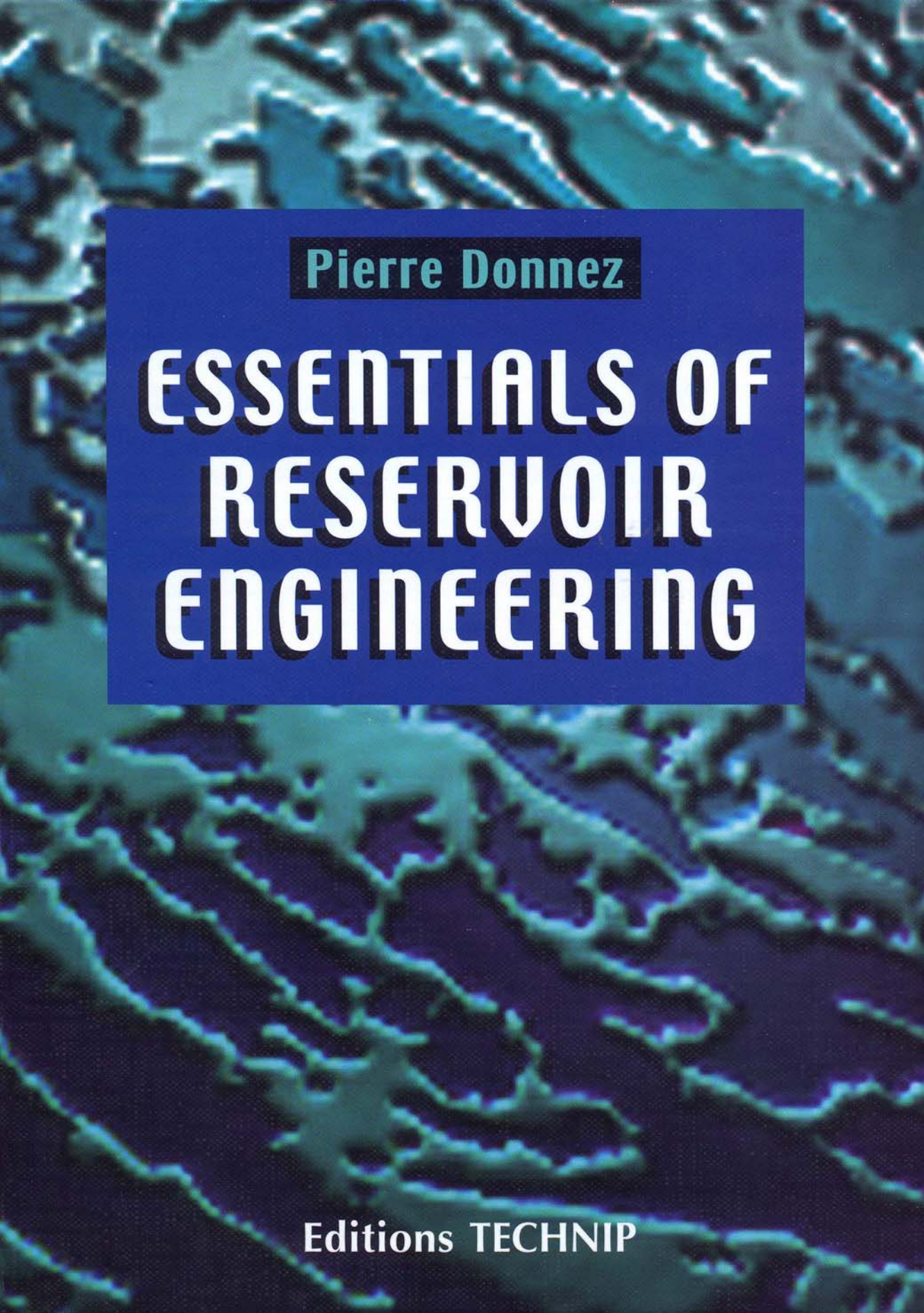
Pierre Donnez
ESSENTIALS OF RESERVOIR ENGINEERING
Editions TECHNIP

ESSENTIALS OF RESERVOIR ENGINEERING

FROM THE SAME PUBLISHER

Well Completion and Servicing
D. PERRIN

Well Testing: Interpretation Methods
G. BOURDAROT

Drilling
J.-P. NGUYEN

Integrated Reservoir Studies
L. COSENTINO

Well Production Practical Handbook
H. CHOLET

Interactive Drilling for Fast Track Oilfield Development
J. LECOURTIER, ed.

Enhanced Oil Recovery
M. LATIL

Abnormal Pressures while Drilling
J.-P. MOUCHET, A. MITCHELL

Drilling Data Handbook
G. GABOLDE, J.-P. NGUYEN

Thermodynamics
J. VIDAL

Properties of Reservoir Rocks: Core Analysis
R.P. MONICARD

Encyclopedia of Well Logging
R. DESBRANDES

Thermal Methods of Oil Recovery
J. BURGER, P. SOURIEAU, M. COMBARNOUS

Directional Drilling and Deviation Control Technology

Dictionary of Drilling and Boreholes. *English-French, French-English*
M. MOUREAU, G. BRACE

Pierre DONNEZ
IFP-School Professor

ESSENTIALS OF RESERVOIR ENGINEERING

2007

Editions TECHNIP 27 rue Ginoux, 75737 PARIS Cedex 15, FRANCE

Printed in France

ISBN 978-2-7108-0892-3

Foreword

Meeting the continuously growing demand in energy will be a major issue of the 21rst century. In addition, the forecasts show that hydrocarbon production will still be the first source of energy for the coming decades. In other words, the Oil and Gas industry should provide more oil and gas than today although the potential for new discoveries is limited. To face this challenge, it will be extremely important to constantly work at optimizing and increasing the recovery factor of the existing fields. And without any doubt, Reservoir Engineering is a key tool to achieve that objective.

So in the future, industry will need a lot of high trained reservoir engineers able to innovate in terms of field development.

Within the past twenty years, the techniques in reservoir engineering have changed. So attention has been given to the problem of technical obsolescence among engineers and the need of overcoming this by means of continuing education. Young engineers must be taught with up to date material and techniques to be rapidly operational in companies.

In this context, a new book is always welcome to improve and extend knowledge in this field.

The author brings here an original contribution based on his personal experience as an expert in the industry and as a teacher in IFP-School.

For each subject, the author develops the links between theory, laboratory measurements, reservoir study practices and field applications.

In addition, practical information is given taking into account different unit systems and mentioning references of key publications to refer to.

This book will be useful for student initial education as well as for updating skills of professionals.

J.P. Roy
Director
Exploration and Production Centre
IFP-School

Preface

The text book is the result of many years of reservoir engineering practice in a major oil company in addition to regular teaching at ENSPM (Ecole Nationale Supérieure des Pétroles et des Moteurs subsidiary of Institut Français du Pétrole at Rueil-Malmaison, France).

The objective of the book was to gather useful material under a single comprehensive manual in relation with the different aspects of Reservoir Engineering.

The book is organised in main chapters that can be read almost independently. Each chapter covers a particular subject always treated in view of the practical use for an engineer. Formulas are generally demonstrated and their use for reservoir studies clearly explained with the limits.

With the rapid development of computers and data processing, during the last forty years, study techniques that were commonly used, have now become obsolete. Some of them are mentioned but not dealt with in details.

Units in Reservoir Engineering is a complex issue since all basic theoretical formulas were deducted from the Darcy unit system and the technical applications with correlations of all sorts were developed in the USA in the so-called field units. The metric system is now commonly used in many countries but differences still remain between the metric system in Europe and America. So the rule in this book is to express all formulas in Darcy units, field units, and the metric system except for some correlations that have not been converted.

Chapter 1 / Reservoir Rock Properties: Rock properties are dealt with under conventional and Special Core Analysis description. Some special physical properties such as natural and induced radioactivity are explained to help the engineer with the basic understanding of log interpretation.

Basic Laboratory techniques are described.

Chapter 2 / Reservoir Fluid Properties: Generalities on hydrocarbon systems encountered are described. The goal is to familiarise the reader with the PVT measurement techniques and their applications in reservoir engineering. A review on the basis of thermodynamics (in appendix) is also presented to introduce the concept of fugacity used in the equation of state.

Chapter 3 / Fluid Flow in Reservoirs: The chapter is focussed on the theory of mechanics of fluid applied to a porous material based on monophasic fluid flow. The diffusivity equation is established and its use in reservoir engineering calculation is explained in details for the Hurst Van Everdingen methodology. Reservoir flow in a gridded reservoir is presented as an introduction to reservoir simulation.

Chapter 4 / Multiphase Flow in Reservoirs: Two-phase and three-phase relative permeabilities are treated with the frontal displacement theory. Some aspects of fractured reservoirs are mentioned.

Chapter 5 / Natural Reservoir Drainage Mechanisms of Hydrocarbon Reservoirs: Classical material balance calculations are explained with a view to using the material balance software MBAL, admitted as a standard in the industry. Water entry calculations by the Hurst Van Everdingen method has been detailed with the symbols used in MBAL.

Chapter 6 / Reservoir Simulation: The basic theoretical foundations of reservoir simulation are explained, to help the reservoir engineer use the tool efficiently. Hardware and associated software have changed during the last forty years. Only the most common present techniques used in the industry to day are dealt with.

Acknowledgements

I wish to express my thanks to ENSPM for granting permission to publish this work, in particular to Jean-Pierre Roy, director of CDEG (Centre D'Exploitation des Gisements). Also all my thanks to the professors who helped me shape the book by their suggestions and corrections, particularly Gérard Lesage and Alain Auriault. I do not forget all the students who attended my lectures for their remarks.

P. Donnez
Paris, September 2007

Symbols and Units

Symbols		US Units	Metric Units
Bg	Gas formation volume factor at pressure P	Bbl/Mscf	ratio
Bgi	Initial gas formation volume factor	Bbl/Mscf	ratio
Bo	Oil formation volume factor at pressure P	ratio	ratio
Bobd	Bo from a differential depletion of an oil at Pb	ratio	ratio
Bobf	Bo from a flash separation of an oil at Pb	ratio	ratio
Bod	Bo from differential depletion at pressure P	ratio	ratio
Boi	Initial oil formation volume factor	ratio	ratio
Bt	Total hydrocarbon formation volume factor	Bbl/bbl	ratio
Bti	Initial total hydrocarbon formation volume factor	Bbl/bbl	ratio
c	Compressibility	psi^{-1}	bar^{-1}
c_e	Equivalent compressibility	psi^{-1}	bar^{-1}
c_o	Oil compressibility	psi^{-1}	bar^{-1}
c_p	Pore compressibility (cf)	psi^{-1}	bar^{-1}
c_t	Total compressibility	psi^{-1}	bar^{-1}
c_w	Water compressibility	psi^{-1}	bar^{-1}
DDI	Depletion drive index	fraction	fraction
G	Initial Gas in place	10^9 or 10^{12} Bcf or Tcf	M m^3 or G m^3
GDI	Gas depletion index	fraction	fraction
GOC	Gas oil contact		
GOR	Gas oil ratio	scf/bbl	m^3/m^3
Gp	Cumulative Gas produced at time t	MMMscf	M m^3 or G m^3
K	Absolute permeability	mD	mD
kg	Effective gas permeability	mD	mD
ko	Effective oil permeability	mD	mD
krg	Gas relative permeability	fraction	fraction
kro	Oil relative permeability	fraction	fraction
krw	Water relative permeability	fraction	fraction
kw	effective water permeability	mD	mD

Symbols		US Units	Metric Units
m	gas to oil pool volume ratio at reservoir conditions	ratio	ratio
N	Initial Oil in Place	MMbbls	M m^3
Np	Cumulative oil produced at time t	MMbbls	M m^3
P	Pressure	psi	bar
Pb	Bubble point pressure	psi	bar
P_{cog}	Capillary pressure oil gas	psi	bar
P_{cow}	Capillary pressure oil water	psi	bar
Pi	Initial pressure	psi	bar
q_D	Dimensionless rate		
Qg	Gas production rate	scf/d	m^3/d
Qo	Oil production rate	Bopd	m^3/d
Qw	Water production rate	Bwpd	m^3/d
Re	Radius exterior	ft	m
r_{eD}	Dimensionless exterior radius		
Rl	Liberated gas	scf/bbl	m^3/m^3
Rp	GOR on cumulatives	scf/bbl	m^3/m^3
Rs	Solution gas at pressure P	scf/bbl	m^3/m^3
Rsd	Solution gas present at pressure P during a differential process	scf/bbl	m^3/m^3
$Rsfb$	Solution gas deduced from a flash liberation of oil at Pb	scf/bbl	m^3/m^3
Rsi	Initial gas in solution at Pi	scf/bbl	m^3/m^3
R_{sid}	Initial total gas in solution deduced from a differential process	scf/bbl	m^3/m^3
Rw	Well radius	ft	m
S	Skin	dimensionless	dimensionless
Sg	Gas saturation	fraction	fraction
So	Oil saturation	fraction	fraction
Swi	Water saturation	fraction	fraction
t_D	Dimensionless time		
V_p	Pore volume	ft^3	m^3
V_r	Rock volume	ft^3	m^3
W	Water volume in the aquifer associated to an oil pool	MMbbls	M m^3
W_D	Dimensionless cumulative water entry		
WDI	Water drive index	fraction	fraction
We	Cumulative water entry	MMbbls	M m^3
WOC	Water oil contact	ft	m
Wp	Cumulative water produced	MMbbls	M m^3
μ_g	Gas viscosity	cp	cp
μ_o	Oil viscosity	cp	cp
μ_w	Water viscosity	cp	cp
ϕ	Porosity	fraction	fraction

Contents

Chapter 2
RESERVOIR FLUID PROPERTIES

Chapter 3
FLUID FLOW IN RESERVOIRS

Chapter 4
MULTIPHASE FLOW IN RESERVOIRS

Chapter 5
NATURAL DRAINAGE MECHANISMS OF HYDROCARBON RESERVOIRS

Chapter 6
RESERVOIR SIMULATION

APPENDICES

CHAPTER 1

Reservoir Rock Properties

1.1 INTRODUCTION

Naturally occurring rocks are in general permeated with fluid, water and hydrocarbons. Geologists and reservoir engineers are concerned with the fluid volumes that have been stored in the formation and the ability for the fluid to move through the porous network that is called the transmissibility capacity.

The rock is made of grains and voids. Grains submitted to violent crushing or grinding may be irregular in shape and with sharp-edges. Sand grains that make up sand beds and fragments of carbonate materials that make up limestone beds usually never fit together perfectly even though submitted to a large overburden pressure. The void space created between grains is the pore space. Pore space or porosity characterizes the rock ability to store fluids.

Knowledge of the physical rock properties is of vital importance in understanding the nature of a given reservoir.

Permeability characterizes the rock ability to let any fluid to move through the porous media.

Laboratory measurements carried out on cores are necessary to:

- Describe the pore system (lithology, geology) and measure the basic properties of the rock.
- To gather the maximum knowledge of the reservoir storage properties in coordination with the data obtained from the mud logging and electric log surveys.

Two kinds of analysis are commonly considered:

- Conventional Core Analysis (CCA) including:
  - Porosity
  - Absolute permeability
  - Grain density.

- Special Core Analysis (SCAL)
  - Wettability
  - Capillary pressure
  - Relative permeability
  - Pore throat size distribution
  - Compressibility
  - Electrical measurements (a, m, n).

Conventional core analysis is carried out on a routine basis as soon as a formation core is available.

1.2 CONVENTIONAL CORE ANALYSIS

1.2.1 Porosity

Porosity is the ratio of the void space volume to the bulk volume of the rock expressed usually in percentage.

An original porosity is developed during the material deposition, and later compaction and cementation reduce it to the primary porosity. Secondary or induced porosity is developed such as fractures in shales and limestones as vugs or solution cavities called kartzs. From the reservoir engineering standpoint, it is necessary to distinguish connected porosity with porosity made of non connected pores. The effective porosity is the ratio of the interconnected void spaces in the rock to the bulk volume of the rock. The total porosity is the sum of the two porosities. Usually, the total porosity is equal to the effective porosity in sandstones. In carbonates as dolomites and limestones, a non connected vuggy porosity may occur. Where water is present in a carbonate formation, there is a continuous process of solution and deposition or recrystallization taking place. This process called diagenesis may affect drastically the porous material and its permeability.

Diagenesis is defined as physical and chemical changes applied to sediment after deposition.

The different processes observed are:

- Mechanical compaction.
- Mineralogical change.
- Cement precipitation.
- Mineral dissolution.

Porosity for a regular cubic stacking packing grain arrangement [1, 2].

Porosity of cubic packed spheres can be calculated as follows:

Considering a cube filled with eight spheres of radius r.

Volume of the cube is: $(4\,r)^3$

Total volume of the eight spheres is: $8 \times 4/3\ \pi r^3$

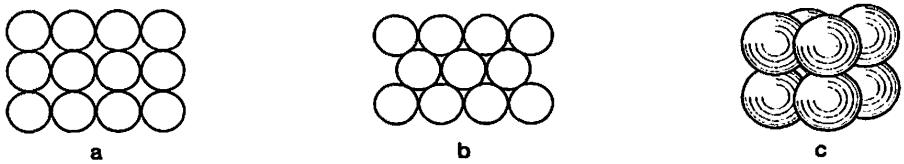

Figure 1.1 *a*: cubic or wide-packed, *b*: rhombohedral or close-packed, *c*: 4 by 4 pack.

Pore space volume is: $(4\,r)^3 - 8 * 4/3\,\pi r^3$

Porosity: $\phi = \frac{V_B - V_s}{V_B} = 1 - \frac{V_s}{V_B}$ $\phi = 1 - \frac{32\pi r^3}{3 * 64 r^3} = 1 - \frac{\pi}{6}$ V_B: bulk volume

V_s: volume of grains

$$\varphi = 0.4764$$

The porosity for cubical packing (the least compact arrangement) is 47.6% (Fig. 1.1.c).

For identical spherical grains, porosity is independent of radius but depends on packing.

The porosity for rhombohedral arrangement in Figure 1.1.b, the most compact arrangement is 25.96%.

Porosity Types:

Interparticle porosity also called "intergranular" is the predominant type found in *sucrosic* (sugar-like) rocks. Pore sizes are of the same order of magnitude as, but usually less than, particule sizes. For uniform spherical grains, interparticle porosity ranges from 47.6% (cubic staking) to 25.9% (close pack) as seen above. In the field, these figures are normally reduced by grain-size variations and shale presence. Permeability in these rocks is affected not only by porosity, sorting, and stacking but also by grain size. The range extends in the order of darcies in large grain sandstones to impervious (to liquids) in chalks and silstones.

Intraparticle porosity is revealed by the SEM (Scanner Electronic Microscope). It is the pore space network within the grains. A significant amount of intraparticle porosity containing connate water is nearly impervious.

Fracture porosity is encountered in fractured reservoirs usually observed in carbonates. The media is then defined as a double porosity media: matrix and fractures. Fractures occur in crystalline or amorphous rocks, which have no "grain size".

Vugs and **molds**, though different in appearance and characteristics, are carried as a single classification on two grounds. First, they are caused by the same mechanism, selective dissolution of sedimentary rock by percolating waters; second they are usually lumped together in log analysis (for lack of a better way). The difference is relative to the sizes. Vugs vary from fingernail size or smaller (micro vugs) to large caves. Molds are normally much smaller. The commonest type results from dissolution of oolites, small calcite spheres often precipitated in sea water. These are consequently called "oolmolds" or

"oolicasts", which porosity can be very high. However, the connectedness is apt to be poor. Vugs tend to be relatively well connected in opposition to the molds case.

1.2.2 Permeability

The term permeability has been adopted as a measurement of the porous rock's ability to conduct fluid. If only one fluid is present in the interstices, this transport coeffioient is called the specific or absolute permeability, but otherwise one must make reference to the effective permeability of each of the immiscible fluids in the connected pore space. Relative permeability is the ratio of the effective to the absolute permeability.

The measurement of permeability is a measurement of the fluid conductivity of the particular material. Analogically with electricity, permeability represents the reciprocal of the resistance which the porous medium offers to flow.

Henry Darcy carried out the pioneer work on permeability when investigating the water flow through filter sands. For that reason the unit of permeability is known as the *Darcy*.

For monophasic flow:

Darcy's equation

$$q = k\frac{A}{\mu L}(P_1 - P_2) \tag{1.1}$$

q: flow rate cc/s
k: permeability of the rock sample (Darcy)
μ: fluid viscosity (cp)
A: cross sample area (cm^2)
L: rock sample length (cm)
P: pressure (atm)

The flow rate is proportional to:

- Rock permeability.
- Cross section area of the sample.
- Pressure gradient.

And is inversely proportional to:

- Fluid viscosity.
- Sample length.

Dimensional analysis:

$$k = \frac{q\mu L}{\Delta P.A} \qquad |k| = \frac{L^3T^{-1}ML^{-1}T^{-1}L}{ML^{-1}T^{-2}L^2} = L^2$$

Permeability has a dimension of an area.

The millidarcy is commonly used in the industry since the Darcy is "large" and convenient only for the very high permeable beds.

The Darcy definition is not issued from a homogenous system of units. Reservoir engineering techniques have been built from that equation. Therefore analytical formulas refer to the Darcy unit system. The other unit systems commonly used in the industry are: field units and metric units. Great care must be taken with reservoir engineering formulas!.

Absolute Permeability:

Initially the Darcy work was carried out to describe the flow of one fluid (water) saturating 100% of the porous media (water). The permeability to a particular fluid is independent of the fluid properties (viscosity). Therefore, the permeability to a 100% saturating fluid is a constant and characteristic of the porous media that is called the absolute permeability or specific permeability.

Remarks:
Building a geological model, implies the allocation of porosity and permeability values to each cell. The permeability to be used is the absolute permeability. An upscaling procedure is usually needed to decrease the number of cells for the future reservoir model. The process consists of filling the geological model with one fluid, and calculating average porosity and permeability dynamically over a group of cells.
Permeability is a key parameter for the reservoir engineer to forecast well flow rates and reserves. A large hydrocarbon quantity may be present, but if permeability is inexistent, the reserves (expected cumulative hydrocarbon volume produced) are nil.

Klinkenberg Effect [2, 3, 4]:

It has been observed that measured absolute permeability of a sample is different when it is measured with air or liquid. In the case of a low pressure gas flow, the free mean path between gas molecules is of the same order of magnitude as the pore size. Therefore the probability of shock between the molecule and the grain is the same as the shock probability between two gas molecules. Consequently the relative weight of the viscous forces involved during the gas displacement is greatly decreased. Applying the Darcy law for the displacement conducts to a higher apparent permeability than the one measured with a liquid.

The linear relationship between the observed permeability and the reciprocal of mean pressure is expressed as:

$$k_L = \frac{k_g}{1+\frac{b}{\overline{P}}} = k_g - m\frac{1}{\overline{P}} \qquad b = \frac{m}{k_L} \tag{1.2}$$

where

k_L: absolute permeability measured with a liquid
k_g: absolute permeability measured with a gas
$\overline{P}$: mean flowing pressure during the displacement
b: constant for a given gas in a given medium (Fig. 1.2)
m: slope of the curve

b depends on the mean free path of the gas and the size of the openings in the porous media. Permeability is also dependent on the size openings in the porous media. Therefore b is a function of permeability.

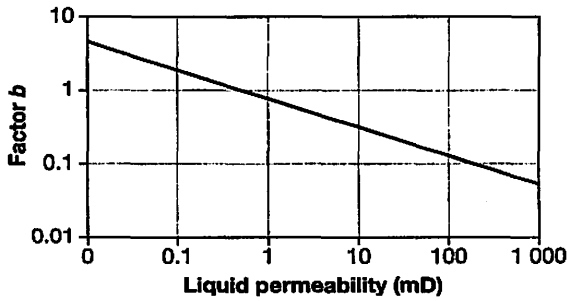

Figure 1.2 Klinkerberg factor *b*.

Effect of Reactive Liquids and Clay on Permeability:

Reservoir rock constituency is not perfectly pure. Often clastic formations contain some percentage of impurities like shale. In the laboratory, core samples are submitted to a severe treatment: drastic pressure and temperature changes, cleaning with water, toluene and drying. Impurities within the rock react differently and alter the internal geometry of the porous media. Therefore measuring air permeability on such a sample may not be representative of the in-situ rock permeability.

Measuring permeability with different salinity waters may conduct to different results. It has been concluded that the degree of hydration of the clays is a function of the water salinity. Fresh water may cause the cementation material in a core to swell owing to hydration. This is why salt saturated water mud is often used for drilling to avoid clay swelling and well obstruction. Consequently it is recommended to use reconstituted formation water for the experiments. Even though laboratory experiments carried out at reservoir conditions may show measured absolute permeability decreased by 10 or 50 fold.

Presence of clay [6] in a reservoir may have a large impact on the in-situ reservoir properties. The clay minerals may be affected during drilling of the well, during completion, during production, and/or injection. Kaolinite, chlorite, illite, and ordered and random mixed layer illite/smectite, may occur simultaneously within the reservoir rock. As little as 2 weight percent clay causes permeability to be drastically reduced.

Formation damage due to clay minerals results from:

- Swelling of smectite caused by injection water or by drilling fluid of low salinity.
- Clay migration and subsequent pore-blockage.
- Precipitation of gelatinous pore-blocking iron hydroxides caused by the dissolution of chlorite by acid.
- High water saturations.
- Desegragation of poorly consolidated parts of the reservoir into its component sand grains if the weak clay cements are disturbed.

Clay control measures may be necessary to increase production while minimizing formation damage.

1.2.3 Grain Density

Grain density is the density of the dried rock material (Table 1.1).

Grain density, also called matrix density is dependent on lithology. Its knowledge is of prime importance to interpret electrical and radioactive logs.

Most reservoir rocks are made of clastics (sandstones) and or carbonates.

Sandstones are sedimentary rocks, while limestones, dolomites, and other carbonate reservoir rock material are frequently derived by precipitation.

Carbonate reservoir rocks can be divided into the following lithologic types: oolitic limestone, limestone, chalk, dolomitic limestone, dolomites and cherty limestones and dolomites.

Usually all rock materials are mixed with impurities (shales or clays). A formation is said to be clean when it is shale free.

Table 1.1 Matrix densities of common clean materials (g/cc)

	From	To
Sandstone	2.65	2.67
Limestone	2.70	2.76
Dolomite	2.82	2.87
Anhydrite	2.90	3.00
Gypsum	2.30	2.40
Clay	2.64	2.66
Salt	2.14	

1.2.4 Laboratory Techniques

1.2.4.1 Core Preparation

Laboratory measurements are carried out on clean samples

The rock sample coming out of the drilling core barrel is saturated with:

- Connate water.
- Mud filtrate and particles.
- Eventually trapped hydrocarbon (liquid and or gas).

The rock sample has been submitted to a drastic treatment during the cutting process and the surface recovery operation:

- Mud products invasion then: partial initial fluid content moved out.
- Depressurization and temperature decrease during the pulling out.

Consequently, in many cases, the surface collected sample is not anymore representative of the in-situ reservoir rock.

Cleaning of the sample is carried out with a Soxhlet type extractor which combines a solvent with heat. The combination of the Soxhlet with centrifugation for conventional core analysis is very efficient.

For large core samples, the "vacuum retorting" (distillation) method is used.

Solvents usually used are:

Toluene, xylem, chloroform, carbon tetrachloride, acetone, chlorothene, hexane...

1.2.4.2 Porosity and Grain Density Measurements [1, 2, 5]

Porosity is: $\Phi = \frac{V_b - V_s}{V_b} \times 100$ V_b: bulk volume V_s: solid volume

Bulk volume V_b determination

Bulk volume can be deducted from measuring the dimensions of the three basic parameters if the geometry of the sample is regular.

Otherwise, the technique is to measure the volume of fluid displaced by the sample, under the condition of preventing fluid penetration into the pore space of the rock. This can be obtained by coating the sample with paraffin or:

- Saturating the rock with the fluid into which it is to be immersed or by using mercury.
- Gravimetric determination.

Solid volume V_s determination

V_s can be obtained by three methods:

- Use of a picnometer.
- Immersion method.
- Use of a pressure chamber.

The two first methods assume a saturated sample. The last is based on the Mariotte-Boyle's law.

Solid volume obtained by the gas expansion method

The equipment consists of two chambers of known volumes connected by tubing equipped with a valve (Fig. 1.3).

First, the dried sample is introduced in the sample chamber and gas is injected at a pressure P_1 with the control valve closed. The expansion chamber is submitted to vacuum.

The communication valve is opened and the gas pressure falls to P_2.

The Boyle's law is written as:

$$(V - V_s)P_1 = (V - V_s + \Delta V)P_2$$

V: volume of the sample chamber V_s: solid volume of the sample
ΔV: volume of the expansion chamber
P_1: initial pressure P_2: final pressure
Usual gas used: helium

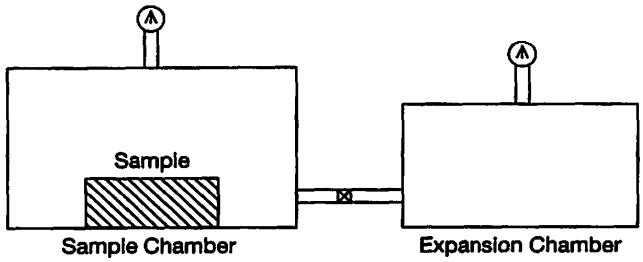

Figure 1.3 Gas expansion method.

$$V_s = V - \frac{P_2}{P_1 - P_2}\Delta V \tag{1.1}$$

The bulk volume is determined from the geometry or with a picnometer (immersion into mercury, measurement of the displaced volume on the pump).

Fluid summation method

The method patented by Core Laboratories is carried out on a non washed sample full of fluids at surface.

It is considered that the pore volume is equal to the sum of water, oil and gas volumes contained in the sample. The method is not accurate and abandoned.

Grain density

$$\rho_{ma} = \frac{\text{mass of dry sample}}{V_s} \text{ (g/cc)}$$

Mass of dry sample is obtained by weighting the sample; V_s is obtained from the gas expansion measurement.

1.2.4.3 Permeability Measurement [2]

The Darcy law is used as:

$$\frac{Q}{A} = \frac{k}{\mu}\frac{dP}{dx} \tag{1.3}$$

Q:	volumetric fluid rate	(cm^3/s)
A:	cross-section	(cm^2)
k:	permeability	(Darcy)
dP/dx:	pressure gradient	(atm/cm)
Q/A:	fluid velocity	
μ:	fluid viscosity	(cp)

Table 1.2 Example of a CCA report

COMPANY EXPLO			DATE: SEP 1979 FORMATION: SAND				FILE NO: SCA 500 ANALYSTS: CRF			
HORIZONTAL PLUGS										
SAMPLE NUMBER	DEPTH	PERMEABILITY		POROSITY		FLUID OIL	SATS. WTR	GRAIN DEN		DESCRIPTION
		KA	KL	GEX	FLD					
364	3 265.25								AA	
365	3 265.50								AA	
366	3 265.75								AA	
367	3 266.00	123	110	15.3	15.2	0.0	55.7	2.64	SS	GY FG SIL CMT
368	3 266.25	506	476	17.3	17.7	0.0	57.4	2.65	SS	GY F-GRAN SIL. CMT
369	3 266.50	126	113	17.4	16.6	0.0	54.8	2.65	AA	
370	3 266.75	653	623	16.5	17.3	0.0	48.2	2.65	AA	
371	3 267.00	176	156	18.1	21.6	0.0	59.2	2.65	AA	
372	3 267.25	1 135	1 085	17.5	17.5	0.0	50.3	2.65	AA	
373	3 267.50	1 821	1 761	15.9	18.2	0.0	55.4	2.66	AA	
374	3 267.75	913	873	17.8	20.4	0.0	65.5	2.65	AA	
375	3 268.00	654	624	15.8	18.7	0.0	55.5	2.70	SS	GY F-GRAN SIL. CMT PY
376	3 268.25	1 519	1 469	18.2	18.7	0.0	60.4	2.65	SS	GY F-GRAN SIL. CMT
377	3 268.50	397	367	18.2	19.3	0.0	49.2	2.65	AA	
378	3 268.75	1 451	1 401	18.1	19.7	0.0	53.5	2.64	AA	
379	3 269.00	177	156	18.2	22.8	4.0	38.5	2.65	SS	GY FG SIL. CMT
380	3 269.25	427	397	16.5	20.6	4.5	38.8	2.63	AA	GY F-GRAN SIL. CMT
381	3 269.50	1 198	1 148	19.5	18.3	0.0	39.8	2.65	SS	GY F-GRAN SIL. CMT
382	3 269.75	1 313	1 263	15.1	19.1	0.0	45.3	2.64	AA	GY F-GRAN SIL. CMT

Table 1.2 Example of a CCA report

383	3 270.00	807	767	18.3	17.5	0.0	54.1	2.66	AA	GY F-GRAN SIL. CMT
384	3 270.25	694	664	17.7	22.1	0.0	36.8	2.64	SS	GY F-GRAN SIL. CMT
385	3 270.50	103	91	16.2	21.6	0.0	52.3	2.65	SS	GY F-GRAN SIL. CMT
386	3 270.75	120	107	18.8	30.0	0.0	51.1	2.64	SS	GY F-GRAN SIL. CMT
387	3 271.00	4 040	3 960	19.8	23.8	3.8	54.8	2.66	SS	GY F-GRAN SIL. CMT
388	3 271.25	3 054	2 974	20.8	24.7	0.0	51.5	2.65	AA	
389	3 271.50	1 119	1 069	21.7	21.9	0.0	58.4	2.65	SS	GY FG SIL. CMT
390	3 271.75	1 101	1 051	21.3	22.9	0.0	59.5	2.65	SS	GY F-GRAN SIL. CMT
391	3 272.00	529	499	15.4	17.5	0.0	46.6	2.66	AA	
392	3 272.25								SHALE/SILTSTONE	
393	3 272.50								AA	

Symbols used:

Permeability

KA: air permeability
KL: liquid permeability
GEX: gas expansion method

Porosity

FLD: fluid summation method to discard
FLUID SATS.: to discard
GRAIN DEN: Grain Density (g/cc)

Geological symbols used

AA: As Above
CMT: Cemented
CARB: Carbon
F: Feldspar
FG: Fine Grains
GY: Grey
VF-FG: Very Fine to Fine Grain
SS: Sandstone
SIL: Silt

All laboratories use gas permeameters for routine analysis since they are accurate and require a short time to be carried out.

Two apparatus are used:

- Variable load gas permeameter (IFP type).
- Fixed load gas permeameter (Core Lab).

Air, nitrogen or helium may be used. The results must be corrected for the Klikenberg effect.

Table 1.2 shows an example of a CCA report.

Concluding remarks:
Permeability values measured with air or liquid should be close. The best porosity measurement is obtained with the gas expansion method (GEX). The fluid summation method should be discarded as well as the fluid saturations measured on cores.

1.3 SPECIAL CORE ANALYSIS (SCAL)

1.3.1 Introduction

Special Core Analysis or Advanced rock properties, includes the study of rock characteristics that are necessary to conduct any reservoir study. Such laboratory experiments are time consuming and expensive. Therefore the end user and the laboratory must collaborate to define the laboratory experiment programme to focus on the essentials, and during the laboratory process to modify eventually the programme if needed.

Each field is a unique entity and the SCAL programme will be defined according to the final objective defined first. To do so, good knowledge of the laboratory techniques with its limits is necessary by all involved actors.

1.3.2 Wettability

Wettability has, in recent years, been recognized as one of the most important parameters for a reservoir. The industry is privileged to have an excellent series of review articles by Anderson [7] (1986-1987) which provides exhaustive discussions on how wettability affects other reservoir parameters. When two immiscible fluids are in contact, due to the interfacial tension forces, the interface will be curved with higher pressure on the concave side than on the convex side.

The grain area in contact with the fluids filling the pores is very high. The smaller the grains are, larger the area is. For example in a rock volume of $1 m^3$, the grain area in contact with reservoir fluids is 83 000 m^2/m^3 for a grain diameter of 0.05 mm. Therefore rock/Fluid properties have a large influence on fluid movements.

The term wettability connotes the preference of a given liquid to spread over a solid surface in the presence of a second liquid. Gas is always a non wetting fluid. Wettability is a very important characteristic of the rock/fluid system as it affects the special core analysis properties which are critical. These properties include: capillary pressure, relative permeability, waterflood behavior, irreducible water saturation and electrical properties [7, 8, 9]. The origin of wettability is not fully understood. It is admitted that wettability is established as a result of the adsorption of molar compounds or deposition of organic material on the rock surface.

It can be imagined that prior to hydrocarbon migration, the reservoir saturated at 100% with water was water wet. The hydrocarbon replacing the water during the migration process modified the rock wettability in the oil zone.

Wettability is influenced by a large number of variables that include temperature; contact time; atmosphere; roughness; crystal structure; composition; surface pre-treatment; and interfacial segregation, adsorption, and reactions. Extensive reviews have been published documenting the role of factors that govern wettability. Basically, three types of interactions can promote wettability in the high-temperature solid-liquid systems: dissociation of surface oxides on liquid metal (oxide scavenging), chemical dissolution of the solid in the melt and interfacial adsorption of reactive solutes and formation of a wettable interfacial compound.

Wettability is quantified by the contact angle defined in Figure 1.4 which represents a drop of liquid deposited on a flat surface. If the angle θ is less than 90°, the surface is wetted by the water. The smaller the angle the higher the wettability is. Conversely, if the angle is higher than 90°, the surface is not wetted by the water.

Wettability may not be uniform on the grain or in the pore of a reservoir. Some authors have identified mixed wettability reservoirs in which the larger pores are oil wet and the smaller are water wet probably indicating that the polar impurities could not reach the wall of the small pores.

The only proper method of measuring wettability is to obtain a contact angle between the two fluids and the rock. If the contact angle measured through a fluid is less than 90°, a neutrally wet situation is said to exist [2]. However, direct measurements are rarely practical with reservoir materials. Actual reservoir materials are sometimes approximated by "pure" smooth surfaces: glass (silica) for sandstones or calcite crystals for carbonates.

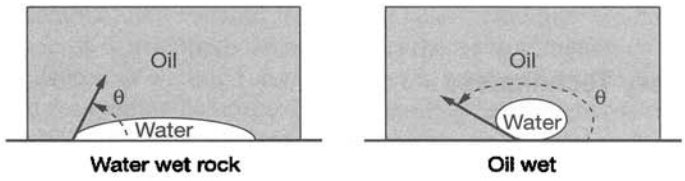

Figure 1.4

An important effect of wettability is the water rise in a water wet capillary which determines the capillary pressure.

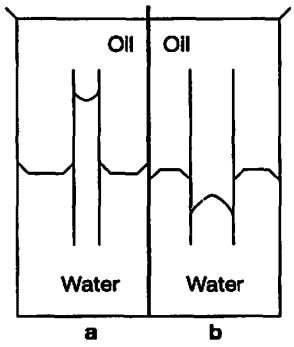

Figure 1.5 *a*: water wetting the tube, *b*: water non wetting the tube.

Water normally wets the glass, capillary inducing a rise.

Crude oil may wet the glass inducing an inverted meniscus and a drop.

If the situation of Figure 1.5a occurs, water is said to wet preferentially the solid surface. If the situation of Figure 1.5b occurs, oil is said to wet preferentially the solid surface.

Factors Affecting Reservoir Wettability [10]:

- Oil composition.
- Rock mineralogy.
- Connate water composition and ph.
- Reservoir pressure and temperature.

Wettability has an impact on the rock water saturation. A highly water wet sandstone will show a high S_{wc} (0.3 to 0.45). Conversely a low water wet rock will show a low S_{wc} (0.05). This affects the amount of oil in place and the displacement efficiency of oil by water.

1.3.3 Laboratory Techniques

The remarks relative to the core treatment for the Conventional Core Analysis are still valid since reservoir cores are submitted to many changes. Then manipulations from the reservoir conditions to the laboratory alter the wettability. Coring with the reservoir oil would be ideal to avoid any wettability change. Wettability is sensitive to surfactants, brine chemistry, ph, and many drilling fluids are known to alter wettability. A water-base mud is required to obtain core material with representative wettability. In addition, the cores should not be cleaned for use in relative permeability tests.

When preserved (non-cleaned) cores are not available, an attempt is made to restore the reservoir wettability. This is accomplished by displacing reservoir oil through the 100% saturated core with reservoir water and "aging" the plug. By "aging" it is meant to store the plug at reservoir temperature in an oven for a four to six week-period.

Normally, the wetting state of a porous medium containing two immiscible fluids should be evaluated in terms of the surface area fraction contacted by each of the fluids [11]. Thus under neutral wetting condition, each of the two fluids should cover 50% of the surface area in the porous medium. In a preferential water-wet system, more that 50% of the surface is covered by water. It is, however, well known that the transport properties of two immiscible fluids in a porous medium are, determined by capillary forces, [12] which are related to capillary pressure. Therefore, the two most used wetting indices, I_{AH} and WI_{USBM}, are defined in terms of capillary pressure and/or fluid flow, spontaneous imbibition/drainage and forced imbibition/drainage. The Amott-Harvey index is based on both of the flow process, i.e. spontaneous imbibition/drainage and forced imbibition/drainage, while WI_{USBM} is related to the area below the capillary pressure imbibition and drainage curves under forced fluid flow. The indices are determined empirically, and they have been used interchangeably within the petroleum industry.

I_w: Amott water index
I_o: Amott oil index
I_{AH}: Amott-Harvey wettability index
WI_{USBM}: Water Index USBM: United States Bureau of Mines

$$I_w = \frac{\Delta S_{ws}}{1 - S_{wr} - S_{or}} = \frac{\Delta S_{ws}}{\Delta S_{wt}} \qquad I_o = \frac{\Delta S_{os}}{1 - S_{wr} - S_{or}} = \frac{\Delta S_{os}}{\Delta S_{ot}} \tag{1.4}$$

ΔS_{ot}: Total increase in oil saturation during spontaneous and forced displacement of water.
ΔS_{os}: Increase in oil saturation during spontaneous imbibition of oil
ΔS_{ws}: Increase in water saturation during spontaneous imbibition of water
ΔS_{wt}: Total increase in water saturation during spontaneous and forced displacement of oil.

Techniques for Monitoring Wettability:

Various experimental techniques have been developed to measure the wettability of surface. These techniques include contact angle measurement [2], two-phase separation, bubble pickup, micro flotation, and vacuum flotation. These techniques are based on the fact that water wetting process is essentially an oil displacement phenomenon on the solid surface. In this process the degree of wetting (or wettability) is governed by the surface free energy of the substrate and the wetting solution. The surface that has a higher surface energy tends to be replaced by a liquid that has a lower surface energy, thus reducing the total free energy of the system.

Wetting has been described in terms of **spreading coefficient**. For a liquid, spreading on solid in the air, the spreading coefficient, σ^{LSG}, is defined as: see Figure 1.6.

$$\sigma^{LSG} = \gamma^{SG} - \gamma^{SL} - \gamma^{LG}$$

where γ^{SG}, γ^{SL}, γ^{LG} are solid/gas, solid/liquid and liquid/gas interface tensions.

When σ^{LSG} is positive, spreading of the liquid occurs spontaneously. Since it is very difficult to determine γ^{SG} directly, Young's equation is employed by considering the equilibrium between force vectors at the S/L/G contact:

$$\gamma^{SG} = \gamma^{SL} + \gamma^{LG} \cos\theta$$

θ is angle of contact that the liquid/gas interface subtends with the solid/liquid interface.

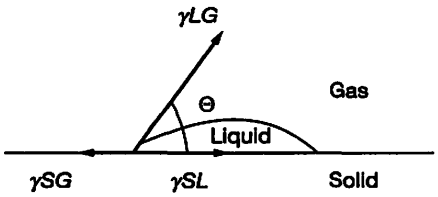

Figure 1.6 Liquid bubble spreading on a surface (L: Liquid; S: surface; G: Gas).

Influence of Wetting Properties on Fluid Flow in Porous Media:

The key parameter that affects the behavior of the porous medium during drainage or imbibition is the spreading coefficient.

Let consider a non wetting fluid on solid surface (S). If a drop of wetting phase is introduced into the system, either the wetting fluid will stay on the surface as a drop, forming contact angle θ, or the wetting fluid will spread over the solid surface, displacing the non wetting fluid. For the second case, we have for the change in interfacial energy between initial stage and final stage:

$$\Delta G = (\gamma_{WS} + \gamma - \gamma_{NS})\,\Delta A$$

where γ_{WS}: interfacial tension between W and S
γ_{NS}: interfacial tension between NW and S (*non wetting and surface*)
γ: interfacial tension between W and NW (*weting and non wetting*)
ΔA: area of the solid surface

In order for the wetting fluid to spread, we must have:

$$\gamma_{WS} + \gamma - \gamma_{NS} < 0. \quad \text{or} \quad \frac{\gamma_{WS} + \gamma}{\gamma_{NS}} < 1$$

The fraction is called spreading coefficient k. So, if $k < 1$, then the wetting fluid will spread over the solid surface. In porous media, it means that the wetting fluid will form thin films on the surfaces of solid grains. The same analysis is valid also for case of curved surface. Moreover, these thin films will not be destroyed during drainage or imbibition, because energetically films are the preferable state for the system. If $k > 1$, then the wetting fluid will remain on the solid surface in the form of the drop, and we need to use the contact angle equation:

$$\gamma_{NS} = \gamma_{WS} + \gamma \cos\theta$$

Fractured Reservoirs:

Fractured reservoirs are often associated with carbonate lithologies. In such a case, a factor that influences wettability is the water acidity. Alkaline waters tend to cause water wetness, while acidic waters may be more commonly associated with oil-wet reservoirs.

Imbibition of water into a reservoir becomes an important factor in the ultimate recovery of oil, because of the tendency for advancing water to seek the fine pores first. This will drive oil out of the fine pores into the larger pores and channels.

Wettability is important, since it will affect the rate and degree of imbibition [13, 14]. For example, if a rock is strongly oil-wet, rather than water-wet, water imbibition will be retarded.

The remaining oil saturation in water invaded regions of fractured, oil-wet, carbonate formations is often high. It may not be possible to apply a large pressure gradient across the matrix, and the oil is retained by capillarity. The oil recovery from the matrix depends on spontaneous imbibition.

1.3.4 Surface Tension, Interfacial Tension

Liquid, contrary to the case of a gas does not tend to occupy all the volume that is offered. Liquid molecules are stuck together by attraction forces. These forces being low in a real gas disappear in a low pressure gas, which then behaves like a perfect gas. Attraction forces decrease quickly with distance. The radius at which the attraction forces become negligible is called the molecular action radius.

Considering a vessel full of water, a molecule within the body of water, is submitted to attraction forces from all directions. Then the molecules are in equilibrium.

At the boundary a molecule has no water molecules above; therefore the resultant force tends to attract the surface molecule into the liquid. Looking at this differently, one can imagine that every new molecule put into the surface area would require that work be done on it. The amount of work that is needed to create 1 cm^2 of a surface is termed the surface energy in ergs (dynes per cm) commonly termed surface tension.

The term *surface tension* is usually used for the tension of a liquid which is in contact with its vapor or with air. Energy between two liquids or a liquid and a surface, is termed *interfacial tension* [15].

The surface tension between liquid and its vapor is a function of pressure, temperature and the phase compositions.

The interfacial tension between two liquids depends on temperature and pressure. For oil and water, the interfacial tension is about 25 dynes/cm at surface conditions. Increasing the temperature and pressure tends to increase interfacial tension. At reservoir conditions, the interfacial tension between oil and water is about 30 dynes/cm (Berg, 1975).

Surface tensions at 20°C

Mercury:	480 dynes/cm
Water:	73
Interfacial tension water/oil:	28 to 30 dynes/cm

The combination of wettability and surface tension or interfacial tension leads to the existence of forces called capillary forces.

1.3.5 Capillary Pressure [5, 8, 14, 15, 16, 17]

The concept of capillary pressure of a particular rock evolved from the representation of the water rise in a water wet capillary tube. The liquid height determines the capillary pressure. Pores in a reservoir rock are analogous to capillary tubes. When the diameters are small, surface forces extend over the entire interface, causing measurable pressure difference between the two fluid phases across the interface.

Another way to look at it consists in saying that the presence of interfacial tension at the contact surface between two immiscible liquids causes a pressure difference across the contact surface called capillary pressure. The capillary pressure p_{cow} between oil and water is linearly proportional to the interfacial tension between the liquids, and inversely proportional to the principal radii of curvature (R_1 and R_2) of the contact surface:

$$p_c = \sigma \cos\theta \left(\frac{1}{R_1} + \frac{1}{R_2} \right)$$

P_c: capillary pressure
σ: interfacial tension
θ: contact angle
R_1, R_2: two principle radii of curvature

If the surface is spherical ($R_1 = R_2$), then

$$p_c = \frac{2\sigma \cos\theta}{R} \tag{1.5}$$

R is the radius of curvature of the contact surface.

Hubbert (1953) defines it as the pressure in the oil minus the pressure in the water (regardless of which is the wetting fluid). Here, we note that for the common case of water-wet rock, the pressure is higher inside the oil (the non wetting fluid) than in water.

An oil/water or an air/water interface in a large tube is flat because the wetting forces at the walls of the tube are distributed over a large perimeter and do not rise or drop into the fluid. Therefore, the pressures of the fluids at the interface are equal. Consequently, at the gas oil contact (GOC), the gas pressure is equal to the oil pressure. At the water oil contact (WOC), the oil pressure is equal to the water pressure.

Capillary pressure data are used in reservoir numerical models to calculate fluid distribution in reservoirs. In any porous material with two fluid phases present, the wetting phase will always have the lowest pressure. Therefore, capillary pressure curves can also be used to determine the wetting characteristics of reservoir rocks.

Figure 1.7 shows the rise of a wetting phase (water) in three different capillary tubes of different diameters in presence of a non wetting phase (oil).

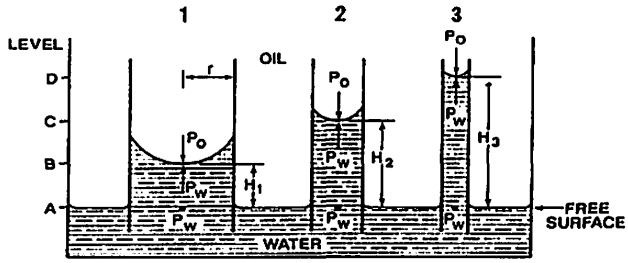

Figure 1.7 Wetting phase rise in capillary tubes.

Lewerett and Lewis first investigated the functions and found some justification to the following conclusions:

- P_{cow} is a function of S_w only and
- P_{cog} is a function of S_g only.

Capillary Pressure J-Function [8, 15]:

Leverett proposed the J-function which describes the heterogeneous rock characteristics by combining porosity and permeability in a dimensionless parameter for correlation. The J-function accounts for changes of permeability, porosity, and wettability of the reservoir when the general pore geometry remains constant. Therefore, different types of rocks exhibit different J functions correlations. All the capillary pressure data from a specific formation can be reduced usually to a single J-function versus the saturation curve.

$$J(S_w) = \frac{P_c}{\sigma \cos\theta}\sqrt{\frac{k}{\varphi}}$$

P_c: dynes/cm^2 σ: dynes/cm k: cm^2 φ: fraction

Capillary function J is a group of physical rock properties and saturating fluid. It was originally proposed as a means of converting all capillary pressure data to a universal curve. It is used to correlate data from one formation.

J function is used in reservoir simulators. $J(S_w)$ is an input; capillary pressure is calculated

From
$$P_c = \text{Cte} \times J(S_w)\sigma\cos\theta\sqrt{\frac{\varphi}{k}} \qquad (1.6)$$

Cte = 4.61678 for field units (psia, mD)

Cte = 0.318319 for metric units (bars, mD)

k is taken as $(k_x + k_y)/2$ $\sigma \cos\theta$ is also required as a function of pressure

1.3.6 Laboratory Measurements Capillary Pressure

Capillary pressures are commonly measured with porous plate de-saturation cells, high-speed centrifuge, or mercury injection techniques. Because of the shorter test times, the centrifuge is the preferred testing technique [5, 18]. The ultra-centrifuge allows testing at temperatures of up to 150°C. Techniques exist for determination of capillary pressures on both consolidated and unconsolidated cores.

Porous Plate Technique:

A core is saturated with water containing salts (NaCl, $CaCl_2$, or Kcl) to stabilize the clay minerals, which tend to swell and dislodge when in contact with freshwater. The saturated core is placed on a porous disk, which also is saturated with water. The disk has finer pores than the rock sample. The pore size of the porous disk should be small enough to prevent penetration of the displacing fluid until the water saturation in the core has reached its irreducible value.

The pressure of the displacing fluid is increased in small increments. For each pressure increase, the amount of displaced water is measured after static equilibrium has been reached. The capillary pressure is plotted function of water saturation. If the rock is water wet, a finite pressure (threshold pressure) will be required before any of the water is displaced from the core. If the core is preferentially oil wet, and oil is the displacing fluid, oil will imbibe into the core, displacing water at zero capillary pressure. The displacement may be reversed.

Laboratory Result Conversions:

Capillary measurements carried out in the laboratory with mercury/air or water/air must be converted to water/oil as found in the reservoir.

$$\frac{P_c H_g \text{ / air}}{P_c \text{water / air}} = \frac{480}{70} = 6.57$$

From experience, the ratio for limestones is about 5 to 8 and for sandstones 7 to 5.

Converting results from laboratory conditions to reservoir conditions:

$$(P_c)_{res} = \frac{\sigma_{\text{water/oil}} \cos\theta_{\text{water/oil}}}{\sigma_{\text{water/gas}} \cos\theta'_{\text{water/gas}}} (P_c')_{lab} \quad \text{or} \quad (P_c)_{res} = \frac{\sigma_{res}}{\sigma_{lab}} (P_c)_{lab} \qquad (1.7)$$

1.3.7 Oil Migration and Entrapment

Because oil is less dense (lighter) than water, droplets of oil immersed in water will tend to rise vertically in the absence of flowing ground water. The net upward force on an oil droplet of volume V can be determined by application of Archimedes's principle. The

downward force of gravity on the oil droplet is $\rho_{oil} \times g \times V$, where ρ_{oil} is the density of oil. The upward force on the oil droplet is equal to the weight of water displaced by the oil droplet, which is $\rho_w \times g \times V$, where ρ_w is the density of water. Therefore, the net upward force (buoyancy force) per unit volume of oil droplet is

$$F_b = (\rho_w - \rho_{oil})\, g$$

In the underground, the oil droplet must rise through the pore space between solid grains.

Whether the buoyancy force is sufficiently large to push an oil droplet through the pore space is the key to petroleum entrapment. To analyze this entrapment mechanism (Berg, 1975) considered a spherical bubble of oil at rest in a pore Figure 1.8.a. The radius of the

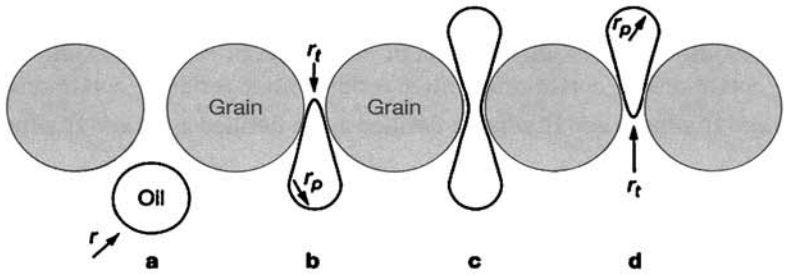

Figure 1.8 Movement of an oil droplet in water wet clastic rock (After Berg, 1975).

Bubble r is approximately equal to the pore radius r_p.

The capillary pressure in the pore is by definition: $p_p = \dfrac{2\sigma}{r_p}$

The bubble to migrate upwards will have to be distorted as shown in Figure 1.8.b.

The capillary pressure at the throat is: $p_t = \dfrac{2\sigma}{r_t}$ with r_t the throat radius

The throat radius r_t being less than r_p, the capillary pressure is greater in the throat than in the pore. This creates a downward force on the oil bubble.

It is worth to note the relation:

Force per unit volume = – pressure gradient

The downward force per unit volume applied on the oil bubble is given by the capillary pressure gradient as:

$$F_c = \frac{p_t - p_p}{H} = \frac{2\sigma}{H}\left(\frac{1}{r_t} - \frac{1}{r_p}\right)$$

H: vertical height of the bubble.

The oil bubble will be able to move upward through the pore throat if the buoyancy force F_b is greater than the pressure gradient F_c or:

$$(\rho_w - \rho_o)g \geq \frac{2\sigma}{H}\left(\frac{1}{r_t} - \frac{1}{r_p}\right)$$

Once the top of the bubble moves past the pore throat Figure 1.8.c & d, the capillary pressure gradient reduces and the rest of the bubble can easily move through the pore throat.

1.3.8 Capillary Number

The concept of capillary number is used to characterize the oil trapping, leading to the residual oil saturation, and the mobilization of residual oil. Models have been developed to simulate the conditions necessary to mobilize residual oil.

Melrose and Bradner [9, 19, 20] have defined a capillary number:

$$Nc = \frac{v\mu}{\phi\sigma} \tag{1.8}$$

v is the Darcy velocity, μ viscosity of the displacing fluid, φ: porosity of the pack, σ: interfacial tension.

1.3.9 Capillary End Effect during a Displacement [9]

During a water injection test through a core sample at a constant water rate, the two forces involved are: friction forces and capillary forces. It is remembered that at maximum water saturation, the P_{cow} is nil. At low water saturation, the oil water capillary pressure is at its maximum.

At the end of the core, the two phases enter a common header where the pressures of both phases are essentially equal. Thus the capillary pressure must undergo a rapid change from finite value in the core to a value close to zero outside the core. For the system to remain at capillary equilibrium, the saturation of the wetting phase must increase to the value corresponding to "zero" capillary pressure. This causes the building of a saturation gradient to be near the end of the core.

At low injection rate, the oil-phase pressure between the core and the end plate exceeds the water-phase pressure. No water flow can occur as long as $p_w < p_o$. As a result water arriving at the end of the core accumulates until the water phase pressure in the core exceeds the oil-phase pressure in the end space of the core holder. This effect can lead to misinterpretation of the core flood since water is accumulated at the end of the core and water breakthrough is delayed, so a displacement test may appear to be stabilized when it is not.

The effect of capillary pressure gradients is minimized when the pressure gradients in both oil and water phases are large in comparison to the capillary pressure gradient.

1.3.10 Rock Compressibility

1.3.10.1 Generalities

The sediment weight on top of the reservoir exerts a constant external pressure called overburden pressure.

The fluid pressure being reduced due to the production process, the bulk rock volume decreases while the volume of the solid rock material (sand grains) increases. Both of these volume changes act to reduce the rock porosity slightly. The porosity changes depend only on the difference between the internal and external pressures and not upon the absolute value of the pressures.

1.3.10.2 Pressure Regimes

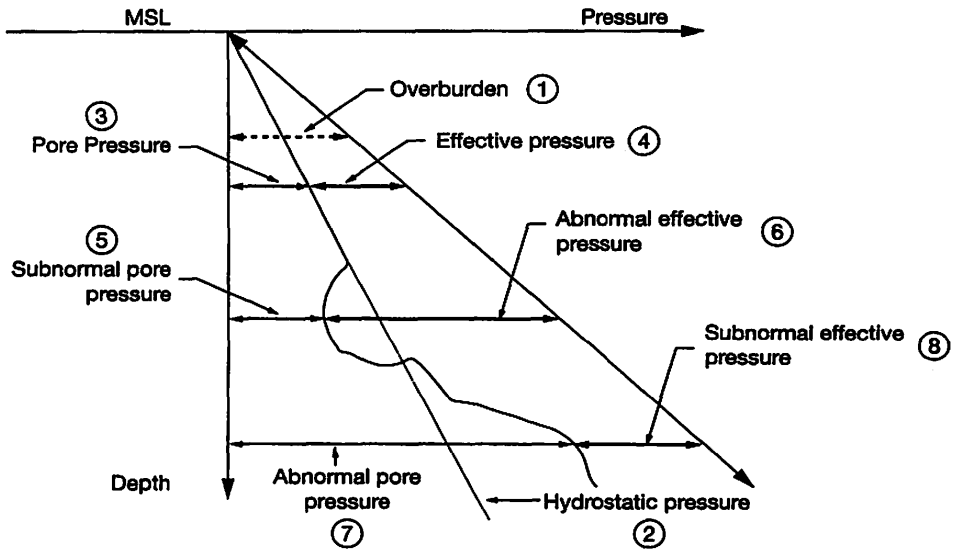

Figure 1.9 Pressure versus Depth.

Pressure gradients are depicted on Figure 1.9.

Label "1" curve is the overburden pressure. That is the pressure created by the weight of the sediments. It is also called the litho static pressure. The average density of the earth crust is about 2.2 g/cm^3, corresponding to a pressure gradient of 0.954 psi/ft or 0.216 bar/m.

Label "2" curve illustrates the hydrostatic pressure. It is the pressure created by a continuous water column from surface, downwards. The gradient is in the range of 0.6 psi/ft or 0.098 bar/m for a water density of 1 000 kg/m^3.

Label "3" At any depth, if a water filled bed is present; in communication up to surface, the fluid pressure is equal to the pore pressure, equal to the hydrostatic pressure. At the same depth, the difference between the overburden pressure and the pore pressure is the effective pressure labeled "4".

Label "5" shows the case of a pore pressure less than the hydrostatic pressure. This proves the existence of an isolated reservoir (no communication to surface). The pore pressure is qualified as subnormal. At the same depth, the average overburden pressure does not change; therefore the effective pressure increases and is qualified as abnormal effective pressure (Label "6").

Label "7" shows a pore pressure higher than hydrostatic pressure; it is called an over pressured reservoir with an abnormal pore pressure. The corresponding effective pressure is then subnormal (Label "8").

When fluid is produced from a porous level, the pore pressure tends to decrease; therefore the effective pressure to increase. In other words, the active pressure exerted at the top of the reservoir increases. If the formation is not consolidated, a collapse of the reservoir takes place, the porous system shrinks; the phenomenon is called compaction.

1.3.10.3 Compressibility

Geertsma [1, 15, 21] states that three kinds of compressibility can be distinguished in rocks:

- Rock bulk compressibility (solids plus pores).
- Rock matrix compressibility (solids).
- Pore compressibility.

Rock bulk compressibility is the fractional change in volume of the bulk rock volume with a unit change in pressure.

$$c_b = -\frac{1}{V_b}\left(\frac{\partial V_b}{\partial p}\right)_T$$

c_b: rock-bulk compressibility, psi^{-1} or, bar^{-1}
V_b: bulk volume
T: subscript means at constant temperature
p: pressure

Rock matrix compressibility is the fractional change in volume of the solid rock material (grains) with a unit change in pressure.

$$c_r = -\frac{1}{V_r}\left(\frac{\partial V_r}{\partial p}\right)_T$$

c_r: rock-matrix compressibility, psi^{-1} or, bar^{-1}
V_r: volume of solids

Pore compressibility is the fractional change in pore volume of the rock with a unit change in pressure.

$$c_p = -\frac{1}{V_p}\left(\frac{\partial V_p}{\partial p}\right)_T$$

c_p: rock-pore compressibility, psi^{-1} or, bar^{-1}
V_p: pore volume

This last equation can be expressed in terms of porosity. It is noted that porosity increases with the increase of pore pressure therefore the compressibility definition is changed to keep the compressibility sign positive.

$$c_p = \frac{1}{\phi}\left(\frac{\partial \phi}{\partial p}\right)_T$$

Combining the compressibilities based on classical linear elasticity theory:

$$c_b = (1-\varphi)\times c_r + \varphi \times c_p$$

The rock (solid) compressibility being negligible, then

$$c_b \approx \varphi \times c_p$$

Several possibilities are offered to measure the rock compressibility. It is possible to vary the external or internal pressure or both.

Hall [22] investigated the pore compressibility at constant overburden pressure. He designated as effective rock compressibility and correlated with porosity. The correlation is shown on Figure 1.10. It can be noted that the compressibility decreases as the porosity increases.

For reservoir applications, the rock and bulk compressibilities are considered small in comparison with the pore compressibility. Therefore the pore compressibility c_p defined by Hall is considered to characterize the compressibility of the system and is sometimes noted as c_f, or c_r.

Fatt found that the pore compressibility is a function of pressure.

$$c_f\, \partial p = \left(\frac{1}{\phi}\right)\partial \phi \qquad \text{integrating the equation}$$

$$c_f \int_{p0}^{p} \partial p = \int_{\phi 0}^{\phi} \frac{\partial \phi}{\phi} \qquad c_f(p-p_0) = \mathrm{Ln}\left(\frac{\phi}{\phi_0}\right) \qquad \text{or} \qquad \phi = \phi_0 e^{c_f(p-p_0)}$$

p_0 = initial pressure
Φ_0 = initial porosity
Φ = porosity at pressure p $\quad e^x = 1 + x + x^2/2! + x^3/3!$ Then

$$\Phi = \Phi_0\,[1 + c_f(p-p_0)] \tag{1.9}$$

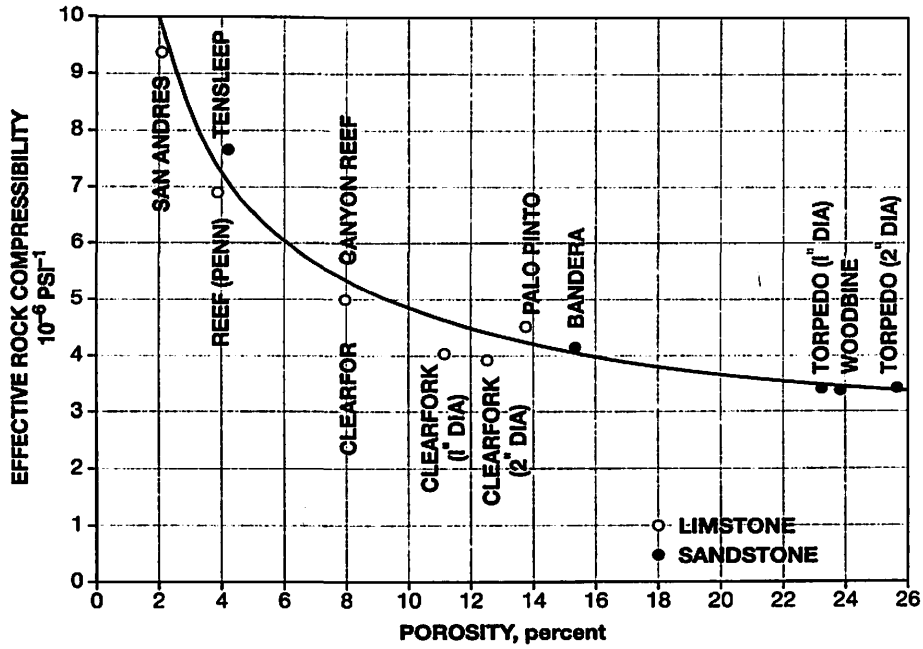

Figure 1.10 Effective formation (rock) compressibility. From Hall, Trans, AIME (1953) 198.

Eq. (1.9) is used in reservoir simulators to update the porosity value when a pressure change occurs and when the pore compressibility is assumed constant. The assumption is valid for most reservoir engineering applications.

Order of magnitude: 3 to 10 10^{-6} psi^{-1} or 4.35 to 14.5 10^{-5} bar^{-1}

1.3.10.4 Engineering applications

A. Compressibility for Transient Flow (Build-Up)

In an under saturated reservoir the total compressibility involved includes: oil, connate water and porous media:

under saturated reservoir: $$c_t = c_o S_o + c_w S_w + c_p \tag{1.10}$$

saturated reservoir: $$c_t = c_o S_o + c_w S_w + c_g S_g + c_p \tag{1.11}$$

B. Compressibility used in Material Balance Calculation

The change of effective volume $c_{ef}V_p$ is equal to the expansion of oil, water and gas plus the reduction of the pore volume resulting from the reservoir pressure decline.

$$c_{ef}V_p = c_o S_o V_p + c_w S_w V_p + c_p V_p$$

Therefore $$c_{ef} = c_o S_o + c_w S_w + c_p \quad (1.12)$$

c_{ef}: effective compressibility

The system made of oil, connate water and formation is replaced by a unique material: oil having an equivalent compressibility c_e.

$$c_e = \frac{c_o S_o + c_w S_w + c_p}{S_o} \quad (1.13)$$

C. Compressibility of an Aquifer

For material balance calculation the total compressibility involved is *(water + porous media)*:

$$c_e V_p = c_w S_w V_p + c_p V_p \qquad \text{with } S_w = 1$$

$$c_t = c_w + c_p \quad (1.14)$$

D. Compaction

In most reservoirs, the pore compressibility is small and can be assumed constant during the depletion.

In some cases, the pore compressibility may start off as small at initial conditions but increases to large values as pressure depletion continues. The voidage created by the fluid production may create a significant collapse (compaction) in the pore volume which is reflected in an increase of the pore compressibility. The logical consequence of such behavior is a decrease of the absolute permeability and therefore a well productivity index drop.

This behavior has been observed and well described in the case of a heavy oil reservoir the Bachaquero Field in Venezuela [23].

The other consequence that has been observed is subsidence at surface or at sea bottom (Ekofisk Field) taking place [24].

The phenomenon occurs generally in reservoirs with high porosity, high permeability and in shallow unconsolidated reservoirs.

1.3.11 Mercury Injection Porosimetry

An analytical technique useful for determining distribution of pore-throat sizes, and thus understanding the structures of pore systems in the reservoir, is capillary pressure analysis. Porous media consists of pores and smaller channels (pore throats) connecting the pores. Pore throats, in conjunction with pore-system geometry and topology, control the movement of fluids. Through the use of capillary pressure curves derived from mercury-injection porosimetry, it is possible to calculate pore-throat size and distribution.

Mercury-injection porosimetry is based on the measurement of the volume distribution of pore throats; the method is based on forcing mercury into small voids, pore throats, within

the rock sample which has been previously evacuated. This process is known as primary drainage (the "wetting" phase is the vacuum). Recording mercury pressures and saturations allows generation of a capillary pressure-saturation curve. Pore throats control access to larger voids (pores) then greater pressures are required to force mercury, or other non wetting fluids, into smaller spaces (Purcell, 1949) [25]. Thus, pore throats are bottlenecks in the system. It is necessary to exceed their critical capillary pressure in order to inject mercury into pores. By injecting mercury at incrementally higher pressures, and allowing time for equilibration between pressure increments, mercury is injected into increasingly smaller pores. It is then possible to calculate the size distribution of pore throats, to determine how pore-throat size is affected by increasing confining stress to approximate reservoir conditions, and to determine how permeability is affected by reduction in pore-throat size.

Injection systems are designed for injection pressures up to 15,000 psi which enable pore entry radius measurements to below 0.01 microns. The process includes software that calculates pore entry radius, converts pressure data to equivalent air/brine, air/oil, and oil/brine systems, and displays the data in tabular form and graphical formats that can be used to correlate the mercury injected data to reservoir capillary pressure characteristics. The measured data is presented in cumulative and incremental tabular form with graphical representations of mercury saturation versus pressure, equivalent system saturation versus pressure, and pore size distribution versus percent pore space in cumulative and incremental (Histogram) formats. A J-Function calculation for correlation of capillary pressure data across several systems is also performed.

Laboratory Measurements

A sample is located into the measuring chamber and vacuum is imposed upon the system. The mercury level is then brought up until the sample is covered. The chamber pressure is raised in an incremental fashion, injecting mercury into the sample. This volumetric data is corrected for system variations to obtain injected volumes. Data is measured from vacuum through the threshold pressure of the sample and on to 15 000 psi. The core holders are located in a temperature controlled ventilated chamber for minimizing operator exposure to mercury vapors.

Laboratory results are depicted in Figure 1.11.

1.3.12 Electrical Properties of Fluid-Saturated Rocks

1.3.12.1 Generalities

The relationship between the electrical properties of a reservoir rock and its interconnected porosity has always been fundamental to quantitative formation evaluation in the petroleum industry. The relationship provides a vital means of estimating water-zone porosity from a downhole measurement of an electrical parameter. This is the basic principle of open hole electric logging.

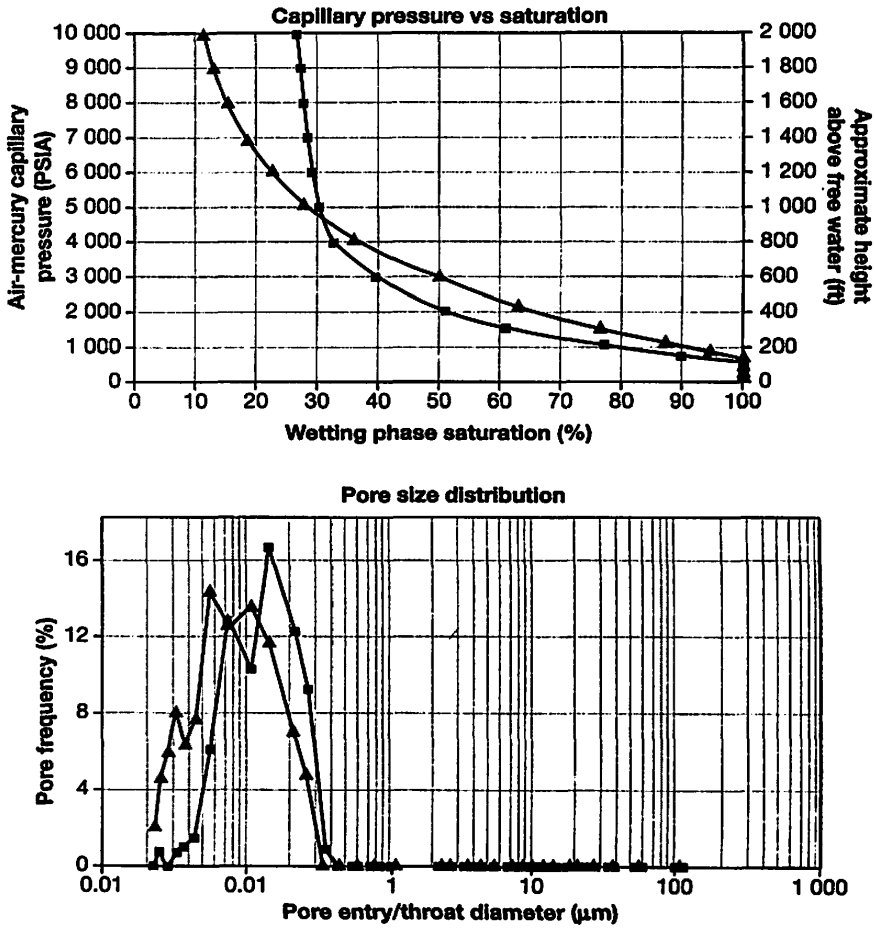

Figure 1.11 Example of capillary pressure and pore throat size distribution.

Porous rocks are made of an aggregate of minerals, rock fragments, and void space. The solids, with the exception of certain clays are non conductors. The electrical properties of a rock depend on the geometry of the voids and the fluids with which those are filled: oil, gas and water. Oil and gas are non conductors. Water is a conductor when it contains dissolved salts. Current is conducted in water by movement of ions and can therefore be termed electrolytic conduction.

The resistivity of a material is the reciprocal of conductivity and is commonly used to define the ability of a material to conduct current.

The resistivity of a material is defined by the following equation:

$$\rho = \frac{rA}{L}$$

ρ: resistivity
r: resistance
A: cross-sectional area of the conductor
L: conductor length

For electrolytes, ρ is reported in ohm-centimeters, r in ohms, A in cm^2, and L in centimetres. In oil field industry, the ohm-meters is used and symbolized by R.

1.3.12.2 Formation Factor or Electrical-resistivity Factor of rocks

It has been established experimentally that the resistivity of a clean formation (no clay content) is proportional to the resistivity of the brine with which it is fully saturated. The constant of proportionality is called formation resistivity factor, F.

The resistivity factor F provides a useful and convenient evaluation of the nature of the pore structure of reservoir rocks. This factor was defined by Archie as the ratio of the electrical resistance R_0 of a sample saturated with a conductive brine to the resistance R_w of a volume of the same brine having the same size and shape as the over-all dimensions of the sample.

$$F = \frac{R_0}{R_w} \tag{1.15}$$

Since the flow of electricity is analogous to the flow of fluid of zero viscosity, pore diameters are not a factor, as, for example, Poiseuille's law for viscous flow. The resistivity factor depends only on the pore length, porosity and not on permeability. F depends upon the available cross-sectional void area of the sample and the increased distance due to the irregular path (tortuosity). For a given porosity, the ratio R_0/R_w remains nearly constant for all values of R_w below about 1 Ω-m.

1.3.12.3 Resistivity Index

If the porous rock sample contains both water and hydrocarbons, the water is still the only conductor. The cross-sectional area available for conduction is reduced and the path length changed.

The second fundamental notion of porous rock electrical properties is that of the resistivity index defined as:

$$I = \frac{R_t}{R_0}$$

R_t: true resistivity of the sample partially saturated with water
R_0: resistivity of the 100% water saturated sample

Archie, in 1942, [26] correlated observed formation factors with porosity and permeability. He concluded that the correlation with porosity was the best and the formation factor could be expressed:

$$F = \frac{a}{\phi^m} \tag{1.16}$$

Φ: porosity
m: cementation factor
a: constant empirically determined

Satisfactory results are obtained with:

$a = 0.81$ in sands and $a = 1$ in compacted formations

Humble proposed $a = 0.62$ and $m = 2.15$ which are used in the Schlumberger charts. The Humble formula is satisfactory for sucrosic rocks. Better results are obtained by using $a = 1$ and m = 2 in chalky rocks.

$a = 1$, $m = 2.2$ to 2.5 in compact or oolicastic rocks.

m may be as high as 3 in some oolicastic rocks.

1.3.12.4 Water Saturation

The formation resistivity [27] is very affected by the presence of hydrocarbon. As a result of numerous observations, for clean formations, Archie expressed water saturation with the empirical relationship:

$$S_w^n = \frac{FR_w}{R_t} \tag{1.17}$$

R_t: true resistivity
R_w: water resistivity
F: formation factor
S_w: water saturation
n: saturation exponent generally = 2

FR_w is equal to R_0: resistivity of the formation when 100% saturated with water of resistivity R_w.

The equation may be written:

$$S_w = \sqrt{\frac{FR_w}{R_t}} \quad \text{or} \quad S_w = \sqrt{\frac{R_0}{R_t}} \tag{1.18}$$

The formula is good in clean formations having a fairly regular distribution of the porosity (inter granular or inter crystalline porosity). In formations with fractures or vugs, the formula can still be used, but the accuracy is not as good.

1.3.12.5 Laboratory Techniques

A good knowledge of the formation electrical properties is necessary for electrical log interpretation to derive water saturation and then initial hydrocarbon in place quantities.

Evaluation of the cementation factor "m"

The resistance of the saturated water sample is measured.

Then R_0 is deducted from: $R_0 = R\frac{S}{L}$ $F = \frac{a}{\phi^m}$

R_0: sample resistivity (ohm-m)
R: sample resistance (ohm)
S: section area (m^2)
L: sample length (m)

Measurements of a and m consists of measuring the formation factor on many samples from the same rock type and draw a straight line through the points according to the equation:

$$F = \frac{a}{\phi^m} \qquad \log(F) = -m\log(\Phi) + \log(a) \tag{1.19}$$

Assuming $a = 1$

$$\frac{1}{\phi^m} = \frac{R_0}{R_w} \quad \text{so} \quad m = -\frac{\log(R_0 / R_w)}{\log\phi}$$

Measurements are carried out on a large number of samples at laboratory conditions. The cementation factor is deducted from the plot illustrating Eq. (1.19).

Usually the electrical properties and porous plate capillary pressure test are combined in the same experiment. The objective is to determine the formation and cementation factor of the sample at different water saturations simultaneous with capillary pressure.

Some authors carried out measurements at reservoir conditions [28].

1.4 ROCK RADIOACTIVITY

1.4.1 Natural Radioactivity

Gamma rays are high energy electromagnetic waves emitted by the nuclei of atoms. A nucleus emits gamma rays when it is naturally unstable. When an atom of matter is disturbed in some way, usually by an external force, it oscillates, gives off the unwanted energy as a gamma ray, and returns to its former stable state. A burst of gamma radiation is sometimes called a photon.

Gamma ray energies are expressed in units of "million electron-volts". Most energies lie in the range from 0.1 to 10 Mev. X-rays are also electromagnetic waves, but usually have lower energies than the gamma rays emitted by atomic nuclei.

The radioactive elements which produce natural gamma rays are inherently unstable, and their atoms have been gradually undergoing spontaneous transformation into different atoms since the formation of the earth billions (10^9) of years ago. Each of these elements has a characteristic "half life", which is the time required for half of the original atoms to undergo transformation (Table 1.3).

Table 1.3 Half-life of some elements

Element	**Half-life** (billions of years)
Uranium-238	4.5
Thorium-232	14
Potassium-40	1.4

Since the age of the earth is about 4 billions years, only half of the uranium which originally existed is left. Most of the thorium still remains, but only about 10% of the original potassium-40.

When a uranium or thorium atom spontaneously transforms into a new atom, the latter is also unstable and sooner or later transforms to another atom. This process continues through about a dozen stages until a stable atom is reached. During this series of transformations a number of gamma rays with different energies are emitted. Consequently one can say only that the average energy of the gamma rays for uranium is about 1 Mev. The same is true for the thorium. However potassium transforms directly to a stable atom so that it emits gamma rays of only a single energy, 1.5 Mev.

1.4.2 Radioactivity Units

For many years geologists expressed radioactivity in μg equivalent of Radium. Radium is one of the intermediate elements in the step by step disintegration of uranium; consequently, there is a fixed uranium/radium ratio, $3 \times 10^6/1$, in the earth. Thus common shale may have a radium equivalent of 0.0007×10^{-6} % can be expressed as 7 micrograms radium-equivalent per metric ton of formation [29].

Usually radioactivity is expressed in API units (American Petroleum Institute). The conversion between old units and API units is:

1 μg = 16.5 API for GNT-F or G and 11.7 API for GNT-J or K

GNT-F,G, GNT-J, K are specific Schlumberger tools measuring natural formation radioactivity and induced radioactivity.

1.4.3 Use of Rock Natural Radioactivity Measurements

The down-hole Gamma-ray log is a measurement of the natural radioactivity of the formations. In sedimentary formations, the log reflects the shale content of the formations since radioactive elements tend to concentrate in clays and shales. Clean formations usually have a very low level of radioactivity, unless radioactive contaminant such as volcanic ash or granite wash is present or the formation waters contain dissolved radioactive salts.

The Gamma ray log can be recorded also in cased hole which is used as a correlation curve in completion and workover operations.

At laboratory, a gamma ray survey performed on the cores is used to adjust the true core depth with the down-hole gamma ray survey curve.

1.4.4 Natural Gamma Ray Spectrometry [30]

As seen before, the gamma-ray survey records the global natural radioactivity of the formations. The radioactivity is due to three main elements (K^{40}, Th^{232} and U^{238}) or to their daughter isotopes which emit at different energy levels.

By examining the emitted energy spectrum it appears that the energy level of the gamma radiation is a characteristic of the emitting element.

Potassium 40 decays directly to stable argon 40 with the emission of a 1.46 Mev gamma ray. However, uranium 238 and thorium 232 decay sequentially through a long sequence of various daughter isotopes before arriving at stable lead isotopes. As a result, gamma rays of many different energies and fairly complex energy spectra are obtained. It is assumed that formations are in equilibrium; that is, the daughter isotopes decay at the same rate as they are produced from the parent isotope. In other words it can be admitted that the relative proportions of parent and daughter elements in a particular series remain fairly constant. Consequently by measuring the gamma ray population in a particular part of the spectrum, it is possible to infer the population at any other point.

Once the parent isotope population is known, the amount of non radioactive isotope can also be found. The ratio of potassium 40 to total potassium is very stable and constant on the earth while, apart from thorium 232, the thorium isotopes are very rare and so can be neglected.

Applications:

Electric logging companies have developed tools to measure the amounts (concentrations) of potassium, thorium, and uranium in the formation. Thorium and uranium concentrations are presented in parts per million (ppm) and potassium concentration in percent.

The NGS log (Natural Gamma Spectrum, Schlumberger log) is used to detect, identify, and evaluate radioactive minerals. It can be used also to identify clay type and calculate clay volumes. This, in turn, can provide information on the source, the depositional environment,

the diagenetic history, and the petrophysical characteristics (surface area, pore structure) of the rock.

The thorium and potassium response or the thorium only response of the NGS log is often a better shale indicator than the simple GR log or other shale indicator.

As usual it is recommended to combine other measurements such as photoelectric absorption, density, neutron, sonic to evaluate the volumetric mineral analysis of complex lithologies.

The NGS tool uses five-window spectroscopy to resolve total gamma ray spectra into the three most common components of naturally occurring radiation-potassium, thorium and uranium.

In addition to the potassium, thorium and uranium curves, the standard gamma ray and the gamma ray minus the uranium component are presented. The computed gamma ray or the thorium curve can be used in evaluating clay content where radioactive minerals are present.

1.4.5 Formation Response to High Energy Neutron Bombardment

The neutron log was first described by Pontecorvo in 1941 [29]. It was used principally in association with the natural gamma ray for delineation of porous formations. After about 1949, attention was given to the neutron log as a porosity indicator.

Neutrons are electrically neutral particles, each having a mass almost identical to the mass of a hydrogen atom.

The neutrons primarily interact with formation nuclei Figure 1.12 in three ways [31]:

1) *Elastic-scattering*: the neutron bounces off the bombarded nucleus without exiting or destabilizing it. With each elastic interaction, the neutron looses energy. Hydrogen, with the mass of its nucleus equal to that of a neutron, is very good at slowing down neutrons. Hence, how efficiently a formation slows down neutrons generally indicates the abundance of hydrogen. Because hydrogen is most abundant in pore fluids, neutron slowdown indicates porosity.
2) *Inelastic neutron scattering*: the neutron bounces off the nucleus, but excites it into quickly giving off what is called inelastic gamma rays. The measurement of emitted gamma ray energies from inelastic neutron scattering yields the relative concentrations of carbon and oxygen, which are then used to calculate water saturation. This is the induced gamma spectrometry survey.
3) *Neutron absorption*: the nucleus absorbs the neutron and becomes exited, typically emitting capture gamma rays. Neutron absorption, or neutron capture, is most common after a neutron has been slowed by elastic and inelastic interactions to thermal energies of about 0.025 ev. This is the diffusion phase. The measurement of capture gamma ray energies is used to estimate the abundances of elements most likely to capture a neutron-silicon, calcium, chlorine, hydrogen, sulphur, iron, titanium and gadolinium.

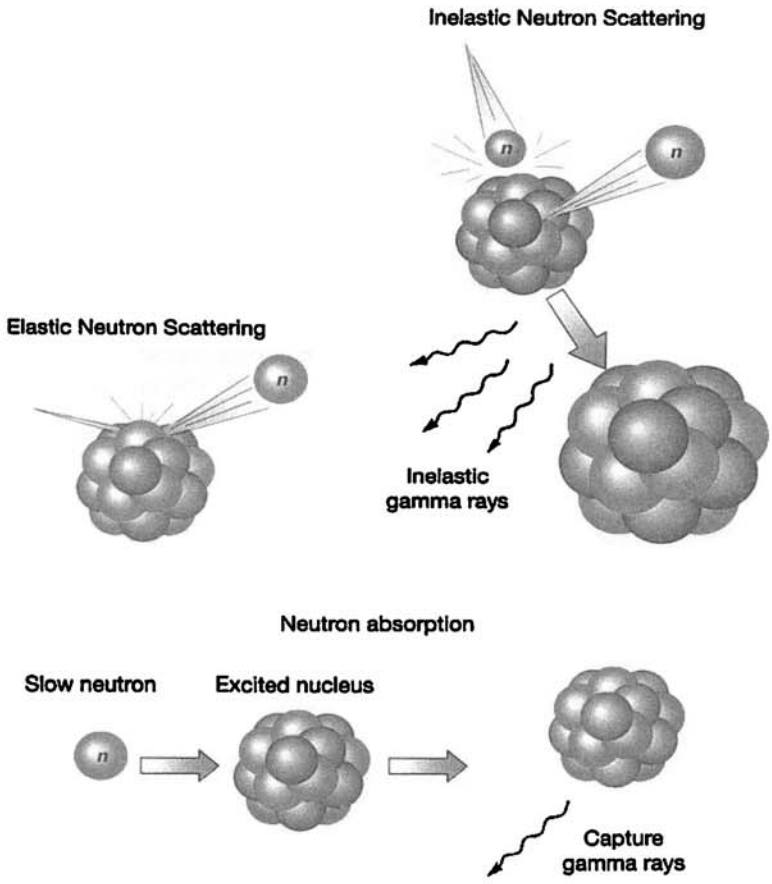

Figure 1.12 Neutron collisions with nucleus.

The collision probability of a neutron with an element is a function of the nucleus concentration of this element per unit of volume and the nuclear cross-section offered. The dimension of this last parameter being a surface, characterizes the target size of the element offered to the neutron. Finally, the cross-section Σ is dependent on the element and also on the neutron energy.

For example the cross-section of a hydrogen nuclei is practically nil for high energy neutrons (>1 Mev). A fast neutron mainly slowed down by hydrogen atoms reaches an energy level called epithermal (0.1 < energy < 100 ev), then to a low energy level called thermal (0.025 ev).

Table 1.4 gives the capture and scatter cross sections [32] of individual nuclei of several common earth elements. Hydrogen is the most important scattering, or slowing-down

Table 1.4 Cross section of elements

Cross section in barns(10^{-24} cm^2/atom) (average values for slow neutron)		
Element	**Capture**	**Scatter**
Chlorine	33.2	10.0
Hydrogen	0.33	20.0
Oxygen	0.0002	4.1
Sodium	0.50	3.5
Silicon	0.16	1.7
Calcium	0.44	9.5
Magnesium	0.40	3.6
Carbon	0.0034	4.8
Boron	755.0	3.0

element, while chlorine is the most important capturing component among those commonly encountered. Note the high capture cross-section value for boron which is used as a moderator in nuclear reactors. Figure 1.13 illustrates the energy history of a neutron.

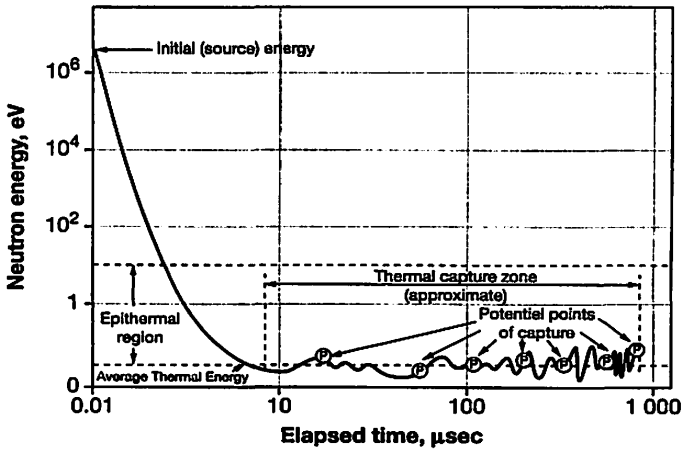

Figure 1.13 Energy history of an average neutron.

Starting from formation fluid filled rocks response to fast neutron exposure, scientists developed different tools and interpretation techniques to investigate and evaluate formation lithology, formation porosity and fluid content.

In the following section, a brief description of the tool principles is presented; technological details and interpretations are found in specialized documents on radioactive logging.

GNT series (Gamma Neutron Tool):

High energy (fast) neutrons are continuously emitted from a radioactive source which is mounted in the sonde. Neutrons strike fluid and matrix nucleus. The greatest neutron energy loss occurs when the neutron strikes hydrogen nucleus due to its equivalent mass with the neutron. Therefore the slowing down of neutrons depends on the concentration of hydrogen atoms encountered. Reaching an energy level of 0.025 electron volts, the neutron diffuses through the formation until it is captured by nuclei such as chlorine, hydrogen, silicon, etc. The exited capturing nuclei emit a high energy capture gamma ray. These gamma rays are counted by a detector located in the sonde.

If the hydrogen concentration is large, most of the neutrons are slowed down and captured within a short distance of the source. On the contrary, if the hydrogen concentration is small, the neutrons travel farther from the source before being captured. Consequently, the counting rate at the detector increases for low hydrogen concentration (with the commonly used source detector spacing) and vice versa.

The GNT tool is sensitive to both high energy capture gamma rays and thermal neutrons. In addition the measurement is greatly affected by bore hole fluid effect.

In the 1960's, a new tool was developed called SNP (Sidewall Neutron Porosity). To decrease the bore hole effect, the source and the detector are mounted on a pad; the pad is applied against the bore hole during the survey. The detector is shielded so that only epithermal neutrons (energy > 0.4 ev) can be counted.

In the late 1960's, the CNL (Compensated Neutron Log) was operational in the field. The CNL is a dual spacing thermal-neutron detection instrument which is also applied against the bore hole during survey.

As explained above, the neutron log is very sensitive to the hydrogen concentration in the pore media. Consequently for a given porosity, the neutron log will show a lower porosity if the formation is gas filled than if it is oil or water filled. For this reason, neutron log is the gas filled formation detector.

GNT, SNP and CNL are trademarks of Schlumberger.

1.5 SEM (SCANNING ELECTRON MICROSCOPE)

1.5.1 Introduction

The Scanning Electron Microscope (SEM) is a microscope that uses electrons rather than light to form an image. There are many advantages to using the SEM instead of a light microscope including, a large depth of field, which allows a large amount of the sample to be in focus at one time, and also the ability to obtain images of high resolution, which means

that closely spaced features can be examined at a high magnification. Preparation of the samples is relatively easy since most SEMs only require the sample to be conductive. Non-conductive samples can be coated using a sputter coater to deposit a thin layer of silver, gold or other conducting material. The combination of higher magnification, larger depth of focus, greater resolution, and ease of sample observation makes the SEM one of the most heavily used instruments in research areas today.

1.5.2 Theory

In light microscopy, a specimen is viewed through a series of lenses that magnify the visible-light image. However, the scanning electron microscope (SEM) does not actually view a true image of the specimen, but rather produces an electronic map of the specimen that is displayed on a cathode ray tube (CRT).

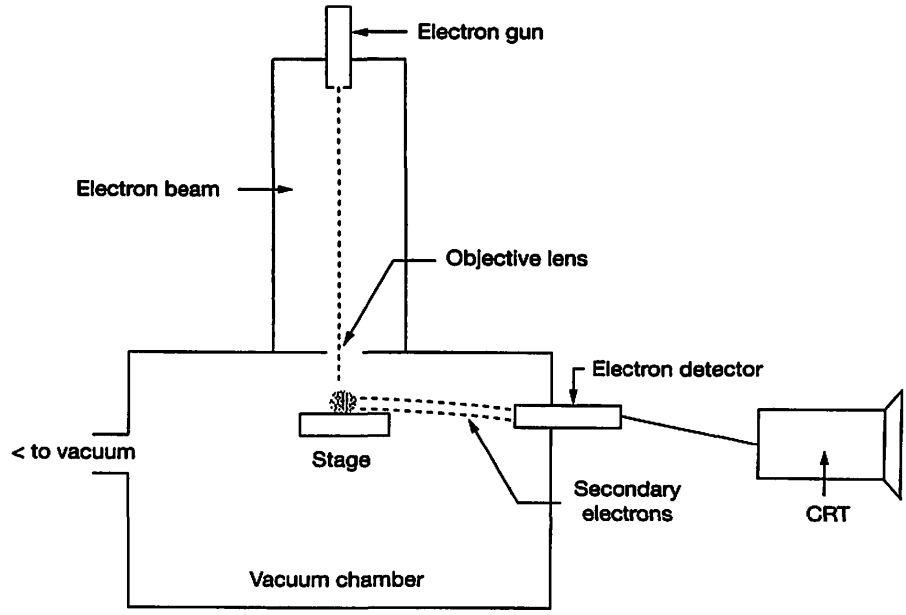

Figure 1.14 Scanning Electron Microscope Principle.

Figure 1.14 shows a schematic for a generic SEM. Electrons from a filament in an electron gun are beamed at the specimen in a vacuum chamber. The beam forms a line that continuously sweeps across the specimen at high speed. This beam irradiates the specimen which in turn produces a signal in the form of either x-ray fluorescence, secondary or backscattered electrons. The SEM has a secondary electron detector. The signal produced by

the secondary electrons is detected and sent to a CRT image. The scan rate for the electron beam can be increased so that a virtual 3-D image of the specimen can be viewed. The image can also be captured by standard photography. By changing the width (w) of the electron beam, the magnification (M) can be changed.

1.5.3 Secondary Electron Images – High Resolution Topographic Imaging

Secondary electrons are low energy electrons ejected from the sample as a result of inelastic collisions with beam electrons. They are produced near the surface of the sample, from a small area around the beam tip. The resolution of the image is therefore very good because the beam is only a few nanometers in diameter.

Backscattered Electron Images – Qualitative Compositional Information:

Backscattered electrons (BSE) are primary electrons emitted as a result of elastic collisions with specimen electrons. BSE emission intensity is a function of the specimen's atomic number; i.e., the higher the atomic number (e.g., Fe (26) vs. Mg (12)), the brighter the signal. BSE images are obtained in exactly the same way as Secondary Electron Images.

X-Ray Microanalysis – Quantitative Compositional Information:

When the beam interacts with the sample, energy is released in the form of radiation over a variety of wavelengths. This energy results from beam electrons ionizing the inner electron shells of an atom. When the excited atom relaxes, i.e., an outer electron filling the inner shell, radiation is released which is characteristic of the atom's electron shells' energy levels. The portion of radiation in the X-Ray part of the spectrum is referred to as Characteristic X-rays. The X-rays generated are collected and plotted as a spectrum. Each peak on the spectrum represents a transition with a characteristic energy – every element has its own "fingerprint" of peaks so we can deduce which elements are present. It is possible to calculate absolute concentrations of individual elements by comparing spectra with others collected from samples of known composition. Not all X-rays are characteristic of the elements present in the specimen – many belong to the background continuum (*Bremstralung*) generated as the beam electrons slow down when they hit the sample.

X-Ray Maps – Areal Compositional Data:

Maps of relative concentration for multiple elements can be generated using the SEM. The electron beam is scanned across the sample, stopping at regular intervals to count the number of X-rays within a predefined energy window arriving at the detector. For example, X-rays which fall in the window (1.64-1.84) may be used to map Silicon (SiKa – 1.74). The number of counts at each stop (pixel) can then be displayed as a map. By maximizing the number of points at which X-rays are counted, and by scanning the beam many times over the sample, high resolution maps can be produced which pick out concentration differences not detectable using backscattered electron images.

Element Maps:

Several maps showing the concentration of various elements in each thin section are available. Element maps are obtained by examining the intensity of the characteristic X-ray emissions of an element. X-rays are produced while the sample is bombarded with electrons. To form the image, the electron beam is moved across the sample. Emitted X-rays are collected and the data are organized into a map. The brightest areas indicate the highest concentrations of the element, while the darkest areas indicate the lowest concentrations. This technique is useful for determining the minerals present as well as their compositions.

SEM is commonly used by geologists, petrophysics to study the sedimentary process of the reservoir rock, to describe the porosity system, to evaluate the mineralogy and a description of the rock lithology (Fig. 1.15).

The images created without light waves are rendered black and white.

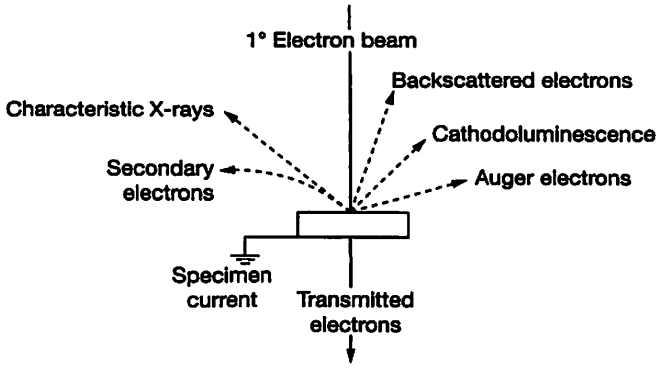

Figure 1.15 Electron/specimen Interactions. When the electron beam strikes the sample, both photon and electron signals are emitted.

1.6 RESERVOIR APPLICATIONS

1.6.1 Porosity Permeability Relationship

The early development of well logging techniques consisted in the determination of parameters like porosity and water saturation deducted from radioactive, sonic and electrical measurements. These parameters are fundamental for the geologist to evaluate the initial hydrocarbon volumes in place. To evaluate the ability of the hydrocarbon to flow through the porous media, the key parameter is permeability.

Absolute permeability is measured on core plugs of small dimensions (a few centimeters) in the laboratory. The other way to assess permeability is through the drill stem

testing (DST) technique where the engineer can deduct $k_e \times h/\mu$ from the interpretation of the build-up period.

k_e: effective permeability of the moving fluid (k_o, or k_g, or k_w)
h: total reservoir thickness contributing to the production and build-up
μ: viscosity of the fluid in movement

Laboratory measurements involve only on a very small rock volume. DST results involving a larger formation volume around the well are dependent on the acting reservoir thickness.

It may be difficult to estimate the true thickness, which brings large errors on the permeability estimation.

Well logging is not able to measure directly formation permeability.

Practically, all the wells are submitted to well logging surveys, with a minimum logging programme. On the other hand, any new well is not submitted to coring. The result of the situation is that for each well crossing a porous interval, the formation porosity is deducted but the permeability is usually unknown.

Intuitively, one can admit that the more porous a rock is, better the permeability will be. This is true and verified when we deal with the same sort of rock (lithology, texture, tortuosity). In many consolidated sandstone and carbonate formations, plots of core data show that the logarithm of permeability (k) is often linearly proportional to porosity (φ). The slope, intercept, and the degree of scatter of these log(k) versus φ trends vary from formation to formation, and these variations are attributed to differences in grain size and sorting, diagenetic history, and compaction history. In unconsolidated sands, better sorting systematically increases both permeability and porosity. In sands and sandstones, an increase in gravel and coarse grain size content causes k to increase even while decreasing φ. Diagenetic minerals in the pore space of sandstones, such as cement and some clay types, tend to decrease log(k) proportionately as φ decreases.

1.6.2 Permeability Prediction [15]

Many investigators worked on the subject:

"How to predict the formation permeability from the known porosity?"

Predictive models were based from various rock and pore parameters. They include

- Grain size and sorting.
- Measures of pore surface area.
- Statistical and data base approaches that incorporate well log measurements.

In addition, laboratory studies show that nuclear magnetic resonance, gas adsorption, cation exchange capacity measured in the laboratory can be correlated with permeability.

Predictive equations use wells where both core and well logs are available. The equations are then applied in wells where well logs are available but core data are not.

A last class of physical models is based on pore throat dimension as measured by mercury injection technique.

1.6.2.1 Wyllie and Rose's model [33, 34]

Wyllie and Rose proposed an empirical relation for sands as:

$$k = \left(\frac{C\phi^3}{S_{wi}} \right)^2 \tag{1.20}$$

$C = 250$ for medium gravity oils and 79 for dry gas.

φ: porosity (fractional decimal)
S_{wi}: water saturation (fractional decimal)

1.6.2.2 Timur's Model

Timur (1968) [35] used a data base of 155 sandstones samples from three oil fields (Gulf Coast field, Colorado Field, California Field). The sandstones exhibit varying degrees of sorting, consolidation, and porosity ranges. S_{wi} was measured using a centrifuge. The following empirical equation was proposed:

$$k = \frac{a \times \phi^b}{S_{wi}^2} \qquad k\text{: absolute permeability (mD)} \tag{1.21}$$

a = 0.136 S_{wi}: irreducible water saturation (percent)
b = 4.4 φ: porosity (percent)

A modification of the previous equation discussed by Schlumberger (1988) and Ahmed *et al.* (1989) proposed:

$$k = \left[\frac{100\phi_e^2 (1 - S_{wi})}{S_{wi}} \right]^2 \tag{1.22}$$

φ_e: effective porosity (fraction decimal)
S_{wi}: irreducible water saturation (fraction decimal)

For example permeability of oil bearing sand with 0.2 porosity and 0.25 water saturation:

Wyllie and Rose: 64 mD Timur: 10 mD Ahmed: 144 mD

Remark:
It has been observed in the Rotliegend sandstone (North Sea), the presence of fibrous illite (clay mineral) within the pore space. The result is a reduction of permeability one or two orders of magnitude compared with rocks in which clay occurs as grain coating. Special core preparation techniques are required to preserve the fibrous illite so the laboratory measurements reflect the in-situ permeability value. (Heaviside et al., 1983).
Clay minerals are very important in petroleum geology and engineering. Some points to consider are:

- *Kaolinite is a chemically stable clay, but can migrate during production to clog pores.*
- *Illite and mixed layer illite/smectite are water-sensitive clays. (contains water molecules layers).*

- *Chlorite contains high amounts of iron and magnesium and is usually very sensitive to HCl acid producing a gelatinous ferric iron that can plug pores.*
- *Smectite (montmorillonite) clay mineral group is highly water sensitive.*

1.6.2.3 Regression model

The simplest regression model takes porosity to be the single independent variable [36].

$$\log(k) = a + b\,\varphi \tag{1.24}$$

When a straight line relationship between $\log(k)$ and φ exists, the computation of a predictor is straight forward.

Plotting φ, vs $\log(k)$ may lead to a cloud of points through which no straight line correlation can be envisaged. This case requires a detailed 'rock typing' study in order to create different families of rock types.

Prediction of permeability in formations with small grain size and an abundance of clay minerals is difficult. Such rocks are called "tight sands".

1.6.3 Hydraulic Flow Units [37]

The relationship between permeability and porosity is not causal. Whereas porosity is generally independent of grain size, permeability is strongly dependent on grain size. In the same reservoir, there may be both high and low permeability with equal porosity values. The different porosity/permeability relationships conduct to the existence of different hydraulic units.

Methodology:

The generalized form of the Kozeny-Carmen relationship is given by:

$$k = \frac{\phi_e^3}{(1-\phi_e)^2}\,\frac{1}{F_s\tau^2 S_{gv}^2} \tag{1.25}$$

k: permeability in μm^2
φ_e: effective porosity (fraction)
F_s: Shape factor = 2 for a circular cylinder
$F_s\tau^2$: Kozeny constant can vary from 5 to 100

Dividing both sides of Eq. (1.25) by φ_e:

$$\sqrt{\frac{k}{\phi_e}} = \frac{\phi_e}{1-\phi_e}\left[\frac{1}{\sqrt{F_s}\;\tau\, S_{gv}}\right] \tag{1.26}$$

When the permability is expressed in mD, the following parameter is defined:

$$\text{Reservoir Quality Index} = \text{RQI}\ (\mu\text{m}) = 0.0314\sqrt{\frac{k}{\phi_e}} \tag{1.27}$$

Defining the pore volume to grain volume ratio φ_Z:

$$\phi_Z = \frac{\phi_e}{1-\phi_e} \tag{1.28}$$

The Flow Zone Indicator is designed as FZI (μm):

$$FZI = \frac{1}{\sqrt{F_s}\ \tau\ S_{gv}} = \frac{RQI}{\phi_Z} \tag{1.29}$$

Substituting Eq. (1.28) and Eq. (1.29) into Eq. (1.25) we obtain:

$$\log RQI = \log \varphi_Z + \log FZI$$

On a log-log plot of RQI versus φ_Z, all samples with similar FZI values will lie on a straight line with unit slope. Samples with different FZI values will lie on other parallel lines. Samples that lie on the same straight line have similar pore throat attributes and, thereby constitute a hydraulic unit.

The method based on petrophysical properties, pore throat geometrical attributes can be used in geological model to define "hydraulic flow units" crossing eventually different rock types. The applications are:

- Improve the definition of the geological model.
- Improve prediction of permeability and permeability distributions from wire line logs in partially cored/uncored intervals and adjacent wells.
- Improve well to well rock properties correlations.

1.6.4 Rock Typing Methodology

Geological observations, based on cores, logs, thin sections, and interpreted data in terms of facies, depositional environments and sequences, are gathered from qualitative or semi-quantitative data. Measurements, based on core analysis and logs, such as porosity, permeability, saturations, (CCA, *Conventional Core Analysis*, SCAL, *Special Core Analysis*) are quantitative data.

Rock typing approach integrates all data from all sources in order to define families of rock properties to better model the reservoir and therefore populate the geological model with reliable data.

CHAPTER 2

Reservoir Fluid Properties

2.1 INTRODUCTION

An accurate description of reservoir rock, fluid contents, rock fluid systems, fluid distribution and flow performance are required to provide sound basis for reservoir engineering studies, to answer the following questions:

- Presence of hydrocarbon
- Quantity in place and reserves
- What is the optimum development strategy?

An integrated data gathering programme is necessary: it is designed in advance to make sure that all required data is obtained.

The interpretation of the collected data for reliability and proper use should include comparison between all sources. Good reservoir engineering judgment is necessary to differentiate and select the best representative data.

Fluid samples taken to a laboratory provide the only way to study volumetric behavior and chemical properties of formation fluids.

Objective of a PVT study is to determine the physical and chemical fluid characteristics to predict its behavior versus pressure and temperature changes.

A PVT study is used by the geologist and reservoir engineer to:

- Evaluate the hydrocarbon in place at surface conditions.
- Simulate the reservoir fluid behavior during all production processes.
- Build a production profile associated with a development plan.

For the process engineer to:

- Build a surface facility project.
- Optimization of surface separators.
- Predict by simulation a gas plant performance.
- Predict transportation performances.

2.2 GENERALITIES

Producing hydrocarbon from a field creates pressure disturbance in the reservoir therefore the hydrocarbon is submitted to pressure changes then to volume changes. Most of the time, it can be assumed that the reservoir temperature is constant over the whole reservoir thickness. Fluid flow taking place from the reservoir into the well up to surface is submitted to depletion and temperature decrease.

In order to control and forecast production performance, it is necessary to investigate the hydrocarbon behavior as early as possible in the production life of the field. It is recommended to test, to collect a hydrocarbon sample as soon a hydrocarbon filled bed has been detected.

The types of hydrocarbon systems encountered in oil field operations range from almost pure methane gas to heavy bituminous material having the nature of road tar or asphalt.

2.2.1 Components Encountered in Reservoir Fluids

Inert gases	Nitrogen (N_2)	
	Helium (He)	
	Argon (Ar)	
Acid gases	Hydrogen Sulfide (H_2S)	
	Carbon Dioxide (CO_2)	
Pure Hydrocarbons	Methane (C_1)	Light ends
	Ethane (C_2)	
	Propane (C_3)	
	i-Butane (*i*-C_4)	
	n-Butane (*n*-C_4)	
	i-Pentane (*i*-C_5)	Heavy ends
	n-Pentane (*n*-C_5)	
	Cyclopentane	
	Hexanes, benzene and heavier (C_{6+})	
Organic Compounds	Hydrocarbons with oxygen, nitrogen, sulphur	
Sulphur Compounds	Mercaptans (R-S-H)	
	Sulfides	
	Disulfides	
	Thio-compounds	
Inorganic Compounds	Hydrocarbons with metal (Nickel, Vanadium, Potassium, Copper, Zinc, Iron)	
	Arsenic compounds (Arsenes)	
Mercury		
Naturally Occurring Radioactive Material		
	Radon, Radium	

Solids	Mill scale and rust
	Iron Sulfide (FeS)
	Reservoir fines
	Solid sulphur
Corrosion Inhibitors	
Hydrate Inhibitors	Methanol (MeOH)
	Diethyleneglycol (DEG) or Monoethylene glycol
Water and Salts	

A typical wellhead stream (natural gas with associated condensate, crude oil with associated gas) contains hundreds of different chemical compounds, and trying to separate or identify it into different chemicals is impractical.

Consequently, wellhead stream composition is defined with a finite number of components: constituents and oil cuts.

Constituents are identified and determined pure components.

They consist of:

- Non hydrocarbon components such as:
  - Nitrogen, helium, carbon dioxide, hydrogen sulfide.
- Light end hydrocarbon components such as:
  - Methane, ethane, propane, isobutene, *n*-butane, isopentane, *n*-pentane.

Oil cuts or crude fractions (or pseudo-components or hypotheticals) are a set of compounds globally determined and of identical behavior with respect to a given analysis method.

All analyses have a limited number of components; constituents and oil cuts, usually listed in the growing order of normal boiling temperature or number of carbons in the molecule. The last oil cut corresponds to the constituent group of highest normal boiling temperature or highest number of carbons in the molecule. It is named "heavy component" or C_{n+}.

Usually each laboratory uses its analytical process and issues its own description. Consequently, the oil "cut" presented in an analysis report may correspond to one criterion or several criteria.

Example:

CRITERIA	ANALYSIS PROCESS
Boiling-point temperature	Distillation or gas chromatography
Molecular mass	Gel permeation chromatography
Chemical family	Liquid chromatography
Functional group	Absorption spectrometry

Differences may appear from one analysis to the other for the main constituents (light ends), but they may be more important for cuts.

2.2.2 Fluid Identification

From geological indices and log interpretation, a production test is carried out to control the formation contents at surface.

When hydrocarbon is present, the well test delivers oil and gas at stock tank conditions.

From the observed GOR and tank density, it may be difficult to identify the hydrocarbon nature in the reservoir as oil, volatile oil, critical fluid or gas condensate. This knowledge is of prime importance for the operator since the proposed development plan is very dependent on the reservoir fluid nature. Table 2.1 can help for fluid identification.

Table 2.1 Reservoir Fluid Identification

	GOR sep		TANK OIL	
	v/v	scf/bbl	Density kg/m^3	°API
Heavy oil	<10	< 56	>900	<25.7
Oil	<500	< 2800	800-900	25.7-45.4
Critical fluid	# 700	# 3930	750-850	35-57
Condensate Gas	700-800	3 930-4 500	700-800	45.4-70
Wet gas	<15 000	< 84 230	700-800	45.4-70
Dry gas	inf			

The term "wet gas" is used for a gas that does not release condensate in the reservoir but gives hydrocarbon liquid at surface.

The term dry gas is used for a gas that does not form any hydrocarbon liquid either in the reservoir or at surface.

2.3 UNITS AND STANDARD CONDITIONS

$$PV = znRT \tag{2.1}$$

The equation of state including the compressibility factor z is convenient and sufficiently accurate for many engineering requirements.

P: pressure, kPa (abs)
V: volume, m^3
z: compressibility factor
n: number of moles, kmol
R: gas constant = 8.31441 10^{-3} m$^3 \cdot$ kPa/(K; mol)
R = 8.31441 J/(K $\cdot$ mol) or 1.985 96 Btu(IT)/(°R $\cdot$ lb-mol)

Standard atmosphere is 76 cm of Hg rise in a capillary tube which corresponds to

1 atm = 101.3250 kPa = 14.69595 psia

The molar volume for gas at 0°C and 1 atm is:

$$V = \frac{Z \times R \times T}{P} = \frac{1 \times 8.31441 \times 10^{-3} \times 273.15}{101.325} = 0.02241383 \text{ m}^3 \text{ or } 22.41383 \text{ liters}$$

Standard conditions or normal conditions in physics refer to: $P = 1$ atm, $T = 0°C$ or 273.15 K *(76 cm of mercury Hg (0.76 × 13.6 × 9.803 = 101.325 kPa))*

The reference conditions (standard conditions) used in the petroleum industry are:

$P = 1$ atm or 1.01325 bar $P = 14.7$ psia

$T = 15.6°C$ $T = 60°F$

The molar volume at standard conditions becomes:

$$V = \frac{22.41383 \times 288.15}{273.15} = 23.645 \text{ liters}$$

Molecular mass of air: 28.9784

Air density: $\rho_{air} = \frac{28.9874}{23.645} = 1.225 \text{ kg/m}^3$

English units

Standard conditions: 60°F 14.7 psia

1 000 000 std cu. ft = 1 MMscf = 2 638 lb mol

1 lb mol of gas occupies a volume of 379 cu. ft at standard conditions [38] *(After Campbell)*.

Some authors use other standard conditions for metric units.

Metric units

Standard conditions: 0°C 100 kPa

1 000 000 std m^3 = 10^6 std m^3 = 44073 kmol at std conditions

1 kmol of gas occupies a volume of 22.7 m^3 at std conditions *(After Campbell)*.

Summary:

Table 2.2 Standard Conditions and Constants

Standard Conditions			
Pressure	1 atm	1.01325 bar	14.7 psia
Temperature		15.5°C	60°F
Constants			
Molar volume of gas at standard conditions			
		1 gmol	23.645 dm^3
		1 kmol	23.645 m^3
		1 lb mol	379 cu. ft
Molar mass of air			28.9784

2.4 DEFINITIONS

2.4.1 Reduced Pressure and Temperature for a Pure Constituent

According to the theorem of corresponding states, the deviation of any actual gas from the ideal gas law is the same for different gases when at the same corresponding state. The same corresponding states are found at the same fraction of the absolute critical temperature and pressure, which are:

$$P_r = \frac{P}{P_c} \qquad T_r = \frac{T}{T_c} \tag{2.2}$$

T, P: temperature and pressure of the gas
T_c, P_c: critical temperature and pressure of the constituent
T_r, P_r: Reduced temperature and pressure of the constituent

2.4.2 Pseudo Reduced Pressure and Temperature for a Multi Component System

Pseudo reduced properties are defined as the ratio of temperature (or pressure) with pseudo reduced critical temperature (or pressure). These pseudo critical properties are an average of the critical properties of the components in the mixture.

Kay extended the theorem of corresponding states to mixtures and defined pseudo reduced temperature and pressure.

$$P_{pc} = \Sigma y_i P_{ci} \quad \text{and} \quad T_{pc} = \Sigma y_i T_{ci}$$

Where y_i is the mole fraction of each component in the mixture and T_{ci} and P_{ci} are critical values for each component.

$$T_{pr} = \frac{T}{T_{pc}} \qquad P_{pr} = \frac{P}{P_{pc}} \tag{2.3}$$

2.5 BASIC DEFINITIONS: OIL FVF (FORMATION VOLUME FACTOR), R_s (SOLUTION GAS RATIO)

2.5.1 Oil PVT Functions

B_o is the ratio of the volume of a given mass of oil plus its dissolved gas, at a given pressure and temperature, to the volume of the same oil at standard (stock tank) conditions.

Remark:
At reservoir conditions liquid only is present. At standard conditions there are two phases. The definition above assumes a constant composition of the two components: oil and gas.

$$B_o = \frac{V_{o(res)}}{V_{o(std)}} \qquad R_s = \frac{V_{g(std)}}{V_{o(std)}} \tag{2.4}$$

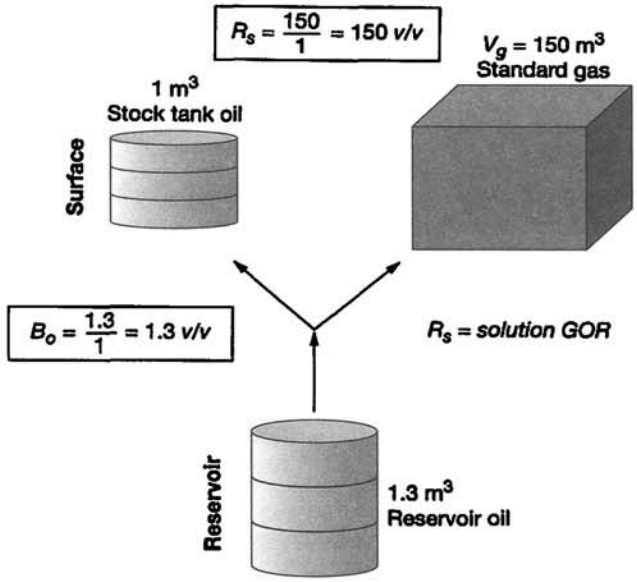

Figure 2.1 B_o, R_s definitions.

Solution Gas-oil Ration, R_s:

R_s is the ratio of the volume of dissolved gas at a specified pressure to the volume of oil in which it is dissolved, both volumes converted to standard conditions Eq. (2.4).

At any pressure, there is a maximum limit on the amount of gas which will dissolve in a certain quantity of oil.

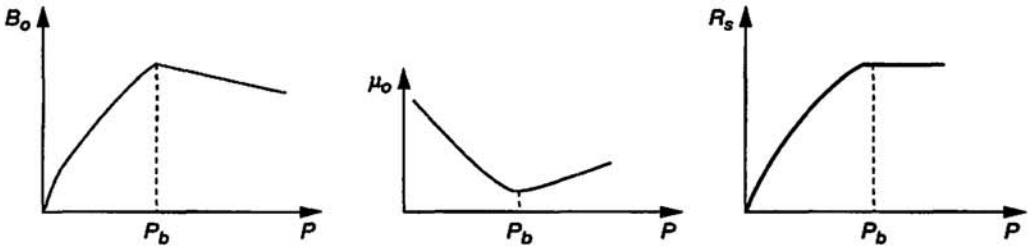

Figure 2.2 B_o, μ_o, R_s versus pressure.

The pressure at which the maximum solution gas is reached is defined as bubble point pressure. In that condition, the oil is qualified as "saturated oil". The term "saturation pressure" is often used for bubble point pressure.

Figure 2.2 illustrates B_o, μ_o and R_s function of pressure.

It can be said that the bubble point pressure is a function of the dissolved gas amount, and conversely.

The term "shrinkage" is often used to describe the phenomenon of liquid volume decrease between reservoir and surface conditions.

Shrinkage factor = $1/B_o$

Symbol R_s (solution gas ratio) defines the amount of gas in solution per unit of liquid volume. GOR defines the amount of gas produced. In an under saturated oil, $GOR = R_s$ (stm^3/m^3).

In field units, R_s is expressed in *scf/bbl std (1 bbl = 5.615 scf)*

Oil viscosity is very dependent on the amount of solution gas. More gas in solution, the lower the viscosity of the oil is. The oil viscosity is minimum at the bubble point pressure (Fig. 2.2).

The term "dead oil" or "stabilized oil" is used to characterize a fluid without gas in solution.

2.5.2 Dry Gas

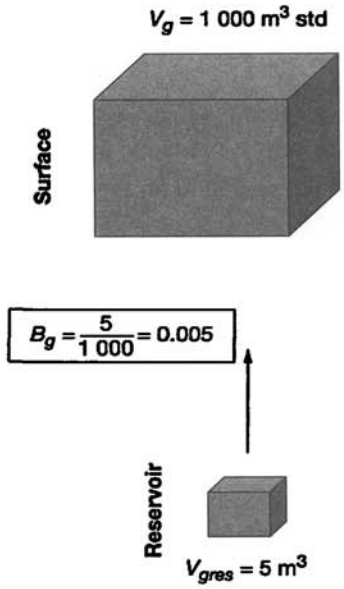

Figure 2.3 Gas formation Factor.

B_g is the ratio of the volume occupied by a unit mass of gas at a given temperature and pressure to the volume occupied by the same unit mass of gas at standard conditions.

Remark:
The nature of the fluid is the same between reservoir and surface conditions.
The mass is kept constant.

B_g is expressed in *V/V* (volume per volume) in the metric system

$E_g = 1/B_g$

E_g gas expansion factor for the illustrated example in Figure 2.3:

$B_g = 0.005$ $E_g = 200$

In field units B_g is often reported in *bbl/Mscf* *(Mscf = 1 000 cft)*

Advantage: with B_g expressed in *bbl/Mscf* and gas cumulative in *Mscf*, the product of the two factors result is reservoir barrels (unit used in material balance calculations).

2.5.3 Wet Gas and Condensate Gas

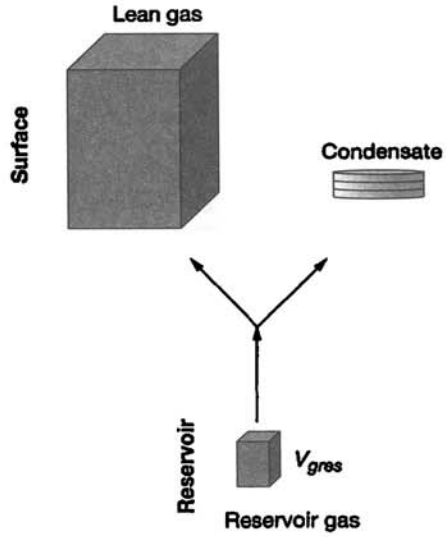

Figure 2.4 Wet and condensate gas relationship.

From a monophasic reservoir gas, condensate and lean gas are obtained at surface (Fig. 2.4).

Yield of condensate is defined as the mass of condensate obtained per mole of reservoir gas.

Yield is calculated from the reservoir gas composition.

Field GOR is measured as lean gas volume produced per volume of condensate produced, both expressed at standard conditions.

Commonly the parameter CGR (Condensate Gas Ratio) is used in addition to the GOR.

CGR = 1/GOR

2.6 FLUID SAMPLING

2.6.1 Purpose

Obtaining a representative sample of hydrocarbons present from a given reservoir in conditions which are as closely similar to reservoir conditions is important because it allows the engineer to:

- Determine the molar composition of the hydrocarbons.
- Measure their physical properties such as density, viscosity, compressibility, etc.
- Determine the variations of the above parameters as a function of pressure, and temperature.

Study the phase diagram of the hydrocarbon and determine the bubble point curve, dew point curve, amount of dissolved gas in the oil, etc.

The validity of the laboratory PVT measurements relies on the representativity of the fluid sample used for the analysis.

Reservoir fluid representativity implies: The collected fluid sample composition is identical to the reservoir fluid composition.

2.6.2 Sampling Methods

Sampling must be conducted with utmost care. Erroneous data about reservoir fluid can lead to errors, amounting to considerable financial consequences. The complexity of reservoir and fluid flow conditions, makes it difficult to define the optimal well conditioning to get representative samples particularly in the case of saturated oil or gas-condensate reservoirs.

There are two methods to collect hydrocarbon samples:

- Bottom hole sampling
- Surface sampling.

2.6.2.1 Bottom Hole Fluid Sampling

To collect fluid, a sample taking tool is lowered into the hole at the producing depth. Sampling is performed during a low production rate flow through the sample taker to avoid a high pressure draw down and gravity segregation.

Therefore *bottom hole fluid sampling must be avoided for saturated oil* but is convenient for under saturated oil.

Sample brought to surface is checked for validity and transferred into a carrying bottle for transportation to the laboratory. A simple check is carried out by measuring the bubble point pressure of the sample at surface temperature. Usually, three samples are taken and consistency of the three bubble point pressures must be observed to qualify the samples for laboratory expertise.

Operation

Before collecting fluid samples from the well, the production must be stabilized which means:

- Constant flow rate
- Constant well head flowing pressure.

Usually the well head flowing pressure is monitored with a dead weight tester. It is admitted that the well head flowing pressure must not fluctuate more than a few psi.

It is important that the sample is taken in conditions as close as possible to reservoir conditions in order to avoid the loss of some hydrocarbon components which occurs during decompression and which may be left in the formation or in the well.

Tool characteristics (PST):

- The sampling capacity is 600 cm^3. The sampler is associated with a Casing Collar Locator (CCL) to ensure an accurate depth positioning.

The sample taken with the tool, meets the following requirements:

- It comes from a well defined depth.
- It is free of atmospheric gases.
- The fluids are kept at down hole pressure during the sampling process and they are recompressed to any desired pressure before transfer into a receptacle for transport to the laboratory.

The well must be producing at a very low rate.

The sampler is positioned at the proper depth with the CCL.

The sample chamber is opened from surface and is slowly filled (about 2 minutes) in order to keep the sample equal to the well pressure during sampling.

The chamber is then closed and the tool brought up to surface.

At surface, the sample is recompressed and transferred into a receptacle.

Other Tools: RFT (Repeat Formation Tester), MDT, (Modular Formation Dynamics Tester), DST (Drill Stem Test) equipped with a sample catcher.

(PST, RFT, MDT are trade marks of Schlumberger)

2.6.2.2 Surface Sampling

Fluid samples are collected from the separator in specialized bottles for liquid and gas. To reconstitute the reservoir fluid, gas and liquid must be recombined at the laboratory in the proper proportions. The ratio is the field measured $GOR = Q_g/Q_o$.

In the field, gas flow rates are measured with an orifice meter [2]. The gas rate is derived from the orifice meter equation:

$$q_g = C' \times \sqrt{h_w p_f} \tag{2.5}$$

with $$C' = F_b \times F_{pb} \times F_{tb} \times F_g \times F_{tf} \times F_r \times Y \times F_{pv} \times F_m \times F_l \times F_a$$

q_g: gas flow rate scf/hr at STD conditions (14.7 psi; 60°F, or 520° Rankine)
h_w: pressure differential across the orifice in inches of water
C': orifice constant
F_b: basic orifice flow factor function of diameter, efficiency factor
F_{pb}: pressure base factor to correct q_g in case of pressure other than STD conditions
F_{tb}: temperature base factor to correct q_g in case of temperature other than 520°R (60°F)
F_g: gas relative density correction $F_g = \sqrt{\frac{1}{\gamma_g}}$ γ_g: (relative density of gas; air = 1)
F_{tf}: correction factor for gas flowing temperature other than 60°F $F_{tf} = \sqrt{\frac{520}{T_f}}$
F_r: correction for variation of the discharge coefficient with Reynolds number
Y: expansion factor due to gas density change across the orifice
F_{pv}: super compressibility factor (deviation from ideal gas law behavior $F_{pv} = \sqrt{\frac{1}{z}}$
F_m: manometer correction
F_l: correction for gauge location (elevation and latitude other than sea level and 45° latitude
F_a: correction for thermal expansion or contraction of the orifice

The orifice equation can be written:

$$q_g = C'' \times \sqrt{\frac{1}{\gamma_g z}} \times \sqrt{h_w p_f} \tag{2.6}$$

All correction factors are published in the form of tables. To compute the gas flow rate the operator needs an evaluation of the gas compressibility factor and the gas relative density.

A field evaluation is carried out by gas chromatography analysis, and retained values for calculation are reported on the test and sample sheets.

Dry Gas Reservoirs

The gas always remains entirely in gas phase at reservoir conditions. At surface conditions, no liquid hydrocarbon is produced.

Wet Gas Reservoirs

At reservoir conditions, the hydrocarbon remains in gas phase. At separator conditions, liquid hydrocarbon is produced with gas. The temperature drop between the reservoir and the separator causes the heavier components to condense.

Gas Condensate Reservoirs

At reservoir conditions, the hydrocarbon remains in gas phase if the reservoir pressure is kept above the gas dew point pressure. At surface, lean gas and condensate are obtained at the output of the separator. If the reservoir pressure is allowed to drop below the gas dew point pressure, some condensate is trapped in the porous space and the collected fluid is not representative of the reservoir fluid.

Operation

The flow stability has to be perfect and should be found for the lowest flow rate. Flow stability criteria are:

- Stabilized gas and oil flow rates and GOR.
- Stabilized well head flowing pressure.
- Stabilized bottom hole flowing pressure.

In the production column, one must make sure that no segregation occurs. Therefore a minimum flow rate is necessary [39], Appendix G.

Remark:
The gas flow rate is deducted from the orifice meter characteristics. The equipment (diaphragm) must be in perfect condition to obtain a reliable flow rate value. The use of damaged equipment will lead to erroneous flow rate calculation, then a wrong GOR. Consequently the fluid recombination in the laboratory will give a non representative reservoir fluid. In such a case, it is not possible to detect and correct the error until a new test is carried out with new equipment.

2.7 BLACK-OIL CONCEPT

From the basic definitions, the reservoir liquid is made of two components: stock tank oil and standard conditions gas. The reservoir oil is made of surface oil mixed with a variable amount of surface gas (R_s) in solution. The mixture is brought to reservoir pressure and temperature.

The black-oil option assumes that during production, the respective molar compositions of the collected surface oil and gas produced, are constant whatever the reservoir pressure temperature and the surface process. Therefore material balance calculations can be expressed in volumes using the formation volume factors (FVF) B_o and B_g to convert surface conditions to reservoir volumes.

The option is valid for most of the reservoir studies. Thermodynamic conditions require for the representative reservoir conditions point on the pressure temperature plot, to be located far from the critical point.

The option cannot be used to treat volatile oil, critical fluids or gas condensate reservoirs when surface fluid compositions are dependent on the surface process applied. Such cases must be treated with an equation of state to work in masses (kmol, kg, or t) and determine at every calculation step (reservoir and surface conditions) the molar composition of the well stream and the split between liquid and vapor at surface.

Oil is qualified "dead or stabilized" when there is no gas in solution in the oil.

2.8 PVT OIL STUDY

The following tables show a typical Oil PVT report, result of a complete study carried out in the laboratory.

In the field, several liquid and gas samples are collected. Upon arrival in the laboratory, the sample bottles are checked. A gas and oil bottles are chosen on which the complete study is carried out.

In the case of under saturated oil samples, a first selection is already done on the well site to discard the non representative sample. This is accomplished by measuring the bubble point pressure obtained at laboratory conditions.

Table 2.3 Summary of Sampling Conditions

Company: COMPANY	**Well: EXPLO**		
Field: CST	**Formation: OIL**		
SUMMARY OF SAMPLING CONDITIONS **Bottles 4458-EA & A0577**			
Reservoir and Well Characteristics:			
Production Zone	3 559-3 590	m BRT	
Datum Level	3523.2	m BRT	11 559 ft BRT
Static Reservoir Pressure at Datum	384.7	bar(g)	5578 psig
Reservoir Temperature	146.0	°C	295°F
Bottomhole Flowing Pressure	366.5	bar(g)	5314 psig
Bottomhole Flowing Temperature	148.1	°C	299°F
Surface Conditions:			
Date of Sampling	26-10-96		
Wellhead Pressure	171.8	bar(g)	2 491 psig
Wellhead Temperature	97.9	°C	208°F
Separator Presure	14.0	bar(g)	203 psig
Separator Temperature	77.0	°C	171°F
Stock Tank Temperature	15.6	°C	60°F
Atmospheric Pressure	1.013	bar(a)	14.7 psig
Stock Tank Oil Rate	325.3	Sm^3/d	2046 bbl/d
First Stage Separator Oil Rate	367.4	m^3/d	2311 bbl/d
First Stage Separator Gas Rate	69 178	Sm^3/d	2.44 MMscf/d
Gas Relative Density (Air = 1)	0.750		
Gas Compressibility Factor (std)	0.976		
Oil Density (std)	850.0	kg/m^3	35.0°API
BSW	0.0	%	
Shrinkage (1)	0.883		
Separator Gas-Stock Tank Oil Ratio	213	Sm^3/m^3	1 194 Scf/Stb
Separator Gas-Separator Oil Ratio	188.1	Sm^3/m^3	1 056 Scf/Stb

Source: Sampling Sheets.

(1) Calculated.

Summary of the Sampling Conditions

Table 2.3 summarizes the bottom and surface conditions that were prevailing during the sampling operation. During the production test, a bottom hole sample was collected in addition to surface sampling.

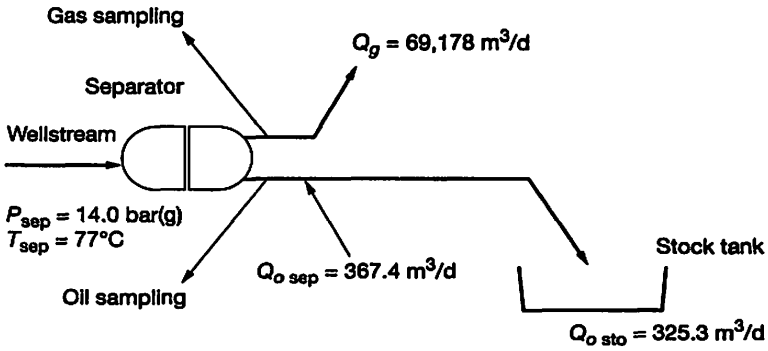

Figure 2.5 Surface sampling.

GOR at separator is:

$$\text{GOR}_{sep} = \frac{\text{Gas rate at sep}}{\text{Oil rate sep}} = \frac{69178}{367.4} = 188\ \text{Sm}^3/\text{m}^3\ \text{sep}$$

Assumed gas relative density: 0.75 (air = 1)

Assumed gas compressibility: $z = 0.976$

BSW: Basic Sediments and Water

Some sediment may be found at the bottom of the separator

$$\text{BSW} = \frac{\text{Sediment + water volumes}}{\text{oil + water volumes}}$$

Table 2.4 Checking of Sample Bottles

Company: COMPANY			**Well: EXPLO**				
Field: CST			**Formation: OIL**				
CHECK OF SAMPLES RECEIVED IN THE LABORATORY							
	Bottom Hole Samples		**Opening Pressure**			**Saturation Pressure**	
			bar(g)	at	°C	bar(g)	at °C
	Fasc N°	Cylinder N°	psig	at	°F	psig	at °F
	#4A	4454-EA	101.0		16.8	285.7	146
			1465		62	4143	295
	#4B	4452-EA	92.0		16.8	212.5	146
			1334		62	3081	295
	Separator Oil		**Opening Pressure**			**Saturation Pressure**	
			bar(g)	at	°C	bar(g)	at °C
	Bottle N°	Bottle N°	psig	at	°F	psig	at °F
	#1A	4442-EA	6.0		18.0	20.8	76.9
			87		64	302	170
	#2A	4441-EA	6.0		18.0	13.7	77.4
			87		64	199	171
(*)	#3A	4458-EA	6.0		18.0	13.8	77.8
			87		64	200	172
	Separator Gas		**Opening Pressure**				
			bar(g)	at	°C		
	Bottle N°	With Oil Bottle	psig	at	°F		
	A0574	4442-EA	16.6		77.0		
			241		171		
	2498A	4442-EA	16.6		77.0		
			241		171		
	A0594	4441-EA	16.6		77.0		
			241		171		
	A0570	4441-EA	2.8		77.0		
			41		171		
	4703A	4458-EA	16.9		77.0		
			245		171		
(*)	A0577	4458-EA	16.4		77.0		
			238		171		

(*) Samples used for Recombination.

Checking samples at Laboratory

Table 2.4 depicts the results of the measurements carried out in the laboratory on the sample bottles.

First the opening bottle pressures are measured at room temperature. All the oil bottle pressures should be consistent.

All the sample bottles are heated up in an oven to the sampling temperature.

Opening pressures are measured and reported. For the oil bottles, the saturation pressure is determined by a constant mass expansion process. The result should be near to the separator pressure at sampling time.

If a pressure anomaly appears; it is explained by a fluid leak during transport; then the bottle sample is discarded.

Finally a couple of bottles (oil and gas) are chosen for recombination and study and, or a bottom hole sample.

Table 2.5 Flash of Separator Oil Sample

Company: COMPANY		**Well: EXPLO**	
Field: CST		**Formation: OIL**	
FLASH OF SEPARATOR OIL SAMPLE **Bottle 4458-EA**			
Production Conditions			
Pressure	14.4	bar(g)	Psat
	209	psig	
Temperature	77.8	°C	
	172	°F	
Separator Conditions			
Pressure	1.013	bar(a)	
	14.69	psig	
Temperature	15.0	°C	
	59	°F	
GOR	8.0	Sm^3/Sm^3	
	45	scf/stb	
Liquid Phase Properties			
Liquid volume factor (1)	1.086		
Oil tank density at 15.6°C	852	kg/m^3	
60°F	34.6	°API	
Gas Phase Property			
Gas Relative Density (Air = 1.00)	0.987		

(1) m^3 of liquid at indicated conditions per m^3 of liquid at 15°C and 1.013 bar(a).

Flash of Separator Oil Sample (Table 2.5)

The separator oil is flashed to standard conditions and the resulting products are analyzed by gas chromatography to determine the composition of each phase (Table 2.6). GOR, liquid density and gas relative density are reported.

Table 2.6 Composition of Separator Oil

Company: COMPANY		**Well: EXPLO**	
Field: CST		**Formation: OIL**	
SINGLE STAGE SEPARATION TO STANDARD CONDITIONS OF SEPARATOR OIL Bottle04458-EA			
Components or Fractions	**Tank Gas (mol %)**	**Tank Liquid (mol %)**	**Separator Oil (mol %)**
Hydrogen Sulfide	0.88	0.00	0.07
Nitrogen	0.08	0.00	0.01
Carbon Dioxide	1.47	0.00	0.12
Methane	58.65	0.00	4.84
Ethane	13.66	0.22	1.33
Propane	11.69	0.97	1.85
***i*-Butane**	2.50	0.42	0.59
***n*-Butane**	5.68	1.59	1.93
***i*-Pentanes**	1.83	1.19	1.24
***n*-Pentanes**	1.80	1.69	1.70
Hexanes	1.09	3.36	3.17
Heptanes	0.58	6.47	5.98
Octanes	0.09	7.94	7.29
Nonanes	0.00	6.65	6.10
Decanes		6.22	5.71
Undecanes		5.20	4.77
Dodecanes		4.80	4.40
Tridecanes		5.11	4.69
Tetradecanes		4.45	4.08
Pentadecanes		3.97	3.64
Hexadecanes		3.31	3.04
Heptadecanes		3.09	2.83
Octadecanes		3.05	2.80
Nonadecanes		2.94	2.70
Eicosanes plus		27.36	25.10
TOTAL	100.0	100.0	100.0
Molecular Mass	28.6	226.6	210.2
Molecular Mass C_{20+}		431(1)	431
Gas Relative Density (air = 1)	0.986		

(1) From simulated distillation.

Composition of Products Resulting of the Flash Liberation of Separator Oil Sample

Chromatograph work with samples at atmospheric conditions. Therefore the separator oil sample is flashed to atmospheric pressure and resulting products (liquid and gas) are analyzed independently with the gas chromatographic technique.

Measured gas and liquid compositions are combined to calculate the separator oil composition.

Table 2.7 Separator Oil Composition Calculation

Name	Formula		Katz Mw (1)	GAS % mole (2)	OIL % mole (3)	gas mass (4)	oil mass (5)	nb of moles in 1 m^3 of oil (6)	nb of gas moles associ with 1 m^3 of oil (7)	total nb of moles (8)	fluid fraction mol % (9)	fluid mass (10)
Hydrogen sulfide	H_2S	H_2S	34.08	0.88		0.300	0.000	0.0000	0.0030	0.0030	0.07	0.025
Nitrogen	N_2	N_2	28.02	0.08		0.022	0.000	0.0000	0.0003	0.0003	0.01	0.002
Carbon dioxyde	CO_2	CO_2	44.01	1.47		0.647	0.000	0.0000	0.0050	0.0050	0.12	0.053
Methane	CH_4	C_1	16.04	58.65		9.407	0.000	0.0000	0.1984	0.1984	4.84	0.777
Ethane	C_2H_6	C_2	30.07	13.66	0.22	4.108	0.066	0.0083	0.0462	0.0545	1.33	0.400
Propane	C_3H_8	C_3	44.1	11.69	0.97	5.155	0.428	0.0365	0.0396	0.0760	1.85	0.818
i-Butane	C_4H_{10}	*i*-C_4	58.12	2.50	0.42	1.453	0.244	0.0158	0.0085	0.0243	0.59	0.344
n-Butane	C_4H_{10}	*n*-C_4	58.12	5.68	1.59	3.301	0.924	0.0598	0.0192	0.0790	1.93	1.120
i-Pentane	C_5H_{12}	*i*-C_5	72.15	1.83	1.19	1.320	0.859	0.0447	0.0062	0.0509	1.24	0.897
n-Pentane	C_5H_{12}	*n*-C_5	72.15	1.80	1.69	1.299	1.219	0.0635	0.0061	0.0696	1.70	1.226
n-Hexane	C_6H_{14}	C_6	84	1.09	3.36	0.916	2.822	0.1263	0.0037	0.1300	3.17	2.665
n-Heptane	C_7H_{16}	C_7	96	0.58	6.47	0.557	6.211	0.2433	0.0020	0.2453	5.98	5.744
n-Octane	C_8H_{18}	C_8	107	0.09	7.94	0.096	8.496	0.2986	0.0003	0.2989	7.29	7.802
n-Nonane	C_9H_{20}	C_9	121	0.00	6.65	0.000	8.047	0.2501	0.0000	0.2501	6.10	7.382
n-Decane	$C_{10}H_{22}$	C_{10}	134	0.00	6.22	0	8.335	0.2339	0.0000	0.2339	5.71	7.647
Undecane	$C_{11}H_{24}$	C_{11}	147	0.00	5.20	0	7.644	0.1955	0.0000	0.1955	4.77	7.013
Dodecane	$C_{12}H_{26}$	C_{12}	161	0.00	4.80	0	7.728	0.1805	0.0000	0.1805	4.40	7.090
Tridecane	$C_{13}H_{28}$	C_{13}	175	0.00	5.11	0	8.943	0.1921	0.0000	0.1921	4.69	8.204
Tetradecane	$C_{14}H_{30}$	C_{14}	190	0.00	4.45	0	8.455	0.1673	0.0000	0.1673	4.08	7.757
Pentadecane	$C_{15}H_{32}$	C_{15}	206	0.00	3.97	0	8.178	0.1493	0.0000	0.1493	3.64	7.503
Hexadecane	$C_{16}H_{34}$	C_{16}	222	0.00	3.31	0	7.348	0.1245	0.0000	0.1245	3.04	6.742
Heptadecane	$C_{17}H_{36}$	C_{17}	237		3.09	0	7.323	0.1162	0.0000	0.1162	2.83	6.719
Octodecane	$C_{18}H_{38}$	C_{18}	251		3.05	0	7.656	0.1147	0.0000	0.1147	2.80	7.024
Nonadecane	$C_{19}H_{40}$	C_{19}	263		2.94	0	7.732	0.1106	0.0000	0.1106	2.70	7.094
Eicosane		C_{20+}	431		27.36	0	117.922	1.0288	0.0000	1.0288	25.10	108.187
			Total	100.00	100.00	28.6	226.6			4.0986	100.00	210.23
						28.98	= air					= Mw
		Oil density		852	kg/m^3							
		GOR		8	v/v	0.986						

Table 2.8 Correction of the Gas Oil Ratio

Company: COMPANY				**Well: EXPLO**	
Field: CST				**Formation: OIL**	
CORRECTION OF THE GAS OIL RATIO DST#1 (A0577 & 4458-EA)					
Corrected GOR			$GOR_{corrected} = GOR_{field} \times \frac{\sqrt{(\gamma \times z)_{field}}}{\sqrt{(\gamma \times z)_{lab}}}$		
with	GOR	:	Gas Oil Ratio (v/v)		
	γ	:	Gas Relative Density (air = 1)		
	z	:	Gas Compressibility Factor		
	γ_{field}			0.750	
	z_{field}			0.976	(=1/fpv^2)
	γ_{lab}			0.717	
	z_{lab}			0.978	
Separator GOR field				188.1	Sm^3/m^{3}sep(1)
				1056	scf/bbl sep
Separator GOR corrected				192.2	Sm^3/m^{3}sep
				1079	scf/bbl sep
Separator Liquid Volume Factor				1.086	(2)
Tank GOR corrected				209	Sm^3/Sm^3
				1174	scf/stb

(1) Sampling sheet.
(2) Laboratory data.

Correction of the Gas Oil Ratio (Table 2.8)

The orifice equation giving the gas flow rate can be written as:

$$q_g = C'' \times \sqrt{\frac{1}{\gamma_g z}} \times \sqrt{h_w p_f}$$

q_g: gas flow rate scf/hr at STD conditions (14.7 psi; 60°F, or 520° Rankine)
h_w: pressure differential across the orifice in inches of water
C'': orifice constant

All correction factors (C'') are published in the form of tables. To compute the gas flow rate the operator needs an evaluation of the gas compressibility factor and the relative density.

For more details see paragraph "sampling"

The correction for the deviation from ideal gas law in the orifice gas meter formula is: *Fpv*.

In the field, *Fpv* is calculated from pressure, temperature, and gas relative density, using procedures given in AGA Report 3 (American Gas Association).

$$Fpv = \sqrt{\frac{1}{z}}$$

Table 2.9 Calculated Well Stream Composition

Company: COMPANY			**Well: EXPLO**
Field: CST			**Formation: OIL**
COMPOSITIONAL ANALYSIS OF THE SEPARATOR FLUIDS AND CALCULATED WELL STREAM (GOR = 192.2 Sm^3/m^3 sep)			
Components or Fractions Bottle N°	**Separator Gas (mol %)** A0577	**Separator Liquid (mol %)** 4458-EA	**Well Stream (mol %)**
Hydrogen Sulfide	0.33	0.07	0.25
Nitrogen	0.34	0.01	0.24
Carbon Dioxide	1.18	0.12	0.85
Methane	83.60	4.84	58.86
Ethane	6.58	1.33	4.93
Propane	3.67	1.86	3.10
***i*-Butane**	0.65	0.59	0.63
***n*-Butane**	1.52	1.93	1.65
***i*-Pentanes**	0.51	1.24	0.74
***n*-Pentanes**	0.57	1.70	0.92
Hexanes	0.47	3.17	1.32
Heptanes	0.38	5.98	2.14
Octanes	0.16	7.30	2.40
Nonanes	0.04	6.10	1.94
Decanes	0.00	5.71	1.79
Undecanes		4.77	1.50
Dodecanes		4.40	1.38
Tridecanes		4.69	1.47
Tetradecanes		4.08	1.28
Pentadecanes		3.64	1.14
Hexadecanes		3.04	0.95
Heptadecanes		2.83	0.89
Octadecanes		2.80	0.88
Nonadecanes		2.70	0.85
Eicosanes plus		25.10	7.88
TOTAL	100.0	100.0	100.0
Molecular Mass	20.8	210.2	80.30
Molecular Mass C_{20+}[(1)]		431	431
Gas Relative Density (air = 1)	0.716		

Calculated Well stream Composition from Separator Fluids

Calculation of the reservoir fluid is carried out from the separator fluid compositions. The physical recombination is performed.

Table 2.10 Calculated Well Stream Composition

Name	Formula		Katz Mw (1)	GAS % mole (2)	OIL % mole (3)	gas mass (4)	oil mass (5)	nb of moles in 1 m^3 of oil (6)	nb of gas moles associ with 1 m^3 of oil (7)	total nb of moles (8)	fluid fraction mol % (9)	fluid mass (10)
Hydrogen sulfide	H_2S	H_2S	34.08	0.33	0.07	0.112	0.024	0.0026	0.0268	0.0294	0.25	0.085
Nitrogen	N_2	N_2	28.02	0.34	0.01	0.095	0.003	0.0004	0.0276	0.0280	0.24	0.066
Carbon dioxyde	CO_2	CO_2	44.01	1.18	0.12	0.519	0.053	0.0045	0.0959	0.1004	0.85	0.373
Methane	CH_4	C_1	16.04	83.60	4.84	13.409	0.776	0.1802	6.7955	6.9757	58.86	9.441
Ethane	C_2H_6	C_2	30.07	6.58	1.33	1.979	0.400	0.0495	0.5349	0.5844	4.93	1.483
Propane	C_3H_8	C_3	44.1	3.67	1.86	1.618	0.820	0.0692	0.2983	0.3676	3.10	1.368
i-Butane	C_4H_{10}	*i*-C_4	58.12	0.65	0.59	0.378	0.343	0.0220	0.0528	0.0748	0.63	0.367
n-Butane	C_4H_{10}	*n*-C_4	58.12	1.52	1.93	0.883	1.122	0.0719	0.1236	0.1954	1.65	0.958
i-Pentane	C_5H_{12}	*i*-C_5	72.15	0.51	1.24	0.368	0.895	0.0462	0.0415	0.0876	0.74	0.533
n-Pentane	C_5H_{12}	*n*-C_5	72.15	0.57	1.70	0.411	1.227	0.0633	0.0463	0.1096	0.92	0.667
n-Hexane	C_6H_{14}	C_6	84	0.47	3.17	0.395	2.663	0.1180	0.0382	0.1562	1.32	1.107
n-Heptane	C_7H_{16}	C_7	96	0.38	5.98	0.365	5.741	0.2226	0.0309	0.2535	2.14	2.054
n-Octane	C_8H_{18}	C_8	107	0.16	7.30	0.171	7.811	0.2718	0.0130	0.2848	2.40	2.571
n-Nonane	C_9H_{20}	C_9	121	0.04	6.10	0.048	7.381	0.2271	0.0033	0.2304	1.94	2.352
n-Decane	$C_{10}H_{22}$	C_{10}	134	0.00	5.71	0	7.651	0.2126	0.0000	0.2126	1.79	2.404
Undecane	$C_{11}H_{24}$	C_{11}	147		4.77	0	7.012	0.1776	0.0000	0.1776	1.50	2.203
Dodecane	$C_{12}H_{26}$	C_{12}	161		4.40	0	7.084	0.1638	0.0000	0.1638	1.38	2.225
Tridecane	$C_{13}H_{28}$	C_{13}	175		4.69	0	8.208	0.1746	0.0000	0.1746	1.47	2.578
Tetradecane	$C_{14}H_{30}$	C_{14}	190		4.08	0	7.752	0.1519	0.0000	0.1519	1.28	2.435
Pentadecane	$C_{15}H_{32}$	C_{15}	206		3.64	0	7.498	0.1355	0.0000	0.1355	1.14	2.356
Hexadecane	$C_{16}H_{34}$	C_{16}	222		3.04	0	6.749	0.1132	0.0000	0.1132	0.95	2.120
Heptadecane	$C_{17}H_{36}$	C_{17}	237		2.83	0	6.707	0.1054	0.0000	0.1054	0.89	2.107
Octodecane	$C_{18}H_{38}$	C_{18}	251		2.80	0	7.028	0.1042	0.0000	0.1042	0.88	2.208
Nonadecane	$C_{19}H_{40}$	C_{19}	263		2.70	0	7.101	0.1005	0.0000	0.1005	0.85	2.231
Eicosane		C_{20+}	431		25.10	0	108.181	0.9345	0.0000	0.9345	7.88	33.984
			Total	100.00	100.00	20.8	210.2			11.8516	100.00	80.27
						28.98	= air					= Mw
			Oil density	782.68	kg/m^3							
			GOR	192.2	v/v	0.716						

Oil density at separator conditions is: $\rho_{oilsep} = \frac{\rho_{ostd}}{1.086} = \frac{850}{1.086} = 782.69$ kg/m^3. 1.086: separator liquid volume factor (Table 2.8).

Table 2.11 Constant Composition Expansion Study

Company: COMPANY				**Well: EXPLO**	
Field: CST				**Formation: OIL**	
PRESSURE VOLUME RELATION OF RESERVOIR FLUID AT T = 146°C (295°F) (Recombined fluid from Bottle A0577 & Bottle 4458EA) **(Constant Composition Study)**					
	Pressure		**Relative Volume**	**Specific Volume**	**Isothermal Compressibility**	
	bar(g)	**psig**	**(V/Vsat)**	**(m^3/kg)**	**(10^{-4} bar^{-1})**	**(10^{-5} psi^{-1})**
			(2)	**(3)**	**(4)**	**(4)**
	447.2	6 484	0.9815	1.64E-03	2.810	4.075
	435.6	6 316	0.9847	0.001642	2.866	4.156
	425.6	6 171	0.9875	0.001647	2.917	4.230
	411.9	5 973	0.9915	0.001653	2.988	4.333
	399.2	5 788	0.9957	0.001661	3.055	4.430
	388.9	5 639	0.9984	0.001664	3.113	4.515
(1)	**384.2**	**5 571**	**1.0000**	**1.667E-03**	**3.139**	**4.552**
	380.3	5 514	1.0027	1.672E-03		
	372.9	5 407	0.0082	1.681E-03		
	361.6	5 243	1.0172	1.696E-03		
	351.1	5 091	1.0263	1.711E-03		
	332.4	4 820	1.0448	1.742E-03		
	308.5	4 473	1.0730	1.789E-03		
	276.7	4 012	1.1205	1.868E-03		
	231.7	3 360	1.2171	2.029E-03		
	188.9	2 739	1.3639	2.274E-03		
	140.1	2 031	1.6607	2.768E-03		
	99.8	1 447	2.1591	3.599E-03		

(1) Saturation Pressure at indicated Temperature.
(2) Volume of fluid at indicated Temperature.
(3) Based on a density at Psat of 600 kg/m^3.
(4) $cT = -dV/Vdp$ determined from smoothe P – V function.

Constant Composition Expansion (Table 2.11)

The saturation pressure is determined by a constant mass depletion study.

All physically measured volumes are referenced to the oil volume at saturation pressure.

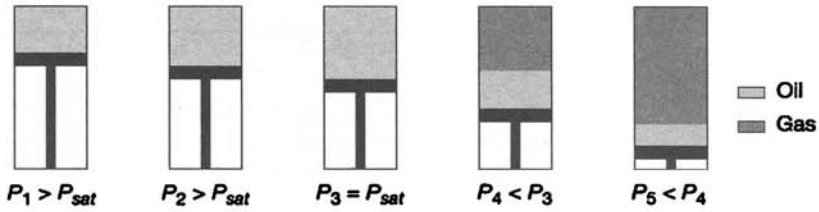

Figure 2.6 Constant Mass Expansion.

The sample at reservoir temperature is over pressurized at a pressure well above bubble point pressure. The sample pressure is decreased by displacing the piston. The bubble point pressure is defined as the pressure at which the first gas bubble appears in the sample.

Relative volume = volume of oil/oil volume occupied at bubble point pressure

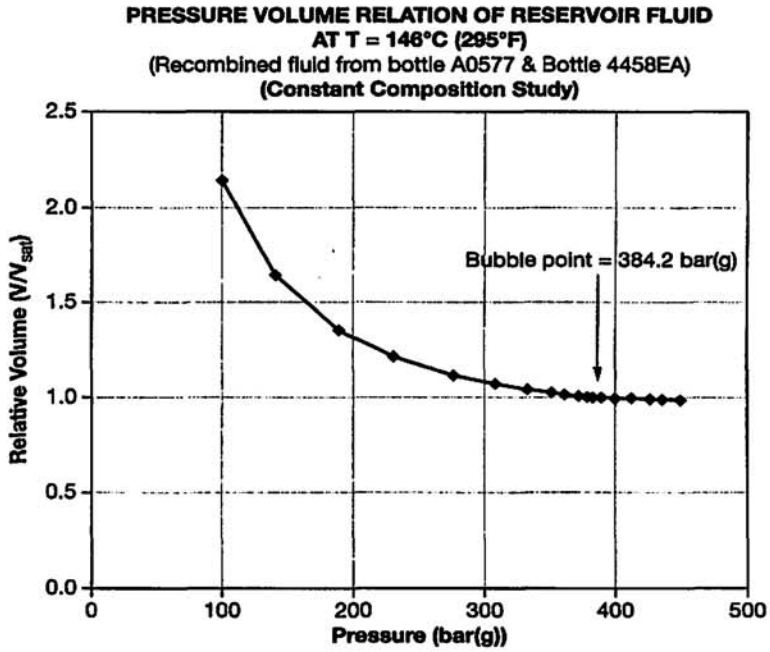

Figure 2.7 Pressure Volume Relation.

Table 2.12 Flash to Standard Conditions of Recombined Reservoir Fluid

Company: COMPANY		**Well: EXPLO**	
Field: CST		**Formation: OIL**	
FLASH TO STANDARD CONDITIONS OF RECOMBINED RESERVOIR FLUID			
Production Conditions			
Pressure	384.2	bar(g)	Psat
	5571	psig	
Temperature	146.0	°C	
	295	°F	
Separator Conditions			
Pressure	1.015	bar(a)	
	14.718	psig	
Temperature	15.0	°C	
	59	°F	
GOR	226.0	Sm^3/Sm^3	
	1 269	scf/stb	
Liquid phase properties			
Oil tank density at 15.6°C	852	kg/m^3	
60°F	34.6	°API	
Gas phase property			
Gas Relative Density (Air = 1.00)	0.725		

Flash to Standard Conditions of Recombined Reservoir Fluid (Table 2.12)

The reservoir fluid at saturation pressure (384.2 bar(g)) and reservoir temperature is flashed to standard conditions. Liquid and gas phase properties are measured.

The resulting products are analyzed through gas chromatography to determine the mole composition of the two phases.

Table 2.13 Gas and Liquid Compositions with calculated well stream composition

Company: COMPANY		**Well: EXPLO**	
Field: CST		**Formation: OIL**	
SINGLE STAGE SEPARATION TO STANDARD CONDITIONS OF RECOMBINED RESERVOIR FLUID Compositional Analysis of Flashed Products And Calculated Wellstream (GOR = 226 Sm^3/Sm^3)			
Components or Fractions	**Flashed Gas (mol %)**	**Flashed Liquid (mol %)**	**Wellsteam (mol %)**
Hydrogen Sulfide	0.37	0.00	0.27
Nitrogen	0.24	0.00	0.17
Carbon Dioxide	1.18	0.00	0.85
Methane	82.50	0.00	59.27
Ethane	6.85	0.15	4.96
Propane	4.13	0.56	3.12
***i*-Butane**	0.80	0.31	0.66
***n*-Butane**	1.88	1.13	1.67
***i*-Pentanes**	0.62	1.00	0.73
***n*-Pentanes**	0.66	1.53	0.91
Hexanes	0.44	3.34	1.26
Heptanes	0.27	6.61	2.06
Octanes	0.06	8.24	2.36
Nonanes	0.00	6.78	1.91
Decanes		6.44	1.81
Undecanes		5.44	1.53
Dodecanes		4.85	1.37
Tridecanes		5.19	1.46
Tetradecanes		4.48	1.26
Pentadecanes		4.01	1.13
Hexadecanes		3.37	0.95
Heptadecanes		3.24	0.91
Octadecanes		3.09	0.87
Nonadecanes		2.99	0.84
Eicosanes plus		27.25	7.67
TOTAL	100.0	100.0	100.0
Molecular Mass	21.0	233(1)	79.1
Molecular Mass C_{20+}		430(2)	430
Gas Relative Density (air = 1)	0.725		

(1) From cryoscopy measurements.
(2) From simulated distillation.

Single Stage Separation to Standard Conditions of Recombined Reservoir Fluid

Gas and liquid compositions from the gas chromatography analysis are reported. The well stream composition is calculated from the two phase compositions. 226 v/v recombination GOR is used, the one obtained during the flash to standard conditions of recombined reservoir fluid (Table 2.12).

Table 2.14 Calculation of well stream composition

Name	Formula		Katz Mw (1)	GAS % mole (2)	OIL % mole (3)	gas mass (4)	oil mass (5)	nb of moles in 1 m^3 of oil (6)	nb of gas moles associ with 1 m^3 of oil (7)	total nb of moles (8)	fluid fraction mol % (9)	fluid mass (10)
Hydrogen sulfide	H_2S	H_2S	34.08	0.37	0	0.126	0.000	0.0000	0.0354	0.0354	0.27	0.091
Nitrogen	N_2	N_2	28.02	0.24	0.00	0.067	0.000	0.0000	0.0229	0.0229	0.17	0.048
Carbon dioxyde	CO_2	CO_2	44.01	1.18	0.00	0.519	0.000	0.0000	0.1128	0.1128	0.85	0.373
Methane	CH_4	C_1	16.04	82.50	0.00	13.233	0.000	0.0000	7.8854	7.8854	59.29	9.509
Ethane	C_2H_6	C_2	30.07	6.85	0.15	2.060	0.045	0.0056	0.6547	0.6603	4.96	1.493
Propane	C_3H_8	C_3	44.1	4.13	0.56	1.821	0.247	0.0210	0.3947	0.4157	3.13	1.378
i-Butane	C_4H_{10}	*i*-C_4	58.12	0.80	0.31	0.465	0.180	0.0116	0.0765	0.0881	0.66	0.385
n-Butane	C_4H_{10}	*n*-C_4	58.12	1.88	1.13	1.093	0.657	0.0423	0.1797	0.2220	1.67	0.970
i-Pentane	C_5H_{12}	*i*-C_5	72.15	0.62	1.00	0.447	0.722	0.0374	0.0593	0.0967	0.73	0.524
n-Pentane	C_5H_{12}	*n*-C_5	72.15	0.66	1.53	0.476	1.104	0.0573	0.0631	0.1203	0.90	0.653
n-Hexane	C_6H_{14}	C_6	84	0.44	3.34	0.370	2.806	0.1250	0.0421	0.1671	1.26	1.055
n-Heptane	C_7H_{16}	C_7	96	0.27	6.61	0.259	6.346	0.2474	0.0258	0.2732	2.05	1.972
n-Octane	C_8H_{18}	C_8	107	0.06	8.24	0.064	8.817	0.3084	0.0057	0.3141	2.36	2.527
n-Nonane	C_9H_{20}	C_9	121	0.00	6.78	0.000	8.204	0.2538	0.0000	0.2538	1.91	2.308
n-Decane	$C_{10}H_{22}$	C_{10}	134		6.44	0.000	8.630	0.2410	0.0000	0.2410	1.81	2.428
Undecane	$C_{11}H_{24}$	C_{11}	147		5.44	0	7.997	0.2036	0.0000	0.2036	1.53	2.250
Dodecane	$C_{12}H_{26}$	C_{12}	161		4.85	0	7.809	0.1815	0.0000	0.1815	1.36	2.197
Tridecane	$C_{13}H_{28}$	C_{13}	175		5.19	0	9.083	0.1942	0.0000	0.1942	1.46	2.556
Tetradecane	$C_{14}H_{30}$	C_{14}	190		4.48	0	8.512	0.1677	0.0000	0.1677	1.26	2.395
Pentadecane	$C_{15}H_{32}$	C_{15}	206		4.01	0	8.261	0.1501	0.0000	0.1501	1.13	2.324
Hexadecane	$C_{16}H_{34}$	C_{16}	222		3.37	0	7.481	0.1261	0.0000	0.1261	0.95	2.105
Heptadecane	$C_{17}H_{36}$	C_{17}	237		3.24	0	7.679	0.1213	0.0000	0.1213	0.91	2.161
Octodecane	$C_{18}H_{38}$	C_{18}	251		3.09	0	7.756	0.1156	0.0000	0.1156	0.87	2.182
Nonadecane	$C_{19}H_{40}$	C_{19}	263		2.99	0	7.864	0.1119	0.0000	0.1119	0.84	2.213
Eicosane		C_{20+}	431		27.25	0	117.448	1.0199	0.0000	1.0199	7.67	33.049
			Total	100.00	100.00	21.001	227.643			13.3007	100.00	79.148
						29.0 = air						= Mw
			Oil density	852	kg/m^3	0.725						
			GOR	226	v/v							

The comparison of the reservoir fluid composition Table 2.14 with the initial calculated well stream composition in Table 2.9 validates the physical fluid recombination.

Remark: The calculated oil molecular mass (column 5 = 227.6) is different to the measured Mw reported in table 2.13 = 233.

Table 2.15 Two Stage Separation of the Reservoir Fluid

Company: COMPANY		**Well: EXPLO**		
Field: CST		**Formation: OIL**		
TWO STAGE SEPARATION OF THE RESERVOIR FLUID				
Production Conditions				
Pressure	bar(g)	384.2		Psat
	psig	5 571		
Temperature	°C	146.0		
	°F	295		
Separator Conditions		**Stage 1**	**Stage 2**	**Total**
Pressure	bar(a)	15	1.013	
	psig	218	15	
Temperature	°C	77.0	20.9	
	°F	171	70	
GOR (1)	Sm^3/Sm^3	193.3	9.15	
	scf/stb	1 085	51	
GOR (2)	Sm^3/Sm^3	213.4	9.2	222.6
	scf/stb	1 198	52	1250
Liquid phase properties				
Oil Formation Factor (3)				1.733
Liquid Volume Factor (4)		1.104	1.005	
Oil Density (5)	kg/m^3	860	850	
	°API	33.0	35.0	
Gas phase property				
Gas Relative Density (Air = 1.00)		0.704	0.966	

(1) m^3 of gas at 15°C and 1.013 bar(a) per m^3 of liquid at indicated conditions.
(2) m^3 of gas at 15°C and 1.013 bar(a) per m^3 of liquid at 15°C and 1.013 bar(a).
(3) m^3 of reservoir oil at saturation pressure per volume of residual oil at 15°C and 1.013 bar(a).
(4) m^3 of liquid at indicated conditions per m^3 of liquid at 15°C and 1.013 bar(a).
(5) at 15°C and 1.013 bar(a).

Two-Stage Separation of the Reservoir Fluid (Table 2.15)

A two-stage separation of the reservoir fluid at bubble point pressure is performed in the laboratory upon request of the end user. Separation conditions (pressures and temperatures) are determined by the operator and common practices in the field. The oil FVF and GOR obtained are the values to be used for material balance reservoir studies.

Operating conditions in the laboratory are not fully representative of the field operating conditions. Flash operations in the lab are carried out over a very short tubing length. Therefore correction may be necessary to apply for field applications.

The under saturated oil Bo can be calculated:

From the B_o definition:

$$B_o = \frac{V_{o(p)}}{V_{o(std)}} = \frac{V_{o(p)}}{V_{o(pb)}} \times \frac{V_{o(pb)}}{V_{o(std)}} = \text{Relative volume multiplied by oil FVF at } P_{bub}$$

Relative volume is found in Table 2.11.

$V_{o(p)}$: oil volume at pressure P
$V_{o(std)}$: oil volume at standard conditions
$V_{o(pb)}$: oil volume at bubble point pressure

Table 2.16 Two Stage Separation of the Reservoir Fluid Compositional Analysis

Company: COMPANY		**Well: EXPLO**	
Field: CST		**Formation: OIL**	
TWO STAGE SEPARATION OF RESERVOIR FLUID COMPOSITIONAL ANALYSIS OF SEPARATOR GAS, RESIDUAL GAS AND RESIDUAL OIL			
	stage 1	**stage 2**	
	from 146°C/ 384.2 barg to 77°C/ 14 barg	from 77°C/14 barg to 20.9°C/0 barg	
Components or Fractions	**Separator gas (mol %)**	**Residual gas (mol %)**	**Residual Liquid (mol %)**
Hydrogen Sulfide	0.43	1.10	0.00
Nitrogen	0.24	0.00	0.00
Carbon Dioxide	1.18	1.50	0.00
Methane	84.25	58.59	0.00
Ethane	6.55	14.44	0.22
Propane	3.54	12.40	1.02
***i*-Butane**	0.63	2.44	0.46
***n*-Butane**	1.43	5.41	1.71
***i*-Pentanes**	0.46	1.48	1.22
***n*-Pentanes**	0.50	1.44	1.76
Hexanes	0.39	0.82	3.35
Heptanes	0.29	0.31	6.35
Octanes	0.10	0.07	7.91
Nonanes	0.01		6.47
Decanes			6.24
Undecanes			5.20
Dodecanes			4.69
Tridecanes			5.05
Tetradecanes			4.37
Pentadecanes			3.91
Hexadecanes			3.28
Heptadecanes			3.04
Octadecanes			3.01
Nonadecanes			2.91
Eicosanes plus			27.83
TOTAL	100.0	100.0	100.0
Molecular Mass	20.4	28.0	230 (1)
Molecular Mass C_{20+}			430.6 (2)
Gas Relative Density (air = 1)	0.725	0.966	

(1) From cryoscopy measuements.
(2) From simulated distillation.

Two-Stage Separation of Reservoir Fluid (Table 2.16)

Gas from the first stage and second stage and residual oil are analyzed by chromatography and reported. The compositions are used for an Equation of State tuning operation.

Table 2.17 Differential Vaporization Study

Company: COMPANY		Well: EXPLO						
Field: CST		Formation: OIL						
DIFFERENTIAL VAPORISATION STUDY AT T = 146°C (295°F) VOLUMETRIC PROPERTIES								
Pressure		Relative Volume (2)	Liquid Density (kg/m^3)	GOR (3)				z factor of liberated gas
				Liberated		Dissolved		
bar(g)	psig			(v/v)	(scf/bbl)	(v/v)	(scf/bbl)	
384.2 (1)	5 571	1.871	600.0	0.0	0	253.0	1 421	
330.4	4 791	1.714	624.0	53.5	300	199.5	1 120	1.019
275.5	3 995	1.592	647.0	97.4	547	155.6	874	0.971
206	2 987	1.473	673.0	141.4	794	111.6	627	0.946
137.4	1 992	1.377	696.0	178.0	999	75.0	421	0.940
68.6	995	1.292	720.0	210.4	1 181	42.6	239	0.948
19.1	277	1.224	740.0	233.8	1 313	19.2	108	0.971
5.2	75	1.192	751.0	242.1	1 359	10.9	61	0.983
0	0	1.112	774.0	253.0	1 421	0.0	0	0.988
0 at 15°C (60°F)	0	1.000	861.0					

(1) Saturation Pressure at indicated temperature.
(2) Relative to Volume of Residual Oil at 15°C (60°F).
(3) GOR measured as gas at 1.013 bar(a) and 15°C per unit of residual oil at 1.013 bar(a) and 15°C.

Differential Vaporization Liberation (Table 2.17)

Starting at saturation pressure, the differential vaporization study is an approach to simulate the physical phenomenon happening in the reservoir far from the producing well.

Liberated gas and residual oil composition are depicted on Table 2.18.

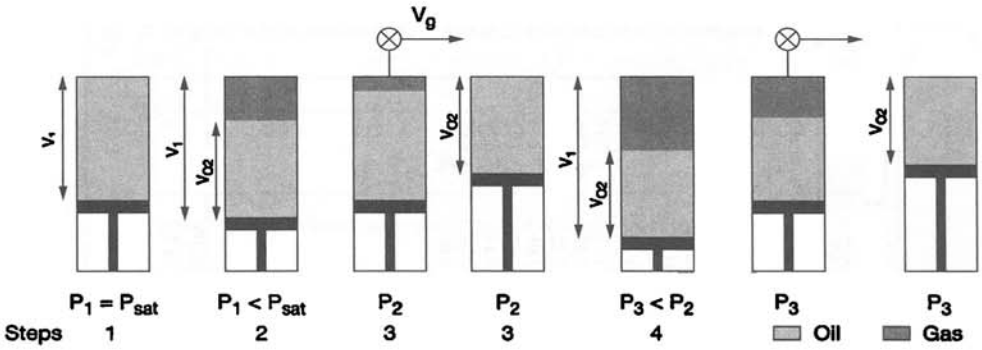

Step 1: sample is at its bubble point pressure
Step 2: sample is depressurized; a gas zone is created at the top of the cell
Step 3: total free gas is produced out of the cell at constant pressure
Step 4: a new pressure step decline is applied

Figure 2.8 Differential Vaporization Experiment.

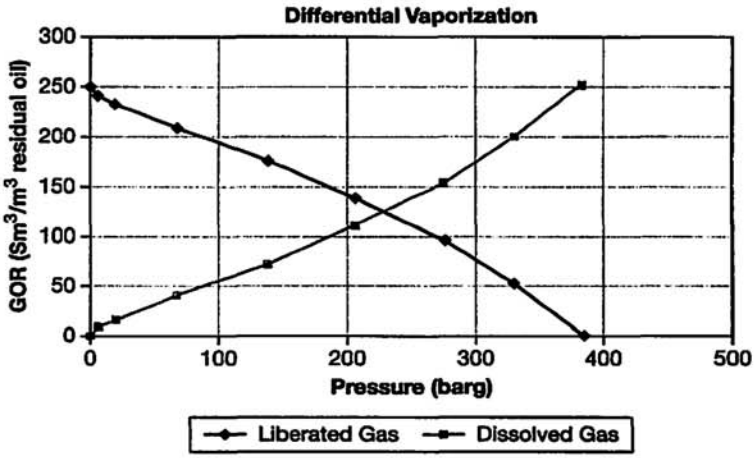

Figure 2.9 Differential Vaporization Liberation.

Table 2.18 Differential Vaporization Study, Compositional Analysis

Company: COMPANY				Well: EXPLO				
Field: CST				Formation: OIL				
DIFFERENTIAL VAPORISATION STUDY at T = 146°C (295°F) Compositional Analysis of Liberated Gases and Residual Oil								Residual liquid (1)
Pressure barg (psig)	330.4 (4 791)	275.5 (3 995)	206.0 (2 987)	137.4 (1 992)	68.6 (995)	19.1 (277)	5.2 (75)	0.0 (0)	0.0 (0)
Components or Fractions	(mol %)	(mol %)	(mol %)	(mol %)	(mol %)	(mol %)	(mol %)	(mol %)	(mol %)
Hydrogen Sulfide	0.20	0.22	0.25	0.31	0.37	0.67	1.30	0.89	0.00
Nitrogen	0.44	0.42	0.27	0.16	0.09	0.05	0.00	0.00	0.00
Carbon Dioxide	1.06	1.07	1.10	1.17	1.31	1.50	1.48	0.47	0.00
Methane	84.68	85.84	86.23	85.69	82.61	70.84	49.09	10.44	0.00
Ethane	5.23	5.13	5.48	6.00	7.48	11.15	15.68	8.08	0.00
Propane	2.59	2.55	2.62	2.87	3.79	7.18	13.74	12.32	0.11
i-Butane	0.48	0.47	0.47	0.50	0.65	1.34	2.96	3.74	0.08
n-Butane	1.15	1.08	1.06	1.13	1.49	3.17	7.17	10.48	0.42
i-Pentanes	0.45	0.41	0.38	0.39	0.50	1.07	2.50	5.15	0.44
n-Pentanes	0.52	0.48	0.44	0.45	0.58	1.22	2.63	6.27	0.72
Hexanes	0.56	0.49	0.43	0.41	0.51	1.01	2.14	8.54	1.86
Heptanes	0.60	0.48	0.40	0.34	0.42	0.62	1.12	11.36	4.47
Octanes	0.37	0.30	0.22	0.17	0.16	0.16	0.18	9.74	6.59
Nonanes	0.27	0.18	0.11	0.07	0.04	0.02	0.01	5.21	6.05
Decanes	0.25	0.16	0.10	0.06	0.00	0.00	0.00	3.08	6.39
Undecanes	0.22	0.14	0.09	0.06	0.00			1.61	5.64
Dodecanes	0.18	0.12	0.07	0.05				0.88	5.23
Tridecanes	0.17	0.11	0.07	0.05				0.62	5.75
Tetradecanes	0.13	0.08	0.05	0.03				0.32	5.04
Pentadecanes	0.11	0.07	0.05	0.03				0.21	4.54
Hexadecanes	0.07	0.04	0.02	0.01				0.11	3.82
Heptadecanes	0.06	0.04	0.02	0.01				0.08	3.57
Octadecanes	0.05	0.03	0.02	0.01				0.08	3.55
Nonadecanes	0.04	0.02	0.01	0.01				0.06	3.44
Eicosanes plus	0.12	0.07	0.04	0.02				0.26	32.29
TOTAL	100.00	100.00	100.00	100.00	100.00	100.00	100.00	100.00	100.00
Molecular Mass	23.0	21.7	20.9	20.6	21.0	24.7	32.4	73.0	253 (2)
Molecular Mass C20+	326.1	321.7	316.1	310.6				319.2	428.7 (3)
Gas Relative Density (air = 1)	0.794	0.749	0.721	0.711	0.725	0.852	1.118	2.519	

(1) Residual oil at 15°C (60°F).

(2) From cryoscopy measurement.

(3) From simulated distillation.

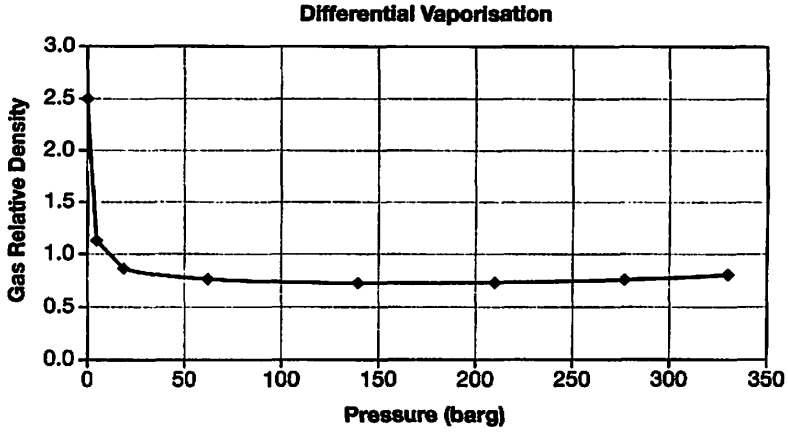

Figure 2.10 Differential Vaporization, Produced Gas Relative Density.

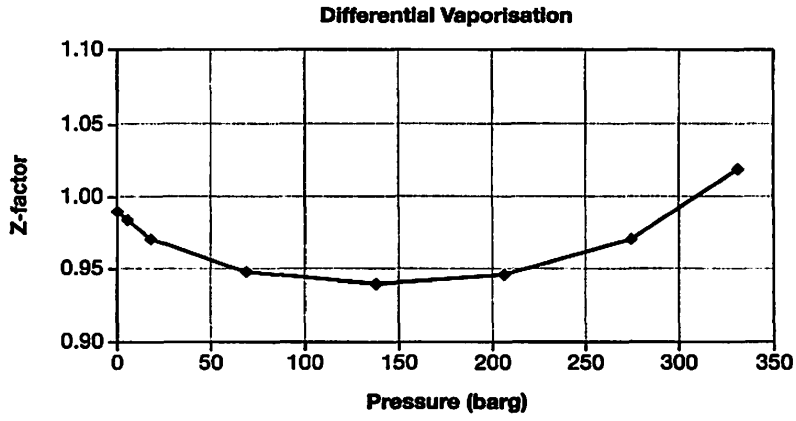

Figure 2.11 Differential Vaporization, Produced Gas Compressibility Factor Z.

Table 2.19 Reservoir Oil Viscosity

Company: COMPANY		**Well: EXPLO**	
Field: CST		**Formation: OIL**	
VISCOSITY OF RESERVOIR FLUID AT T = 146°C (295°F)			
	Pressure		**Viscosity of the liquid phase**
	bar(g)	**psig**	**(cp)**
	447.2	6 484	0.29
	429.9	6 234	0.28
	415.8	6 029	0.27
	398.9	5 784	0.26
	387	5 612	0.26
(1)	**384.2**	5 571	**0.25**
	348.0	5 046	0.26
	282.1	4 090	0.28
	209.8	3 042	0.36
	173.4	2 514	0.40
	135.9	1 971	0.46
	103.9	1 507	0.51
	72.8	1 056	0.57
	56.6	821	0.62
	32.5	471	0.68
	0	0	1.30

(1) Saturation Pressure at indicated Temperature.

Table 2.19 depicts the viscosity of reservoir oil measured through a capillary tube.

Figure 2.10 shows the relative density of produced gas.

Figure 2.11 shows the produced gas compressibility factor Z.

Figure 2.12 depicts the reservoir oil viscosity versus pressure.

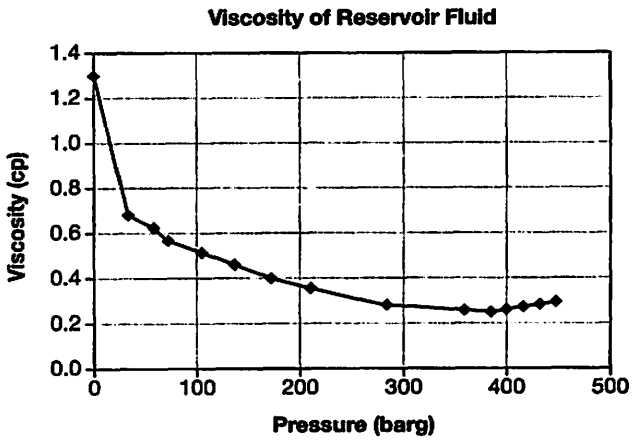

Figure 2.12 Reservoir Oil Viscosity.

Remark:
The minimum oil viscosity is at the bubble point pressure.

2.9 PVT GAS STUDY

The following tables show a typical Gas PVT report, result of a complete study carried out in the laboratory. In the case of a dry gas reservoir, only gas bottles are available. For wet gas and gas condensate, liquid and gas samples are collected, similarly to the oil reservoir (Table 2.20). Upon arrival in the laboratory, the sample bottles are checked. A gas and oil bottles are chosen on which the complete study is carried out (Table 2.21).

Reservoir fluid recombination (calculated and physical) from the two samples must be carried out in the same conditions as the one prevailing during sampling.

The oil sample collected at the separator has been flashed to atmospheric pressure and laboratory temperature. Both fluids (liquid and vapor) obtained were analyzed by gas chromatography for composition determination and results reported on Table 2.23. The separator oil composition is calculated by mathematical recombination applying the measured GOR and oil density during the flash operation (calculation Table 2.24).

Oil density = 808.5 kg/m^3

GOR = 24.4 Sm^3/Sm^3

Gas sample is analyzed by gas chromatography; the resulting compositions are depicted on Table 2.26. The gas rate is measured through an orifice meter. Usually the GOR (gas Oil Ratio) is determined from the oil rate measured at separator conditions and gas rate converted to standard conditions. The measuring conditions are reported on the test sheet. Knowing the sampled gas and oil compositions, the recombination is calculated with the proper corrected GOR and the measured stock tank oil density (Table 2.25).

Table 2.20 Summary of Sampling Conditions

Company: COMPANY	**Well: KOT-1**		
Field: CST	**Formation: GAS**		
SUMMARY OF SAMPLING CONDITIONS SEPARATOR SAMPLES 0459 N 257 & S543203			
Reservoir and Well Characteristics: (1)			
Production Zone	3 700-3 732	m BRT	
Datum Level	3 675	m BRT	12 057 ft BRT
Static Reservoir Pressure	478.7	bar(g)	6 941 psig
Reservoir Temperature	161.7	°C	323 °F
Bottomhole Flowing Pressure	n.a.		n.a. psig
Bottomhole Flowing Temperature	n.a.		n.a. °F
Surface Conditions: (2)			
Date of Sampling	06.07.96		
Wellhead Pressure	285.6	bar(g)	4 141 psig
Wellhead Temperature	120.3	°C	249° F
Separator Presure	35.2	bar(g)	510 psig
Separator Temperature	82.0	°C	180 °F
Stock Tank Temperature	n.a.	°C	n.a. °F
Atmospheric Pressure	n.a.	bar(g)	n.a. psig
Stock Tank Oil Rate	n.a.	Sm^3/d	n.a. bbl/d
First Stage Separator Oil Rate	367	m^3/d	2,308 bbl/d
First Stage Separator Gas Rate	586 201	Sm^3/d	2.07E+07 scf/d
Gas Relative Density (Air = 1)	0.720		
Gas Compressibility Factor (std)	0.944		
Oil Density (std)	810.4	kg/m^3	43.1 °API
BSW	0.0	%	
Shrinkage	n.a.		n.a.
Separator Gas-Stock Tank Oil Ratio	n.a.	Sm^3/m^3	n.a. scf/stb
Separator Gas-Separator Oil Ratio	1 596.5	Sm^3/m^3	scf/stb

(1) Test Report.
(2) Sampling Sheets.

Table 2.21 Checking of Sample Bottles

Company: COMPANY					**Well: KOT-1**		
Field: CST					**Formation: GAS**		
CHECK OF SAMPLES RECEIVED IN THE LABORATORY							
	Separator Oil		**Opening Pressure**			**Saturation Pressure**	
			bar(g)	at	°C	bar(g)	at °C
	Sample N°	Cylinder N°	psig	at	°F	psig	at °F
	1	8008 N 148	0.0		15.0	34.4	82
			0		59	499	180
(*)	2	0459 N 257	33.9		83.0	33.9	82
			492		181.4	492	180
	Separator Gas		**Opening Pressure**				
			bar(g)	at	°C		
	Bottle N°	With Oil Bottle	psig	at	°F		
	S 543175	1	42.0		80		
			609		176		
	S 543187	1	42.0		80		
			609		176		
	S 615927	2	45.0		80		
			653		176		
(*)	S 543203	2	42.5		80		
			616		176		

(*) Samples used for Recombination.

Table 2.22 Flash of Liquid sample

Company: COMPANY		**Well: KOT-1**	
***Field:* CST**		***Formation:* GAS**	
FLASH OF SEPARATOR OIL SAMPLE **Sample N° 0459N257**			
Production Conditions			
Pressure	33.9	bar(g)	Psat
	492	psig	
Temperature	82.0	°C	
	180	°F	
Separator Conditions			
Pressure	1.013	bar(a)	
	14.69	psig	
Temperature	15.0	°C	
	59	°F	
GOR (1)	24.4	Sm^3/Sm^3	
	137	scf/stb	
Liquid phase properties			
Liquid volume factor (2)	1.156		
Oil tank density at 15.6°C	808.5	kg/m^3	
60°F	44	°API	
Gas phase property			
Gas Relative Density (Air = 1.00)	0.942		

(1) m^3 of gas at 15°C and 1.013 bar(a) per m^3 of residual liquid at 15°C and 1.013 bar(a).
(2) m^3 of liquid at indicated conditions, per m^3 of liquid at 15°C and 1.013 bar(a).

Table 2.23 Liquid and gas Compositions; calculated oil composition

Company: COMPANY		**Well: KOT-1**	
Field: CST		**Formation: GAS**	
SINGLE STAGE SEPARATION TO STANDARD CONDITIONS OF SEPARATOR OIL Sample N° 0459N257			
Components or Fractions	**Tank Gas (mol %)**	**Tank Liquid (mol %)**	**Separator Oil (mol %)**
Hydrogen Sulfide	8.40	0.00	1.49
Nitrogen	0.17	0.00	0.03
Carbon Dioxide	2.70	0.00	0.48
Methane	61.90	0.00	10.95
Ethane	7.94	0.12	1.50
Propane	8.26	0.69	2.03
***i*-Butane**	1.97	0.53	0.78
***n*-Butane**	3.86	1.57	1.98
***i*-Pentanes**	1.38	1.45	1.44
***n*-Pentanes**	1.42	2.06	1.95
Hexanes	1.08	4.82	4.16
Heptanes	0.62	8.91	7.44
Octanes	0.29	11.93	9.87
Nonanes	0.01	10.43	8.59
Decanes	0.00	9.08	7.47
Undecanes	0.00	7.13	5.87
Dodecanes	0.00	5.56	4.58
Tridecanes	0.00	5.55	4.57
Tetradecanes	0.00	4.49	3.70
Pentadecanes	0.00	3.86	3.18
Hexadecanes	0.00	2.99	2.46
Heptadecanes	0.00	2.65	2.18
Octadecanes	0.00	2.36	1.94
Nonadecanes	0.00	2.14	1.76
Eicosanes plus	0.00	11.68	9.61
TOTAL	100.00	100.00	100.00
Molecular Mass	27.3	168.4	143.3
Molecular Mass C20+ (1)		377	377
Gas Relative Density (air = 1)	0.942		

(1) From simulated distillation results.

Table 2.24 Recombination Calculation of Table 2.23

Name	Formula		Katz Mw (1)	GAS % mole (2)	OIL % mole (3)	gas mass (4)	oil mass (5)	nb of moles in 1 m^3 of oil (6)	nb of gas moles associ with 1 m^3 of oil (7)	total nb of moles (8)	Recombined fluid fraction mol % (9)	Recombined fluid mass (10)
Hydrogen sulfide	H_2S	H_2S	34.08	8.40	0.00	2.863	0.000	0.0000	0.0867	0.0867	1.49	0.506
Nitrogen	N_2	N_2	28.02	0.17	0.00	0.048	0.000	0.0000	0.0018	0.0018	0.03	0.008
Carbon dioxyde	CO_2	CO_2	44.01	2.70	0.00	1.188	0.000	0.0000	0.0279	0.0279	0.48	0.210
Methane	CH_4	C_1	16.04	61.90	0.00	9.929	0.000	0.0000	0.6388	0.6388	10.95	1.756
Ethane	C_2H_6	C_2	30.07	7.94	0.12	2.388	0.036	0.0058	0.0819	0.0877	1.50	0.452
Propane	C_3H_8	C_3	44.1	8.26	0.69	3.643	0.304	0.0331	0.0852	0.1184	2.03	0.895
i-Butane	C_4H_{10}	*i*-C_4	58.12	1.97	0.53	1.145	0.308	0.0254	0.0203	0.0458	0.78	0.456
n-Butane	C_4H_{10}	*n*-C_4	58.12	3.86	1.57	2.243	0.912	0.0754	0.0398	0.1152	1.98	1.148
i-Pentane	C_5H_{12}	*i*-C_5	72.15	1.38	1.45	0.996	1.046	0.0696	0.0142	0.0839	1.44	1.037
n-Pentane	C_5H_{12}	*n*-C_5	72.15	1.42	2.06	1.025	1.486	0.0989	0.0147	0.1136	1.95	1.405
n-Hexane	C_6H_{14}	C_6	84	1.08	4.82	0.907	4.049	0.2314	0.0111	0.2426	4.16	3.493
n-Heptane	C_7H_{16}	C_7	96	0.62	8.91	0.595	8.554	0.4278	0.0064	0.4342	7.44	7.146
n-Octane	C_8H_{18}	C_8	107	0.29	11.93	0.310	12.765	0.5728	0.0030	0.5758	9.87	10.562
n-Nonane	C_9H_{20}	C_9	121	0.01	10.43	0.012	12.620	0.5008	0.0001	0.5009	8.59	10.390
n-Decane	$C_{10}H_{22}$	C_{10}	134		9.08	0	12.167	0.4360	0.0000	0.4360	7.47	10.015
Undecane	$C_{11}H_{24}$	C_{11}	147		7.13	0	10.481	0.3424	0.0000	0.3424	5.87	8.627
Dodecane	$C_{12}H_{26}$	C_{12}	161		5.56	0	8.952	0.2670	0.0000	0.2670	4.58	7.368
Tridecane	$C_{13}H_{28}$	C_{13}	175		5.55	0	9.713	0.2665	0.0000	0.2665	4.57	7.994
Tetradecane	$C_{14}H_{30}$	C_{14}	190		4.49	0	8.531	0.2156	0.0000	0.2156	3.70	7.022
Pentadecane	$C_{15}H_{32}$	C_{15}	206		3.86	0	7.952	0.1853	0.0000	0.1853	3.18	6.545
Hexadecane	$C_{16}H_{34}$	C_{16}	222		2.99	0	6.638	0.1436	0.0000	0.1436	2.46	5.464
Heptadecane	$C_{17}H_{36}$	C_{17}	237		2.65	0	6.281	0.1272	0.0000	0.1272	2.18	5.170
Octodecane	$C_{18}H_{38}$	C_{18}	251		2.36	0	5.924	0.1133	0.0000	0.1133	1.94	4.876
Nonadecane	$C_{19}H_{40}$	C_{19}	263		2.14	0	5.628	0.1028	0.0000	0.1028	1.76	4.633
Eicosane		C_{20+}	377		11.68	0	44.034	0.5608	0.0000	0.5608	9.61	36.244
			Total	100.00	100.00	27.29	168.380			5.8336		143.4
						28.98	= air					= Mw
		Oil density		808.5	kg/m^3	0.942						
		GOR		24.4	v/v							

Based on the computed composition, (Tables 2.23, 2.24) the physical recombination of the samples is carried out.

Once the separator products have been recombined with the corrected GOR (Table 2.25), the well stream composition is measured (by flashing the reservoir fluid to standard conditions and gas chromatography) and compared with the calculated composition. The objective of this operation is to validate the physical recombination and check consistency of measurements.

The final composition and data obtained are the one to use for further reservoir engineering work.

Table 2.25 Correction of Field measurements

Company: COMPANY			**Well: KOT-1**	
Field: CST			**Formation: GAS**	
CORRECTION OF THE GASOIL RATIO BOTTLES 0459N257 & S 543203				
Corrected GOR		$GOR_{corrected} = GOR_{field} \times \frac{\sqrt{(\gamma \times z)_{field}}}{\sqrt{(\gamma \times z)_{lab}}}$		
with	GOR	: Gas Oil Ratio (v/v)		
	γ	: Gas Relative Density (air = 1)		
	z	: Gas Compressibility Factor		
	γ_{field}		0.720	
	z_{field}		0.945	(= $1/fpv^2$)
	γ_{lab}		0.704	
	z_{lab}		0.947	
Separator GOR_{field}			1 596.5	Sm^3/m^3sep
			8 964	scf/bbl sep
Separator $GOR_{corrected}$			1 612.9	Sm^3/m^3sep
			9 056	scf/bbl sep
Separator Liquid Volume Factor			1.156	(1)
Tank $GOR_{corrected}$			1 864	Sm^3/Sm^3
			10 466	scf/stb

(1) Laboratory data.

Table 2.26 Calculated Well stream Composition.

Company: COMPANY			**Well: KOT-1**
Field: CST			**Formation: GAS**
COMPOSITIONAL ANALYSIS OF THE SEPARATOR FLUIDS AND CALCULATED WELL STREAM (GOR = 1 612.9 Sm^3/m^3 sep)			
Components or Fractions Bottle N°	**Separator Gas (mol %)** S 543203	**Separator Liquid (mol %)** 0459N257	**Wellstream (mol %)**
Hydrogen Sulfide	5.08	1.49	4.84
Nitrogen	1.08	0.03	1.01
Carbon Dioxide	2.20	0.48	2.08
Methane	83.09	10.95	78.27
Ethane	3.44	1.50	3.31
Propane	2.30	2.03	2.28
***i*-Butane**	0.44	0.78	0.46
***n*-Butane**	0.88	1.98	0.95
***i*-Pentanes**	0.35	1.44	0.42
***n*-Pentanes**	0.38	1.95	0.48
Hexanes	0.33	4.16	0.59
Heptanes	0.22	7.44	0.70
Octanes	0.16	9.87	0.81
Nonanes	0.05	8.59	0.62
Decanes	0.00	7.47	0.50
Undecanes	0.00	5.87	0.39
Dodecanes	0.00	4.58	0.31
Tridecanes	0.00	4.57	0.31
Tetradecanes	0.00	3.70	0.25
Pentadecanes	0.00	3.18	0.21
Hexadecanes	0.00	2.46	0.16
Heptadecanes	0.00	2.18	0.15
Octadecanes	0.00	1.94	0.13
Nonadecanes	0.00	1.76	0.12
Eicosanes plus	0.00	9.60	0.64
TOTAL	100.0	100.0	100.0
Molecular Mass	20.40	143.4	28.6
Molecular Mass C20+ (1)		377	377
Gas Relative Density (air = 1)	0.704		

Well stream composition is calculated from gas and liquid separator compositions with a recombination GOR of 1612.9 v/v = corrected separator GOR obtained in Table 2.25.

Table 2.27 Calculation of Well Stream Composition.

Name	Formula		Katz Mw (1)	GAS % mole (2)	OIL % mole (3)	gas mass (4)	oil mass (5)	nb of moles in 1 m^3 of oil (6)	nb of gas moles associ with 1 m^3 of oil (7)	total nb of moles (8)	Recombined fluid fraction mol % (9)	Recombined fluid mass (10)
Hydrogen sulfide	H_2S	H_2S	34.08	5.08	1.49	1.731	0.508	0.0727	3.4652	3.5379	4.84	1.650
Nitrogen	N_2	N_2	28.02	1.08	0.03	0.303	0.008	0.0015	0.7367	0.7382	1.01	0.283
Carbon dioxyde	CO_2	CO_2	44.01	2.20	0.48	0.968	0.211	0.0234	1.5007	1.5241	2.09	0.918
Methane	CH_4	C_1	16.04	83.09	10.95	13.328	1.756	0.5341	56.6783	57.2124	78.28	12.555
Ethane	C_2H_6	C_2	30.07	3.44	1.50	1.034	0.451	0.0732	2.3465	2.4197	3.31	0.995
Propane	C_3H_8	C_3	44.1	2.30	2.03	1.014	0.895	0.0990	1.5689	1.6679	2.28	1.006
i-Butane	C_4H_{10}	*i*-C_4	58.12	0.44	0.78	0.256	0.453	0.0380	0.3001	0.3382	0.46	0.269
n-Butane	C_4H_{10}	*n*-C_4	58.12	0.88	1.98	0.511	1.151	0.0966	0.6003	0.6969	0.95	0.554
i-Pentane	C_5H_{12}	*i*-C_5	72.15	0.35	1.44	0.253	1.039	0.0702	0.2387	0.3090	0.42	0.305
n-Pentane	C_5H_{12}	*n*-C_5	72.15	0.38	1.95	0.274	1.407	0.0951	0.2592	0.3543	0.48	0.350
n-Hexane	C_6H_{14}	C_6	84	0.33	4.16	0.277	3.494	0.2029	0.2251	0.4280	0.59	0.492
n-Heptane	C_7H_{16}	C_7	96	0.22	7.44	0.211	7.142	0.3629	0.1501	0.5130	0.70	0.674
n-Octane	C_8H_{18}	C_8	107	0.16	9.87	0.171	10.561	0.4814	0.1091	0.5906	0.81	0.865
n-Nonane	C_9H_{20}	C_9	121	0.05	8.59	0.061	10.394	0.4190	0.0341	0.4531	0.62	0.750
n-Decane	$C_{10}H_{22}$	C_{10}	134		7.47	0	10.010	0.3644	0.0000	0.3644	0.50	0.668
Undecane	$C_{11}H_{24}$	C_{11}	147		5.87	0	8.629	0.2863	0.0000	0.2863	0.39	0.576
Dodecane	$C_{12}H_{26}$	C_{12}	161		4.58	0	7.374	0.2234	0.0000	0.2234	0.31	0.492
Tridecane	$C_{13}H_{28}$	C_{13}	175		4.57	0	7.998	0.2229	0.0000	0.2229	0.30	0.534
Tetradecane	$C_{14}H_{30}$	C_{14}	190		3.70	0	7.030	0.1805	0.0000	0.1805	0.25	0.469
Pentadecane	$C_{15}H_{32}$	C_{15}	206		3.18	0	6.551	0.1551	0.0000	0.1551	0.21	0.437
Hexadecane	$C_{16}H_{34}$	C_{16}	222		2.46	0	5.461	0.1200	0.0000	0.1200	0.16	0.364
Heptadecane	$C_{17}H_{36}$	C_{17}	237		2.18	0	5.167	0.1063	0.0000	0.1063	0.15	0.345
Octodecane	$C_{18}H_{38}$	C_{18}	251		1.94	0	4.869	0.0946	0.0000	0.0946	0.13	0.325
Nonadecane	$C_{19}H_{40}$	C_{19}	263		1.76	0	4.629	0.0859	0.0000	0.0859	0.12	0.309
Eicosane		C_{20+}	377		9.60	0	36.192	0.4683	0.0000	0.4683	0.64	2.415
			Total	100.00	100.00	20.4	143.4			73.0910	100.00	28.60
						28.98	= air					= Mw
		Oil density		699.39	kg/m^3	0.704						
		GOR		1 612.9	v/v							

Table 2.28 Constant Composition Expansion

Company: COMPANY			**Well: KOT-1**			
Field: CST			**Formation: GAS**			
PRESSURE VOLUME RELATION OF RESERVOIR FLUID AT T = 161.7°C (323°F) (1) (Constant Composition Study)						
	Pressure		**Relative Volume (V/Vsat) (4)**	**Specific Volume (m^3/kg)**	**Compressibility Factor z (5)**	**Retrograde Liquid (%) (6)**
	bar(g)	**psig**				
	557.9	8 090	0.9112	2.901E-03	1.301	
(2)	520.6	7 549	0.9388	2.989E-03	1.251	
	490.6	7 114	0.9644	3.071E-03	1.211	
	460.6	6 679	0.9943	3.166E-03	1.173	
(3)	**455.5**	6 605	**1.0000**	**3.184E-03**	**1.166**	**0.000**
	454.8	6 595	1.0008	3.18E-03		0.046
	453.7	6 579	1.0020	3.190E-03		0.117
	452.4	6 560	1.0035	3.195E-03		0.198
	450.0	6 525	1.0061	3.203E-03		0.339
	447.6	6 490	1.0092	3.213E-03		0.476
	444.8	6 450	1.0104	3.217E-03		0.639
	440.2	6 383	1.0186	3.243E-03		0.934
	434.8	6 305	1.0257	3.266E-03		1.375
	429.9	6 234	1.0326	3.288E-03		1.916
	404.6	5 867	1.0688	3.403E-03		4.118
	380.1	5 511	1.1106	3.536E-03		6.133
	350.5	5 082	1.1718	3.731E-03		8.212
	305.4	4 428	1.2917	4.113E-03		10.519
	249.9	3 624	1.5150	4.825E-03		12.266
	204.5	2 965	1.8035	5.742E-03		12.955
	151.1	2 191	2.3946	7.624E-03		13.156
	126.3	1 831	2.8523	9.082E-03		12.981

(1) Reservoir Temperature.
(2) Reservoir Pressure.
(3) Saturation Pressure at indicated Temperature.
(4) Vsat = Volume of fluid at Saturation Pressure and indicated Temperature.
(5) z = PV/nRT, with n = moles at Saturation Pressure.
(6) Retrograde Liquid Volume at indicated Pressure/Total Volume at Saturation Pressure.

Constant Composition Expansion (CCE) (Table 2.28)

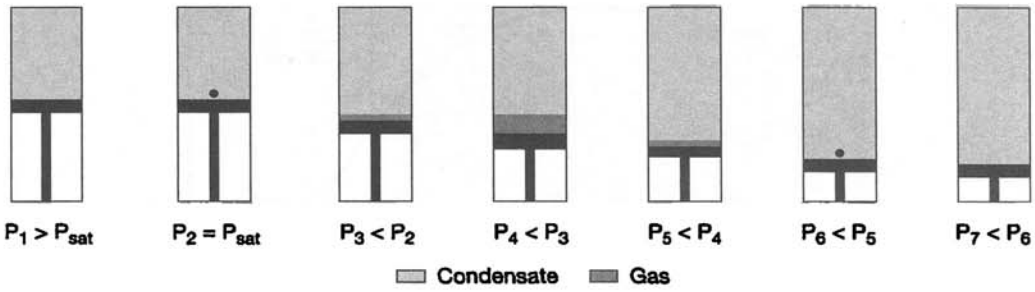

Figure 2.13 Constant Composition Expansion.

At reservoir temperature, the dew point pressure (or saturation pressure) is the pressure at which the first bubble of condensate appears in the cell during the depletion process.

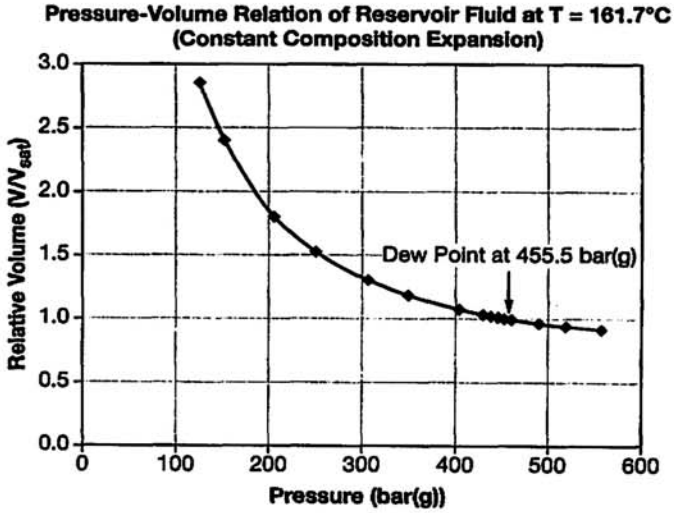

Figure 2.14 Constant Composition Expansion Graph.

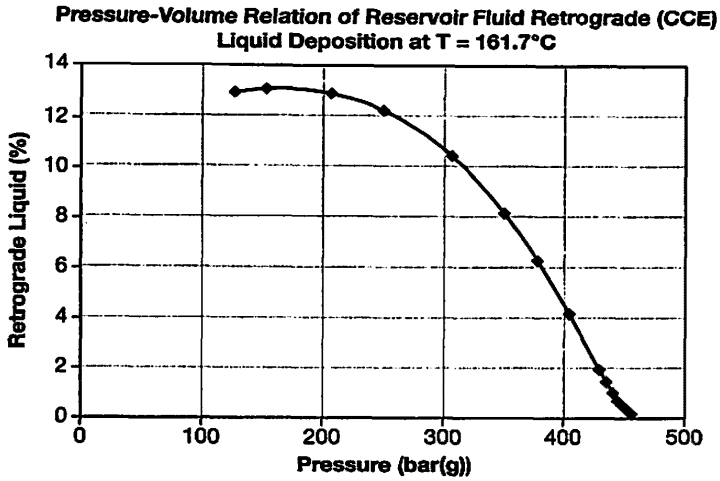

Figure 2.15 Constant Composition Expansion Liquid drop.

Table 2.29 Reservoir Fluid Flash to Standard Conditions

Company: COMPANY		**Well: KOT-1**	
Field: CST		**Formation: GAS**	
RESERVOIR FLUID FLASH TO STANDARD CONDITIONS			
Production Conditions			
Pressure	455.5	bar(g)	**Psat**
	6 605	psig	
Temperature	161.7	°C	
	323	°F	
Separator Conditions			
Pressure	1.013	bar(a)	
	14.69	psig	
Temperature	0.0	°C	
	32	°F	
GOR (1)	1 834.1	Sm^3/Sm^3	
	10 298	scf/stb	
Liquid phase properties			
Oil tank density at 15.6°C	806.7	kg/m^3	
60°F	44	°API	
Gas phase property			
Expansion volume factor (1)	241.1		
Gas Relative Density (Air = 1.00)	0.703		

(1) m^3 of gas at 15°C and 1.013 bar(a) per m^3 of residual liquid at indicated conditions.

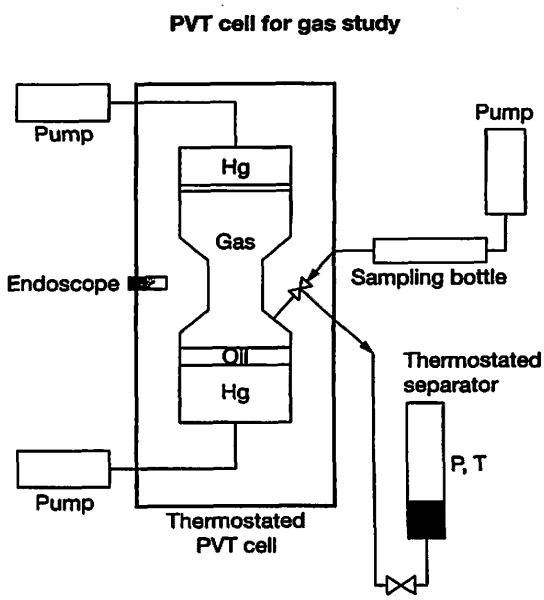

Figure 2.16 Thermo stated cell to study gas condensate gases.

CCE

Gas is introduced between two floating pistons. Floating piston displacements are controlled by mercury pumps. In the middle of the cell, a sapphire window allows the operator to have an inside visual control thanks to an endoscope.

Visual control is necessary to detect the first liquid drop (dew point pressure) or critical conditions and measure in-situ volumes.

Flash Liberation

The reservoir fluid at its dew point pressure is flashed to standard conditions and resulting fluids are analyzed by gas chromatography. Finally, from the composition obtained, the well stream composition is calculated by recombination of oil and gas associated with a recombination GOR of 1834.1 v/v, obtained in Table 2.29.

This final well stream composition is the one to use for further reservoir study.

Table 2.30 Reservoir Fluid Flash to Standard Conditions; Compositions

Company: COMPANY		**Well: KOT-1**	
Field: CST		**Formation: GAS**	
RESERVOIR FLUID SINGLE STAGE SEPARATION TO STANDARD CONDITIONS **Compositional Analysis of Flashed Products** **And Calculated Reservoir Fluid Composition (GOR = 1834.1 Sm^3/Sm^3)**			
Components or Fractions	**Flashed Gas (mol %)**	**Flashed Liquid (mol %)**	**Wellsteam (mol %)**
Hydrogen Sulfide	5.53	0.00	5.21
Nitrogen	0.43	0.00	0.41
Carbon Dioxide	2.09	0.00	1.97
Methane	83.28	0.00	78.51
Ethane	3.55	0.06	3.35
Propane	2.19	0.24	2.08
***i*-Butane**	0.46	0.15	0.44
***n*-Butane**	0.93	0.62	0.91
***i*-Pentanes**	0.39	0.74	0.41
***n*-Pentanes**	0.43	1.22	0.48
Hexanes	0.37	4.01	0.58
Heptanes	0.20	8.99	0.70
Octanes	0.12	13.00	0.86
Nonanes	0.03	11.41	0.68
Decanes	0.00	9.69	0.55
Undecanes		7.47	0.43
Dodecanes		5.78	0.33
Tridecanes		5.75	0.33
Tetradecanes		4.65	0.27
Pentadecanes		4.03	0.23
Hexadecanes		3.12	0.18
Heptadecanes		2.80	0.16
Octadecanes		2.54	0.15
Nonadecanes		2.33	0.13
Eicosanes plus		11.40	0.65
TOTAL	100.0	100.0	100.0
Molecular Mass	20.4	171.2	29.0
Molecular Mass C_{20+}		377	377
Gas Relative Density (air = 1)	0.703		

Table 2.31 Calculation of Table 2.30

Name	Formula		Katz Mw (1)	GAS % mole (2)	OIL % mole (3)	gas mass (4)	oil mass (5)	nb of moles in 1 m^3 of oil (6)	nb of gas moles associ with 1 m^3 of oil (7)	total nb of moles (8)	Recombined fluid fraction mol % (9)	Recombined fluid mass (10)
Hydrogen sulfide	H_2S	H_2S	34.08	5.53	0.00	1.885	0.000	0.0000	4.2895	4.2895	5.21	1.777
Nitrogen	N_2	N_2	28.02	0.43	0.00	0.120	0.000	0.0000	0.3335	0.3335	0.41	0.114
Carbon dioxyde	CO_2	CO_2	44.01	2.09	0.00	0.920	0.000	0.0000	1.6212	1.6212	1.97	0.867
Methane	CH_4	C_1	16.04	83.28	0.00	13.358	0.000	0.0000	64.5988	64.5988	78.51	12.593
Ethane	C_2H_6	C_2	30.07	3.55	0.06	1.067	0.018	0.0028	2.7537	2.7565	3.35	1.007
Propane	C_3H_8	C_3	44.1	2.19	0.24	0.966	0.106	0.0113	1.6987	1.7101	2.08	0.917
i-Butane	C_4H_{10}	*i*-C_4	58.12	0.46	0.15	0.267	0.087	0.0071	0.3568	0.3639	0.44	0.257
n-Butane	C_4H_{10}	*n*-C_4	58.12	0.93	0.62	0.541	0.360	0.0292	0.7214	0.7506	0.91	0.530
i-Pentane	C_5H_{12}	*i*-C_5	72.15	0.39	0.74	0.281	0.534	0.0349	0.3025	0.3374	0.41	0.296
n-Pentane	C_5H_{12}	*n*-C_5	72.15	0.43	1.22	0.310	0.880	0.0575	0.3335	0.3910	0.48	0.343
n-Hexane	C_6H_{14}	C_6	84	0.37	4.01	0.311	3.368	0.1889	0.2870	0.4759	0.58	0.486
n-Heptane	C_7H_{16}	C_7	96	0.20	8.99	0.192	8.630	0.4236	0.1551	0.5787	0.70	0.675
n-Octane	C_8H_{18}	C_8	107	0.12	13.00	0.128	13.910	0.6125	0.0931	0.7056	0.86	0.918
n-Nonane	C_9H_{20}	C_9	121	0.03	11.41	0.036	13.806	0.5376	0.0233	0.5609	0.68	0.825
n-Decane	$C_{10}H_{22}$	C_{10}	134	0.00	9.69	0	12.985	0.4566	0.0000	0.4566	0.55	0.744
Undecane	$C_{11}H_{24}$	C_{11}	147		7.47	0	10.981	0.3520	0.0000	0.3520	0.43	0.629
Dodecane	$C_{12}H_{26}$	C_{12}	161		5.78	0	9.306	0.2723	0.0000	0.2723	0.33	0.533
Tridecane	$C_{13}H_{28}$	C_{13}	175		5.75	0	10.063	0.2709	0.0000	0.2709	0.33	0.576
Tetradecane	$C_{14}H_{30}$	C_{14}	190		4.65	0	8.835	0.2191	0.0000	0.2191	0.27	0.506
Pentadecane	$C_{15}H_{32}$	C_{15}	206		4.03	0	8.302	0.1899	0.0000	0.1899	0.23	0.475
Hexadecane	$C_{16}H_{34}$	C_{16}	222		3.12	0	6.926	0.1470	0.0000	0.1470	0.18	0.397
Heptadecane	$C_{17}H_{36}$	C_{17}	237		2.80	0	6.36	0.1319	0.0000	0.1319	0.16	0.380
Octodecane	$C_{18}H_{38}$	C_{18}	251		2.54	0	6.375	0.1197	0.0000	0.1197	0.15	0.365
Nonadecane	$C_{19}H_{40}$	C_{19}	263		2.33	0	6.128	0.1098	0.0000	0.1098	0.13	0.351
Eicosane		C_{20+}	377		11.40	0	42.978	0.5371	0.0000	0.5371	0.65	2.461
			Total	100.00	100.00	20.4	171.2			82.2798	100.00	29.02
		Oil density		806.7	kg/m^3	28.98	= air					= Mw
		GOR		1834.1	v/v	0.703						

Table 2.32 Constant Volume Depletion

Company: COMPANY					Well: KOT-1					
Field: CST					Formation: GAS					
CONSTANT VOLUME DEPLETION STUDY AT T = 161.7°C (323°F) (Measured Properties)										
Pressure		Cumulative Production (%) (2)	Produced Gas Relative Density (air = 1)	Compressibility Factor z (3)	Retrograde Liquid (%) (4)	Liquid Content of Produced well stream kg/m³			Cumulative Liquid Recovery (%)		
bar(g)	(psig)					Propanes+	Butanes+	Pentanes+	Propanes+	Butanes+ (5)	Pentanes+
455.5 (1)	6605	0.00	1.002	1.167	0.00	0.536	0.497	0.464	0.00	0.00	0.00
393.0	5699	7.24	0.924	1.098	5.38	0.431	0.394	0.363	5.83	5.74	5.66
330.2	4788	16.52	0.868	1.044	8.97	0.357	0.321	0.289	12.00	11.73	11.45
268.6	3895	28.07	0.828	1.011	10.53	0.303	0.267	0.236	18.53	17.93	17.34
205.0	2973	41.84	0.796	0.987	11.02	0.259	0.223	0.193	25.19	24.12	23.08
141.6	2053	58.69	0.776	0.979	10.56	0.232	0.195	0.164	31.69	30.01	28.41
79.7	1156	76.25	0.762	0.984	9.74	0.208	0.178	0.148	39.21	36.95	34.58

(1) Saturation Pressure at indicated temperature.
(2) Moles of wet gas produced per moles of fluid at Saturation Pressure.
(3) z = PV/nRT, with n = nb of moles at Saturation Pressure.
(4) Volume of Retrograde Liquid at indicated Pressure/Total Volume at Saturation Pressure.
(5) Mass of recovered Compound/Total mass of the same Compound in the initial Fluid.

Constant Volume Depletion (CVD) (Table 2.32)

The experiment simulates the depletion of a closed gas reservoir. At reservoir temperature, the operation consists in increasing the cell volume creating a pressure drop in the gas from the initial state set at the dew point pressure. Liquid drop is observed in the cell. Some gas is produced out the cell by displacing the piston at constant gas pressure, back to the initial position (initial pore volume). Liquid drop occurring in the cell is measured, and the produced gas analyzed through a gas chromatograph and measured. The operation is repeated six to ten times.

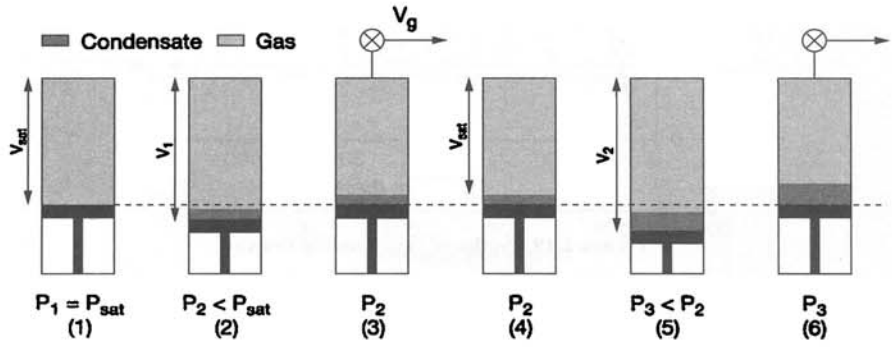

Step 1: gas sample at reservoir temperature and saturation pressure P_{dew}
Step 2: pressure step decline to P_2
Step 3: gas production at constant pressure P_2
Step 4: cell volume back at initial V_{sat} of step 1
Step 5: new pressure step decline to P_3

Figure 2.17 Constant Volume Depletion (CVD).

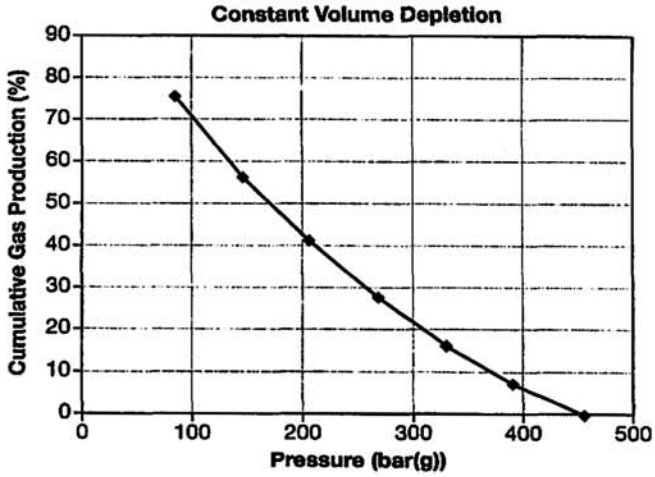

Figure 2.18 Cumulative Gas Produced.

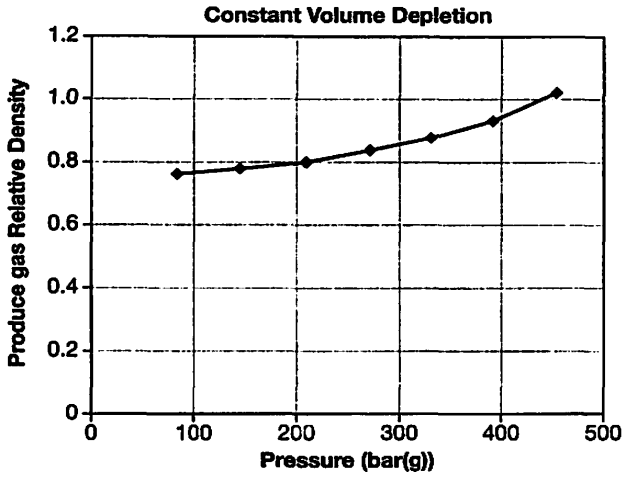

Figure 2.19 Produced Gas Relative Density.

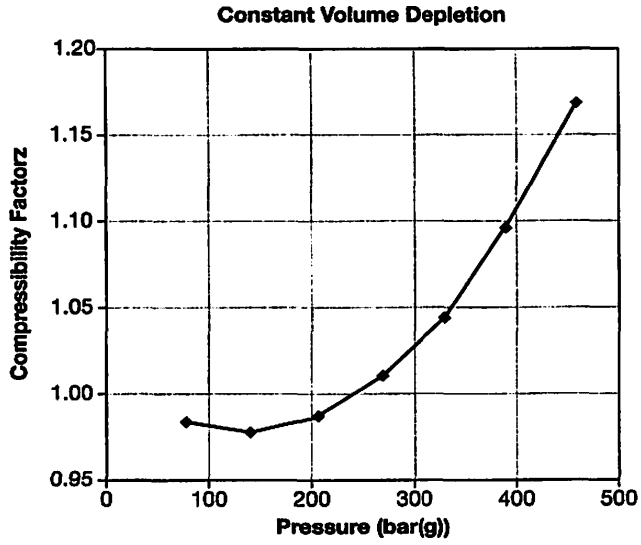

Figure 2.20 Produced Gas Compressibility Factor Z.

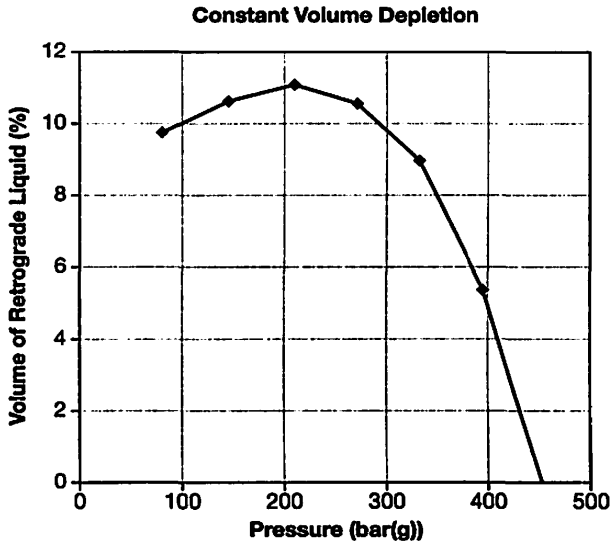

Figure 2.21 Retrograde Liquid Volume.

Figure 2.17 illustrates the CVD steps.
Figure 2.18 shows the cumulative gas produced (from Table 2.32).
Figure 2.19 shows the produced gas relative density (from Table 2.32).
Figure 2.20 shows the produced gas compressibility factor Z (from Table 2.32).
Figure 2.21 shows the retrograde liquid volume (from Table 2.32).
Table 2.33 gives the composition of produced gas.
Figure 2.22 shows the liquid content of produced gas (from Table 2.32).
Figure 2.23 shows the cumulative liquid recovery (from Table 2.32).

Table 2.33 Compositional Analysis of Liberated Gas

Company: COMPANY Field: CST				Well: KOT-1 Formation: GAS				
CONSTANT VOLUME DEPLETION STUDY at T = 161.7°C (323°F) Compositional Analysis of Liberated Gas								Residual liquid (1) at 79.7 bar(g) T = 161.7°C
	Reservoir Fluid							
Pressure bar(g) (psig)	455.5 6 605	393.0 5 699	330.0 4 785	268.6 3 895	205.0 2 973	141.6 2 053	79.7 1 156	1 156 psig and 323°F
Components or Fractions	(mol %)	(mol %)	(mol %)	(mol %)	(mol %)	(mol %)	(mol %)	(mol %)
Hydrogen Sulfide	5.21	5.20	5.26	5.27	5.29	5.32	4.23	1.44
Nitrogen	0.41	0.46	0.47	0.45	0.48	0.44	3.55	0.05
Carbon Dioxide	1.97	1.99	1.99	2.01	2.00	2.05	1.60	0.70
Methane	78.51	79.68	80.47	81.18	81.73	81.97	81.01	19.77
Ethane	3.35	3.35	3.35	3.34	3.35	3.40	3.40	1.78
Propane	2.08	1.99	1.93	1.92	1.92	1.98	1.62	1.78
i-Butane	0.44	0.42	0.42	0.41	0.40	0.40	0.36	0.56
n-Butane	0.91	0.87	0.85	0.84	0.82	0.83	0.87	1.38
i-Pentanes	0.41	0.39	0.38	0.38	0.37	0.37	0.33	0.88
n-Pentanes	0.48	0.45	0.45	0.43	0.42	0.44	0.39	1.12
Hexanes	0.58	0.56	0.53	0.52	0.51	0.50	0.52	2.28
Heptanes	0.70	0.66	0.62	0.59	0.56	0.54	0.55	4.22
Octanes	0.86	0.77	0.74	0.67	0.63	0.59	0.59	6.03
Nonanes	0.68	0.59	0.54	0.50	0.45	0.41	0.41	5.82
Decanes	0.55	0.49	0.43	0.36	0.31	0.25	0.24	5.71
Undecanes	0.43	0.34	0.30	0.25	0.20	0.16	0.14	5.00
Dodecanes	0.33	0.27	0.23	0.19	0.14	0.10	0.07	4.34
Tridecanes	0.33	0.28	0.23	0.17	0.12	0.08	0.05	4.71
Tetradecanes	0.27	0.22	0.17	0.12	0.08	0.05	0.03	4.09
Pentadecanes	0.23	0.19	0.14	0.09	0.06	0.03	0.02	3.69
Hexadecanes	0.18	0.14	0.10	0.06	0.04	0.02	0.01	3.01
Heptadecanes	0.16	0.12	0.08	0.05	0.03	0.01	0.01	2.79
Octadecanes	0.15	0.10	0.07	0.04	0.02	0.01		2.59
Nonadecanes	0.13	0.09	0.06	0.04	0.02	0.01		2.43
Eicosanes plus	0.65	0.38	0.19	0.12	0.05	0.02		13.83
TOTAL	100.00	100.00	100.00	100.00	100.00	100.00	100.00	100.00
Molecular Mass	29.0	26.8	25.1	24.0	23.1	22.5	22.1	151.7
Molecular Mass C_{20+}	377	350	319	319	312	311	313	380
Gas Relative Mass Density (air = 1)		0.925	0.866	0.828	0.797	0.776	0.763	

(1) Residual oil at 15°C (60°F).

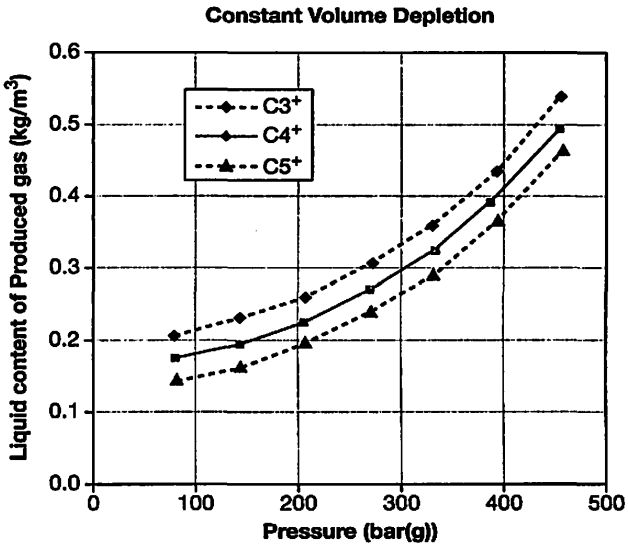

Figure 2.22 Liquid Content of Produced gas.

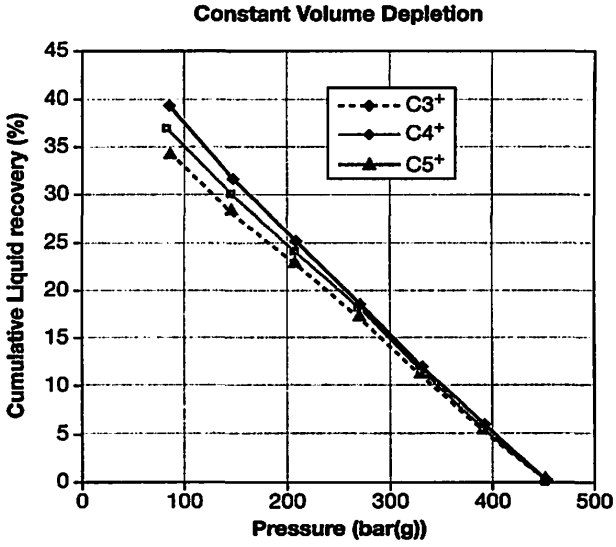

Figure 2.23 Cumulative Liquid Recovery.

2.10 ANALYTICAL ANALYSIS

2.10.1 Compositional Analysis of Pressurized Oil Samples

Gas chromatography analysis of oil is always performed on atmospheric oil samples. High pressure oil samples like separator oil or bottom hole sample, must be separated in stabilized conditions to atmospheric pressure to be analyzed.

Separated fluids, oil and gas are analyzed separately and their composition is recombined with the measured gas-oil ratio to obtain the high pressure sample composition.

2.10.2 Composition Analysis of Atmospheric Oil Sample up to C_{11+}

The analysis is performed by gas chromatography on a single injection upon a specific column by the use of a standard method. Components up to decanes are separated. Weight percentage are calculated and compared to standards. The undecanes plus fraction ($C1_{11+}$) is obtained by material balance calculation.

To characterize the heavy ends (undecanes plus fraction), atmospheric oil is distillated at atmospheric pressure or under vacuum up to a given temperature to vaporize the components up to decanes. Finally the characteristics of the residue (C_{11+}) are determined:

- Density at 15°C with a picnometer or an automatic densimeter.
- Average molecular mass.

The accuracy of the molecular mass depends on the method used, and on the range of the value. Usually cryometric method is used in the range of 100-500 with benzene as a solvent.

2.10.3 Compositional Analysis of Atmospheric Oil Sample up to C_{20+}

The analysis is carried out as a combination of several techniques:

- Light ends are analyzed by chromatography in standard column and capillary column.
- Components from hexane are analyzed by gas chromatography in capillary column and by TBP (True Boiling Point) distillation.

Measured properties:

- Density at 15°C
- Average molecular mass
- Mid average boiling point (optional)
- PNA (Paraffin, Naphtanic, Aromatic) analysis.

The residue of the distillation is considered as the heavy end fraction; its properties are estimated as for the distillation cuts.

Chromatographic Analysis

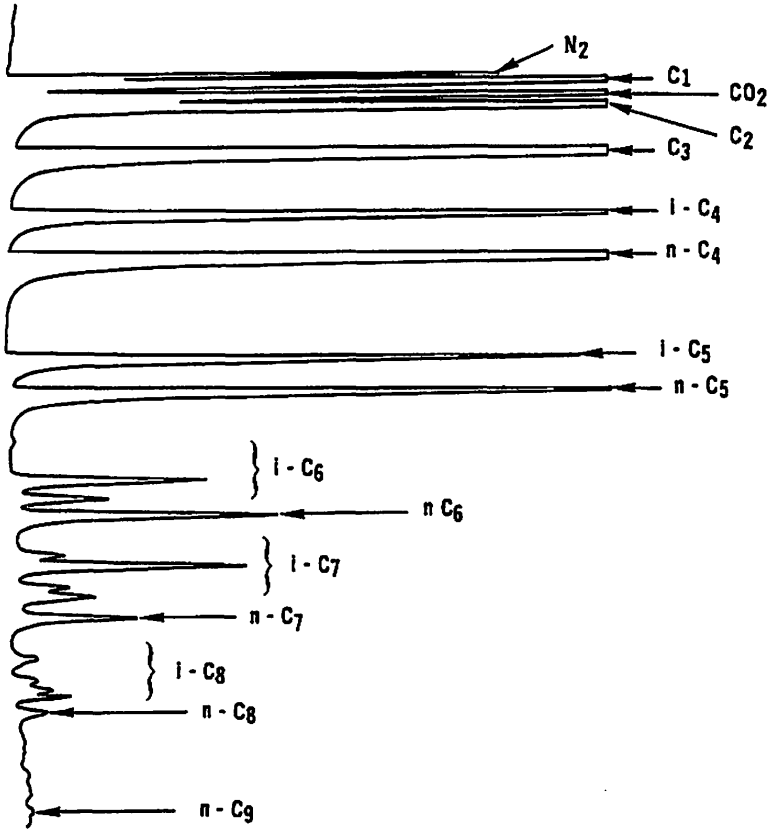

Figure 2.24 Example of a Standard Chromatographic Analysis of a Natural Gas.

Standard Chromatographic Analysis

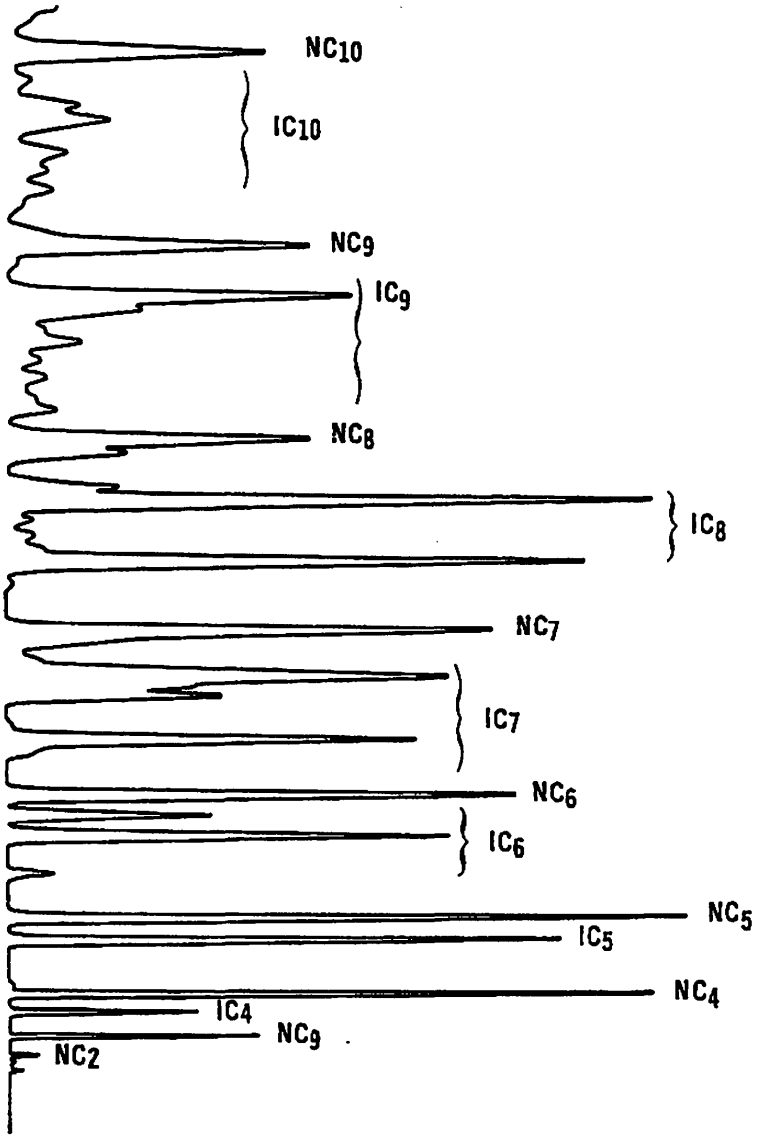

Figure 2.25 Example of a Standard Chromatographic Analysis of Stock Tank Oil.

Oils are usually defined up to C_{10} cut, plus a C_{11+} tail. This practice is justified by the fact that a more extending definition will not bring much additional information but increases the computation time.

The C_{n+} component is characterized by its molecular mass (M_w) and its density at Standard conditions measured in the laboratory. Other thermodynamic properties are calculated from correlations built in the thermodynamic simulator.

The molecular mass is usually obtained by cryoscopy in benzene, by a C_{10}-C_{95} simulated distillation chromatography, or by osmometry.

Two methods are used to measure the density, both defined with an ASTM standard test:

Hydrometer	± 5 to 10 kg/m^3
Digital density meter	± 3 kg/m^3

Remark:
If the molecular mass of the "C_{n+}" fraction is modified, during the tuning procedure of the Equation of state, the molar fluid composition of the fluid defined by the laboratory must be re-calculated since the total mass must remain invariant.
ASTM (American Society for Testing and Materials).

2.10.4 Laboratory Techniques

2.10.4.1 Oil Viscosity Measurement

Usually the capillary tube method is used. The Darcy law is applied to deduct the oil viscosity at reservoir conditions. The rolling ball type is abandoned.

2.10.4.2 Gas Chromatography

Gas Chromatography is an instrumental method for the separation and identification of chemical compounds.

Principle:

A fluid sample is introduced into a heated injector port where it is vaporized. An inert gas is used to carry the sample through a separating column. The component presence is detected by a captor as a series of peaks on a recorder when the component leaves the column.

Chromatographic separation involves the use of a stationary phase and a mobile phase. Components of a mixture carried in the mobile phase are differentially attracted to the stationary phase and thus move through the stationary phase at different rates. In gas chromatography, the mobile phase is an inert carrier gas and the stationary phase is a solid or a liquid coated on a solid contained in a coil column. Different columns are available: short, large diameter or very small capillary columns. Each has its own use and associated advantages and disadvantages. The column is contained in a heated oven that is preceded by a heated detector unit which produces the output. A set of pre-programmed parameters regulate the operation of the system. Separation of the components occurs in the column. Compounds differentially retained in the stationary phase, reach the detector at different

times to produce a set of peaks along the time line (Fig. 2.24, 2.25). Each component of the mixture reaches the detector at different time and produces a signal at a characteristic time called a retention time. The area under a peak is related to the amount of that component present in the mixture. The number of peaks correlates with the number of components in the sample. With component references used for calibration, the retention time under defined conditions is used to identify each component.

Gas compositions are sometimes defined to C_{7+}. Such a definition is not sufficient to model accurately the retrograde behavior of the fluid. In such cases, it is necessary to split the C_{7+} fraction into a more detailed analysis [40].

The method is based on empirical observations:

Plot the molecular mass ratio M_{wn+}/M_{w7+} versus the number of carbons in the molecule (n) results a straight line.

The family of straight lines corresponding to different relative densities of C_{7+} converge at the common point $M_{wn+}/M_{w1+} = 1$ for $n = 7$.

2.10.4.3 Gel Permeation Chromatography [41]

(GPC) also known as Size Exclusion Chromatography (SEC) is a chromatographic method in which molecules are separated based on their size. This method is most widely used in the analysis of polymer molecular masses. The term GPC was used in the beginning of polymer analysis when glass columns filled with gels to perform GPC were used. Nowadays more and more automated and high pressure liquid chromatographic columns are used. Therefore GPC is an old terminology and size-exclusion chromatography (SEC) is the correct expression for the determination of molecular masses.

2.10.4.4 TBP

(True Boiling Point distillation) is performed in columns with 15 to 100 theoretical plates at relatively high reflux ratios (5 to 1 or greater). The high degree of fractionation gives accurate component distributions for mixtures.

2.10.4.5 Cryoscopy

Cryoscopy is a technique for determining the molecular mass of a solute by dissolving a known quantity of it in a solvent and recording the amount by which the freezing point of the solvent drops.

2.10.4.6 Average Molar Mass

Measurements on petroleum distillation residues are mainly carried out by cryoscopy or vapor pressure osmometric methods based on the application of Raoult's law.

2.10.4.7 Detailed hydrocarbon analysis via IFP carburane Software

"Carburane" is a chromatographic data processing program for detailed petroleum hydrocarbon characterization which is operated in a Windows environment. It carries out automatic identification of capillary chromatograms in a temperature programmed mode, and various physical calculations based on analysis of all individual hydrocarbons.

2.11 HYDROCARBON PROPERTY CORRELATIONS

The physical properties discussed next, apply only to black-oils.

Values of reservoir liquid and gas properties are often needed when laboratory PVT data are not available.

During the prospect phase, when only produced fluid properties are available from flowing test, one can resort to empirically derived PVT relations.

Different authors derived equations for estimating saturation pressure, oil formation volume factor (FVF) at saturation pressure, and two phase FVF derived as a function of reservoir temperature, total surface gas relative density, producing GOR, and stock tank oil density. The equations should be valid for all types of oil/gas mixtures after correcting for non hydrocarbons in surface gases and paraffinicity of oil.

Table 2.34 shows the most commonly used correlations [42]. Many others have been published that refer to particular petroleum basins [43]

Table 2.34 Usual Correlations

Fluid Property Correlations	
Fluid Property	**Correlation**
Bubble-point Pressure	Standing, Lasater Vasquez & Beggs, Glasφ
Solution GOR	Standing, Lasater Vasquez & Beggs, Glasφ
FVF	Standing, Vasquez & Beggs Glasφ
Isothermal compressibility	Calhoun, Trube Vasquez & Beggs
Dead-oil viscosity	Beal, Beggs & Robinson Glasφ
Gas saturated oil viscosity	Chew & Connally Beggs & Robinson
Under saturated oil viscosity	Beal, Vasquez & Beggs

2.11.1 Standing Correlation [15, 44, 45]

In 1947, Standing proposed a correlation for determining the formation volume factor of gas saturated oil. A total of 105 experimentally determined data points on 22 different crude oil gas mixtures from California fields were utilized in arriving at the correlation. No corrections for oil type or non hydrocarbon content were introduced.

All data were obtained in the laboratory with a two-stage flash separation designed to duplicate average field conditions in California.

Determination of the Bubble Point Pressure and Oil FVF at Pbub:

From: oil tank gravity (°API)
Gas relative density (air = 1)
Dissolved gas-oil ratio (*scf/bbl*)
Reservoir temperature (°F)

Bubble Point Pressure:

$$P_b = 18 \times \left(\frac{R_{sb}}{\gamma_g}\right)^{0.83} \times 10^{y_g} \quad \text{with} \quad y_g = 0.00091T - 0.0125\gamma_{API} \tag{2.7}$$

P_b: bubble point pressure *(psi)*
R_s: total gas-oil ratio *(scf/bbl) (separator gas plus vent gas)*
γ_{API}: tank oil density *(°API)*
γ_g: gas relative density (air = 1)
T: reservoir temperature *(°F)*

Oil FVF at Pressures Equal to or Below P_b:

$$B_{ob} = 0.972 + 0.000147 \times F^{1.175} \qquad F = R_s \times \left(\frac{\gamma_g}{\gamma_{API}}\right)^{0.5} + 1.25T \tag{2.8}$$

The relation is valid for any pressure equal to or below the bubble point by using the corresponding GOR value.

Solution GOR for Saturated Oils:

$$R_s = \gamma_g \left(\frac{P}{18 \times 10^{y_g}}\right)^{1.204} \quad \text{with} \quad y_g = 0.00091 \times T - 0.0125 \times \gamma_{API} \tag{2.9}$$

R_s: solution GOR, (scf/bbl)
P: pressure (psia)

γ_g: relative gas density/air
γ_{API}: tank oil density (°API)
T: temperature (°F)

Figures 2.26 and 2.27 illustrate the correlation in the form of charts.

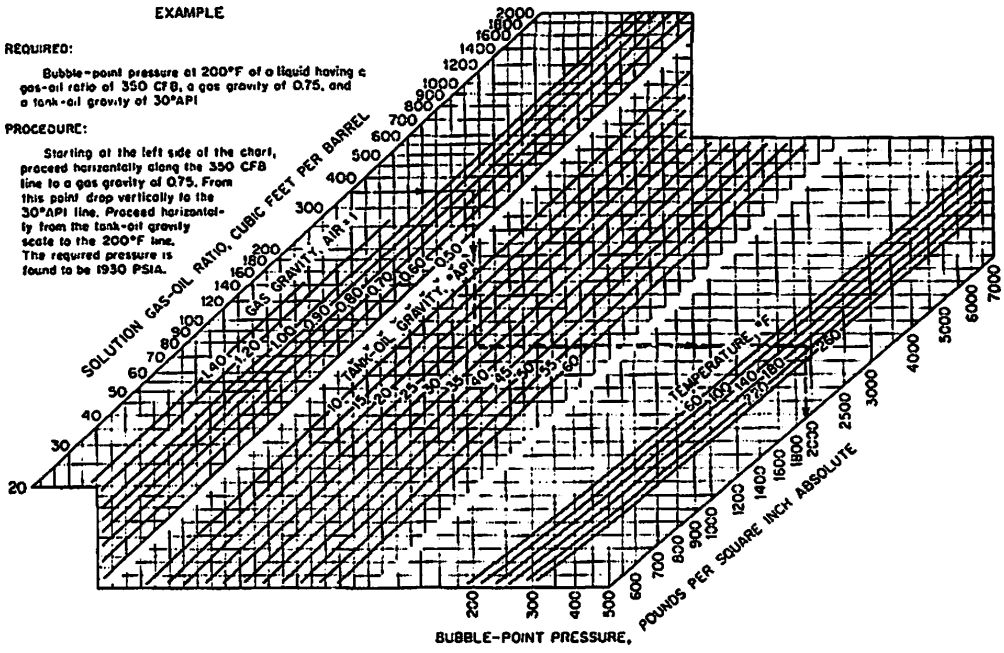

Figure 2.26 Chart to determine bubble point pressure by Standing's correlation.

2.11.2 Lasater Correlation [15, 40, 46]

Lasater presented a bubble-point pressure correlation in 1958. A total of 158 experimentally measured bubble-point pressures from 137 independent crude oil systems from Canada, western and mid-continental U.S., and South America was used in its development. The associated gas of these crudes was essentially free of non hydrocarbon components. Lasater used Henry's law to derive a "bubble-point pressure factor" and correlated it with the mole fraction of gas in solution to obtain the curve. The mole fraction of gas in solution is calculated from values of solution GOR, oil density and molecular mass. Lasater provided the relationship of molar mass versus oil density.

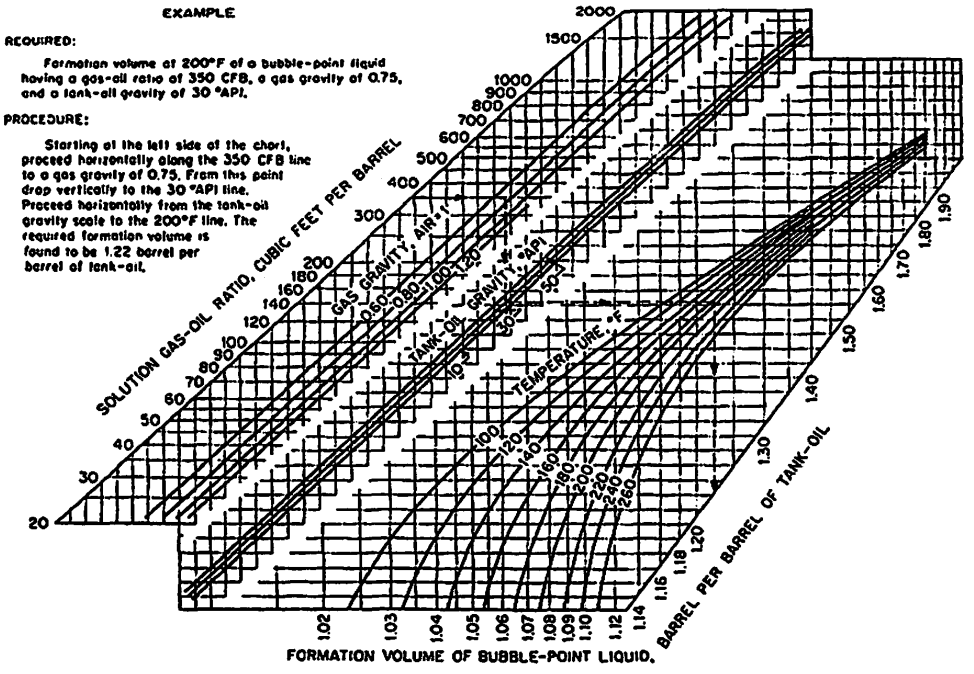

Figure 2.27 Chart to determine oil formation volume by Standing's correlation.

Bubble Point Pressure Determination:

Procedure:

1) Determine the effective molecular mass of the stock-tank oil from its API density (Fig. 2.28).
2) Calculate the mole fraction of gas in the system with equation:

$$y_g = \frac{R_{sb} / 379.3}{R_{sb/} / 379.3 + 350\gamma_o / M_o} \tag{2.10}$$

Nb of gas moles: Rsb/379.3 Nb of corresponding stock tank oil moles: $62.428 \times 5.615 \times \gamma_o/M_o$
62.428 lb/cu. ft: water density 5.615 cu. ft = 1 Bbl M_o: stock tank oil molar mass
γ_o: tank oil relative density (water = 1)
Volume of 1 lb-mole of gas at 14.7 psia and 60°F = 379.3 cu. ft

3) Find the bubble point pressure factor $\left(\frac{P_b \gamma_g}{T_R}\right)$ from Figure 2.29

4) Calculate the bubble point pressure

$$P_b = \left(\frac{P_b \gamma_g}{T}\right) \times \frac{T_R}{\gamma_g} \qquad T_R\text{: in °Rankine} \qquad T\text{: reservoir temperature in °F} \qquad (2.11)$$

Figure 2.28 gives the relationship between tank oil molar mass and tank oil density

Figure 2.29 gives the correlation between bubble point factor and gas mole fraction

Equations for Figure 2.28:

For API ≤ 40 $$M_o = 630 - 10\gamma_{API} \qquad (2.12)$$

For API > 40 $$M_o = 73110\left(\gamma_{API}\right)^{-1.562} \qquad (2.13)$$

Equation for Figure 2.29:

For $\gamma_g \leq 0.60$ $$\frac{P_b \gamma_g}{T_R} = 0.679 \times e^{2.786 \times y_g} - 0.323 \qquad (2.14)$$

For $\gamma_g > 0.60$ $$\frac{P_b \gamma_g}{T_R} = 8.26 y_g^{3.56} + 1.95 \qquad (2.15)$$

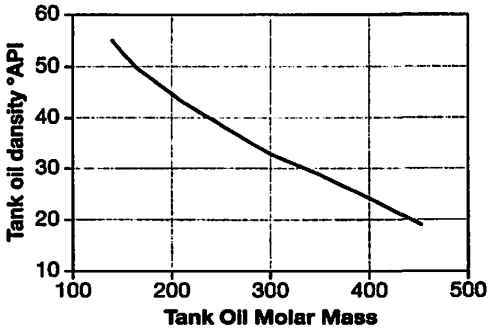

Figure 2.28 Tank oil Molar mass versus tank oil density (after Lasater).

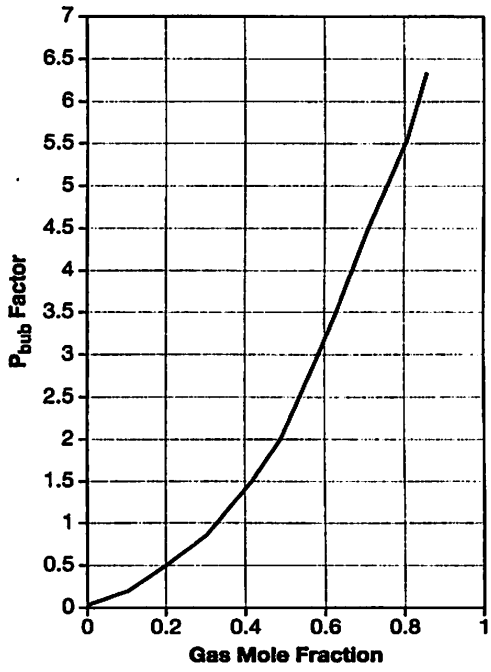

Figure 2.29 Lasater's correlation of bubble point factor with gas mole fraction.

Solution GOR for Saturated Oils:

$$R_s = \frac{132755 \times \gamma_{API} y_g}{M_o(1-y_g)} \tag{2.16}$$

For $\frac{P_b \gamma_g}{T_R} < 3.29$ $$y_g = 0.359 \text{Ln}\left(\frac{1.473 P \gamma_g}{T_R} + 0.476\right) \tag{2.17}$$

For $\frac{P_b \gamma_g}{T_R} \geq 3.29$ $$y_g = \left(\frac{0.121 P \gamma_g}{T_R} - 0.236\right)^{0.281} \tag{2.18}$$

M_o is obtained from Eq. (2.12) or (2.13). γ_g from Eq. (2.14) or (2.15).

2.11.3 Vasquez and Beggs Correlation [15, 40, 47]

In 1976, Vasquez and Beggs presented relationships for determining the solution GOR and formation volume factor of a gas saturated oil. A total of 6004 data points were used in the development of these correlations. The data were separated in two groups because of crude volatility:

1st group for oil densities ≤ 30°API (≥0.88 g/cm^3).
2nd group for oil densities > 30°API (<0.88 g/cm^3).

Vasquez and Beggs normalized gas relative density to a separation pressure of 100 psig (690 kPa) considered as an average representative of field practice.

The following equation gives the proper relative gas density to use if the first stage separation is other than 100 psig.

$$\gamma_{gc} = \gamma_{g(p)}\left[1.0 + (5.912 \times 10^{-5}) \times \gamma_{API} \times T_{sp} \times \log(p_{sp}/114.7)\right] \tag{2.19}$$

γ_{gc}: corrected gas relative density
$\gamma_{g(p)}$: gas relative density resulting from a separation at p_{sp} and T_{sp}
T_{sp}: actual separator temperature (°F)
p_{sp}: actual separator pressure (psia)
γ_{API}: oil density (°API)

Bubble Point Pressure:

The **bubble point pressure** is calculated from:

$$P_b = \left\{\frac{R_{sb}}{C_1 \times \gamma_g \times e^{\left[C_3 \times \gamma_{API}/(T+460)\right]}}\right\}^{1/C_2} \tag{2.20}$$

P_b: bubble point pressure (psia)
R_{sb}: solution GOR at P_b, (scf/bbl)
γ_{API}: oil density (°API)
T: reservoir temperature (°F)

Dissolved gas Correlation:

$$R_s = C_1 \times \gamma_g \times P^{C_2} \times e^{\left[C_3 \times (\gamma_{API}/(T+460))\right]} \tag{2.21}$$

R_s: gas in solution at P and T, (scf/bbl)
γ_g: gas relative density
P: pressure of interest (psia)
γ_{API}: stock tank oil density (°API)
T: temperature of interest (°F)
C_1, C_2, C_3 obtained from table below

Coefficient	$\gamma_{API} \leq 30$	$\gamma_{API} > 30$
C_1	0.0362	0.0178
C_2	1.0937	1.1870
C_3	25.7240	23.9310

Formation Volume Factor B_o for $P \leq P_b$:

$$B_o = 1 + C_1 R_s + C_2 (T-60)(\gamma_{API}/\gamma_{gc}) + C_3 R_s (T-60)(\gamma_{API}/\gamma_{gc}) \tag{2.22}$$

Coefficient	$\gamma_{API} \leq 30$	$\gamma_{API} > 30$
C_1	4.677×10^{-4}	4.67×10^{-4}
C_2	1.751×10^{-5}	1.10×10^{-5}
C_3	-1.811×10^{-8}	1.337×10^{-9}

Formation Volume Factor B_o for $P \geq P_b$:

$$B_o = B_{ob} \times e^{\left[c_o (p_b - p)\right]} \tag{2.23}$$

A correlation for the oil compressibility was developed from a total of 4 036 data points.

$$c_o = \frac{a_1 + a_2 R_s + a_3 T + a_4 \gamma_{gc} + a_5 \gamma_{API}}{a_6 P} \tag{2.24}$$

Where:

$a_1 = -1\,433.0$ $a_2 = 5.0$ $a_3 = 17.2$
$a_4 = -1\,180.0$ $a_5 = 12.61$ $a_6 = 10^5$

2.11.4 Glasφ Correlation [40, 48]

In 1980, Glasφ presented a correlation for calculating formation volume factor. A total of 45 oil samples obtained mostly from the North Sea Region, were used in the correlation.

An adjustment to the API density term in the equations was suggested when the correlations are used with oils of a different compositional nature. A bubble point pressure correlation is provided for volatile oils with a method for correcting the bubble point pressure for the presence of CO_2, N_2, and H_2S in the surface gas.

Bubble Point Pressure Determination:

$$\log P_b = 1.7669 + 1.7447 \log p_b^* - 0.30218 \left(\log p_b^*\right)^2 \tag{2.25}$$

Where $p_b^* = \left(\frac{R_s}{\gamma_g}\right)^{0.816} \times \frac{T^{0.172}}{\left(\gamma_{API}\right)^{0.989}}$

R_s: gas in solution at P and T, (scf/bbl)
γ_g: gas relative density
γ_{API}: stock tank oil density (°API)
T: temperature (°F)
p_b^*: correlating number to calculate bubble point pressure

Oil FVF at Saturation Pressure:

$$\log(B_{ob} - 1) = -6.58511 + 2.91329 \log B_{ob}^* - 0.27683 \left(\log B_{ob}^*\right)^2 \tag{2.26}$$

Where $B_{ob}^* = R_s \left(\frac{\gamma_g}{\gamma_o}\right)^{0.526} + 0.968T$

B_{ob}^*: correlating number to calculate B_{ob}
γ_o: oil relative density at stock tank from flash separation (water = 1)

Total FVF Below P_b:

$$\log B_t = 8.0135 \times 10^{-2} + 4.7257 \times 10^{-1} \times \log B_t^* + 1.7351 \times 10^{-1} \times \left(\log B_t^*\right)^2 \tag{2.27}$$

Where $B_t^* = R_s \frac{T^{0.5}}{\gamma_g^{0.3}} \times \gamma_o^{2.9 \times 10^{-0.00027 Rs}} \times p^{-1.1089}$

B_t^*: correlating number
p: pressure of interest (psia)

Correcting Saturation Pressure for Non hydrocarbons.

The presence of CO_2, N_2 and H_2S in the surface gas, affect the bubble point pressure.

$$P_{b,est,CO_2} = \frac{P_{bCO_2}}{P_{bh}} P_{b,est} \qquad P_{b,est,N_2} = \frac{P_{bN_2}}{P_{bh}} P_{b,est} \qquad P_{b,est,H_2S} = \frac{P_{bH_2S}}{P_{bh}} P_{b,est}$$

$P_{b,est}$ is the estimated pressure calculated from Eq. (2.25). The value is corrected for content of CO_2, N_2, and or H_2S in surface gases by the factors:

$$\frac{P_{bCO_2}}{P_{bh}} \qquad \frac{P_{bN_2}}{P_{bh}} \qquad \frac{P_{bH_2S}}{P_{bh}}$$

Terms developed from laboratory experiments.

$$\frac{P_{bCO_2}}{P_{bh}} = 1.0 - 693.8 y_{CO_2} \times T^{-1.553}$$

$$\frac{P_{bN_2}}{P_{bh}} = 1.0 + \left[\left(-2.65 \times 10^{-4} \gamma_{API} + 5.5 \times 10^{-3}\right) T + \left(0.0931 \gamma_{API} - 0.8295\right)\right] \times y_{N_2} + \left[\left(1.954 \times 10^{-11} \gamma_{API}^{4.699}\right) T + \left(0.027 \gamma_{API} - 2.366\right)\right] \left(y_{N_2}\right)^2$$

$$\frac{P_{bH_2S}}{P_{bh}} = 1.0 - \left(0.9035 + 0.0015 \gamma_{API}\right) y_{H_2S} + 0.019 \left(45 - \gamma_{API}\right) \left(y_{H_2S}\right)^2$$

where y_{CO_2}, y_{N_2}, y_{H_2S}, are mole fraction of CO_2, N_2, H_2S in total surface gases.

In 1988, Al-Marhoun [49] presented a correlation for calculating the formation volume factor. A total of 160 experimentally determined data points on 69 different crude oils from the Middle East were used in the correlation.

2.11.5 Oil Viscosity [15]

Viscosity is the internal friction or the resistance offered by a fluid to relative motion of its parts.

The absolute viscosity unit in the metric system is:

Poise = 1 dyne.sec/cm^2 = 1 g/(sec.cm)

The kinematic viscosity of a fluid is the absolute viscosity divided by the fluid density.

$$\nu = \frac{\mu}{\rho} = \frac{Poises}{g/cc} = \frac{\text{cm}^2}{\text{sec}} \text{ defined as stoke}$$

Reservoir engineering uses only absolute viscosity μ expressed in centipoises (cp).

Viscosity of crudes varies from low values 0.2 cp to 2 000 cp and even 100 000 cp for heavy oils. The centipoise is commonly used in reservoir engineering field units for viscosity.

Beal's Correlation:

In 1946, Beal published graphical correlations for determining the viscosity of dead crude oil. A total of 655 values for dead oil viscosity at 100°F (38°C) were obtained from 492 oil fields, 358 of which are located in the US.

In addition, Beal presented a curve for estimating the viscosity of under saturated oil. The curve was the result of correlating 52 samples taken from California and other locations.

Chew and Connally Correlation:

In 1959, Chew and Connally presented a correlation to predict the oil viscosity change as a function of the solution GOR. The correlation was obtained from 457 crude oil samples from Canada, the U.S., and South America. The "dead oil" viscosity is adjusted for the amount of dissolved gas it contains at reservoir pressure by means of Chew and Connally's correlation.

Beal's correlation is used to obtain gas-free crude oil viscosity at reservoir temperature as a function of its API density.

Dead oil viscosity at stock tank condition:

$$\mu_{oD} = \left(0.32 + \frac{1.8\times10^{7}}{\gamma_{API}^{4.53}}\right)\left(\frac{360}{T+200}\right)^{a} \quad \text{with} \quad a = 10^{\left[0.43+\left(8.33/\gamma_{API}\right)\right]} \tag{2.28}$$

Beggs and Robinson [15, 40]:

In 1975, Beggs and Robinson published equations for calculating dead-oil and gas saturated-oil viscosities. The study involved 2533 viscosity measurements, (460 dead-oils and 2073 gas-saturated oils) from 600 different crude oil systems.

Saturated oil viscosity is calculated in terms of dead oil viscosity Eq. (2.28)

The general equation is:

$$\mu_{ob} = A_1\left(\mu_{oD}\right)^{A_2} \tag{2.29}$$

μ_{ob}: saturated oil viscosity μ_{oD}: dead oil viscosity A_1, A_2: functions of R_s

Different authors gave specific values for A_1 and A_2:

Standing:

$$A_1 = anti\log\left[-7.4\times10^{-4}R_s + 2.2\times10^{-7}R_s^2\right] \quad (anti\log(X) = 10^{(X)})$$

$$A_2 = \frac{0.68}{10^{8.62\times10^{-5}R_s}} + \frac{0.25}{10^{1.1\times10^{-3}R_s}} + \frac{0.062}{10^{3.74\times10^{-3}R_s}}$$

Beggs and Robinson:

$$A_1 = 10.715(R_s + 100)^{-0.515}$$

$$A_2 = 5.44(R_s + 150)^{-0.338}$$

Aziz *et al.*:

$$A_1 = 0.2 + (0.8 \times 10^{-0.00081 R_s})$$

$$A_2 = 0.43 + (0.57 \times 10^{-0.00072 R_s})$$

2.11.6 Example

Estimate the bubble pressure with the Standing procedure with:

$R_s = 350$ *scf/bbl*, $T = 200°F$, $\gamma_g = 0.75$, $\gamma_{API} = 30$

Solution:

$$P_b = 18 \times \left(\frac{350}{0.75}\right)^{0.83} \times 10^{0.00091 \times 200 - 0.0125 \times 30} = 1\,895 \text{ psia}$$

Estimate the bubble point pressure with the Lasater method with:

$R_{sb} = 500$ *scf/bbl*, $T = 200°F$, $T_R = 660°R$, $\gamma_g = 0.80$, $\gamma_{API} = 30$, $\gamma_o = 0.786$

Solution:

$M_o = 630 - 10 \times 30 = 330$

$$\gamma_g = \frac{500/379.3}{500/379.3 + 350(0.876)/330} = 0.587$$

$$\frac{P_b \gamma_g}{T_R} = 0.679 e^{2.786 \times 0.587} - 0.323 = 3.161 \qquad P_b = \frac{3.161 \times 660}{0.80} = 2608 \text{ psia}$$

2.12 ASPHALTENES [50, 51, 52]

A common practice in the petroleum industry is to separate crude oil into chemically distinct fraction: Saturates, Aromatics, Resins, and Asphaltenes (SARA).

If oil temperature drops below the cloud point, wax crystals precipitate from the oil phase. Accumulation of these solids can impact subsurface and surface equipment

operations. Paraffin deposits occur usually with changes of pressure or temperature. Crude is submitted to a pressure drop across perforations, through tubing or a choke. Gas bubbles and light ends separate from the liquid phase. These light ends helped to keep the heavy-end paraffin in solution, then precipitation occurs.

Asphaltene deposition is less driven by temperature and pressure. The deposition is affected more by chemistry changes in the crude.

Asphaltene molecules are not dissolved in the crude, but are dispersed, or 'floating' in it. Lowering the ph of the system (making it more acid) or introducing carbon dioxide (CO_2), or nonaromatic solvents can strip away the asphaltene molecule's outer part that helps keep the asphaltene molecules dispersed.

Asphalt is a complex mixture of hydrocarbons which can be separated into two mayor fractions: asphaltenes and maltenes (petrolenes).

Separating of asphaltenes and maltenes fractions is done by diluting asphalt with straight chain, saturated hydrocarbons (*n*-alkanes) such as: Pentane (C_5H_{12}).

Asphaltene molecules carry a core of stacked, flat sheets of condensed (fused) aromatic rings linked at their edges by chains of alipathic and/or naphthenic-aromatic ring systems.

Asphaltenes are defined as the non-volatile and polar fraction that is insoluble in *n*-alkanes (pentane). Resins are defined as the non-volatile and polar fraction of crude oil that is soluble in *n*-alkanes (pentane) and aromatic solvents (toluene) and insoluble in ethyl acetate. A commonly accepted view in the industry is that asphaltenes form micelles which are stabilized by adsorbed resins kept in solution by aromatics.

Two key parameters control the stability of asphaltene micelles in a crude oil:

- Ratio of aromatics to saturates
- Ratio of resins to asphaltenes.

When the ratios decrease, asphaltene micelles flocculate and form large aggregates.

The precipitation of asphaltene aggregates can generate severe problems in the reservoir: plugging the porous media around the well and wettability reversal in addition to surface facility troubles. The adsorption of asphaltene aggregates at oil water interface has been shown to cause the steric stabilization of water oil emulsions.

De Boer *et al.* [53] observed that the relative change in asphalt solubility in the crude per unit of pressure drop is higher for light under saturated crudes, which usually contain small amount of asphaltenes. Depressurizing the crude below the bubble point pressure will cause a rapid increase in asphalt solubility. Heavy crudes usually present fewer problems with asphalt precipitation, despite their higher asphaltene content, certainly if the reservoir pressure is close to the bubble point pressure.

Haskett and Tartera [54] presented results observed in the Hassi-Messaoud field in Algeria. One well, which produced at a well head pressure considerably higher than the bubble point pressure, showed asphaltene deposition up to the surface, except on the downstream side of the choke where the pressure was below the bubble point.

Many researchers work on the problem of asphaltene flocculation to explain the phenomena and build models based on thermodynamics associated with an EOS in order to simulate and predict the behavior of light as well as heavy crudes containing asphaletenes.

Historical Note
The classic definition of asphaltenes is based upon the solution properties of petroleum residuum in various solvents. The word asphaltene was coined in France by J.B. Boussingault in 1837. Boussingault described the constituents of some bitumens (asphalts) found at that time in Eastern France and in Peru. He named the alcohol insoluble, essence of turpentine soluble solid obtained from the distillation residue "asphaltene", since it resembled the original asphalt.

2.13 GAS PROPERTIES

2.13.1 Definition Review Bg

The gas formation volume factor is defined as: $B_g = \frac{V_{res}}{V_{std}}$

gas FVF = ratio of the volume occupied by a mass of gas at reservoir conditions to the volume of the same mass of gas at standard conditions.

The real gas equation of state is: $p\,v = z\,R\,T$		Field units	metric	SI
p:	gas absolute pressure	psia	bars(a)	Pa(a)
v:	gas volume	cu. ft	m^3	m^3
R:	gas constant			
z:	gas compressibility (gas deviation factor)			
T:	absolute gas temperature	°Rankine	K	K

Writing the equation for the same gas at two conditions: reservoir and standard conditions gives:

$P_{res} \times V_{res} = Z_{res}\,R\,T_{res}$

$P_{std} \times V_{std} = Z_{std}\,R\,T_{std}$

At low pressure, real gases behave like ideal gas. Then $Z_{std} = 1$

The B_g definition becomes:

$$B_g = \frac{V_{res}}{V_{std}} = \frac{P_{std}}{T_{std}} Z \frac{T_{res}}{P_{res}}$$

B_g depends on the standard conditions chosen, gas composition (Z), and reservoir conditions (pressure, temperature).

Standard conditions used in the industry:

	Field units	metric	SI
P_{std} = (1 atm)	14.7 psia	1.01325 bars	101325 Pa
T_{std} =	520°R (60°F + 460)	288 K (15°C+273)	288 K

Remark: P_{std} = 100 kPa is used by some authors.

B_g becomes: $B_g = \text{Cte}\dfrac{ZT}{P}$

Cte = 0.028269 for field units
0.00352 metric units (bars a)
351.8 SI

- The relationship to convert gas mass into volume for any gas is:
  1 g mole of gas at 1 atm and 15.5°C occupies 23.645 dm^3
  1 lb-mole of gas at 14.7 psia and 60°F occupies 379.4 cu. ft

2.13.2 B_g Determination [55]

When only the relative gas density and pressure are available, the gas formation volume factor can be estimated from the chart published by Standing and Katz (Fig. 2.30, 2.31).

2.13.3 Law of Corresponding States [40, 56]

J.D. Van der Waals proposed the theorem of corresponding states. The principle states that two substances have similar properties at corresponding conditions with reference to some basic property such as the critical temperature and pressure. Two parameters are used: reduced temperature and reduced pressure.

$$Z = f(P_r, T_r) \tag{2.30}$$

$T_r = \dfrac{T}{T_c}$ $P_c = \dfrac{P}{P_c}$ T and P are absolute temperature and pressure of the system

This concept would be true absolutely if the Z_c, compressibility factor at T_c and P_c was the same value of 0.375 for all molecules (as predicted by the Van der Waals equation). Therefore the corresponding state concept is an approximation only.

Mixture Combination Rules

Kay has applied the concept for mixtures. He suggested to use the molal average critical pressure and temperatures for mixtures in place of the critical pressures and temperatures used for pure compounds. The critical values found from the combination rule are not true values. These molal average properties are called pseudo critical temperatures and pseudo critical pressures.

Katz Correlation and Kay's Rule

The method to calculate the Z factor assumes that Eq. (2.30) is valid. Figure 2.32 illustrates the correlation prepared by Katz *et al.* (upper limit: $P_{pr} = 15$).

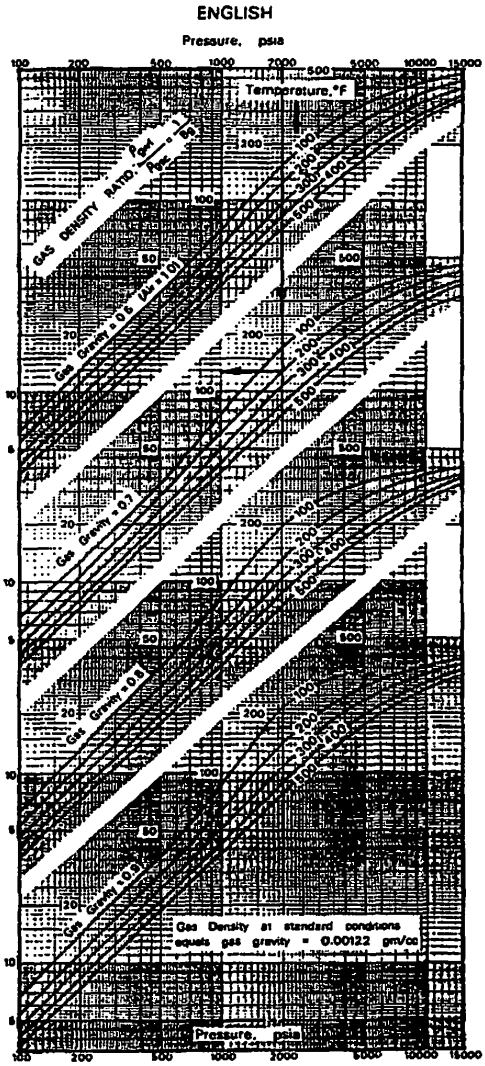

Figure 2.30 B_g, vs γ, P and T, English.

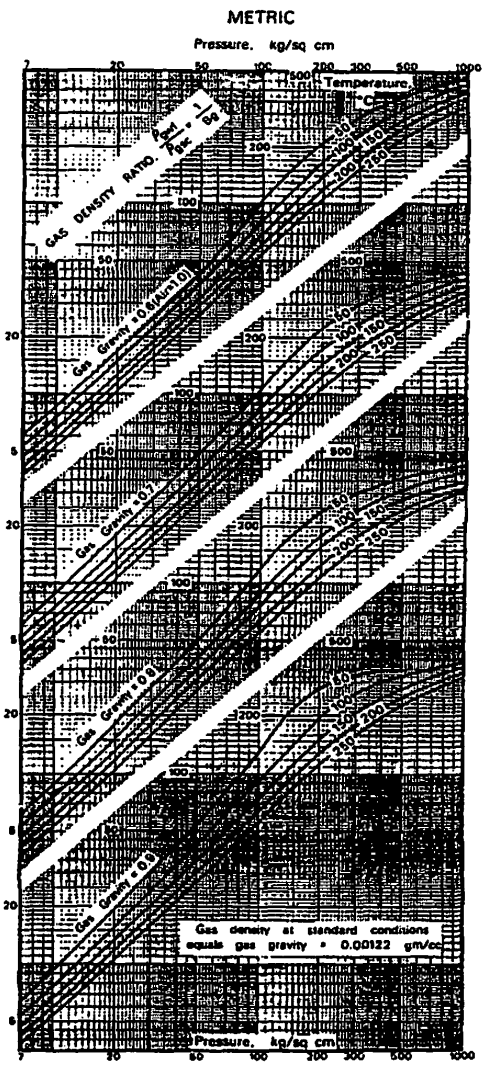

Figure 2.31 B_g, vs γ, P and T, Metric.

Standing, M. B. and Katz, D. L.; "Density of Crude Oils Saturated with Natural Gas", Trans, AIME, Vol 146 (1942).

The values of P_{pr} and T_{pr} for use of the correlation are determined from Kay's rule:

$$P'_c = \Sigma y_i P_{ci} \quad \text{and} \quad T'_c = \Sigma y_i T_{ci}$$

Where y_i is the mole fraction of each component in the mixture and T_{ci} and P_{ci} are critical values for each component found in table 2.35.

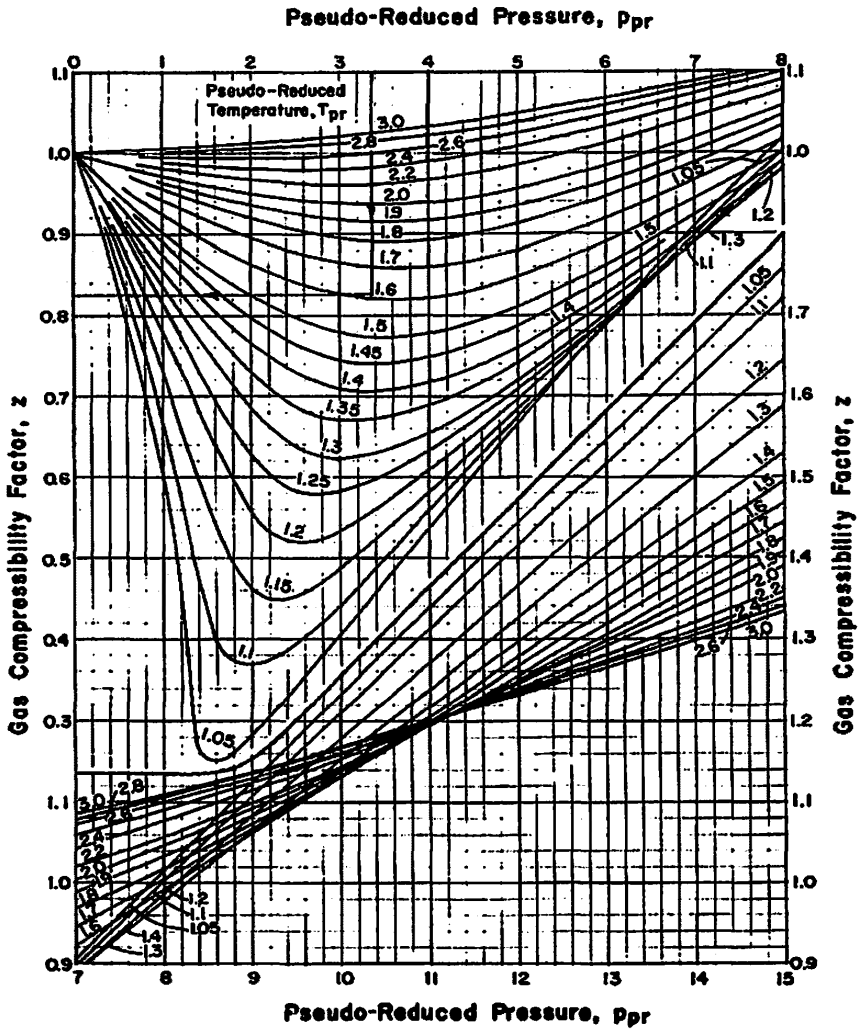

Figure 2.32 Compressibility Factors for Natural Gas (1941).

2.13.4 Other Characterizing Parameters

It has been found that Eq. (2.30) is not always adequate for complex mixtures of gas, [38] and was modified as:

$$Z = f(Pr, Tr, \text{third parameter}) \tag{2.31}$$

The third parameter is used to characterize the mixture behavior.

Acentric Factor (ω)

Pitzer defined the acentric factor [38, 56] to describe the deviation of a fluid from simple fluid behaviour, or its nonconformity with the corresponding states principle. ω represents the non sphericity of a molecule. For high molecular mass hydrocarbons, ω increases. For simple gases like argon, xenon, hydrogen, ω is equal to zero.

ω is defined from the equation:

$$\varpi = -\log_{10}\left(\frac{P}{P_c}\right) - 1 \quad \text{at} \quad T_r = \frac{T}{T_c} = 0.7 \qquad (2.32)$$

P: vapor pressure at T

T_c: component critical temperature

ω is widely used as a correlating parameter.

Critical Compressibility (Z_c)

Each component exhibits its own critical compressibility factor Z_c. Table 2.35 shows the physical constants for main gas components.

Molecular Refraction [38, 56, 57]

The parameter is related to the refractive index and molecular mass of a fluid. There are two forms: Lorentz and Eykman. The Eykman (EMR) value may be determined from the molecular mass and relative density of the heaviest fraction (usually C_{7+}) (table 2.35).

Table 2.35 Physical Properties

Constituent	Molecular mass	Zc	Critical Pressure		Critical Temperature		EMR	Acentric Factor ω
			Bar(a)	psia	K	°R		
C_1	16.042	0.29	46.39	673.10	190.72	343.30	14.115	0.0140
C_2	30.068	0.288	48.81	708.30	305.43	549.77	24.365	0.0990
C_3	44.094	0.278	42.55	617.40	370.00	665.95	34.628	0.1520
iso-C_4	58.120	0.283	36.46	529.10	408.14	734.65	44.741	0.1850
n-C_4	58.120	0.274	37.95	550.70	425.17	765.31	44.243	0.2010
iso-C_5	72.146	0.269	33.29	483.00	461.00	829.80	55.302	0.2220
n-C_5	72.146	0.268	33.74	489.50	469.78	845.60	55.267	0.2540
n-C_6	86.172	0.264	30.3	439.70	507.89	914.20	65.575	0.3010
n-C_7	100.198	0.26	27.35	396.90	540.17	972.31	75.875	0.3500
n-C_8	114.224	0.256	24.96	362.10	569.06	1024.31	86.193	0.4020
n-C_9	128.250	0.25	23.78	345.00	596.11	1073.00	96.529	0.4460
n-C_{10}	142.276	0.246	21.09	306.00	619.28	1114.70	106.859	0.4890
n-C_{11}	156.302	0.243	19.43	282.00	640.94	1153.70	117.173	0.5010
n-C_{12}	172.378	0.237	18.13	263.00	659.83	1187.70	127.499	0.5390
N_2	28.016	0.292	33.91	492.00	126.22	227.20	9.407	0.0400
CO_2	44.010	0.275	73.95	1073.00	304.44	548.00	15.750	0.2250
H_2S	34.076	0.284	90.01	1306.00	373.72	672.70	19.828	0.1000
O_2	32.000	0.292	50.31	730.00	154.44	278.00	8.495	0.0213
H_2	2.016	0.304	12.96	188.10	33.44	60.20	4.450	0.0000

Example:

Calculate the Z factor for the following gas at 139 bars (a) and 331 K

Table 2.36 Calculation Example

Constituent	(a) Composition y_i	(b) Critical P_c bars (a)	c = (a) × (b) $P'c$	(d) Critical Tc K	e = (a) × (d) $T'c$
N_2	0.0046	33.91	0.1560	126.22	0.58
CO_2	0.0030	73.95	0.2219	304.44	0.91
H_2S	0.1438	90.01	12.9434	373.72	53.74
C_1	0.8414	46.39	39.0325	190.72	160.47
C_2	0.0059	48.81	0.2880	305.43	1.8
C_3	0.0008	42.55	0.034	370.00	0.3
i-C_4	0.0003	36.46	0.0109	408.14	0.12
n-C_5	0.0002	33.74	0.0067	469.78	0.09
	1.0000		52.694		218.02
$P/P'c$ =	139/52.7 =	2.64	$T/T'c$ =	331/218 =	1.52

Finally From Figure 2.32 Z = 0.8.

2.13.5 Hall and Yarborough Correlation

The Standing-Katz Z factor chart Figure 2.32 has been used for reservoir gas and gas condensate systems during a long period. An equation applicable to high P_{pr} and to sour gases was needed in the industry. (Upper limit of the original chart; $P_{pr} = 15$).

Hall and Yarborough [58, 59, 60] proposed a methodology from the equation of state developed by Starling-Carnahan based on the concept of inelastic spheres rather than real molecules. Real fluids behave similarly to hard-sphere fluids.

The direct Z calculation is:
$$Z = \frac{0.06125 P_{p_r} \times t \times \exp\left[-1.2(1-t)^2\right]}{y} \tag{2.33}$$

Where P_{pr} = pseudo reduced pressure
t = reciprocal of pseudo reduced temperature
y = "reduced density" which is obtained from the equation:

$$F = -0.06125P_{pr} \times t \times e^{-1.2(1-t)^2} + \frac{y + y^2 + y^3 - y^4}{(1-y)^3} - \left(14.76t - 9.76t^2 + 4.58t^3\right)y^2$$
$$+ \left(90.7t - 242.2t^2 + 42.4t^3\right)y^{(2.18+2.82t)} = 0 \qquad (2.34)$$

The equation is nonlinear and must be solved by trial and error method, the Newton-Raphson technique.

The required derivative is:

$$\frac{dF}{dy} = \frac{1 + 4y + 4y^2 - 4y^3 + y^4}{(1-y)^4} - \left(29.52t - 19.52t^2 + 9.16t^3\right)y$$
$$+ \left(2.18 + 2.82t\right) \times \left(90.7t - 242.2t^2 + 42.4t^3\right)y^{(1.18+2.82t)} \qquad (2.35)$$

Calculation methodology:

- Start with an initial value of y^k, where k is an iteration counter ($y^1 = 0.001$).
- Substitute the value into Eq. (2.34) the result will have some small value F^k.
- Using the first order Taylor series expansion, a better estimate of y is determined by:

$$y^{k+1} = y^k - \frac{F^k}{\frac{dF^k}{dy}} \qquad (2.36)$$

- Iterate using Eq. (2.33) and Eq. (2.34) until satisfactory convergence is obtained ($F^k = 0$).

The gas constant R does not appear in any of the required equations, so any consistent units may be used for pressure, volume, and temperature.

The resulting correlation has been tested for rich and lean gas condensates which contain significant amounts of non hydrocarbon components (up to 33% N_2, 8.5% CO_2, 40% H_2S).

Figure 2.33 illustrates the extended Standing-Katz Z-factor chart obtained *(reduced pressure up to 24 instead of 15)* from the correlation.

2.13.6 Influence of non Hydrocarbon Constituents

Natural gases contain frequently non hydrocarbon constituents in sufficient quantities so that their influence must be taken into account to correct the non conformity to the corresponding state concept. Hydrocarbon gases are qualified as "sweet" or "sour" depending on the hydrogen sulphide content. Both sweet and sour gases may contain nitrogen, carbon dioxide, or both.

Many investigators worked on the influence of the effect of the presence of nitrogen and carbon dioxide in gases on the compressibility factor.

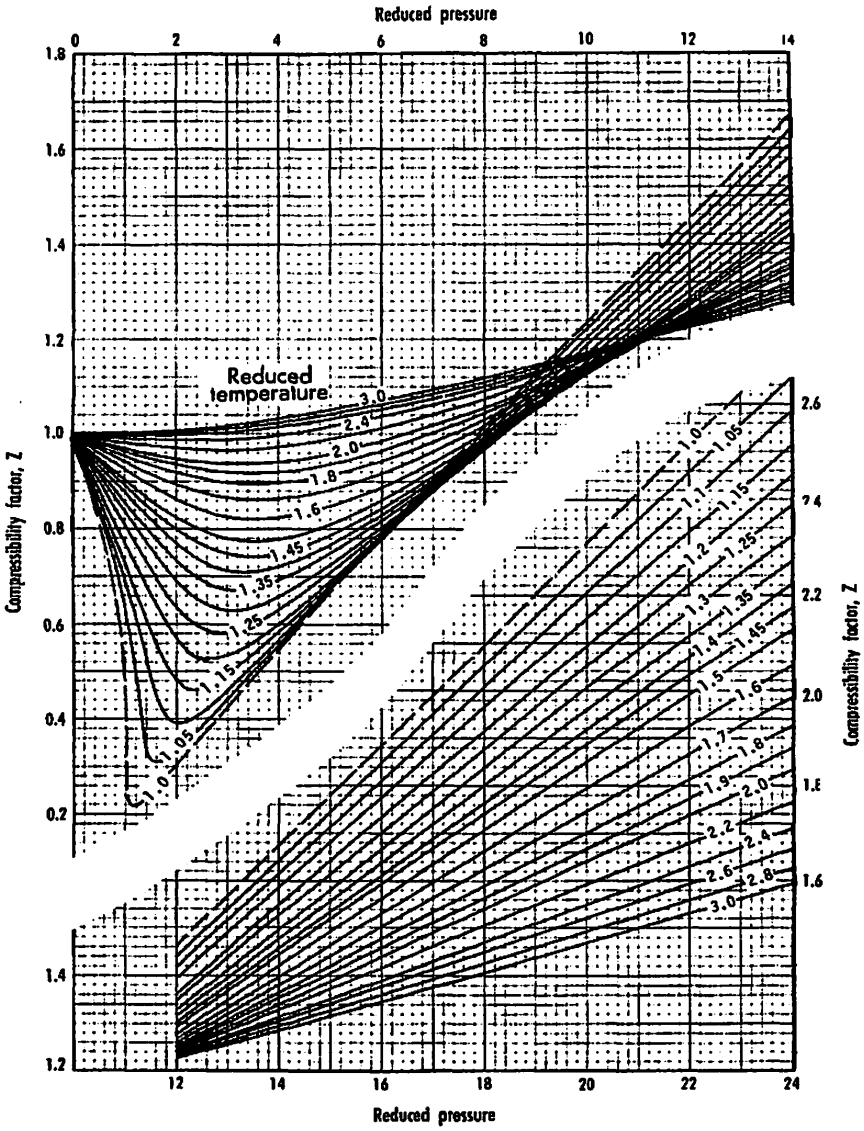

Figure 2.33 Extended Standing-Katz Z-factor chart.

Wichert and Aziz [61] proposed a method consisting of adjusting the pseudo critical parameter found from Kay's combination rule. The adjusted values are then used to find the reduced pressure and temperature for input to Figure 2.32.

The adjustment equations are:

Metric $T_c'' = T_c' - 0.556\varepsilon$ $\qquad P_c'' = \dfrac{P_c' T_c''}{T_c' + B(1-B)\varepsilon \times 0.556}$

P'' in MPa

Field units $T_c'' = T_c' - \varepsilon$ $\qquad P_c'' = \dfrac{P_c' T_c''}{T_c' + B(1-B)\varepsilon}$

T_c' and P_c': pseudo critical parameters from Kay's rule

ε: found from Figure 2.34 B: H_2S mole fraction in the gas

Finally, the adjusted pseudo critical pressure and temperature are used to read the Z factor from the extended Standing-Katz chart Figure 2.33.

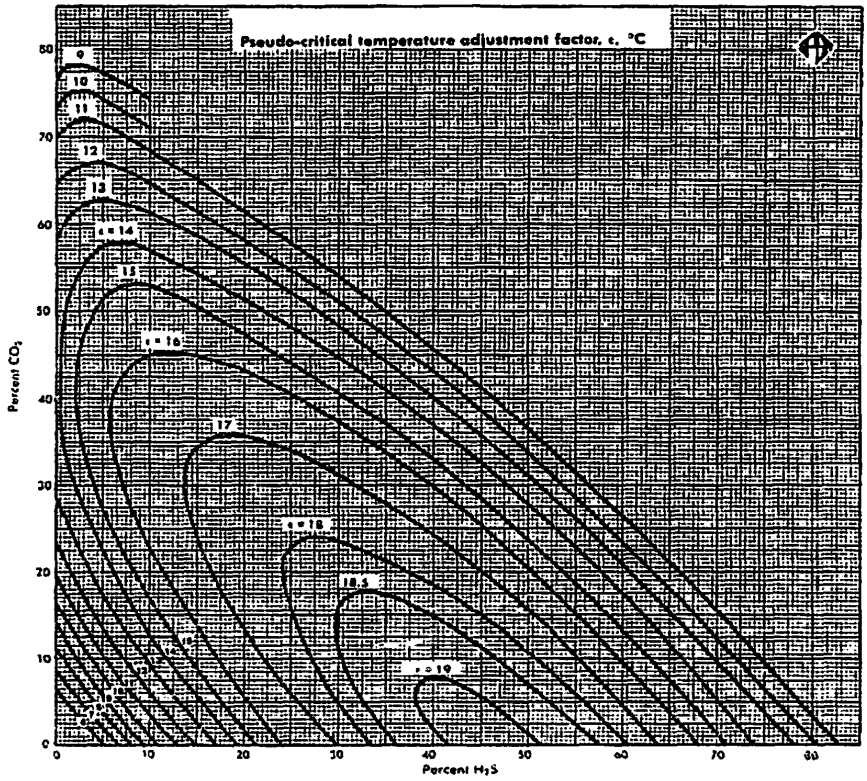

Figure 2.34 Correction Factor Chart for Sour Gases (GPSA) [62].

2.13.6.1 Gas and Liquid Isothermal Compressibility

Definition:
$$c = -\frac{1}{V}\left(\frac{\delta V}{\delta P}\right)_T = \frac{1}{\rho}\left(\frac{\delta \rho}{\delta P}\right) \tag{2.37}$$

c: *compressibility at constant temperature T*
V: *initial volume*
δV: *volume change*
δP: *pressure change*
ρ: *fluid density*
δρ: *density change*

Compressibility has to be a positive value. Therefore when c is defined from volume or density variations, the sign is changed.

Calculation of the real gas compressibility

$$c = -\frac{1}{V}\left(\frac{\delta V}{\delta P}\right)_T \qquad \text{with} \qquad pv = znRT \qquad v = \frac{1}{p}nzRT$$

$$\frac{\delta v}{\delta p} = nRT\frac{\delta}{\delta p}\left(\frac{z}{p}\right) = \frac{nzRT}{p}\left[\frac{1}{z}\frac{\delta z}{\delta p} - \frac{1}{p}\right]$$

Substituting into the compressibility definition Eq. (2.37):

$$c_g = -\frac{1}{v}\frac{nRTz}{p}\left[\frac{1}{z}\frac{\delta z}{\delta p} - \frac{1}{p}\right] = \frac{1}{p} - \frac{1}{z}\frac{\delta z}{\delta p} \cong \frac{1}{p} \tag{2.38}$$

If z changes are small, the gas compressibility can be approximated to $1/p$.

Gas compressibility is very pressure dependent.

Liquid compressibility can be considered constant in the pressure range of interest.

$$c = \frac{1}{\rho}\frac{d\rho}{dp} \qquad \int\frac{d\rho}{\rho} = c\int dp \qquad Ln\frac{\rho}{\rho_0} = c(p - p_0)$$

So
$$\rho = \rho_0 e^{c(p-p_0)} \qquad e^x = 1 + x + x^2/2! + x^3/3! + \ldots$$

$$e^{c(p-p_0)} = 1 + c(p-p_0) + \left[\frac{c(p-p_0)}{2!}\right]^2 + \ldots..$$

Since c is very small, higher order terms can be neglected

$$e^{c(p-p_0)} = 1 + c(p-p_0)$$

then
$$\rho = \rho_0[1 + c(p-p_0)] \tag{2.39}$$

The above formulation is used for most reservoir oils and reservoir waters. For gases, the approximation is not valid, and the complete equation must be used.

2.13.7 Gas Condensate

2.13.7.1 Gas FVF

The compressibility factor Z, normally used in the equations PV = nZRT should apply only in the pressure and temperature range in which the system remains in a single phase.

Other way to quote: the conventional gas FVF definition assumes that the number of gas moles at surface is equal to the number of gas moles at reservoir conditions. This is obviously false if the reservoir gas yields condensate at surface. However the concept of gas FVF is still used by defining a wet gas Z^* or FVF (Bg^*) in case of liquid-yielding reservoir gases. The surface volume is a hypothetical wet-gas volume consisting of the dry surface gas plus the surface condensate volume converted into an equivalent surface-gas volume.

2.13.7.2 Relative Density of Reservoir gases calculation from high Pressure Separator Stream

The reservoir relative gas density is calculated from the production data, by adding the dry gas mass with the condensate mass, divided by the sum of dry gas volume and equivalent vaporized condensate volume, assuming additive gas volumes [63, 64].

Air density at standard conditions:1.225 kg/m^3

Mass of gas corresponding to 1 m^3 of high pressure separator condensate:

$$m_g = \rho_c + GOR \times \gamma_g \times \rho_{air}$$

Total volume of gas ("dry" gas out of separator + virtual gas corresponding to the mass of condensate obtained in the stock tank):

$$v_{total} = GOR + V_c$$

Mass of air of the volume above:

$$m_{air} = (GOR + V_c) \times \rho_{air}$$

The relative density of the reservoir gas is: $\gamma_{gres} = \dfrac{m_g}{m_{air}}$

$$\gamma_{gres} = \frac{\rho_c + GOR \times \gamma_g \times \rho_{air}}{(GOR + V_c) \times \rho_{air}} = \frac{\dfrac{\rho_c}{\rho_{air}} + GOR \times \gamma_g}{GOR + V_c}$$

Or:
$$\gamma_{gres} = \frac{\gamma_g + \frac{\rho_c}{\rho_{air} \times GOR}}{1 + \frac{V_c}{GOR}} \tag{2.40}$$

m_g: mass of gas
ρ_c: density of the high pressure (hp) separator condensate at 15°C (kg/m^3)
GOR: gas condensate ratio, m^3 separator gas per m^3 separator condensate (1.01325 bars, 15°C)
V_c: condensate vaporization volume ratio, m^3 per m^3 separator condensate (1.01325 bars, 15°C)
γ_g: relative density of high pressure (hp) separated gas (air = 1)
ρ_{air}: air density at standard conditions = 1.225 kg/m^3
γ_{gres}: relative density of reservoir gas (air = 1)

The required data from the field needed to use Eq. (2.40) are:

- Flow rates of the high-pressure separator gas and condensate streams obtained from field measurements.
- Relative density of the high-pressure separator gas and condensate obtained from laboratory measurements.
- Condensate vaporizing volume ratio V_c.

V_c is deducted from the curve Figure 2.35

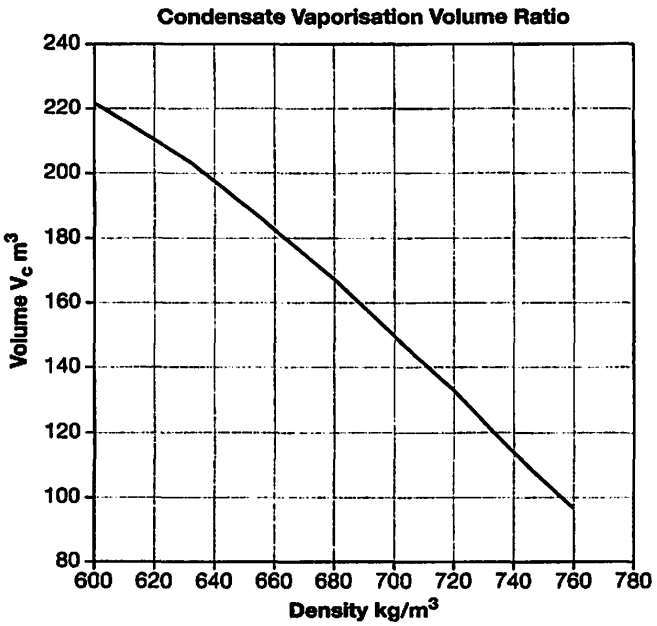

Figure 2.35 Relationship between Condensate Vaporization Volume Ratio and Density at 15°C.

The graph Figure 2.35 is applicable only for converting high-pressure separator condensate to an equivalent gas volume.

Example:

Gas relative density of hp separator gas: $\gamma_g = 0.65$
Density of hp separator condensate: $\rho_c = 750$ kg/m^3
Gas Condensate Ratio: GOR = 3500 v/v

From Figure 2.35 $V_c = 105$

$$\gamma_{gres} = \frac{0.65 + \dfrac{750}{1.225 \times 3500}}{1 + \dfrac{105}{3500}} = 0.8$$

In cases where measurements are made on stock tank condensate, instead of the high pressure separator condensate, the following procedure provides the way for calculating the relative density of a reservoir gas.

$$\gamma_{gres} = \frac{\gamma_g + \dfrac{\rho_{csto}}{\rho_{air} \times GOR_{sto}}}{1 + \dfrac{V_{csto}}{GOR}} \tag{2.41}$$

γ_{gres}: relative density of reservoir gas (air = 1)
ρ_{csto}: density of stock tank condensate at 15°C, kg/m^3
GOR_{sto}: gas stock tank condensate ratio, m^3 separator gas per m^3 stock tank condensate (1.01325 bars, 15°C)
V_{cs}: stock tank condensate vaporization volume ratio, m^3 per m^3 stock tank condensate (1.01325 bars, 15°C)
γ_g: relative density of the high pressure (hp) separator gas (air = 1)
ρ_{air}: air density at standard conditions = 1.225 kg/m^3

The required data from the field needed to use Eq. (2.41):

- Flow rate of the high-pressure separator gas stream and the accumulation rate of the stock tank condensate obtained from field measurements.
- Operating pressure of the high pressure separator from field measurements.
- Relative density of the high-pressure separator gas and the density of the stock tank condensate obtained from laboratory measurements.
- Stock tank condensate vaporizing volume ratio obtained from Figure 2.36

The stock tank condensate vaporizing ratio V_{cs} is dependent on density and separator pressure, see Figure 2.36 [65].

To sum up, the calculation of the reservoir gas relative density is carried out with Eq. (2.40) or Eq. (2.41). The difference being the evaluation of the equivalent gas volume of the condensate Vc. Vc is estimated from Figure 2.35 if the data origin is separator conditions or from Figure 2.36 if production data come from stock tank conditions to correct for working separator pressure.

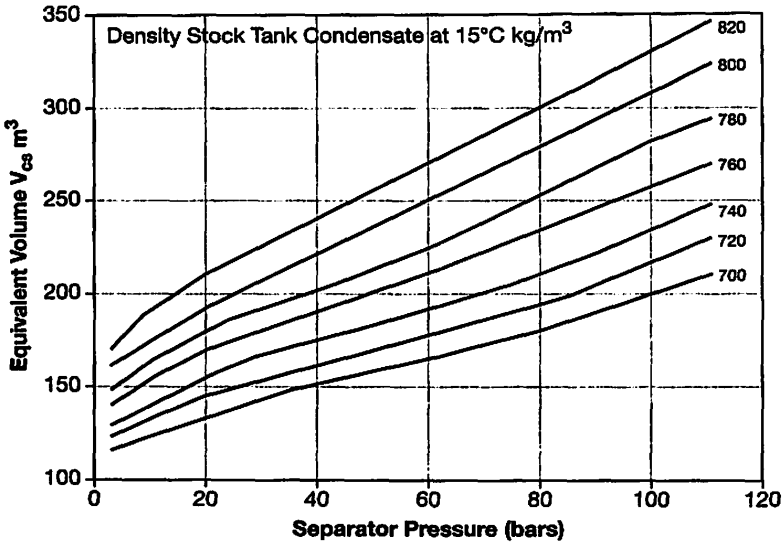

Figure 2.36 Equivalent Gas Volume of Stock Tank Condensate Adapted from Leshikar (1961).

The reservoir gas relative density may be calculated also by determining the molar mass of the gas M_g, and dividing M_g by 28.966 (molar mass of air).

Reservoir gas mass corresponding to $1m^3$ of high pressure separator condensate:

$$m_g = \rho_c + GOR \times \gamma_g \times \rho_{air}$$

Number of corresponding moles of separator gas: GOR/23.6

Number of condensate moles at stock tank: ρ_c/M_c

Adding the moles

The molar mass of the reservoir gas is then: *(data measured at stock tank conditions)*

$$M_{gres} = \frac{\rho_c + GOR \times \gamma_g \times \rho_{air}}{(GOR/23.6) + (\rho_c / M_c)} \tag{2.42}$$

Molar mass of condensate is evaluated from Figure 2.37 [38].

The molecular mass versus relative density is not an exact correlation since these are not dependent variables. It is an approximate correlation that should be used only when data do not permit use of a better one.

Finally, the reservoir gas relative density is:

$$\gamma_{gres} = \frac{M_{gres}}{28.966} \tag{2.43}$$

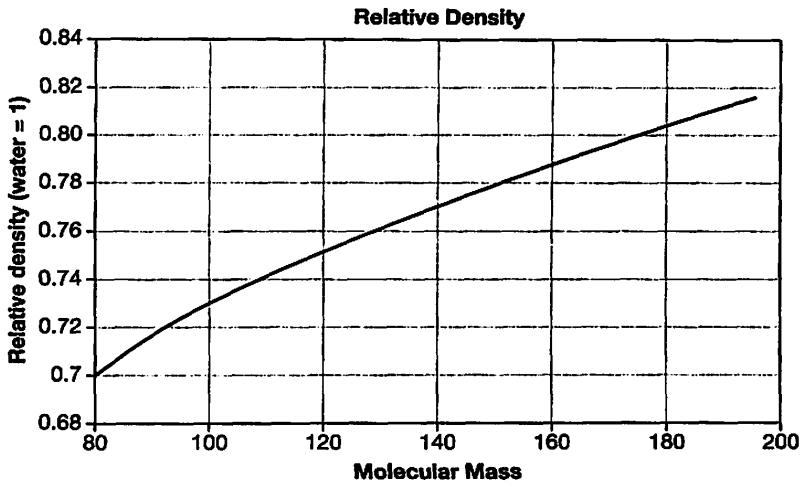

Figure 2.37 Molecular mass versus Relative Density for typical crudes and condensates at 15°C and 100 kPa.

Remark:
These procedures to calculate the reservoir gas relative densities may be applied only when detailed information regarding the compositions of the various separator streams is not available.

2.13.7.3 Gas condensate richness

Associated liquid hydrocarbons in natural gases are called "Natural Gas Liquids" (NGL). They are very valuable by-products of natural gas processing. NGLs include ethane, propane, butane, iso-butane and natural gasoline. These NGLs are sold separately and have a variety of different uses; including enhanced oil recovery, providing raw materials for oil refineries or petrochemical plants, and as sources of energy.

The initial NGL yield is calculated from the gas composition.

It is usual in the industry to separate LPG (Liquid Petroleum Gas: C_3 and C_4) with condensate: C_{5+} also called gasoline.

For a gas condensate reservoir, the NGL yield produced decreases with time if the reservoir pressure declines due to heavy component trapping in the porous media *(reservoir pressure below the gas dew point pressure)*. Therefore the production GOR increases with time. This is one of the reasons why it is important to identify the fluid nature at time of discovery in order to build a reliable production forecast profile. The phenomenon does not occur in the case of a wet gas since no liquid deposit occurs in the porous media.

2.13.8 Gas Heating Value

A gas producing operator does not sell volumes but gas heating capacity.

Units:

The basic field unit in use is the Btu (British Thermal Unit).

For the metric system the unit is Joule.

Sometimes the "therm" is used. (1 therm = 100 000 Btu)

The calorie or kcal units are no longer valid.

Conversion: 1 kJ = 0.948 Btu or 1 Btu = 1.055 kJ

The heating value of natural gas [62] is the heat liberated when a unit of fuel is burned under specific conditions. The heating value is the negative of the enthalpy of combustion $-\Delta$ Hc of a gas or liquid in its standard state at 15°C to give combustion products in their standard states, all at 1 atm (101.325 kPa abs).

For the gross heating value, the water produced by the combustion is in the liquid form. For the net heating value, the water is in the gas state.

Gross heating value of a natural gas is calculated from the complete analysis of the mixture.

Ideal gas heating value H is:

$$H = x_1H_1 + x_2H_2 + \ldots x_nH_n$$

$x_1, x_2, \ldots x_n$ = mole fractions of the components

$H_1, H_2, \ldots H_n$ = Ideal gas heating values of the components

The ideal gas heating value H, is corrected to the real gas heating Hr by dividing H by the compressibility factor Z for the gas mixture at standard conditions.

Hr = H/Z

2.13.9 Calculation of Gas Properties from Composition

From a detailed gas composition, many properties can be deducted with Tables 2.37, 2.38.

2.14 VAPOR LIQUID EQUILIBRIUM (VLE) [2, 15, 38, 40, 44]

The produced well stream at surface is submitted to a separator process, liquid is stored in a tank and gas collected for further conditioning. The processing and conditioning implies the control of the vapor-liquid ratio. The design and specifications of the installations necessitates the ability to predict the bubble point and dew point conditions as well as the vapor liquid behavior anywhere within the phase envelope.

In a compositional reservoir simulation, it is necessary to know the nature of the fluid (vapor, or liquid or both and amounts) in each grid cell and at each timestep. A vapor liquid equilibrium calculation is the answer to the question.

The calculations are based on the assumption of instantaneous equilibrium. The hydrocarbon systems are made of many components. Each component is present in the vapor and liquid phase.

Considering z_i, the mole fraction of any component in the total feed stream.

y_i: mole fraction of any component in the vapor phase.

x_i: mole fraction of any component in the liquid phase.

The split of the component i between the vapor phase and the liquid phase, is characterized by the ratio:

Equilibrium constant $$k_i = \frac{y_i}{x_i} \tag{2.44}$$

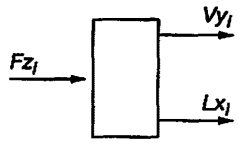

Figure 2.38 Liquid Vapor Split.

F: total moles of feed
L: total moles of liquid
V: total moles of vapor

k value is function of pressure, temperature and composition

over all balance is: $$F = L + V \tag{2.45}$$

Material balance equation for each component:

$$Fz_i = Lx_i + Vy_i \tag{2.46}$$

Compositions are given in moles fractions so:

$$\Sigma z_i = \Sigma x_i = \Sigma y_i = 1 \tag{2.47}$$

Equilibrium is reached when for each component within the hydrocarbon mixture; the number of moles transferring from liquid to vapor is equal to the number of moles moving from vapor to liquid.

The thermodynamic criteria for equilibrium, states that the fugacities in the liquid and the vapor phase must be equal (Appendix H):

$$f_{iL} = f_{iV}$$

In an equation of state approach, the fugacities are calculated from the equation of state. The fugacity depends on temperature, pressure, composition and the phase type considered.

$$Fi = fi\ (T, P, x_i, \text{type})$$

Table 2.37 Calculation Example of Gas Properties

RAMH

Name	Formula	GAS (E) Mw	COMPOSITION (F) % mole	(G) LPG C3/C4	(H) Condensate C5+	(I) F/100 %mole C3/C4 from gas	(J) I/Sig(I) frac for each comp	(K) GPSA table liq volume m^3/kgmole	(L) K*J volume C3/C4	(M) E*F/100 Mw calc 0.54905 0.37409 12.7831 2.3304	(N) F/100 compo C5+ from gas	(O) N/Sig(N) fraction C5+ each compo	(P) K*O vol C5+	(Q) E*O Mw C 5+ calc	(R) GPSA table Liq density std g/cm³	(S) G or H/R Liq vol std cm³
Nitrogen	N2	28.013	1.96													
Carbon dioxyde	CO2	44.010	0.85													
Hydrogen sulfide	H2S	34.076	0.00													
Methane	CH4	16.043	79.68													
Ethane	C2H6	30.070	7.75													
Propane	C3H8	44.097	3.10	1.367		0.031	0.5545	0.08684	0.04816	1.3870					0.5078	2.6920
i Butane	C4H10	58.124	1.18	0.886		0.012	0.2111	0.10320	0.02178	0.6859					0.5632	1.2178
n Butane	C4H10	58.124	1.31	0.761		0.013	0.2343	0.09949	0.02332	0.7614					0.5842	1.3034
i Pentane	C5H12	72.151	0.76		0.548			0.11560		0.5483	0.0076	0.1823	0.02107	13.14982	0.6244	0.8782
n Pentane	C5H12	72.151	0.54		0.390	0.0559	1	0.11430	0.09326	0.3896	0.0054	0.1295	0.01480	9.34329	0.6310	0.6175
n Hexane	C6H14	84.000	0.78		0.655			0.12980		0.6552	0.0078	0.1871	0.02428	15.71223	0.6640	0.9557
n Heptane	C7H16	96.000	0.63		0.605			0.14560		0.6048	0.0063	0.1511	0.02200	14.50360	0.6882	0.8788
n Octane	C8H18	107.000	0.58		0.621			0.16160		0.6206	0.0058	0.1391	0.02248	14.88249	0.7068	0.8780
n Nonane	C9H20	121.000	0.38		0.460			0.17770		0.4598	0.0038	0.0911	0.01619	11.02638	0.7217	0.6371
n Decane	C10H22	134.000	0.22		0.295			0.19390		0.2948	0.0022	0.0528	0.01023	7.06954	0.7341	0.4016
Undecane	C11H24	172.000	0.28		0.482			0.23243		0.4816	0.0028	0.0671	0.01561	11.54916	0.7400	0.6508
Dodecane	C12H26															
Tridecane	C13H28															
Tetradecane	C14H30															
Pentadecane	C15H32															
Hexadecane	C16H34															
Heptadecane	C17H36															
Octodecane	C18H38															
Nonadecane	C19H40															
Eicosane	C20+															
	Mw gas =	22.9	100	Yield 119.10 g/m³	171.59 g/m³					Mw gas 22.9057	total mole 0.0417	1	total m³ 0.14665	Mw C5+ 97.24		total cm³ 11.1419

Mw C3/C4 = 50.35
Rho C3/C4 = 539.8 kg/m³

Mw C11 + = 172 Rho C11 + = 740 kg/m³
Mw C5+ = 97.2 Rho C5+ = 663.0 kg/m³

YIELD / std well stream	C3/C4	C5+	units	C4 +	C3 +
	119.1	171.6	g/sm³	232.8	290.7
	221	259	cm³/sm³		
	39.3	46.1	bbls/MMscf		
		1.68	gpm	2.67	3.53

GOR / std well stream	C3/C4	C5+	units
	4533	3864	m³/sm³
	25452	21696	scf/std bbl

Table 2.38 Detailed Calculation Example of Gas Properties

RAMAH Gas Composition

From a complete gas composition, important engineering data can be deducted.

The calculated results refer to a given composition. During field production history, the produced gas composition changes. The produced gas heavy component yield decreases. Therefore the production GOR increases.

LPG or GPL Liquid Petroleum Gas is the mixture of C3/C4 or GPL (french)

GPSA = Gas Processors Suppliers Association

LNG = Liquefied Natural Gas

Calculations are based on the hypothesis of adding volumes is valid

Column	
(E)	molar mass of each component
(F)	mole percent of each component
(G)	= (E) * (F) for C3 & C4 mass content in one mole of feed
(H)	= (E) * (F) for C5+ mass content in one mole of feed
(I)	mole fraction of each component 0.0559 = sigma of mole frac for C3/C4
(K)	liquid specific volume from GPSA table
(L)	= (K) * (J) liquid volume of each component 0.0933 = sig of volumes
(M)	= (E) * (F)/100 : mass of each component in one mole of feed 22.9057 = feed gas molar mass
(N)	= (F)/100 mole frac for C5+ 0.0417 = sig of mole frac for C5+
(O)	= (N)/ 0.0417 mole frac of each component within the C5+
(P)	= (K) * (O) volume contribution of each component in C5+ 0.14677 m^3 = C5+ liquid volume in 1 kmole of feed gas
(Q)	= (E) * (O) mass of each component in 1 mole of C5+ 97.24 = molar mass of C5+
(R)	= Liquid density at std conditions from GPSA table
(S)	= liquid volume contribution of each component of C3+ 11.1419 = total liquid volume in 1 mole of feed gas
Yield	calculated from the composition, knowing that the volume of 1 feed gas mole at std conditions is 23.63 dm^3

units

bbls/MMscf	used in international contracts	a rich gas can be as high as 230 bbls/MMscf
gpm	stands for gallons per 10^3 scf	1 US gallon = 3.785 dm^3

remark : The deducted GOR is not representative of a classical field GOR
it is calculated relative to a standard condition well stream mole of feed gas

With the cubic equations of state, the same equation is used for both the liquid and the vapor phase. A cubic equation may give 3 solutions in volume. The smallest volume is chosen for the liquid phase and the greatest volume for the vapor phase.

2.14.1 Flash Calculation

The objective of each flash calculation on a two phase system is to determine the amounts of vapor and liquid and the composition of each [2, 66].

Combining Eq. (2.45) with Eq. (2.46) gives:

$$z_i F = \frac{y_i}{k_i} L + y_i V \tag{2.48}$$

$$y_i = \frac{z_i F}{L/k_i + V} = \frac{F}{V} \frac{k_i z_i}{k_i + L/V}$$

for F = 1 mole

$$y_i = \frac{k_i z_i}{(k_i - 1)V + 1}$$

For all components:

$$\sum y_i = 1 = \sum \frac{F}{V} \frac{k_i z_i}{k_i + L/V} \tag{2.49}$$

Similarly

$$x_i = \frac{F}{V} \frac{z_i}{k_i + L/V} = \frac{z_i}{(k_i - 1)V + 1}$$

$$\sum x_i = 1 = \sum \frac{F}{V} \frac{z_i}{k_i + L/V} \qquad \text{with F = 1 mole} \tag{2.50}$$

$$V = \sum \frac{k_i z_i}{k_i + L/V} = \sum \frac{z_i}{k_i + L/V} \tag{2.51}$$

Given a composition of feed and equilibrium constants k_i for a selected pressure and temperature, a value of V is assumed and $\Sigma z_i/(k_i + L/V)$ terms are calculated to find whether the V value is correct.

Alternative methods of combining Eq. (2.44) with Eq. (2.45) lead to the following try and error solution handling method:

Subtracting Eq. (2.50) from Eq. (2.49) one obtains:

$$\sum y_i - \sum x_i = 0 = \sum \frac{z_i (k_i - 1)}{V(k_i - 1) + 1} \tag{2.52}$$

After the first trial value V, the Newton's numerical method is used to converge to the satisfactory V value. This implies the derivative of Eq. (2.50) with respect to V.

$$\frac{\delta}{\delta V}\left[\sum \frac{z_i(k_i-1)}{V(k_i-1)+1}\right]=\sum \frac{z_i(k_i-1)^2}{\left[V(k_i-1)+1\right]^2} \tag{2.53}$$

When the solution of Eq. (2.52) is outside of the interval [0, 1], this indicates a single phase state. Then the non-existing phase composition is calculated as if the system was at the saturation pressure:

If V < 0, V is set to 0, and $x_i = z_i$ $\quad y_i = \dfrac{k_i x_i}{\sum k_i x_i}$

If V > 1, V is set to 1, and $y_i = z_i$ $\quad x_i = \dfrac{y_i / k_i}{\sum y_i / k_i}$

An initial k_i value estimation is necessary to start the iterative process (Eq. (2.54)).

$$k_i = \frac{1}{p_{ri}} \exp\left[5.37(1+\varpi_i)(1-1/T_{ri})\right] \tag{2.54}$$

2.14.2 k Values Determination

As seen above, *k* values are function of pressure, temperature and overall composition. *k* values can be estimated with empirical correlations or by satisfying the equal fugacity constraint with an equation of state (EOS).

The generalized use of EOS has decreased the interest in correlations. Nevertheless empirical methods are still used for multistage separation process.

Before the extensive use of EOS, a method to estimate equilibrium constants k_i based on the concept of convergence pressure was used.

The method is not detailed here, only the basic concept is evoked.

2.14.3 Convergence Pressure Concept [62, 66]

It has been observed that, at high pressures, the *k* values of all components in a mixture tend to converge to unity at the same pressure. This pressure is called the convergence pressure and for binaries, represents the actual mixture critical pressure.

k equilibrium constants have been correlated as a function of temperature, pressure and convergence pressure. These correlations led to the following postulate:

"The equilibrium vaporization constant for one component in a complex system is the same as the equilibrium constant at the same temperature and pressure for the same component in another system whether or not composed of the same number or kind of

components, providing only that the convergence pressures of the two systems are exactly the same at the same temperature and that the components are of the same homologous series."

2.14.4 Low Pressure k_i Determination [67, 68, 69]

Composition dependency usually is indicated by the apparent convergence pressure value (for example, 5 000 psia, and 10 000 psia). However, at pressures below 1 000 psia, the effect of the system composition is small and often may be neglected. The basic k data involved are those developed by Katz and Hachmuth on recombined samples of gas and oil from the Wilcox sand of the Oklahoma City Field. The k values corresponded to pressures of 14, 200, 400, 600, 800, 800, and 1 000 psia, at temperatures of 40°, 120°, and 200°F.

Hoffman *et al.* [68], proposed a correlation which is widely used in the industry for low pressures:

$$k = (1/p)10^{(a+cF)} \qquad F = b(1/T_B - 1/T) \tag{2.55}$$

k: equilibrium ratio y/x
p: pressure, psia or (Mpa)
T_B: boiling point of the compound at 14.7 psia, °R (K) see Table 2.39
b: slope of the straight line connecting the critical point and the atmospheric boiling point on a log vapor pressure vs. 1/T plot (Table 2.39).

Table 2.39 Values of b and T_B For use in the Low pressure K value Correlation

Component	(Cycle °R)	T_B (°R)
N_2	470	109
CO_2	652	194
H_2S	1 136	331
C_1	300	94
C_2	1 145	303
C_3	1 799	416
iso-C_4	2 037	471
n-C_4	2 153	491
iso-C_5	2 368	542
n-C_5	2 480	557
C_6 (lumped)	2 738	610
n-C_6	2 780	616
n-C_7	3 068	669
n-C_8	3 335	718
n-C_9	3 590	763
n-C_{10}	3 828	805

$$b = \frac{\log(p_c / 14.7)}{\left(1/T_B - 1/T_C\right)} \tag{2.56}$$

T: temperature °R (K)
T_c: critical temperature of the compound, °R (K)
p_c: critical pressure of the compound; psia (Mpa)

$$a(intercept) = 1.2 + 4.5(10^{-4})\,p + 15(10^{-8})\,p^2$$
$$c(slope) = 0.89 - 1.7(10^{-4})\,p - 3.5(10^{-8})\,p^2$$

For heptanes and heavier components:

$$n_{C7+} = 7.3 + 0.0075T(°F) + 0.0016\,p$$
$$b_{C7+} = 1013 + 324\,n_{C7+} - 4.256\,n^2_{C7+}$$
$$T_{BC7+} = 301 + 59.85\,n_{C7+} - 0.971 n^2_{C7+}$$

n_{C7+}: effective carbon number

2.15 EQUATION OF STATE (EOS)

Since the time of Van der Waals, (1873), engineers imagined lots of equations of state to represent the pressure-volume-temperature fluid behavior. These equations range from simple expressions with one or two constants to complicated forms with up to more 50 constants. The longer equations have been used for high accuracy work; those can be found in the literature. Semi empirical relationships have been proposed in order to try combining simplicity and accuracy.

One of the most successful was proposed by Redlich and Kwong in 1949. Since that time, numerous modifications have been suggested to fit pure substance PVT data and equation's capability for vapor-liquid equilibrium (VLE) predictions.

In 1972 Soave modified the Redilch Kwong equation which gave birth to the Soave-Redlich-Kwong equation (SRK). This new equation gained rapidly acceptance by the hydrocarbon processing industry [56, 70] because of its relative simplicity and its capability of generating reasonable accurate VLE calculations. However the SRK equation fails to generate satisfactory liquid densities even though vapor density values are acceptable.

The same form of equation used for gas is also employed for liquid.

2.15.1 Van Der Waals Equation

Van der Waals modifies the perfect gas expression by adding two correction terms:

- Internal pressure or cohesion pressure:
  - The kinetic theory of gas neglects the cohesion forces existing between moles. Near a boundary or an interface, the resulting force is not nil, so that the measured pressure is lower than the one would exist if the gas was perfect.

- The proposed correction is:

$$P_{int} = \frac{a}{V^2} \qquad P_{measured} = P_{perfect\ gas} - \frac{a}{V^2} \tag{2.56}$$

– Co-volume:
  - The molecules have a finite volume which limits the free space to move about. The measured volume is then corrected by the term *b* called the co-volume.

The resulting Van der Waals Equation is:

$$\left(P + \frac{a}{V^2}\right)(V - b) = RT \qquad \text{or} \qquad P = \frac{RT}{V - b} - \frac{a}{V^2} \tag{2.57}$$

At the critical point, the curvature of the isotherm *P(V)* reverses and the tangent is horizontal.

Therefore a value of *a* and *b* can be obtained in terms of the critical properties:

$$\left(\frac{\delta P}{\delta V}\right)_{P_c,T_c} = \left(\frac{\delta^2 P}{\delta V^2}\right)_{P_c,T_c} = 0$$

$$\left(\frac{\delta P}{\delta V}\right)_T = -\frac{RT}{(V-b)^2} + \frac{2a}{V^3} \qquad \left(\frac{\delta^2 P}{\delta V^2}\right)_T = \frac{2RT}{(V-b)^3} - \frac{6a}{V^4}$$

$$\text{With } Z = \frac{PV}{RT} \qquad a = \frac{27}{64}\frac{R^2 T_c^2}{P_c} \qquad b = \frac{RT_c}{8P_c} \qquad Z_c = \frac{3}{8} = 0.375$$

The equation is superior to the ideal gas law and does not predict the formation of a liquid phase. The agreement with experimental data is limited for conditions where the liquid forms.

The Van der Waals equation may be considered as "improved" ideal gas law limited for use to low pressure and low temperature ranges.

2.15.2 Redlich-Kwong Equation of State (1949)

$$P + \frac{a}{\sqrt{T}\,V(V+b)}(V-b) = RT$$

The equation is similar to the one proposed by Van der Waals. The internal pressure term has been modified to improve the representativity in the high temperature domain (above *Tc*). The equation is simple and can be used to model the liquid phase in addition to the vapor phase and the phase change.

$$P = \frac{RT}{V-b} - \frac{a}{\sqrt{T}\,V(V+b)} \tag{2.58}$$

The Redlich-Kwong equation has been commonly used in the industry to perform phase equilibrium calculations of hydrocarbon mixtures.

In 1971, Soave proposed to modify the Redlich-Kwong equation in order to closely reproduce saturation pressure of pure components by assuming the parameter a in the original equation to be temperature dependent. With the introduction of the acentric factor as a third parameter, a generalized correlation for the modified parameter can be derived.

Acentric Factor (ω):

The factor ω [56] was developed by Pitzer in 1955 to describe the deviation of a fluid from simple fluid vapor, or its non conformity with the corresponding states principle. For the simple gases like argon, xenon, ω is equal to zero.

Other way to characterize the factor consists of saying that Pitzer developed a way of accounting for the "non-central" or "acentric" (non spherical size-shape) interactions empirically. The acentric factor ω is defined as:

$$\varpi = -\log_{10} P_r - 1 \quad \text{with} \quad P_r = \frac{P^*}{P_c}$$

P^*: saturation pressure at $T = 0.7\ T_c$ P_c: critical pressure

2.15.3 Soave-Redlich-Kwong EOS (SRK) [66]

The term $\frac{a}{\sqrt{T}}$ from Eq. (2.58) was replaced by a more general temperature dependent term $a(T)$: to obtain the Soave-Redlich-Kwong EOS:

$$P = \frac{RT}{V-b} - \frac{a(T)}{V(V+b)} \tag{2.59}$$

Letting:

$$V = Z\frac{RT}{P} \qquad A = \frac{aP}{R^2T^2} \qquad B = \frac{bP}{RT} \tag{2.60}$$

Eq. (2.59) can be written:

$$Z^3 - Z^2 + Z(A - B - B^2) - AB = 0 \tag{2.61}$$

Pure Substances:

Similarly to the Van der Waals equation, at the critical point for each pure substance, the first and second derivative of pressure with respect to volume is zero. Then we obtain:

$$a_i(T_{ci}) = a_{ci} = 0.42747\frac{R^2T_{ci}^2}{P_{ci}} \qquad b_i = 0.08664\frac{RT_{ci}}{P_{ci}} \tag{2.62}$$

At temperatures other than the critical, let:

$$a_i(T) = a_{ci}\alpha_i(T) \tag{2.63}$$

$\alpha_i(T)$ is an dimensionless factor = *1* at $T = T_{ci}$

Applying Eq. (2.62), Eqs. (2.60) become for pure substances:

$$A = 0.42747\alpha_i(T)\frac{P/P_{ci}}{(T/T_{ci})^2} \qquad B = 0.08664\frac{P/P_{ci}}{T/T_{ci}} \tag{2.64}$$

The fugacity of a pure component is calculated from the thermodynamic relationship (Appendix H):

$$\mathrm{Ln}\frac{f}{P} = \int_0^P\left(\frac{V}{RT} - \frac{1}{P}\right)dp \tag{2.65}$$

Applying the relationship Eq. (2.65) to Eq. (2.59)

$$\mathrm{Ln}\frac{f}{P} = Z - 1 - \mathrm{Ln}(Z - B) - \frac{A}{B}\mathrm{Ln}\left(\frac{Z+B}{Z}\right) \tag{2.66}$$

For a real gas of free enthalpy G at pressure P, the fugacity of the gas is the virtual pressure f at which it should be if it behaved as a perfect gas.

Solving Eq. (2.61) generally gives one or three roots depending on the number of phases present. Only the positive roots can be retained. In the two-phase region, the largest root is for the compressibility factor of the vapor while the smallest positive root corresponds to that of the liquid.

2.15.4 Peng-Robinson Equation

Peng-Robinson EOS [66] was developed specifically for light hydrocarbons. It was to improve performance or rectify defects of previous EOS. But, since there are only a limited number of parameters available, all defects cannot be corrected.

Din-Yu Peng and Donald B. Robinson proposed a new semi-empirical equation of state in 1976 in order to satisfy the following goals:

The parameters should be expressible in terms of the critical properties and the acentric factor.

- The model should provide accuracy near the critical point, particularly for calculations of the compressibility factor and liquid density.
- The mixing rules should not employ more than a single binary interaction parameter, which should be independent of temperature and composition.
- The equation should be applicable to all calculations of all fluid properties in natural gas processes.

For the most part, the Peng-Robinson Equation exhibits performance similar to the Soave equation, although it is generally superior in predicting the liquid densities of many materials, especially non polar ones.

Semi-empirical equations of state are expressed as the sum of two terms, a repulsion pressure P_R and an attraction pressure P_A as follows:

$$P = P_R + P_A$$

$$P_R = \frac{RT}{v-b} \qquad P_A = -\frac{a}{g(v)}$$

b is related to the size of the hard spheres; $g(v)$ is a function of the molar volume v; parameter a characterizes the intermolecular force. The pressure exerted on the container wall is reduced by the intermolecular attraction.

a and b can be expressed in terms of critical properties:

$a = f(P_c, T_c, v_c)$

$b = g(P_c, T_c, v_c)$

Peng-Robinson proposed the equation:

$$P = \frac{RT}{v-b} - \frac{a(T)}{v(v+b)+b(v-b)} \tag{2.67}$$

Letting:

$$A = \frac{aP}{R^2T^2} \qquad B = \frac{bP}{RT} \qquad Z = \frac{Pv}{RT}$$

Eq. (2.67) expressed in terms of Z becomes:

$$Z^3 - (1-B)Z^2 + (A - 3B^2 - 2B)Z - (AB - B^2 - B^3) = 0 \tag{2.68}$$

The solution of Eq. (2.68) leads to one or three roots depending upon the number of phases. In the two-phase system, the largest root corresponds to the vapor phase and the smallest to the liquid phase.

Applying the critical point conditions to Eq. (2.67) leads to:

$$\left(\frac{\delta P}{\delta V}\right)_{P_c,T_c} = \left(\frac{\delta^2 P}{\delta V^2}\right)_{P_c,T_c} = 0$$

$$a(T_c) = 0.45724\frac{R^2T_c^2}{P_c} \qquad b(T_c) = 0.07780\frac{RT_c}{P_c} \qquad Z_c = 0.307 \tag{2.69}$$

At temperatures other than the critical, let

$$a(T) = a(T_c) \times \alpha(T_r, \omega) \qquad b(T) = b(T_c) \tag{2.70}$$

$\alpha(T_r, \omega)$:dimensionless function of reduced temperature T_r and acentric factor ω; for $T = T_c$, $\omega = 1$.

Applying the relationship Eq. (2.65) to Eq. (2.67) the fugacity of a pure component is derived:

$$\text{Ln}\frac{f}{P} = Z - 1 - \text{Ln}(Z - B) - \frac{A}{2\sqrt{2}B}\text{Ln}\left(\frac{Z + 2.414B}{Z - 0.414B}\right) \tag{2.71}$$

Equilibrium is reached when the fugacity in the liquid phase is equal to the one in the vapor phase for each component.

$\alpha(T_r, \omega)$ can be expressed as: $$\sqrt{\alpha} = 1 + k\left(1 - \sqrt{T_r}\right) \tag{2.72}$$

where k is correlated with the acentric factor ω

$$k = 0.37464 + 1.54226\,\omega - 0.26992\,\omega^2 \tag{2.73}$$

The mixture parameters to be used in Eq. (2.68) and Eq. (2.71) are defined by the mixing rules:

$$a = \sum_i \sum_j x_i x_j a_{ij} \qquad b = \sum_i x_i b_i \tag{2.74}$$

With $$a_{ij} = \left(1 - \delta_{ij}\right)\sqrt{a_i}\sqrt{a_j}$$

δ_{ij} is an empirically determined binary interaction coefficient between component i, and component j.

The fugacity coefficient of component k in a mixture is calculated from:

$$\text{Ln}\frac{f_k}{x_k P} = \frac{b_k}{b}(Z - 1) - \text{Ln}(Z - B) - \frac{A}{2\sqrt{2}B} \times \left(\frac{2\sum X_i a_{ik}}{a} - \frac{b_k}{b}\right) \times \text{Ln}\left(\frac{Z + 2.414B}{Z - 0.414B}\right) \tag{2.75}$$

2.15.5 Volume Translation for Cubic Equation of State

Peneloux and Rauzy [71] (1982) introduced a volume correction parameter c into the SRK Equation of Sate to improve the calculated volume. The improvement was to minimize the errors in the saturated liquid volumes as predicted by the SRK EOS at Tr = 0.7. The third parameter c does not change the vapor-liquid equilibrium conditions determined by the EOS

equation, but affects the liquid and gas volumes by a volume translation along the volume axis. The correction is particular for each substance and is independent of temperature.

For mixture:

$$V_L = V_L^{EOS} - \sum_{i=1}^{N} x_i c_i \qquad \text{and} \qquad V_V = V_V^{EOS} - \sum_{i=1}^{N} y_i c_i$$

V_L^{EOS}, and V_V^{EOS} = EOS calculated liquid and vapor molar volumes
x_i, y_i: liquid and vapor compositions
c_i: individual component dependent volume shift parameter that is found experimentally and being generalized as:

$$c_i = 0.40768(0.29441 - Z_{RA})\frac{RT_c}{P_c}$$

Z_{RA}: Rackett compressibility calculated from (Reid *et al.*, 1987) [72]

$$Z_{RA} = 0.29056 - 0.08775\varpi$$

P_c, T_c: critical pressure and temperature of the substance
ω: acentric factor

B. Hoyos [73] showed that a constant specific volume shift like that of Peneloux *et al.* (1982) applied to the SRK or the Peng-Robinson EOS is not completely satisfactory for calculations of liquid volumes of hydrocarbons. He proposed a generalized temperature function, which does not require additional parameters for each substance and produces lower relative deviations than Peneloux model.

Watson *et al.* (1986) proposed a correction equation for specific volume of liquids for the Peng-Robinson EOS. The correction is an exponential function of temperature that can be used in the region close to the critical point only. Other authors proposed a correction function of temperature which necessitates an additional parameter.

2.15.6 Vapor Liquid Equilibrium Calculation with an EOS

Figure 2.39 depicts the algorithm used for the Vapor Liquid Equilibrium Calculation with an Equation of State.

Fussell and Yanosik [66] published a method to accelerate the convergence to the solution of the algorithm.

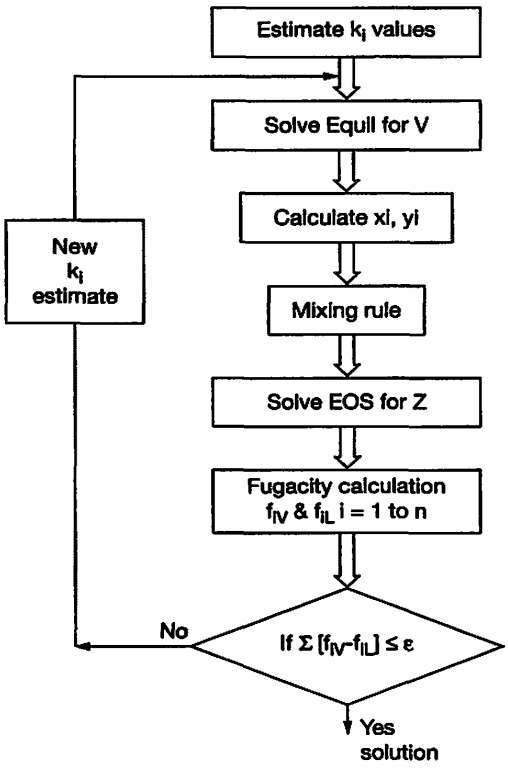

At pressure P and temperature T_r

Step 1 estimate an initial k_i with Eq. (2.54)
Step 2 solve VLE for V with Eq. (2.52)
Step 3 calculate the liquid and vapor compositions x_i, y_i.
Step 4 use the mixing rule
Step 5 build and solve the EOS in terms of Z
Step 6 calculate the vapor and liquid fugacity of each component
Step 7 convergence test on errors $\Sigma|f_{iV}-f_{iL}| \leq \varepsilon$

If test is verified then the solution is reached otherwise step 8

Step 8 estimate new values of k_i, go to step 2

Figure 2.39 VLE Calculation Algorithm.

2.16 APPLICATIONS TO RESERVOIR ENGINEERING

2.16.1 Determination of Initial Reservoir Fluid Nature

At time of discovery, it may be difficult to distinguish whether the reservoir fluid is liquid or gas. From experience, based on surface liquid color, density, and production GOR, general rules of thumbs have been established. Nevertheless, in the field during a production test, the results may be ambiguous. It is necessary to know as soon as possible the nature of the reservoir fluid with its properties to build an appropriate field development plan (Fig. 2.40). Fluid sampling must be carried out with great care.

Usually a gas condensate reservoir is associated with an oil rim. This option must be kept in mind until a gas water contact is encountered.

The Black oil option is valid when the fluid representing point on the pressure temperature plot is far from the critical point (Fig. 2.40).

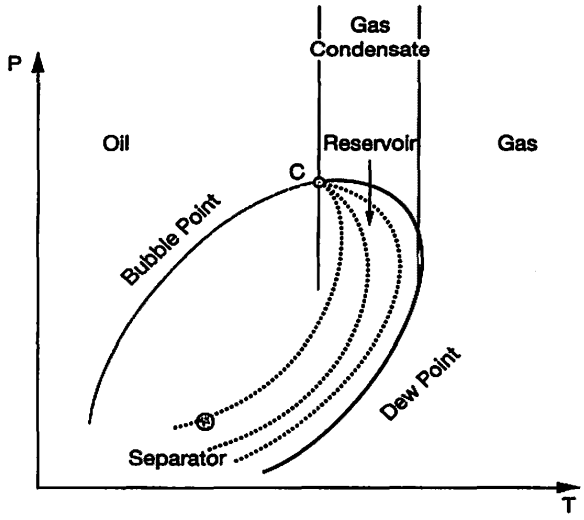

Figure 2.40 Phase Envelope on a pressure, temperature Plot.

2.16.2 Total Formation Volume Factor: Diphasic FVF

Let's consider a constant mass hydrocarbon system in a cell. At a pressure higher than bubble point pressure, the total hydrocarbon is totally monophasic liquid. The Bo increases when the pressure decreases until the bubble point pressure is reached.

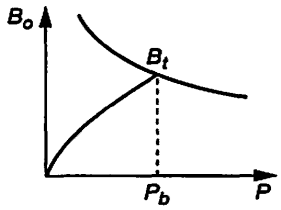

Figure 2.41 Oil FVF.

More depletion creates a gas phase in the cell and the total hydrocarbon formation volume factor is the sum of the oil FVF + the contribution of the free gas FVF:

$$B_t = B_o + R_l \times B_g$$

R_l: liberated gas $= R_{si} - R_s$

Therefore:

$$B_t = B_o + (R_{si} - R_s)\, B_g$$

R_{si}: initial gas in solution per unit volume of liquid (both at STD conditions)
R_s: gas in solution at current pressure P

The total formation volume factor is used in the material balance calculations.

2.16.3 Composite PVT Functions [1, 59]

To conduct a material balance calculation, the engineer needs of a unique set of PVT properties to convert surface measurements into reservoir conditions data.

The laboratory report gives results of different experiments that have been ordered by the operator:

Usually the results are:

- Constant mass study to define the saturation point pressure *(bubble point or dew point pressure)*
- Flash liberation of bubble point oil to standard conditions
- Flash liberation of bubble point oil through separators and to stock tank
- Differential vaporization liberation.

For each process, values of formation volume factor B_o and dissolved gas R_s ratios are reported. The difficulty is that none of these processes simulates properly the field operation.

The differential vaporization process is an approximation of what is taking place far away from the production well in the reservoir. Gas being highly mobile, under a small pressure gradient it moves quickly to the production well.

Flash liberation is considered to occur between the reservoir and the surface separators. There are some differences between the process simulated in the laboratory and the field operations. In the field, the oil and gas moving through the tubing are submitted to a progressive pressure and temperature changes. The result is gas comes out of solution gradually in the tubing. In addition to this, the two phases: gas and oil flow at different velocities in the casing and tubing. The complex process is not reproducible in the laboratory.

Therefore a compromise is elaborated under the name of "composite" PVT properties. From the two laboratory experiments, a composite PVT is built to be used for material balance calculations.

$$\text{Composite FVF} \quad B_o = B_{od}\frac{B_{ofb}}{B_{odb}} \tag{2.76}$$

B_{od} oil FVF obtained during the differential process function of pressure f(P)

B_{ofb} oil FVF obtained from the flash liberation through separators of the oil at its bubble point pressure

B_{odb} oil FVF measured during the differential process of the oil at its bubble point pressure

Interpretation: using the FVF differential as a reference, it is corrected by a constant value B_{ofb}/B_{odb} (<1) over the pressure range.

The relationship between the two FVF (flash and differential) is assumed to be constant over the entire pressure range of interest.

$$R_s \text{ composite} \quad R_s = R_{sfb} - (R_{sid} - R_{sd}) \times \frac{B_{ofb}}{B_{obd}} \tag{2.77}$$

R_{sfb} solution gas oil ratio obtained from bubble point oil during flash liberation through separators

R_{sid} solution gas oil ratio calculated during differential process of the oil at its bubble point pressure

R_{sd} gas in solution calculated during differential process f (P)

$(R_{sid} - R_{sd})$ represents the amount of liberated gas during the differential process at each pressure step.

Interpretation: the flash liberation through separators (Rsfb) is taken as a reference. The composite solution gas is computed as equal to the total liberated gas during the flash through separators, minus the calculated liberated gas during the differential process at each pressure step; corrected by the FVF ratio. (The liberated gas during the differential process is considered too high).

2.16.4 Reservoir Oil Density Calculation

In the black-oil concept, the stock tank oil and the surface gas densities are assumed to be constant.

The reservoir oil mass is equal to mass of oil plus the associated gas mass.

The reservoir oil density is surface oil density/B_o.

The mass of 1 m^3 of stock tank oil is ρ kg/m^3

The associated gas mass is: GOR × ρ_g

$$\rho_{ores} = \frac{\rho_o + GOR \times \rho_g}{B_o} \tag{2.78}$$

ρ_{ores}: reservoir oil density (kg/m^3)
ρ_o: stock tank oil density (kg/m^3)
ρ_g: surface gas density (kg/m^3)
B_o: oil FVF
GOR: m^3/m^3

ρ_g may be expressed in term of gas relative density/air γ_g *(SG old symbol for gas gravity)* then associated gas mass is:

$$gas\ mass = GOR \times \gamma_g \times \rho_{air}$$

The calculated reservoir oil density can be compared with the in-situ measurement obtained from the RFT (Repeat Formation Tester or MDT) survey. Two identical values within engineering accuracy validate the well testing and RFT survey data.

The surface oil density in field unit system is expressed in °API.

$$°API = \frac{141.5}{\rho} - 131.5 \qquad \rho_o = \frac{141.5}{131.5 + °API} \tag{2.79}$$

ρ_o: oil density g/cm^3

Remark:
10°API corresponds to the pure water density.

2.16.5 Variable Bubble Point Pressure Concept

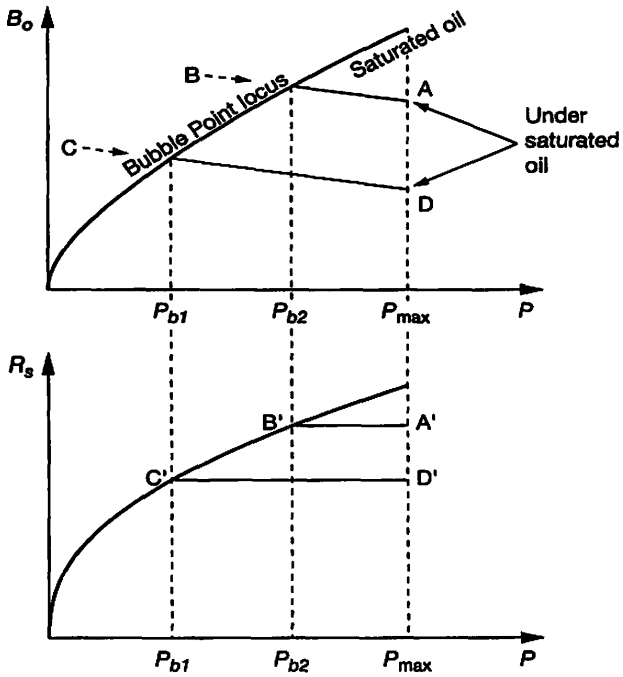

Figure 2.42 Variable Bubble Point.

Considering an under saturated oil reservoir (Fig. 2.42) at pressure P_{max} (point A). During the natural depletion, the oil FVF follows the under saturated line AB until the oil bubble point pressure is reached (B). Continuing the reservoir depletion, the oil FVF follows the curve BC (P_{b1}), the saturated line. Assuming a shut in of all producing wells and implementation of a water injection scheme, the reservoir pressure will increase and the oil FVF follows the line CD: the under saturated line parallel to AB.

The corresponding solution gas Rs in the oil path during the above process is: A', B', C', D'.

Remark: during the process described above, the oil plus gas system do not vary at constant mass.

Considering an under saturated oil reservoir starting at pressure P_{max} (point D, Fig. 2.42). During a natural depletion process, the oil FVF follows the under saturated line D to C. At pressure P_{b1} (point C) assuming a shut in of all producing wells and a gas injection scheme implemented, the reservoir pressure increases and the oil FVF follows the line C to B. At pressure P_{b2} (point B), let us stop the gas injection and implement a water injection scheme instead, the oil FVF will follow the line B to A.

The corresponding solution gas Rs path during the process is: D', C', B', A'.

Remark: during the reservoir pressure change illustrated by the line BC, the bubble point pressure is equal to the reservoir pressure. During the process AB or CD, the bubble point pressure is lower than the reservoir pressure.

It can be said that the bubble point pressure is a measure of the amount of gas in solution and conversely.

2.16.6 Variable Bubble and Dew Point Pressure Versus Depth

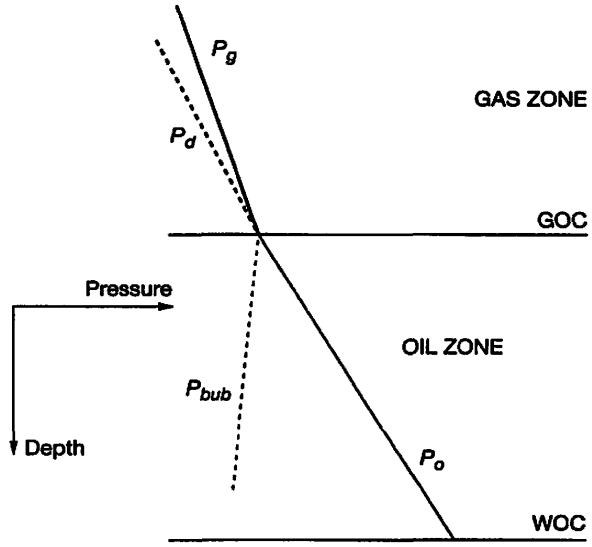

Figure 2.43 Variable P_{dew} and P_{bub} versus depth.

In the black-oil option, it may be necessary to introduce a variable bubble point versus depth in the oil column to match the observed GOR during production well tests carried out at different depths. At the gas oil contact (GOC, Fig. 2.43) the reservoir pressure is equal to the bubble point pressure by definition. It can be said that at the GOC a maximum gas quantity is in solution in the oil. As we investigate deeper in the oil column, the gas in solution Rs may decrease, therefore the bubble point pressure decreases. The same concept can be applied in the gas cap with the dew point pressure. The maximum condensate yield occurs at GOC. As we travel higher in the gas column, the condensate yield may decrease; therefore the dew point pressure decreases.

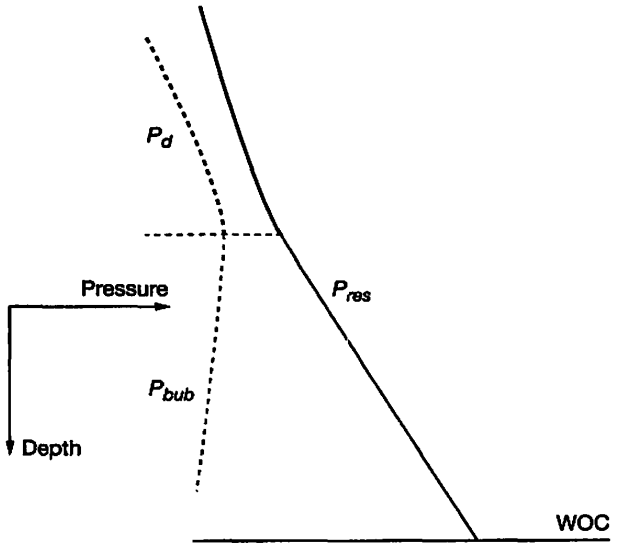

Figure 2.44 Reservoir pressure versus depth.

Figure 2.44 shows a case where no GOC is present in the hydrocarbon column. Reservoir pressure is above dew point pressure and bubble point pressure.

2.16.7 Saturation Pressure Calculation with an EOS

The saturation pressure of a single phase fluid of fixed composition at fixed temperature is defined as the pressure at which a second phase begins to form. If the fluid initially is vapor, the pressure at which a second phase (in equilibrium with the vapor) begins to form is called a dew point pressure. If the fluid initially is a liquid, the pressure at which an equilibrium vapor forms is called a bubble point.

For a saturation pressure calculation, the composition of one phase (liquid, for a bubble point; vapor for a dew point) is known and equal to the feed composition.

Equilibrium constant is defined as: $k_i = \dfrac{y_i}{x_i}$

k_i: equilibrium constant of component i
y_i: mole fraction of component i present in vapor
x_i: mole fraction of component i present in liquid

$$z_i = V \times y_i + L \times x_i$$

V: vapor fraction
L: liquid fraction

constraints: $\Sigma z_i = 1 \quad \Sigma x_i = 1 \quad \Sigma y_i = 1 \quad V + L = 1$

For a bubble point calculation:

$x_i = z_i$ the vapor composition in equilibrium is: $y_i = k_i \times x_i$

For a dew point calculation:

$y_i = z_i$ the liquid composition in equilibrium is: $x_i = k_i/y_i$

The calculation procedure is:

Step

1 choose a (low) starting pressure
2 estimate k_i from the same correlation as for VLE calculation or modify k_i from previous iteration
3 solve VLE for V with Eq. (2.52)
4 calculate the liquid and vapor compositions x_i, y_i
5 use the mixing rule
6 build and solve the EOS in terms of Z
7 calculate the vapor and liquid fugacity for each component
8 test on errors $\Sigma|f_{iV} - f_{iL}| \leq \varepsilon$
If test is verified then equilibrium solution is reached; go to 10 otherwise step 9
9 estimate new values of k_i, go to step 3
10 test on V to conclude if monophasic or diphasic status

Step 10: if $0 < V < 1$ fluid is diphasic, the initial chosen pressure is too low and calculation is resumed with a higher pressure until $V = 0$ for bubble point or $V = 1$ for dew point.

2.16.8 Depletion Performance Prediction of a Volatile Crude Oil

Jacoby and Berry [74, 75] worked on a method to predict the depletion performance of a volatile oil reservoir. The method was developed at times when no computing facilities were available. A PVT package or a compositional reservoir model are used today.

2.16.9 Reservoir Energy

Associated water with the matrix contributes to the reservoir fluid energy by its expansion during the reservoir depletion. The contribution is limited due to the low water compressibility, but can be significant if a large volume is involved. Connate water saturation may be as high as 45% in a water-wet reservoir.

Aquifer may have a large impact on the reservoir behavior depending on its volume and connection with the oil pool. This is why it is important at the beginning of a reservoir study to evaluate the size of the aquifer and determine its strength when possible.

Before implementing a water injection scheme, it is necessary to carry out a water compatibility study between the formation water and the programmed injected water. The objective is to determine the domain interval (pressure, temperature) where solids

precipitate when the two waters are in contact in the porous media. Precipitates in the reservoir plug the formation and increase the operating costs due to production interruption and necessity to clean the porous media around the wells. Usually commercial software is used to evaluate the risks of solid precipitates from the water analysis shown in Table 2.40.

In a material balance calculation, the water Formation Volume Factor can be considered as 1, the error is negligible.

Water compressibility is small and generally considered constant in the interval of interest at reservoir conditions. Water viscosity is also assumed to be constant in the range of 0.35 to 0.5 cp.

2.16.10 Reservoir Monitoring

Detailed ionic composition of produced water can be used to identify the water source: water coming from the same aquifer, or from different compartments.

Injected water can be used as a vector to carry a radioactive tracer in order to evaluate the connectivity between two wells.

2.16.11 Production and Process

At surface, oil produced is usually carrying some formation water. The two fluids are separated in a three phase separator (oil, water and gas).

Produced gas also carries some water. At surface, gas is dehydrated with glycol. Glycol agent has a chemical affinity for water. Glycol solution absorbs water, becomes heavier and sinks to the bottom of the container.

Glycol solutions are also used to avoid hydrate formation in surface facilities. Usually it is injected upstream of the production wellhead.

2.17 FORMATION WATER

2.17.1 Generalities [2]

Water is always associated with a hydrocarbon bearing reservoir.

The water can be present as trapped (immobile) or free to flow simultaneous with the hydrocarbon or filling at 100% saturation the pore volume: aquifer.

At sediment deposition time, the sea or river water was filling at 100% the voids (pores).

The water was in contact with the matrix grains for a long period of time until hydrocarbon molecules migrating through the porous media replaces the water in place. The result of such a process is called drainage, in water wet environment which is generally the

case of clastic (sandstone) reservoirs. When the process is complete, the residual amount of water in place that can't be moved is called the irreducible water.

Many different words are used and their meaning. is sometimes confusing. A few definitions are depicted below [15].

Connate Water Saturation (S_{wc}):

"Connate" implies born, originated with the formation rock.

Water saturation trapped in the pores during formation of the rock. The composition of the water can change throughout the history of the rock.

Irreducible Water Saturation (S_{wirr}):

The lowest water saturation that can be obtained in a core plug by displacing water with oil or gas. The final saturation level is dependent on the laboratory conditions (pressure gradient across the plug).

Interstitial Water (S_{wi}):

Water from fluids introduced to a formation through drilling or other interference, such as mud or sea water. Interstitial water might not have been the water present when the rock originally formed.

Initial Water Saturation (S_{wi}):

Reservoir water saturation present at initial time, before any drilling. The saturation may be higher than the connate water saturation due to an incomplete hydrocarbon migration filling process of the trap. Consequently some of the present water is mobile at initial time.

Condensate Water:

Reservoir gas has been in contact with formation water for a long time. Therefore when produced, the gas carries water as vapor to surface. In the surface separator, vapor condenses and precipitates because of temperature and pressure changes.

For water laboratory analysis purposes, a sample of water is collected at the bottom of the separator "hoping" that it is representative of the formation water.

Shale Compaction and Membrane Filtration:

Some authors believe that the salinity variations are the result of filtration of water through shale. Shale acts as semi-permeable membranes causing the water on the down flow side to contain less dissolved ions than on the upstream side.

Dual Water Model:

The model is used for the log interpretation of shaly sand formation. The concept (Waxman and Smith) consists of distinguishing the formation water filling the pores and the clay-bound water. The clay being a non porous material is made of water which salinity may differ to the pore water salinity. The concept being used for the interpretation of resistivity in shaly sands is also useful in the interpretation of nuclear and nuclear magnetic resonance logs.

The waters which are contained in the pores of the reservoir can vary considerably with geographic location, depth, and geological age.

Shallow ground waters are usually fresh, frequently used for domestic purposes, and their resistivities are comparatively high. They may also contain considerable amounts of calcium and magnesium salts, which make them "hard".

In deeper formations, the waters are generally saltier, although there is nothing uniform and regular about this. Many factors can influence the salinity of deeper formation waters, such as the saltiness of the seas present when the sediments were deposited; proximity to ancient river mouths with their fresher waters; increased salt concentration by leaching when the sediments were younger, etc.

2.17.2 Physical and Chemical Properties

2.17.2.1 pH

The pH of a water sample is a measure of the concentration of hydrogen ions. The term pH was derived from the manner in which the hydrogen ion concentration is calculated: it is the negative logarithm of the hydrogen ion (H+) concentration. This means that at higher pH, there are fewer free hydrogen ions, and that a change of one pH unit reflects a tenfold change in the concentrations of the hydrogen ion. For example, there are 10 times as many hydrogen ions available at a pH of 7 than at a pH of 8. The pH scale ranges from 0 to 14. A pH of 7 is considered to be neutral. Substances with pH of less that 7 are acidic. Substances with pH greater than 7 are basic.

A saline water contains significant amounts (referred to as "concentration") of dissolved salts. The concentration is the amount (by mass) of salt in water, is expressed in "parts per million".

Parts per million works like percent by mass, but is more convenient when there is only a small amount of solute present. ppm is defined as the mass of the component in solution divided by the total mass of the solution multiplied by 10^6.

Typical values:

Fresh water:	Less than 1 000 ppm
Slightly saline water:	From 1 000 ppm to 3 000 ppm
Moderatly saline water:	From 3 000 ppm to 10 000 ppm
Highly saline water:	From 10 000 ppm to 35 000 ppm
Sea water:	about 35 000 ppm
	Salt saturated water: 300 000 ppm

2.17.2.2 Conductivity, Resistivity

The conductivity is the ability of a material (water) to conduct electricity. It is the inverse of resistivity and is measured in mho/m. The conductivity is a property of the material, whereas the conductance also depends on the volume measured. In the most general case, the conductivity is the current density divided by the electric field and depends on the frequency of the applied signal.

Conductivity or resistivity of the water is an indicator of the amount of dissolved material in the water. The unit is Ω-m.

The resistivity of the water is dependent on the chemical content and temperature. At a given temperature, the resistivity of formation water varies with a concentration and the nature of the dissolved chemicals. In most cases, the predominant solute is sodium chloride; therefore the NaCl (Fig. 2.45) [76] may be used to obtain resistivity from concentration. If other components are present in relatively large amounts, it is possible to convert the concentrations of such chemicals into equivalent concentrations of sodium chloride to determine the resistivity.

The resistivity of water decreases as its temperature increases.

2.17.2.3 Chemical Analysis

The Units mg/l or ppm may be converted to milliequivalents/l by dividing the milligrams per liter by the combining mass of the appropriate ions.

For example the calcium content in the analysis depicted in Table 2.40 is 1 681 mg/l

The combining mass is: atomic mass/2 = 40.078/2 = 20.04

The milliequivalent meq/l is then: 1 681/20.04 = 83.9 meq/l

In an analysis expressed in milliequivalents per liter, unit concentrations of all ions are chemically equivalent. This means that all ions have been correctly determined the total meq/l of cations is equal to the total meq/l of anions.

The relationship of water composition to solid mineral composite is made more clearly evident when expressed in meq/l.

The quantitative analysis for sodium is long and tedious; it is seldom determined but is calculated from the difference between the positive and negative ions.

Table 2.40 exhibits a typical formation water analysis.

2.17.2.4 Solubility of gas in water

The solubility of natural gas in pure water has been studied and has been shown to be dependent upon the temperature and pressure. At temperature less than 150°C (300°F) the solubility is less than 0.4 mol % or approximately 5 vol/vol (28 scf/STB). According to Dodson and Standing [77], the amount of dissolved gas increases the water compressibility of 25%. (e.g. from 3.8 10^{-6} to 4.8 10^{-6} psi^{-1}).

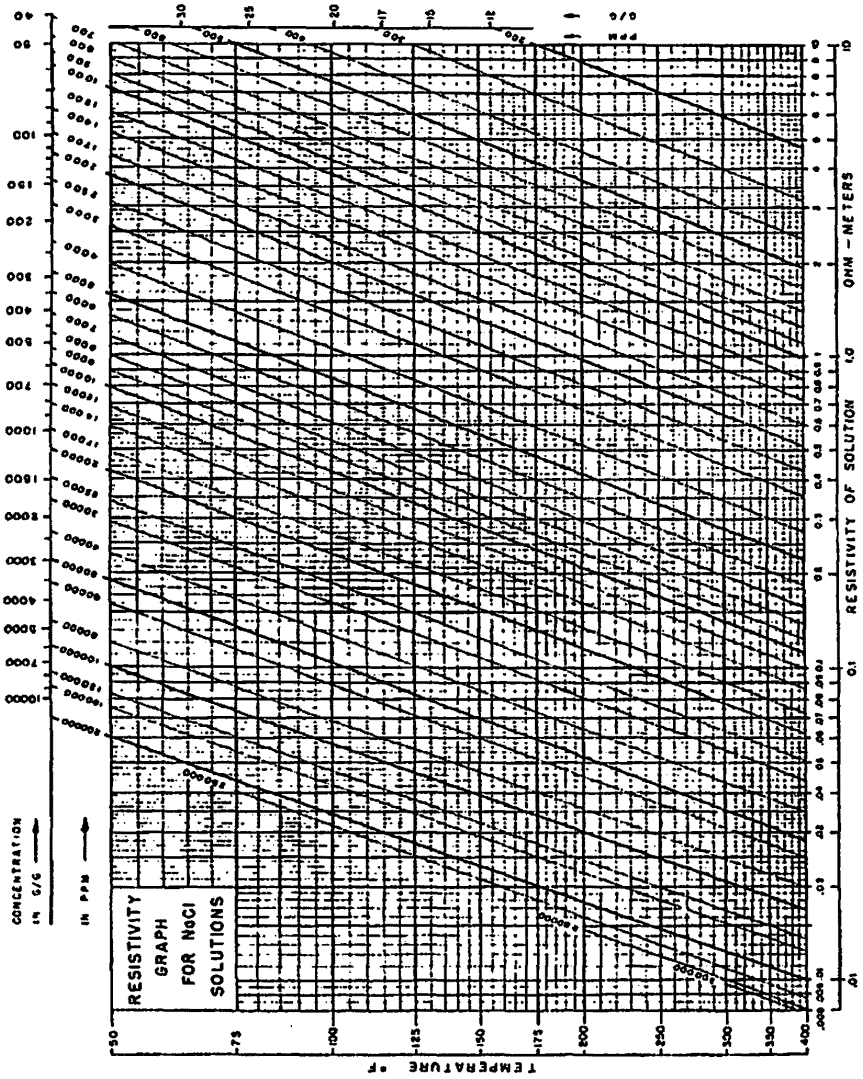

Figure 2.45 Water Resistivity (*From Schlumberger*).

2.17.2.5 Water Compressibility and density

Dodson and Standing [77] have shown that the compressibility of pure water is dependent upon pressure, temperature, and gas in solution in the water.

Table 2.40 Example of Water Composition, Milliequivalent Calculation

Company: COMPANY		**Well: Wildcat**	
Field: CST		**Formation: OIL**	
Sampled: 27/11/1996 Reference: J1010			
Water sample under atmospheric conditions pH = 6.28 @ 20°C			
		mg/L	meq/l
cations:	Na^+	43 498.94	1 892.08
	K^+	875	22.38
	Ca_2+	1 681	84.05
	Mg_2+	307	25.27
	Sr_2+	19	0.43
	Ba_2+	0.05	0.00
	Iron	38	1.36
			2 025.6
anions:	Cl^-	69 450	1 956.34
	HCO_3-	842	13.8
	$CO_{3,2}-$	2	0.07
	$SO_{4,2}-$	2 655	55.3
	NO_3-	2	0.03
			2 025.6
TDS	(calculated):	119 370 mg/L	
(Total Dissolved Salts)			
	Deposits:	– mg/L	

Milliequivalent Calculation					
		atomic mass	**active**	**mg/L**	**meq/l**
sodium	Na^+	22.99	22.99	**43 498.94**	1 892.10
potassium	K^+	39.10	39.10	**875**	22.38
calcium	Ca_2+	40.08	20.04	**1 681**	83.89
magnesium	Mg_2+	24.31	12.15	**307**	25.26
Strontium	Sr_2+	87.62	43.81	**19**	0.43
barium	Ba_2+	137.33	68.66	**0.05**	0.00
iron	Fe_2	55.85	27.92	**38**	1.36
					2 025.42
chloride	Cl^-	35.5	35.5	69 450	1 956.34
bicarbonate	HCO_3-	61	61	842	13.80
carbonate	$CO_{3,2}-$	30	30	2	0.07
sulfate	$SO4._2-$	48	48	2 655	55.31
nitrate	NO_3-	62	62	2	0.03
					2 025.55

$$c_w = -\frac{1}{V_w}\left(\frac{\partial V_w}{\partial p}\right)_T$$

c_w: water compressibility (bar^{-1} or psi^{-1})
V_w: volume of water
δV_w: volume change
δp: pressure change

Increasing pressures have the effect to reduce the compressibility, whereas increasing temperature have the effect of producing an increase. At a given pressure and temperature, the effect of gas in solution in pure water is to increase the compressibility. Interpreting Dodson and Standing data, Jones proposed the following correlation to estimate the compressibility:

$$c_w = c_{wp}(1 + 0.0088\, R_{sw})$$

c_w: compressibility of reservoir water 1/psi
c_{wp}: compressibility of pure water, 1/psi
R_{sw}: solubility of gas in reservoir water cu. ft/bbl

Water compressibility expressed in terms of density

$$c_w = -\frac{1}{V}\left(\frac{\delta V}{\delta P}\right)_T = \frac{1}{\rho_w}\left(\frac{\delta \rho_w}{\delta P}\right) \qquad \int \frac{d\rho_w}{\rho_w} = c_w \int dp \qquad \text{Ln}\frac{\rho_w}{\rho_{w0}} = c(p - p_0)$$

so $$\rho_w = \rho_{w0} e^{c(p-p_0)} \qquad e^x = 1 + x + x^2/2! + x^3/3! + \ldots.$$

$$e^{c(p-p_0)} = 1 + c(p-p_0) + \left[\frac{c(p-p_0)}{2!}\right]^2 + \ldots..$$

p_0, ρ_{w0}: reference oil pressure and reference water density

since c is very small, higher order terms can be neglected

$$e^{c(p-p_0)} = 1 + c(p-p_0) \qquad \text{then} \qquad \rho_w = \rho_{w0}\left[1 + c\left(p - p_0\right)\right]$$

2.17.2.6 Water Formation Volume Factor

The formation volume factor for pure water is dependent upon its pressure and temperature. An increase in pressure produces a decrease in the volume factor whereas, at constant pressure, an increase in temperature produces an increase in the volume factor. At a given pressure and temperature, gas saturated pure water has a higher volume factor than pure water. In addition to gas, formation water contains dissolved salts. It has been observed that gas solubility in water is decreased with increasing salinity.

2.17.2.7 Water Viscosity

Few data have been published on the viscosity of water. The pressure effect on viscosity is negligible for all practical purposes.

2.17.3 Density, Relative Density, Pressure Gradient Relationships

Table 2.41 depicts the relation between pure water density and pressure gradient in all common unit systems.

Note: the gallon used in the petroleum industry is the US gallon = 3.785 liter.

Table 2.41 Pressure Gradient, Density Relationship

Pressure Gradient	Units	DENSITY			
		g/cm^3	kg/m^3	Lbs/cu. ft	Lbs/gal
0.100	$kgf/cm^2/m$	1.000	1 000.0	62.428	8.345
0.098	Bars/m	1.000	1 000.0	62.428	8.345
1.422	psi/m	1.000	1 000.0	62.428	8.345
0.434	psi/ft	1.000	1 000.0	62.428	8.345

Relative Density (/water)
1

DENSITY		PRESSURE GRADIENT	
1.000	g/cm^3	0.100	$kgf/cm^2/m$
1 000.0	kg/m^3	0.098	Bars/m
62.428	Lbs/cu. ft	1.422	psi/m
8.345	Lbs/gal	0.434	psi/ft

2.18 HYDRATES [2]

A hydrate is a solid built by the physical combination of water molecules and certain gas molecules. It is solid like ice but possesses different properties. All hydrates crystallize in a combination of two cubic structures, in which gas molecules are trapped in cavities. These cavities occur in a framework composed of water molecules linked together by hydrogen bonds. The structure is very weak and will collapse unless supported by any mass occupying the cavities.

Hydrates are generated at the gas water boundary with most of the molecules coming from those in solution in the water phase. H_2S and CO_2 accelerate hydrate formation (at high temperatures) since they are more soluble in water than in most hydrocarbons.

Hydrates grow like crystals. They build up and plug a line at orifice plates and valves. High turbulence helps to avoid hydrate formation.

Vast deposits of natural gas hydrates exist in the Artic. Recovery of natural gas entrapped in the deposits located in permafrost regions has been studied recently [78].

A lot of research is been carried out to explain, and predict the formation of hydrates.

CHAPTER 3

Fluid Flow in Reservoirs

3.1 INTRODUCTION

Reservoir engineers should not ignore the origin of the development of this "invisible science" to which famous individuals are attached. Reservoir study can be traced as early as 1856 when Frenchman H. Darcy became interested in the flow characteristics of sand filters for water purification. He started the real foundation of the quantitative theory of the flow of homogenous fluids through porous media. In 1857, Darcy published "Recherches Expérimentales Relatives au Mouvement de l'eau Dans les Tuyaux", (Experimental Research Relating to the Movement of Water in Pipes). This paper presented his research on pipe flow resistance and was the first work to suggest the existence of the boundary layer in fluid flow. This publication provides the basis for his credit in the "Darcy-Weisbach" equation, even though Wiesbach published before him in 1845.

Fluid Flow

Hydrocarbons are complex fluids that generally exist in an untapped reservoir in liquid and gaseous states and are considered to be at equilibrium. Likewise, they are expected to behave in accordance with predictable functional pressure/volume/temperature (PVT) relationships. If all the gas is dissolved in the oil, the single phase is considered to be a liquid phase, and the reservoir is called a "dissolved-gas" reservoir. On the other hand, if there are hydrocarbons as vaporized gas that are recoverable as natural gas liquids on the surface, the single phase is considered to be a gas phase, and the reservoir is called a "wet-gas" reservoir. In some reservoirs, both liquid and gaseous phases may exist. These are called "gas-cap reservoirs." If an artesian water supply is directly associated with any of these reservoirs or expanding water is the dominant producing force, the reservoir is termed a "water drive reservoir.

Challenges to reservoir engineers begin when the reservoir is opened to production and the flow of hydrocarbons begins. At this point, reservoir pressures drop; fluids comprising gas, oil, and water expand; phase equilibrium is disturbed; and alterations in the physical properties of the fluid phases occur in various degrees throughout the entire reservoir. In

short, the oil has become "active." With further withdrawal of fluids, changes continue and difficult second-order partial-differential equations are needed to describe the unsteady-state flow of expansible fluids.

From 1927 to 1930, Jan Versluys, a well-known hydrologist working for Royal Dutch Shell, wrote numerous articles on the physics of oil producing formations that were widely published. In 1931, Morris Muskat and H.G. Botset wrote several papers on the flow of reservoir fluids. These papers and articles were instrumental in advancing the knowledge of reservoir dynamics to its present state.

"Today, most reservoir engineers consider that, of the many great reservoir-engineering pioneers, Muskat probably had the greatest impact," relates Joe Warren, a personal friend of the late Morris Muskat. A native of Riga, Latvia, Muskat attended Marietta College and Ohio State U. and ultimately received a PhD degree in physics from the California Inst. of Technology in 1929. Following his graduation from Cal Tech, Muskat joined the Gulf Research and Development Co. where, at the age of 31, he wrote "The Flow of Homogeneous Fluids through Porous Media", a seminal publication for reservoir engineering. Twelve years later, in 1949, he wrote a second book, Physical Principles of Oil Production. Together, these books provided a sound analytical foundation for reservoir engineering by combining fluid mechanics with phase behavior.

"Muskat also published technical papers in such diverse fields of interest as hydrodynamics, lubrication theory, and the mechanics of shaped charges," Warren recalls. "As a matter of fact, he received an original patent for his work on the use of shaped charges in oil well perforating applications."

A paper written in 1933 by TV Moore, Ralph J. Schilthuis, and William Hurst advanced reservoir science further. The paper presented the first equation for unsteady-state radial flow of expansible reservoir fluids. It reported the development of a linear second-order equation similar to the classic heat-flow equation that adequately described the flow of a single-phase compressible (or expansible) liquid in a reservoir. A year later, in 1934, Schilthuis and Hurst published the application of the equation to the calculation of reservoir-pressure changes in an east Texas field and to the prediction of the effect thereon of changes in production rates.

3.2 VISCOSITY

The porous media contains an enormous internal surface area as compared with that represented by their macroscopic dimensions. As a result, the viscous resistance reactions will be far greater than the inertia and acceleration forces. The forces present for fluid movement through porous media involve only the dynamic equilibrium between viscous shearing resistance and driving forces as pressure gradients.

Viscosity is an important fluid property used in fluid flow calculations. It represents the drag forces caused by the attractive forces in adjacent fluid layers.

Since the intermolecular forces are a function of the distance between molecules, viscosity depends on whether the fluid is a liquid or gas. The distance between molecules has a direct impact in the gas behavior: perfect gas or real gas. The liquid viscosity is much higher than gas, at the same conditions (pressure, temperature).

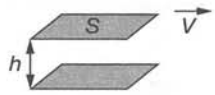

Figure 3.1 Laminar flow.

Considering two adjacent planes (Fig. 3.1) within the fluid, one static and S moving at velocity V, the resistance to the movement is:

- Proportional to the velocity.
- Proportional to the contact area S.
- Inversely proportional to the distance h between the two planes.

The coefficient of proportionality is defined as viscosity μ.

$$F = \mu \frac{V \times S}{h}$$

		CGS units	SI units
F:	viscosity force	dynes	Newtons
V:	fluid velocity	cm/s	m/s
S:	area	cm^2	m^2
h:	distance	cm	m
μ:	viscosity	poise	Pa.s

Dimensional analysis:

$$\mu = \frac{F \times h}{V \times S} \qquad |\mu| = \frac{FL}{LT^{-1}L^2} = \frac{FT}{L^2} \approx \frac{\text{dynes}.s}{cm^2}$$

1 "mPa.s" = 1 "cp"

1 mPa = 10^{-3} Pa

The dimension of viscosity is equivalent to a "pressure multiplied by time".

The commonly unit used is the centipoise (cp).

At 20°C and atmospheric pressure, the pure water viscosity is 1 cp.

The viscosity of reservoir water is function of temperature. The pressure effect on water viscosity is negligible for all practical purposes. The viscosity of brine is higher than that of pure water; however reservoir waters with gas in solution may have less viscosity than the corresponding brine with no solution gas.

As a rule of thumb, water viscosity at reservoir conditions is in the range of 0.4 to 0.55 cp.

3.3 DARCY'S LAW

In 1856, Darcy investigated the flow of water through sand filters for water purification. Interpretation of his observations gave birth to Darcy's law.

Darcy's law defines the permeability parameter "k".

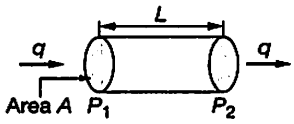

Figure 3.2 Flow through a cylindrical sample.

$$q = k\frac{P_1 - P_2}{\mu L}A \tag{3.1}$$

Neglecting the gravity influence, the Darcy's law expresses the monophasic fluid flow rate through the porous sample (Fig. 3.2) as:

- Being proportional to the pressure gradient $(P_1 - P_2)$.
- Proportional to the cross area of the sample.
- Inversely proportional to the sample length and fluid viscosity.

The coefficient of proportionality is defined as permeability k

	Darcy units	SI
q: fluid flow rate	cm^3/s	m^3/s
P: pressure	atm	Pa
A: area	cm^2	m^2
μ: fluid viscosity	cp	Pa.s
L: sample length	cm	m
k: permeability	Darcy	m^2

These units define what is called the Darcy unit system.

The "mD" (10^{-3} D) is commonly used in the industry since the Darcy is large.

The single-fluid permeability is regarded as a constant for the media if the flow is in the viscous range. It is called the absolute permeability characterizing an intrinsic property of the media.

The general equation form is: $$\frac{q}{A} = v = -\frac{k}{\mu}\frac{\delta P}{\delta x} \quad (3.2)$$

Sign (–) due to velocity and pressure gradient varying in opposite directions

If gravity cannot be neglected then: $v = -\frac{k}{\mu}\text{grad}\,\Phi$

Where Φ is the potential:

$$\Phi = P + \rho g h$$

Φ: potential
P: pressure
ρ: fluid density
g: gravitational acceleration
h: height above a datum

Dimensional analysis:

$$k = \frac{q\mu L}{\Delta P.A} \qquad |k| = \frac{L^3T^{-1}ML^{-1}T^{-1}L}{ML^{-1}T^{-2}L^2} = L^2$$

Permeability has a dimension of an area.

1 mD = 9.86923×10^{-16} m^2 preferred SPE metric unit: μm^2 1 mD = 9.86923×10^{-4} μm^2

3.4 RADIAL STEADY-STATE OF AN INCOMPRESSIBLE FLUID FLOW

3.4.1 Well Flow Equation

A monophasic flow of an incompressible fluid through a homogenous porous media is considered where gravity forces are neglected.

Steady-state implies that at any reservoir location, no pressure change occurs versus time.

The continuity equation states that the total flow through any cylindrical surface coaxial with the well bore is constant.

$$q = 2\pi r h v = \text{Cte}$$

Fluid velocity is:

$$v = -\frac{q}{2\pi r h}$$

Fluid velocity from Darcy law is:

$$v = -\frac{k}{\mu}\frac{\delta p}{\delta r} = -\frac{q}{2\pi r h}$$

rearranging and separating variables

$$dp = \frac{q\mu}{2\pi kh}\frac{dr}{r} \tag{3.3}$$

Integration gives:

$$p = \frac{q\mu}{2\pi kh}\text{Ln}\frac{r}{r_w} + p_w$$

The pressure versus radii has a logarithmic shape.

Other writing:

Steady-state flow equation:

$$Q = \frac{2\pi kh}{\mu B}\frac{(p - p_w)}{\text{Ln}\left(\frac{r}{r_w}\right)} \qquad (Q\text{: surface rate, SI or Darcy units}) \tag{3.4}$$

B is the fluid formation volume factor, Q expressed in surface volume
k is the effective fluid permeability when more than one fluid is present

Steady-state flow can be reached at the laboratory when high permeability samples are used (linear flow). Physically it means a constant input and output rates in addition to stabilized input and output pressures. Neglecting gravity effect, (horizontal plug) the flow is linear and the pressure profile is a straight line between input and output.

In a radial configuration, well rate is constant and pressures at well radii r_w and at r_e (exterior radii) are constant. The pressure profile is logarithmic between r_w and r_e.

Boundary conditions are expressed as:

$$dp/dt = 0 \text{ at } r_w \text{ and } r_e$$

The steady-state regime in the field can be observed when a strong water drive or a water injection scheme compensates the fluid withdrawal created by the production wells.

3.4.2 Average Pressure Calculation in a Segmented Circular Reservoir

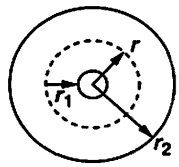

Figure 3.3 Segmented Circular Reservoir.

Considering a segmented radial reservoir limited by radius r_1 and r_2 submitted to a steady-state flow regime (Fig. 3.3).

The pressure distribution between two radii has a logarithmic shape. It is expressed for incompressible fluid:

$$p - p_{r_1} = \frac{q\mu}{2\pi kh} \operatorname{Ln} \frac{r}{r_1} \tag{3.5}$$

The average reservoir pressure between r_1 and r_2 is defined as

$$\bar{p} = \frac{1}{V} \int_{r_1}^{r_2} p dV$$

with $V = \pi h \phi (r_2^2 - r_1^2)$ volume element: $dV = 2\pi h \phi r \, dr$

$$\bar{p} - p_{r_1} = \frac{2}{r_2^2 - r_1^2} \int_{r_1}^{r_2} p r dr = \frac{2}{r_2^2 - r_1^2} \int_{r_1}^{r_2} \left[\frac{q\mu}{2\pi kh} \operatorname{Ln} \frac{r}{r_1} \right] r dr$$

integrating by parts

$$\int_{r_1}^{r_2} \left[\operatorname{Ln} \frac{r}{r_1} \right] r dr = \left[\frac{r^2}{2} \operatorname{Ln} \frac{r}{r_1} \right]_{r_1}^{r_2} - \int_{r_1}^{r_2} \frac{r^2}{2} \frac{1}{r} dr$$

$$= \left[\frac{r_2^2}{2} \operatorname{Ln} \frac{r_2}{r_1} \right] - \frac{r_2^2 - r_1^2}{4}$$

$$\bar{p} - p_{r_1} = \frac{q\mu}{2\pi kh} \left[\frac{r_2^2}{r_2^2 - r_1^2} \operatorname{Ln} \frac{r_2}{r_1} - \frac{1}{2} \right] \tag{3.6}$$

Eq. (3.6) gives the average pressure in a segmented circular reservoir limited by radii r_1 and r_2.

Particular case when $r_1 = r_w$ (well radius) and $r_2 = r_e$ (exterior radius).

with $r_w \ll r_e$ $\quad \dfrac{r_e^2}{r_e^2 - r_w^2} = \dfrac{1}{1 - \dfrac{r_w^2}{r_e^2}} \approx 1$

Average reservoir pressure in a steady-state flow:

$$\bar{p} - p_w = \frac{q\mu}{2\pi kh} \left[\operatorname{Ln} \frac{r_e}{r_w} - \frac{1}{2} \right] \textit{ (reservoir conditions, SI or Darcy units)}$$

$\bar{p}$ is the average pressure in the circular segmented reservoir.

3.4.3 Radius Determination at which the Average Pressure is Found

Identification between Eq. (3.5) and (3.6) is carried out:

$$\mathrm{Ln}\frac{\bar{r}}{r_1} = \frac{r_2^2}{r_2^2 - r_1^2}\mathrm{Ln}\frac{r_2}{r_1} - \frac{1}{2}$$

Other writing:

$$\mathrm{Ln}\frac{\bar{r}}{r_1} = \mathrm{Ln}\left(\frac{r_2}{r_1}\right)^a - \mathrm{Ln}\sqrt{e} \qquad \text{with } a = \frac{r_2^2}{r_2^2 - r_1^2}$$

$$\frac{\bar{r}}{r_1} = \frac{1}{\sqrt{e}}\left(\frac{r_2}{r_1}\right)^a \qquad \bar{r} = \frac{1}{\sqrt{e}}\frac{r_2^a}{r_1^{(a-1)}}$$

$$a - 1 = \frac{r_1^2}{r_2^2 - r_1^2} = b$$

$$\text{then } \bar{r} = \frac{1}{\sqrt{e}}\frac{r_2^a}{r_1^b} \qquad \text{with } a = \frac{r_2^2}{r_2^2 - r_1^2} \qquad \text{and } b = \frac{r_1^2}{r_2^2 - r_1^2}$$

Some reservoir simulators in the radial mesh option identify reference radius at which all block parameters are attached as the average radii defined above.

3.5 RADIAL PSEUDO STEADY-STATE FLUID FLOW

In the steady-state flow the fluid flow rate is the same whatever the section location in the radial circular reservoir, in particular at the well radius r_w and at the outer boundary r_e. This means that production from the well is continually replenished by flow into the drainage area across r_e. For many reservoirs producing under natural depletion, the production fluid originates from the well drainage area and no flow occurs across the external drainage radius r_e. When the flow becomes stabilized, it is called pseudo steady-state flow. The well flow rate is constant at r_w but varies across sections according to the surface distance from the well.

3.5.1 Well Flow Equation

A closed reservoir at a distance r_e is assumed. Therefore no flow occurs at r_e ($dp/dr = 0$).

At r_w, the well constant flow rate is q_w. Production is the result of fluid movement created by the pressure gradient in the drainage area (Fig. 3.4).

Fluid volume between r and r_e is: $V(r) = \pi(r_e^2 - r^2)\,\varphi h$

Total fluid volume between r_w and r_e: $V_{res} = \pi(r_e^2 - r_w^2)\,\varphi\, h$

Assuming a constant bottom hole well production rate q_w of an incompressible fluid from the well.

At any radii r, the flow entering rate is proportional to the reservoir fluid contained between r and r_e.

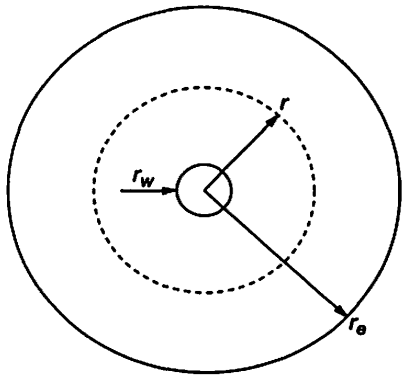

Figure 3.4 Well Flow in a Radial Circular Reservoir.

The rate at any radius r is:

$$q = q_w \frac{(r_e^2 - r^2)}{(r_e^2 - r_w^2)} \qquad r_w \text{ being negligible compared to } r_e$$

$$\frac{(r_e^2 - r^2)}{(r_e^2 - r_w^2)} = \frac{r_e^2}{r_e^2 - r_w^2} - \frac{r^2}{r_e^2 - r_w^2} = \frac{1}{1 - \frac{r_w^2}{r_e^2}} - \frac{r^2}{r_e^2\left(1 - \frac{r_w^2}{r_e^2}\right)} \cong \left(1 - \frac{r^2}{r_e^2}\right)$$

$q_r = q_w\left(1 - \frac{r^2}{r_e^2}\right)$ from Eq. (3.3) Darcy's law is: $q = \frac{2\pi kh}{\mu} r \frac{dp}{dr}$ both rate expressions above are the same at radius r.

q_w: constant well flow rate.

Integration from well boundary r_w to radius r

$$q_w\left(1-\frac{r^2}{r_e^2}\right)=\frac{2\pi kh}{\mu}r\frac{dp}{dr}$$

$$q_w\left(\frac{dr}{r}-\frac{1}{r_e^2}rdr\right)=\frac{2\pi kh}{\mu}dp$$

$$q_w\mathrm{Ln}\frac{r}{r_w}-\frac{q_w}{r_e^2}\left(\frac{r^2}{2}-\frac{r_w^2}{2}\right)=\frac{2\pi kh}{\mu}(p_r-p_w)$$

solving for q_w

$$q_w=\frac{2\pi kh}{\mu}\frac{(p_r-p_w)}{\left[\mathrm{Ln}\left(\frac{r}{r_w}\right)-\frac{r^2}{2r_e^2}+\frac{r_w^2}{2r_e^2}\right]}$$

neglecting r_w in comparison with r_e

$$q_w=\frac{2\pi kh}{\mu}\frac{(p_r-p_w)}{\left[\mathrm{Ln}\left(\frac{r}{r_w}\right)-\frac{r^2}{2r_e^2}\right]} \tag{3.7}$$

Eq. (3.7) gives the well flow rate function of the reservoir pressure p_r located at r particular case when $r = r_e$

$$q_w=\frac{2\pi kh}{\mu}\frac{(p_e-p_w)}{\left[\mathrm{Ln}\left(\frac{r_e}{r_w}\right)-\frac{1}{2}\right]} \tag{3.8}$$

(reservoir conditions, SI or Darcy units)

Introducing the fluid formation factor B to convert bottom to surface rates:

$$Q_w=\frac{2\pi kh}{\mu B}\frac{(p_e-p_w)}{\left[\mathrm{Ln}\left(\frac{r_e}{r_w}\right)-\frac{1}{2}\right]}$$

(Q_w: surface rate, SI or Darcy units)

Since there is no compressibility term, the equation is valid for a non variable compressibility fluid in the well drainage area. The assumption is acceptable for liquids but not for gases.

This is the well inflow equation under pseudo steady-state conditions (also called semi-steady state regime) and is similar to the equation for steady state Eq. (3.4).

Generally p_w is measured but p_e (pressure at external boundary) is not known. In the field, the average reservoir pressure is deducted from pressure build-up test.

Discussion

For the same boundary conditions p_e and p_w, the constant well flow in the pseudo-steady state flow regime is slightly higher than the one obtained in the case of steady-state regime. The difference is explained by the fact that most of the produced fluid travels a shorter distance in the pseudo steady-state case than in the steady-state flow regime.

3.5.2 Average Pressure Calculation of a Radial Reservoir in Pseudo Steady-state Regime

From Eq. (3.8) $$p_e - p_w = \frac{q\mu}{2\pi kh}\left[\mathrm{Ln}\left(\frac{r_e}{r_w}\right) - \frac{1}{2}\right]$$

at radius r:

From Eq. (3.7) $$q_w = \frac{2\pi kh}{\mu}\frac{(p_r - p_w)}{\left[\mathrm{Ln}\left(\frac{r}{r_w}\right) - \frac{r^2}{2r_e^2}\right]} \tag{3.9}$$

The volume averaged pressure is defined as:

$$\bar{p} = \frac{1}{V}\int_{r_w}^{r_e} p\,dV \qquad \text{with } V = \pi(r_e^2 - r_w^2)\,\varphi h \qquad \text{and } dV = 2\pi h\varphi\, r\,dr \tag{3.10}$$

From Eqs. (3.9) and (3.10) $$\bar{p} - p_w = \frac{2}{r_e^2 - r_w^2}\int_{r_w}^{r_e} p r dr$$

$$r_e^2 - r_w^2 = r_e^2\left(1 - \frac{r_w^2}{r_e^2}\right) \approx r_e^2 \qquad \text{neglecting } r_w \text{ in comparison with } r_e$$

$$\bar{p} - p_w = \frac{2}{r_e^2}\int_{r_w}^{r_e} p r dr = \frac{2}{r_e^2}\frac{q\mu}{2\pi kh}\int_{r_w}^{r_e}\left[\mathrm{Ln}\left(\frac{r}{r_w}\right) - \frac{r^2}{2r_e^2}\right] r dr \tag{3.11}$$

$$\int_{r_w}^{r_e}\left[\mathrm{Ln}\left(\frac{r}{r_w}\right) - \frac{r^2}{2r_e^2}\right] r dr = \int_{r_w}^{r_e}\mathrm{Ln}\left(\frac{r}{r_w}\right) r dr - \frac{1}{2r_e^2}\int_{r_w}^{r_e} r^3 dr \quad \text{integrating by parts:}$$

$$= \left[\frac{r^2}{2}\mathrm{Ln}\left(\frac{r}{r_w}\right)\right]_{r_w}^{r_e} - \frac{1}{2}\int_{r_w}^{r_e}\frac{r^2 dr}{r} - \frac{1}{2r_e^2}\int_{r_w}^{r_e} r^3 dr$$

$$= \frac{r_e^2}{2}\mathrm{Ln}\left(\frac{r_e}{r_w}\right) - \left[\frac{r^2}{4}\right]_{r_w}^{r_e} - \frac{1}{2r_e^2}\left[\frac{r^4}{8}\right]_{r_w}^{r_e} \qquad \text{neglecting } (r_w)^4$$

$$\approx \frac{r_e^2}{2}\mathrm{Ln}\left(\frac{r_e}{r_w}\right) - \frac{r_e^2}{4} - \frac{r_e^2}{8}$$

back to Eq. (3.11) $$\bar{p} - p_w = \frac{2}{r_e^2}\frac{q\mu}{2\pi kh}\left[\frac{r_e^2}{2}\mathrm{Ln}\left(\frac{r_e}{r_w}\right) - \frac{3r_e^2}{8}\right]$$

The pseudo steady-state flow regime average reservoir pressure is:

$$\bar{p} - p_w = \frac{q\mu}{2\pi kh}\left[\mathrm{Ln}\left(\frac{r_e}{r_w}\right) - \frac{3}{4}\right]$$

Introducing the fluid formation factor B to convert bottom to surface rates

$$Q_w = \frac{2\pi kh}{\mu B}\frac{(\bar{p} - p_w)}{\left[\mathrm{Ln}\left(\frac{r_e}{r_w}\right) - \frac{3}{4}\right]}$$

(Q_w: surface rate, SI or Darcy units)

No formation damage ($S = 0$)

The pseudo steady-state flow is characterized by:

a) a constant well flow rate
b) a finite reservoir geometry at r_e
c) no flow condition at external radius r_e $dp/dr = 0$ at r_e
d) the reservoir pressure decreases uniformly versus time $dp/dt \approx$ Cte at any r (Fig. 3.5).

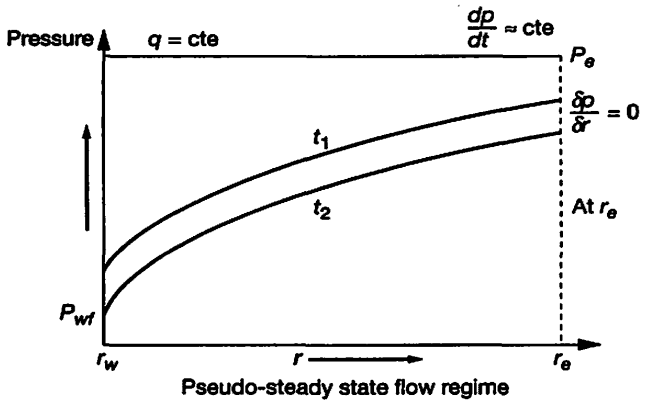

Figure 3.5 Pressure profile.

3.5.3 Drawdown and Well Productivity Index [79, 80]

The well producing pressure p_w or p_{wf} is generally measured and known as the bottom hole flowing pressure. The difference between p_{wf} and the well static pressure p_s or p_r is the

drawdown. The ratio of the surface producing rate of a well to its drawdown is defined as the productivity index, *PI* or *J*.

$$J = \frac{Q}{p_s - p_{wf}} \qquad \text{Bbl/d/psi} \quad \text{or} \quad \text{m}^3\text{/d/bar} \qquad p_s\text{: static pressure}$$

The specific productivity index is the productivity index per unit of pay thickness:

$$J_s = \frac{J}{h} = \frac{Q}{h(p_s - p_{wf})} \qquad \text{Bbl/d/psi/ft} \quad \text{or} \quad \text{m}^3\text{/d/bar/m}$$

Q: fluid surface rate
h: net pay thickness

***PI* formulas for oil** *SI or Darcy units*

	Steady state	**Pseudo steady state**
In terms of $p = p_e$ at $r = r_e$	$J_o = \frac{q_o}{(p_e - p_{wf})} = \frac{k_{ro}}{\mu_o B_o} \frac{2\pi kh}{\text{Ln}\left(\frac{r_e}{r_w}\right)}$	$\frac{q_o}{(p_e - p_{wf})} = \frac{k_{ro}}{\mu_o B_o} \frac{2\pi kh}{\left(\text{Ln}\frac{r_e}{r_w} - \frac{1}{2}\right)}$
In terms of Average pressure	$J_o = \frac{q_o}{(\bar{p} - p_{wf})} = \frac{k_{ro}}{\mu_o B_o} \frac{2\pi kh}{\left(\text{Ln}\frac{r_e}{r_w} - \frac{1}{2}\right)}$	$\frac{q_o}{(\bar{p} - p_{wf})} = \frac{k_{ro}}{\mu_o B_o} \frac{2\pi kh}{\left(\text{Ln}\frac{r_e}{r_w} - \frac{3}{4}\right)}$

Remarks:
The above PI expressions assume a non damaged and non stimulated well: (S = 0)
The PI expression is made of two terms:
- *a constant, based on petrophysical properties: k: absolute permeability, reservoir thickness h and geometry r_e,*
- *a variable term function of pressure and saturation changes around the well:*
  μ_o, B_o function of pressure
  k_{ro} function of oil saturation S_o

Consequently the well PI varies during the well production life. The oil rate can be written as:

$$q_o = W_k \frac{k_{ro}}{\mu_o B_o} (P_r - P_{wf})$$

W_k is the well connection factor which includes the well geometry, the absolute formation permeability and skin factor.

r_e is seldom known. The $\text{Ln}(r_e/r_w)$ can be approximated between 7 to 9 in many circumstances.

3.6 DIFFUSIVITY EQUATION

3.6.1 Equation of Continuity or Conservation Mass Law [63, 80, 81, 82]

Considering an element of a reservoir through which a single phase is flowing in the x direction, at any time:

Mass rate in – Mass rate out = Mass rate of accumulation

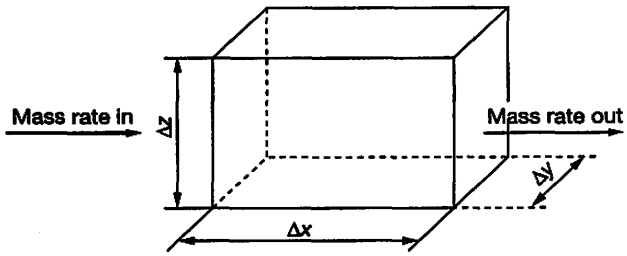

Figure 3.6 Reservoir element for 1 dimension flow.

$$(\rho_x v_x \Delta y \Delta z) - (\rho_{x+\Delta x} v_{x+\Delta x} \Delta y \Delta z) = (\Delta x \Delta y \Delta z)\ \phi \frac{(\rho_{t+\Delta t} - \rho_t)}{\Delta t}$$

dividing both sides by Δx. Δy. Δz:

$$-\frac{(\rho_{x+\Delta x} v_{x+\Delta x}) - (\rho_x v_x)}{\Delta x} = \frac{\phi(\rho_{t+\Delta t} - \rho_t)}{\Delta t}$$

when Δx and Δt tend to zero simultaneously then: $\frac{\delta(\rho v)}{\delta x} = -\phi \frac{\delta \rho}{\delta t}$

continuity equation for three dimensions: $\frac{\delta(\rho v)}{\delta x} + \frac{\delta(\rho v)}{\delta y} + \frac{\delta(\rho v)}{\delta z} = -\phi \frac{\delta \rho}{\delta t}$ (3.12)

Other form: $div(\rho \vec{V}) = -\phi \frac{\delta \rho}{\delta t}$

Darcy's law from Eq. (3.2) $v = -\frac{k}{\mu} \frac{\delta P}{\delta x}$

combination of the continuity equation Eq. (3.12) with Darcy's law (1 dimension) gives:

$$\frac{\delta}{\delta x}\left(-\frac{k\rho}{\mu}\frac{\delta P}{\delta x}\right)=-\phi\frac{\delta\rho}{\delta t} \tag{3.13}$$

expanding:
$$-\left(\frac{k}{\mu}\frac{\delta^2 P}{\delta x^2}\rho+\frac{k}{\mu}\frac{\delta P}{\delta x}\frac{\delta\rho}{\delta x}\right)=-\phi\frac{\delta\rho}{\delta t}$$

$$\frac{\delta\rho}{\delta x}=\frac{\delta\rho}{\delta P}\frac{\delta P}{\delta x}\qquad\frac{\delta\rho}{\delta t}=\frac{\delta\rho}{\delta P}\frac{\delta P}{\delta t}$$

for radial flow Eq. (3.13) becomes: $\frac{1}{r}\frac{\delta}{\delta r}\left(\frac{r\rho k}{\mu}\frac{\delta P}{\delta r}\right)=\phi\frac{\delta\rho}{\delta t}$

An equation of state is needed to express the density in terms of pressure. In the field, reservoir densities are not measured but pressures are.

Most oil field liquid systems are considered slightly compressible:

Compressibility is defined as:

$$c=-\frac{1}{V}\left(\frac{\delta V}{\delta P}\right)_T=\frac{1}{\rho}\left(\frac{\delta\rho}{\delta P}\right)$$

at constant temperature

c: compressibility
V: initial volume
δV: *volume change under*
δP: *pressure variation*

Then:
$$\rho=\rho_0 e^{c(P-P_0)}$$

ρ: fluid density at pressure P
ρ_0: density at reference pressure p_0

(The change of sign in the compressibility definition is necessary to keep $c > 0$; volume and pressure variations are opposite while density and pressure change in the same direction); c can be assumed constant for liquids over the pressure range of interest.

3.6.2 Diffusivity Equation

Eq. (3.13) becomes:
$$-\left[\frac{k}{\mu}\frac{\delta^2 P}{\delta x^2}\rho+\frac{k}{\mu}\frac{\delta\rho}{\delta P}\left(\frac{\delta P}{\delta x}\right)^2\right]=-\phi\frac{\delta\rho}{\delta P}\frac{\delta P}{\delta t} \tag{3.14}$$

neglecting term $(\delta P/\delta x)^2$ since small pressure gradients are assumed and μ independent of pressure.

$$\frac{\delta^2 P}{\delta x^2} = \frac{\phi \mu c}{k}\frac{\delta P}{\delta t} \text{ for three dimensions } \frac{\delta^2 P}{\delta x^2} + \frac{\delta^2 P}{\delta y^2} + \frac{\delta^2 P}{\delta z^2} = \frac{\phi \mu c}{k}\frac{\delta P}{\delta t} \tag{3.15}$$

other writing: $\nabla^2 P = \dfrac{\phi \mu c}{k}\dfrac{\delta P}{\delta t}$ $\nabla^2 P$ is the Laplacian of P

in radial coordinates $\dfrac{1}{r}\dfrac{\delta}{\delta r}\left(r\dfrac{\delta P}{\delta r}\right) = \dfrac{\phi \mu c}{k}\dfrac{\delta P}{\delta t}$

Diffusivity equation for radial flow:

$$\frac{\delta^2 P}{\delta r^2} + \frac{1}{r}\frac{\delta P}{\delta r} = \frac{\phi \mu c}{k}\frac{\delta P}{\delta t} \tag{3.16}$$

$\dfrac{k}{\phi \mu c}$ is the hydraulic diffusivity

The equation is similar to the one describing the heat diffusion through a material.

The diffusivity equation has been built for low compressible fluids: (liquids) by using the equation of state defining compressibility.

If the hydraulic diffusivity is pressure independent then the equation is linear.

If the hydraulic diffusivity is pressure dependent then the equation is non linear (case of gas flow).

3.6.3 Single-Phase Gas Flow

Gas flow needs a particular equation of state to characterize the relationship between pressure, volume and temperature.

3.6.3.1 Ideal gas

It is expressed as:

$$pv = nRT$$

- p: absolute pressure
- v: volume occupied by gas at pressure p
- n: gas moles number of volume v at pressure p and temperature T
- R: universal gas constant
- T: Absolute temperature

This equation is valid for low pressures $p < 4$ bars, R = 0.08314 (bar) (m^3)/(kmol) (K)

n number of moles is equal to:

$$n = \frac{m}{M_w}$$

m: mass of gas
M_w: *gas molecular mass* *gas density:* $\rho = \frac{m}{v}$

The equation of state can be written:

$$\rho = \frac{M_w}{RT} p \text{ then: } \frac{\delta \rho}{\delta t} = \frac{M_w}{RT} \frac{\delta p}{\delta t}$$

The combination of continuity equation with Eq. (3.13) in 3 Dimensions becomes:

$$\frac{\delta}{\delta x}\left(p \frac{\delta p}{\delta x}\right) + \frac{\delta}{\delta y}\left(p \frac{\delta p}{\delta y}\right) + \frac{\delta}{\delta z}\left(p \frac{\delta p}{\delta z}\right) = \frac{\phi \mu}{k} \frac{\delta p}{\delta t} \tag{3.17}$$

The equation can be rewritten:

$$\frac{\delta^2 p^2}{\delta x^2} + \frac{\delta^2 p^2}{\delta y^2} + \frac{\delta^2 p^2}{\delta z^2} = \frac{2\phi \mu}{k} \frac{\delta p}{\delta t} \tag{3.18}$$

for radial flow:

$$\frac{\delta^2 p^2}{\delta r^2} + \frac{1}{r} \frac{\delta p^2}{\delta r} = \frac{2\phi \mu}{k} \frac{\delta p}{\delta t} = \frac{\phi \mu}{kp} \frac{\delta p^2}{\delta t} \tag{3.19}$$

3.6.3.2 Real gas or non-ideal gas [82]

The gas deviation factor z is introduced. It is also called the gas compressibility factor.

The corresponding equation of state is:

$$pv = znRT$$

The gas density can be evaluated as before:

$$\rho = \frac{M_w}{RT} \frac{p}{z}$$

Assuming a laminar flow and neglecting gravity, Eq. (3.13) in 3 D becomes:

$$\frac{\delta}{\delta x}\left(\frac{p}{\mu z} \frac{\delta p}{\delta x}\right) + \frac{\delta}{\delta y}\left(\frac{p}{\mu z} \frac{\delta p}{\delta y}\right) + \frac{\delta}{\delta w}\left(\frac{p}{\mu z} \frac{\delta p}{\delta w}\right) = \frac{\phi}{k} \frac{\delta}{\delta t}\left(\frac{p}{z}\right)$$

To avoid confusion, the symbol w is used for the third dimension while z is the gas deviation factor.

For radial flow:

$$\frac{\delta^2 p}{\delta r^2} + \frac{1}{r} \frac{\delta p}{\delta r} = \frac{\phi}{k} \frac{\mu z}{p} \frac{\delta}{\delta t}\left(\frac{p}{z}\right) \tag{3.20}$$

The equation is nonlinear since z and μ are functions of the unknown p.

The pseudo-pressure concept $m(p)$ was introduced by Al-Hussainy *et al.* [59, 63, 83].

$$m(p) = \int_{p_o}^{p} \frac{2p'}{z(p')\mu(p')} dp'$$

Where p_0 is the base pressure and p: pressure of interest

Al-Hussainy, Ramey, and Crawford replaced the dependent variable p by the real gas pseudo pressure $m(p)$ in the diffusivity equation.

$$\frac{\delta m(p)}{\delta r} = \frac{\delta m(p)}{\delta p} \times \frac{\delta p}{\delta r} \text{ and } \frac{\delta m(p)}{\delta p} = \frac{2p}{\mu z}$$

then:
$$\frac{\delta m(p)}{\delta r} = \frac{2p}{\mu z} \frac{\delta p}{\delta r}$$

similarly:
$$\frac{\delta m(p)}{\delta t} = \frac{2p}{\mu z} \frac{\delta p}{\delta t}$$

substituting into the diffusivity equation for radial flow gives:

$$\frac{\delta^2 m(p)}{\delta r^2} + \frac{1}{r} \frac{\delta m(p)}{\delta r} = \frac{\phi \mu c}{k} \frac{\delta m(p)}{\delta t} \tag{3.21}$$

Eq. (3.21) is similar to Eqs. (3.16) and (3.19) except for the pressure and pressure squared variables which are replaced by $m(p)$, the pseudo-pressure. The term $\varphi\mu c/k$ is not constant as it was in the case of liquid flow, since c and μ are very pressure dependent. Consequently the resulting equation is non-linear.

See $m(p)$ calculation example in Appendix D.

3.7 SOLUTION FOR RADIAL LIQUID FLOW

3.7.1 Generalities Engineering Applications

Assumptions:

- radial flow
- homogenous isotropic porous media
- uniform thickness of the medium
- constant porosity and permeability (independent of pressure)
- fluid of small and constant compressibility
- constant fluid viscosity
- small pressure gradients; gravity neglected.

The solution of the diffusivity equation is dependent on the boundary conditions (inner and outer).

Inner Boundary Conditions:

Referring to a well drilled through an ideal reservoir, two main boundary conditions are commonly used:

- the constant terminal rate case
- the constant terminal pressure case.

In the constant terminal rate case, a unit rate of production is made to flow across the terminal boundary (well) from time 0 onward. The ensuing pressure drop is computed as a function of time.

This condition is used to establish the well build-up analysis.

In the constant terminal pressure case, the terminal boundary pressure is lowered by unity at time 0 and kept constant. The resulting cumulative amount of fluid flowing across the boundary is computed as a function of time.

This condition is used to calculate the water influx into an oil reservoir. The oil pool is considered as a large hole into which water from an aquifer flows in as a result of a pressure drop imposed at the inner boundary. This pressure drop is deducted from the oil zone pressure history.

Van Everdingen and Hurst published a solution (1949) for both conditions by using the Laplace transformation [85].

Outer Boundary Conditions:

a. Infinite Reservoir Case

At all times, pressure at the outer boundary (radius infinite) is the same as the initial pressure p_i for all t.

$p \rightarrow p_i$ as $r \rightarrow \infty$ for all t infinite reservoir.

The pressure wave created by the constant rate fluid withdrawal diffuses continuously through the reservoir.

The flow is in unsteady conditions since pressure is changing permanently everywhere in the reservoir with time.

b. Bounded Reservoir Case

$p = pi$ at $t = 0$ for all r.

$$\left(\frac{\delta p}{\delta r}\right)_{r_e} = 0 \text{ for all } t \text{ (no flow at } r = r_e, \text{ sealed reservoir)}$$

3.7.2 Constant Rate, Infinite Reservoir Case [80, 82, 83]

Diffusivity equation

$$\frac{\delta^2 p}{\delta r^2} + \frac{1}{r}\frac{\delta p}{\delta r} = \frac{\phi \mu c}{k}\frac{\delta p}{\delta t}$$

Boundary conditions at initial time:

1) $p = p_i$ at $t = 0$ for all r

2) $\left(r\frac{\delta p}{\delta r}\right)_{r_w} = \frac{q\mu}{2\pi kh}$ for $t > 0$(constant rate flow)

3) $p \to p_i$ as $r \to \infty$

The second condition is replaced by:

$\lim_{r\to 0}\left(r\frac{\delta p}{\delta r}\right) = \frac{q\mu}{2\pi kh}$ for $t > 0$ "line source approximation" to develop a solution, change of variable is used (Boltzman transformation).

$$y = \frac{\phi\mu c r^2}{4kt}$$ substituting into the diffusivity equation

$$y\frac{d^2p}{dy^2} + \frac{dp}{dy}(1+y) = 0 \qquad \text{let} \qquad p' = \frac{dp}{dy}$$

the equation becomes:

$$y\frac{dp'}{dy} + (1+y)p' = 0$$

Separation of variables and integration leads to

$$\frac{dp'}{p'} = -\frac{dy}{y} - dy \qquad \text{then} \qquad \text{Ln}(p') = -\text{Ln}(y) - y + C$$

$$\text{Ln}(p'y) = -y + C \qquad p'y = e^{-yC_1}$$

$$p' = \frac{dp}{dy} = \frac{C_1}{y}e^{-y}$$ C and C_1 are integration constants

From boundary condition (2) above

$$\lim_{y\to 0} 2y\frac{dp}{dy} = \lim_{y\to 0} 2C_1 e^{-y} = \frac{q\mu}{2\pi kh} \qquad \text{then} \qquad C_1 = \frac{q\mu}{4\pi kh}$$

$$p' = \frac{dp}{dy} = \frac{q\mu}{4\pi kh}\frac{e^{-y}}{y} \qquad p = \frac{q\mu}{4\pi kh}\int_{\infty}^{y}\frac{e^{-y}}{y}dy + C_2$$ or changing the limits

$$p = -\frac{q\mu}{4\pi kh}\int_{y}^{\infty}\frac{e^{-y}}{y}dy + C_2$$

with the first boundary condition: $C_2 = p_i$ finally the solution is:

$$p_i - p(r,t) = \frac{q\mu}{2\pi kh}\left[-\frac{1}{2}E_i\left(-\frac{\phi\mu c r^2}{4kt}\right)\right]$$

E_i is the exponential integral

$$E_i(-x) = -\int_x^{\infty}\frac{e^{-u}du}{u} = \left[\mathrm{Ln}(x) - \frac{x}{1!} + \frac{x^2}{2\times 2!} - \frac{x^3}{3\times 3!} + \ldots.\right]_x^{\infty}$$

The integral has been worked out in the form of a table (Appendix J).

Nisle [82] has shown that the exponential integral may be expressed by the series

$$E_i(-x) = \mathrm{Ln}(x) + 0.5772 - x + \frac{x^2}{2\times 2!} - \frac{x^3}{3\times 3!} + \ldots.\frac{x^n}{n\times n!}$$

$$\gamma = e^{0.5772} = 1.781 \qquad 0.5772 \text{ is the Euler's constant}$$

$$\lim_{n\to\infty}\left[1 + \frac{1}{2} + \ldots\ldots\ldots + \frac{1}{n} - \mathrm{Ln}(n)\right] = 0.5772$$

For $x < 0.01$, the value of $Ei(-x)$ is approximated by $(\mathrm{Ln}(1/x) - 0.5772)$.

The exponential integral, solution of the diffusivity equation is used for well interference test analysis (see example Appendix I).

The solution becomes: *(SI or Darcy units)*

$$p(r,t) = p_i + \frac{q\mu}{4\pi kh}\mathrm{Ln}\left(\frac{\gamma\phi\mu c r^2}{4kt}\right) \quad \text{or} \quad p(r,t) = p_i - \frac{q\mu}{4\pi kh}\left[\mathrm{Ln}\frac{kt}{\phi\mu c r^2} + 0.80907\right]$$

$\mathrm{Ln}(4/\gamma) = 0.80907$ The expression at the well bore $r = r_w$

$$p_{wf} = p_i + \frac{q\mu}{4\pi kh}\mathrm{Ln}\left(\frac{\gamma\phi\mu c r_w^2}{4kt}\right) \quad \text{or} \quad p_{wf} = p_i - \frac{q\mu}{4\pi kh}\left[\mathrm{Ln}\frac{kt}{\phi\mu c r_w^2} + 0.80907\right] \quad (3.22)$$

Data for Figure 3.7:

$q =$ 24 m^3/d
$\mu =$ 0.4 cp
$k =$ 0.2 Darcy
$h =$ 20 m
porosity = 0.2

As expressed above, the $Ei(x)$ solution can be approximated by a Ln expression for $x < 100$. The approximation is quickly valid with time for small r like the well radius r_w.

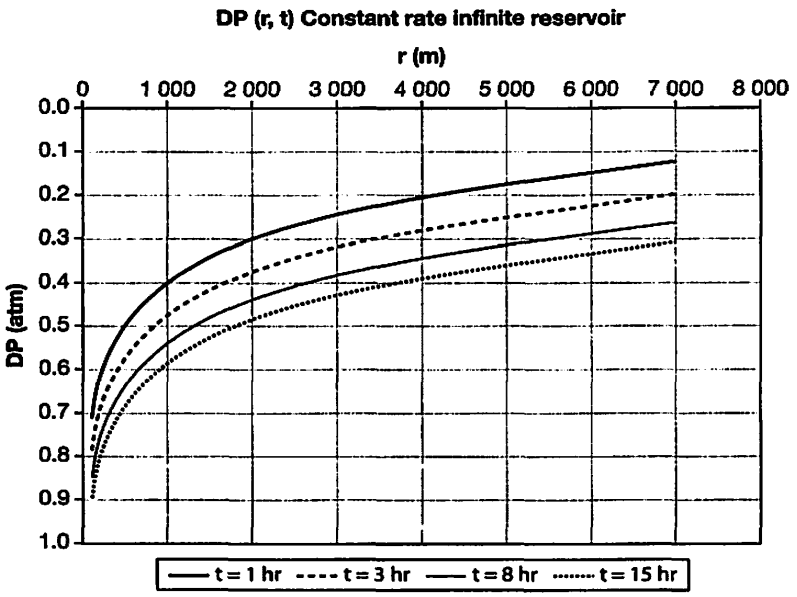

Figure 3.7 Pressure profile of a constant rate producing well flowing in an infinite reservoir.

To evaluate the pressure drop at a distance r far from the well, (interference test), the use of $Ei(x)$ solution is necessary [84].

The reservoir is said to be in an **unsteady state** regime or transient regime. An observer located at a distance r from the well, would measure a continuous pressure change.

3.7.3 Dimensionless Variables and Units

It is convenient to express the diffusivity equation in terms of dimensionless variables. The objectives of such a form are multiple: [63]

The number of parameters upon which the solution depends is reduced:

Δp_D, q_D, t_D. Subscript $_D$ means dimensionless terms.

The three cases: "liquid" (pressure), "pressure-squared", and "pseudo-pressure", are all represented by only one equation.

The diffusivity equation is equivalent to the standard heat conduction equation for which solutions with various boundary conditions can be applied.

$$\nabla^2(\Delta p_D) = \frac{\delta}{\delta t_D}(\Delta p_D)$$

The diffusivity equation was built from Darcy's law. Consequently all resulting formulas are governed by the Darcy units. In practice the oilfield units and practical metric units are used.

Tableau 3.1 Variables in practical unit systems

Parameter	Darcy	Oilfield Units	European Metric	Canadian Metric	SI
r, h	cm	ft	m	m	m
k	darcy	mD	mD	mD	m^2
t	s	h	h	h	s
μ	cp	cp	cp	cp	Pa.s
p	atm	psia	bara	kPa	Pa
V	cm^3	ft^3	m^3	m^3	m^3
q(oil)	cm^3/s	bbl/d	m^3/d	m^3/d	m^3/s
q(gas)	cm^3/s	MMcf/d	m^3/d	m^3/d	m^3/s

Dimensionless variables:

$$r_D = \frac{r}{r_w} \qquad t_D = \alpha \frac{kt}{\phi \mu c r_w^2} \qquad \Delta p_D = \frac{p_i - p}{\frac{q\mu}{2\pi kh}} \qquad q_D = \beta \frac{q\mu}{kh\Delta p}$$

α and β are constants dependent on the unit system in use.

Tableau 3.2 Constants for Dimensionless Variables

Dimensionless parameters for Radial Flow			
		$t_D = \frac{\alpha\, kt}{\phi \mu c r_w^2}$	$q_D = \frac{\beta\, q\, \mu}{kh\, \Delta p}$
		α	β
Darcy units		1	$1/2\pi$
Oilfield units	t: hours t: days t: years	0.000264 0.006327 2.309	141.2
European Metric *(bars)*	t: hours t: days t: years	3.553E-04 8.527E-03 3.112	18.66
Canadian Metric *(kPa)*	t: hours t: days t: years	3.553E-06 8.527E-05 0.03112	1 866
SI	t: seconds	1	$1/2\pi$

3.7.4 Constant Rate at Inner Boundary, Bounded Reservoir Case

In this configuration a well is flowing at a constant rate in a radial cylindrical flow. The inner boundary is the well radius; the reservoir is limited with a no flow condition at the outer boundary.

The well flow rate is constant:

$$\left(r\frac{\delta p}{\delta r}\right)_{r_w} = \frac{q\mu}{2\pi kh} \quad \text{for } t > 0$$

in dimensionless terms: $$r_D \frac{\delta(\Delta p_D)}{\delta r_D} = -1 \quad \text{at } r_D = 1 \text{ for } t_D > 0$$

The no flow condition at the outer boundary implies a zero pressure gradient at the boundary:

$$\frac{\delta p}{\delta r} = 0 \quad \text{at } r_e \text{ for all } t$$

r_e is the radius of the external boundary

in dimensionless terms: $$\frac{\delta(\Delta p_D)}{\delta r_D} = 0 \quad \text{at } r_{eD} \text{ for all } t_D$$

At initial time, the reservoir pressure is uniform:

$$\Delta p_D = 0 \text{ at } t_D = 0 \text{ for all } r_D$$

The diffusivity equation becomes:

$$\frac{\delta^2(\Delta p_D)}{\delta r_D^2} + \frac{1}{r_D}\frac{\delta(\Delta p_D)}{\delta r_D} = \frac{\delta(\Delta p_D)}{\delta t_D}$$

with $$r_D = \frac{r}{r_w} \qquad r_{eD} = \frac{r_e}{r_w}$$

Hurst and Van Everdingen solved the equation by using the Laplace transform [63, 85].

The final general solution is:

$$\Delta p_D = \frac{2}{r_{eD}^2 - 1}\left(\frac{r_D^2}{4} + t_D\right) - \frac{r_{eD}^2 \operatorname{Ln} r_D}{r_{eD}^2 - 1} - \frac{3r_{eD}^4 - 4r_{eD}^4 \operatorname{Ln} r_{eD} - 2r_{eD}^2 - 1}{4(r_{eD}^2 - 1)^2}$$
$$+\pi \sum_{n=1}^{\infty} \frac{e^{-\alpha_n^2 t_D} J_1^2(\alpha_n r_{eD})\left[J_1(\alpha_n) Y_0(\alpha_n r_D) - Y_1(\alpha_n) J_0(\alpha_n r_D)\right]}{\alpha_n\left[J_1^2(\alpha_n r_{eD}) - J_1^2(\alpha_n)\right]} \qquad (3.23)$$

α_n are the roots of: $$J_1(\alpha_n r_{eD}) Y_1(\alpha_n) - J_1(\alpha_n) Y_1(\alpha_n r_{eD}) = 0$$

J_1 and Y_1 are the Bessel functions of the first and second kind respectively and both of order one. The roots may be obtained by iterative numerical methods.

The solution at the well, is obtained by evaluating Eq. (3.23) at $r_D = 1$

Δp_D at well:

$$|\Delta p_D|_{r_w} = \frac{2t_D}{r_{eD}^2} + \text{Ln}\, r_{eD} - \frac{3}{4} + 2\sum_{n=1}^{\infty} \frac{e^{-\alpha_n^2 t_D} J_1^2(\alpha_n r_{eD})}{\alpha_n^2 \left[J_1^2(\alpha_n r_{eD}) - J_1^2(\alpha_n)\right]} \tag{3.24}$$

For values of $t_D < 0.25\ r_{eD}^2$, $|\Delta p_D|_{rw}$ is equivalent to Eq. (3.22); that is the boundary effect is negligible and the reservoir behaves as if it were infinite.

As t_D increases, the summation term becomes negligible. The pressure at the well is expressed by:

$$|\Delta p_D|_{r_w} = \frac{2t_D}{r_{eD}^2} + \text{Ln}\, r_{eD} - \frac{3}{4} \quad \text{for} \quad \frac{t_D}{r_{eD}^2} > 0.25 \tag{3.25}$$

Discussion:

At production start up time, the resulting pressure wave generated at well diffuses outwards in the reservoir as if the reservoir was infinite. This is the transient or **unsteady-state** regime. Then the disturbance hits the reservoir boundary; after some transient time, the reservoir pressure declines at a constant rate. This is the **semi-steady-state** flow regime (or pseudo steady-state).

$$\frac{\delta p}{\delta t} \equiv \text{Cte} \quad \text{for all } r$$

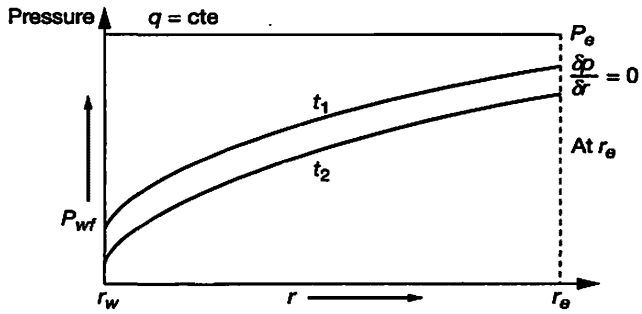

Figure 3.8 Pressure profile in a pseudo-steady state regime for a bounded reservoir.

3.7.5 Constant Rate at Inner Boundary, Constant Pressure at Outer Boundary [63, 85]

Diffusivity equation

$$\frac{\delta^2(\Delta p_D)}{\delta r_D^2}+\frac{1}{r_D}\frac{\delta(\Delta p_D)}{\delta r_D}=\frac{\delta(\Delta p_D)}{\delta t_D}$$

boundary conditions:

- at initial time $p = p_i = p_e$ for all r
- in dimensionless terms: $\Delta p_D = 0$ at $t_{Dw} = 0$ for all r_D

$$\text{for } t>0 \quad \left(r\frac{\delta p}{\delta r}\right)_{r_w}=\frac{q\mu}{2\pi kh} \text{ (constant rate) or } r_D\frac{\delta(\Delta p_D)}{\delta r_D}=-1 \text{ for } t_{Dw}>0$$

p at $r_e = p_i$ for all t or $\Delta p_D = 0$ at $r_D = r_{eD}$ for all t_{Dw}

The pressure behavior solution at the well is:

$$\left|\Delta p_D\right|_{r_w}=\text{Ln } r_{eD}-2\sum_{n=1}^{\infty}\frac{e^{-\beta_n^2 t_D}J_0^2(\beta_n r_{eD})}{\beta_n^2\left[J_1^2(\beta_n)-J_0^2(\beta_n r_{eD})\right]} \tag{3.26}$$

β_n is a root of:

$$J_1(\beta_n)\,Y_0(\beta_n r_{eD})-Y_1(\beta_n)\,J_0(\beta_n r_{ed})=0$$

As t_D increases, the summation term decreases (due to e^{-tD}) and Eq. (3.26) reduces to:

$$\left|\Delta p_D\right|_{r_w}=\text{Ln } r_{eD} \qquad \text{for } t_D > 1.0\, r_{eD}^2 \tag{3.27}$$

In the early part of the production period, the well acts as if it were an infinite reservoir. After some time, boundary effects become noticeable, and a transition period precedes the steady-sate condition illustrated by Eq. (3.27).

This situation occurs in oil reservoirs which are connected to a strong active aquifer or submitted to an adapted water injection scheme. In laboratory experiments, the regime can be reached on good quality samples during a permeability measurement or a water flood experiment.

3.7.6 Constant Well Pressure, Infinite Reservoir, or Finite Circular Reservoir with no Flow at Outer Boundary

In the field, a producing well usually operates against a fixed back pressure (constant surface separator pressure, then constant P_{wf}). The flow rate varies with time.

Another field application is to assume a circular oil pool as a huge production well into which an aquifer produces water. The driving parameter of the water influx is the pressure drop history that has been measured at the oil water boundary. This condition is used to calculate water entries. Hurst and Van Everdingen [59, 85] developed the method.

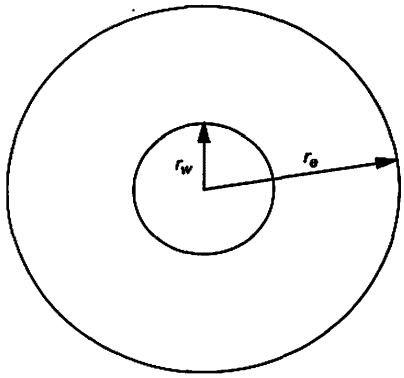

Figure 3.9 Finite Circular Reservoir.

Diffusivity equation: $$\frac{\delta^2(\Delta p_D)}{\delta r_D^{\,2}} + \frac{1}{r_D}\frac{\delta(\Delta p_D)}{\delta r_D} = \frac{\delta(\Delta p_D)}{\delta t_D}$$

Boundary conditions:

At initial time $p = p_i = p_e$ for all r

In dimensionless terms: $\Delta p_D = 0$ at $t_{Dw} = 0$ for all r_D

The flow rate is given by Darcy's law,

for $t > 0$ $$\left(r\frac{\delta p}{\delta r}\right)_{r_w} = \frac{q\mu}{2\pi kh}$$

dimensionless rate is: $$q_D(t_D) = \frac{q\mu}{2\pi kh\Delta p} \quad \textit{(SI or Darcy units)} \tag{3.28}$$

$q_D(t_D)$ is the dimensionless influx rate evaluated at $r_D = 1$, describes the change in rate from zero to q due to a pressure drop Δp applied at the reservoir boundary r_w or r_0 at time $t = 0$. It is convenient to express the solution in terms of cumulative water influx rather than rate of influx.

Results are presented in the form of tables, giving the elementary dimensionless influx W_D, function of dimensionless entries: t_D and r_D.

Note: the calculated solution is the production rate at the well radius r_w or the water influx calculated at the oil water boundary located at radius r_0.

The cumulative fluid produced is calculated from Eq. (3.28)

$$\frac{\mu}{2\pi kh\Delta p}\int_0^t q\,dt = \int_0^{t_D} q_D(t_D)\frac{dt}{dt_D}dt_D \text{ gives:}$$

$$\frac{W_e\mu}{2\pi kh\Delta p} = W_D(t_D)\frac{\phi\mu c r_0^2}{k}$$

$$\text{so } W_e = 2\pi\Phi hcr_0^2\Delta p W_D(t_D) \qquad \textit{(SI or Darcy units)} \tag{3.29}$$

W_e: cumulative fluid entry due to pressure drop Δp set at $r = r_0$
$W_D(t_D)$: cumulative fluid influx giving the dimensionless influx per unit pressure drop imposed at r_0 at $t = 0$
Φ: formation porosity.
h: formation thickness
r_w, r_0: well radius or oil pool radius
Δp: pressure drop set at inner boundary

Eq. (3.29) is used to calculate water entries in a reservoir. The method is detailed in Appendix M.

3.8 APPLICATION OF THE DIFFUSIVITY EQUATION TO THE WELL FLOW

Radial well flow in a homogenous reservoir.

Considering the diffusivity equation in the radial flow for incompressible fluid, implies the second member to be zero ($c = 0$). The diffusivity equation reduces to:

$$\frac{1}{r}\frac{\delta}{\delta r}\left(r\frac{\delta P}{\delta r}\right) = 0 \tag{3.30}$$

The general solution of Eq. (3.30) is:

$$p = c_1 \log r + c_2$$

where c_1 and c_2 are integration constants

The boundary conditions to be honored are:

at $r = r_w$ $\quad p = p_w$
at $r = r_e$ $\quad p = p_e$

The final solution is expressed as:

$$p = p_w + \frac{p_e - p_w}{\text{Ln } r_e / r_w}\text{Ln}\frac{r}{r_w} \tag{3.31}$$

Eq. (3.31) gives the pressure at any point between r_w and r_e. The pressure varies logarithmically between the two radii.

The Darcy law expresses the fluid velocity as:

$$v = -\frac{k}{\mu}\frac{\delta p}{\delta r} = -\frac{k}{\mu r}\frac{p_e - p_w}{\mathrm{Ln}(r_e / r_w)} \tag{3.32}$$

From Eq. (3.32), the total fluid flow through the formation (thickness h) and into the well can be calculated as:

$$q = -h\int_0^{2\pi} rvd\theta = \frac{2\pi kh(p_e - p_w)}{\mu\,\mathrm{Ln}(r_e / r_w)} \qquad \textit{(SI or Darcy units)}$$

The sign has been changed to obtain a production rate positive.

The steady-state oil well flow equation is then:

oil well: $$Q_o = \frac{2\pi k_o h}{\mu_o B_o}\frac{(p_e - p_w)}{\mathrm{Ln}(r_e / r_w)}$$ *Darcy units*:

Q_o:	surface oil flow rate	cm^3/s
k_o:	oil effective permeability	D
h:	formation thickness	cm
B_o:	oil formation factor	
Ln:	natural logarithm *(base e)*	
P:	pressure	atm
μ_o:	oil viscosity	cp

See well formulas in Appendix L.

3.9 WELL FLOW IN A GRID

3.9.1 Well Flow in a Regular Grid [86]

Let's assume grid block 0 at pressure P_B (numerically calculated block pressure), surrounded by four adjacent blocks at pressure P_e (Fig. 3.10). A well is drilled at the centre of block 0 and perforated over the full block thickness h. All adjacent P_e pressures are assumed to be equal.

It is convenient to associate an equivalent radius r_0 with the well block. r_0 is the radius at which the steady-state flowing pressure is found for the actual well and equal to the numerically calculated pressure P_B for the well block.

With P_B at r_0 and P_{wf} at r_w, the well flow rate expressed in the radial geometry is: *(SI or Darcy units)*

$$Q = \frac{2\pi kh}{\mu B}\frac{P_B - P_{wf}}{\mathrm{Ln}\left(\frac{r_0}{r_w}\right)} \tag{3.33}$$

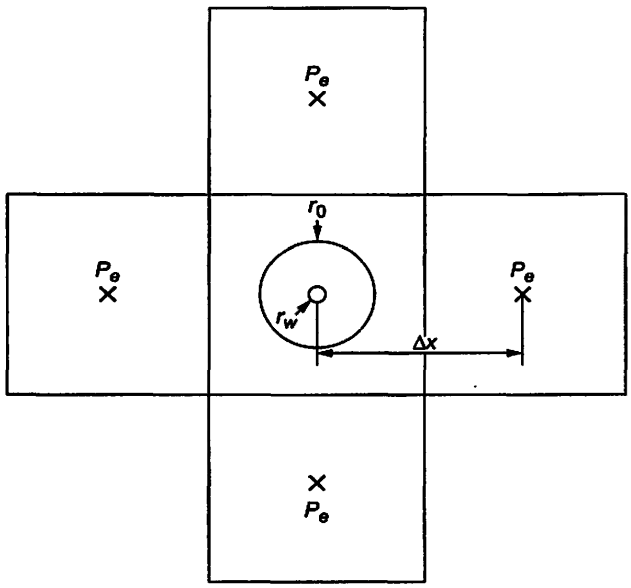

Figure 3.10 Well in a regular grid.

In the square mesh: P_e at Δx and P_{wf} at r_w, the radial flow is:

$$Q = \frac{2\pi kh}{\mu B} \frac{P_e - P_{wf}}{\mathrm{Ln}\left(\frac{\Delta x}{r_w}\right)} \tag{3.34}$$

In the square mesh: P_e at Δx and P_B at r_0 the radial flow is:

$$Q = \frac{2\pi kh}{\mu B} \frac{P_e - P_B}{\mathrm{Ln}\left(\frac{\Delta x}{r_0}\right)} \tag{3.35}$$

In the mesh geometry, the linear flow rate is:

$$Q = 4\frac{k\Delta x \times h}{\mu B \Delta x}(P_e - P_B) = 4\frac{kh}{\mu B}\left(P_e - P_B\right) \tag{3.36}$$

Elimination of $(P_e - P_B)$ from Eqs. (3.35) and (3.36) gives:

$$\frac{Q\mu B}{2\pi kh}\mathrm{Ln}\left(\frac{\Delta x}{r_0}\right) = \frac{Q\mu B}{4kh}$$

$$\text{Ln}\left(\frac{\Delta x^2}{r_0^2}\right)=\pi \qquad \text{so} \qquad r_0=\frac{\Delta x}{\sqrt{e^{\pi}}}=0.208\,\Delta x \tag{3.37}$$

The calculated block pressure P_B is found at a radius 0.208 Δx from the block centre in the actual radial well steady-state flow configuration.

The simulator well flow without skin is found from Eq. (3.33):

$$Q=\frac{2\pi kh}{\mu B}\frac{P_B-P_{wf}}{\text{Ln}\left(\frac{0.208\Delta x}{r_w}\right)} \quad \textit{(SI or Darcy units)}$$

The well connection is:

$$W_k=\frac{2\pi kh}{\text{Ln}\left(\frac{0.208\Delta x}{r_w}\right)} \quad \text{or} \quad W_k=\frac{4\pi kh}{\text{Ln}\frac{\Delta x^2}{r_w^2}-\pi} \quad \textit{(SI or Darcy units)}$$

k: absolute permeability of the well block
h: block thickness
$\Delta x = \Delta y$ block size

The simulator well productivity index for oil without skin is:

$$PI_{sim}=W_k\frac{k_{ro}}{\mu_o B_o}$$

k_{ro}: oil relative permeability of the well block
μ_o: oil viscosity
B_o: oil formation factor

3.9.2 Well Flow in a non Square Grid

3.9.2.1 Isotropic Permeability ($k_x = k_y$) [87]

r_0 is the radius in the well block at which the steady-state flowing pressure for the actual well is equal to the numerically calculated block pressure P_B (Fig. 3.11).

The steady-state well flow rate is expressed in the two directions between P_1 and P_B (Δx, r_0)

$$P_1-P_B=P_3-P_B=\frac{Q\mu B}{2\pi kh}\text{Ln}\left(\frac{\Delta x}{r_0}\right) \tag{3.38}$$

between P_2 and P_B (Δy, r_0)

$$P_2-P_B=P_4-P_B=\frac{Q\mu B}{2\pi kh}\text{Ln}\left(\frac{\Delta y}{r_0}\right) \tag{3.39}$$

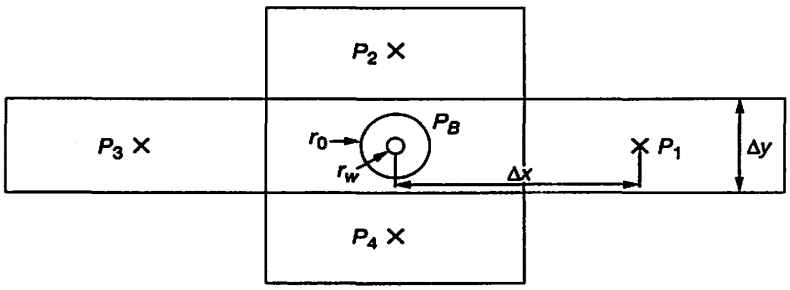

Figure 3.11 Well in a Non square grid.

The well flow rate in the rectangular mesh is:

$$Q=\frac{kh}{\mu B}\frac{\Delta y}{\Delta x}\left[\left(P_1-P_B\right)+\left(P_3-P_B\right)\right]+\frac{kh}{\mu B}\frac{\Delta x}{\Delta y}\left[\left(P_2-P_B\right)+\left(P_4-P_B\right)\right] \tag{3.40}$$

Substituting Eqs (3.38) and (3.39) into (3.40):

$$\pi=\frac{\Delta y}{\Delta x}\mathrm{Ln}\left(\frac{\Delta x}{r_0}\right)+\frac{\Delta x}{\Delta y}\mathrm{Ln}\left(\frac{\Delta y}{r_0}\right) \tag{3.41}$$

aspect ratio definition: $$\alpha=\frac{\Delta y}{\Delta x}$$

from Eq. (3.41) $$\alpha\,\mathrm{Ln}\left(\frac{\Delta x}{r_0}\right)+\frac{1}{\alpha}\mathrm{Ln}\left(\frac{\Delta y}{\Delta x}\frac{\Delta x}{r_0}\right)=\pi$$

$$\alpha\,\mathrm{Ln}\left(\frac{\Delta x}{r_0}\right)+\frac{1}{\alpha}\mathrm{Ln}\,\alpha+\frac{1}{\alpha}\mathrm{Ln}\left(\frac{\Delta x}{r_0}\right)=\pi$$

$$\text{so: } \mathrm{Ln}\left(\frac{\Delta x}{r_0}\right)=\frac{\alpha\pi-\mathrm{Ln}\,\alpha}{1+\alpha^2} \quad \text{or} \quad \mathrm{Ln}\left(\frac{r_0}{\Delta x}\right)=\frac{\mathrm{Ln}\,\alpha-\alpha\pi}{1+\alpha^2} \tag{3.42}$$

The well flow rate without skin in the well block is:

$$Q=\frac{2\pi kh}{\mu B}\frac{P_B-P_{wf}}{\mathrm{Ln}\left(\frac{r_0}{r_w}\right)} \qquad Q=\frac{2\pi kh}{\mu B}\frac{P_B-P_{wf}}{\mathrm{Ln}\left(\frac{r_0}{\Delta x}\frac{\Delta x}{r_w}\right)}$$

The well connection *(or well index)* is: $W_k=\dfrac{2\pi kh}{\mathrm{Ln}\left(\frac{r_0}{\Delta x}\frac{\Delta x}{r_w}\right)}$ *(SI or Darcy units)*

k: absolute permeability of the well block
h: block thickness
r_0: radius at which P_B is found; calculated from Eq. (3.42)

D.W. Peaceman [87] derived the equivalent well-block radius for an isotropic reservoir with an aspect ratio $\Delta y/\Delta x$ as:

$$r_0 = 0.14(\Delta x^2 + \Delta y^2)^{1/2} \tag{3.43}$$

The relation was obtained by mathematical derivation based on an infinite non square grid, using the finite Fourier series. The same result was obtained by careful numerical simulation.

Eq. (3.37) must be replaced by the more general rule expressed by Eq. (3.43).

3.9.2.2 Anisotropic Permeability ($k_x \# k_y$)

Darcy's law for homogeneous but anisotropic medium can be written:

$$v_x = -\frac{k_x}{\mu}\frac{\delta p}{\delta x} \qquad v_y = -\frac{k_y}{\mu}\frac{\delta p}{\delta y}$$

Assuming that the individual permeabilities k_x, k_y are uniform, x and y are principal axes of the porous media and applying the equation of continuity, it is found that the pressure distribution (x, y) for steady-state homogeneous liquid flow is given by:

$$k_x \frac{\delta^2 p}{\delta x^2} + k_y \frac{\delta^2 p}{\delta y^2} = 0 \tag{3.44}$$

Transforming the coordinate system defined by:

$$u = \left(\frac{k_y}{k_x}\right)^{1/4} x \qquad v = \left(\frac{k_x}{k_y}\right)^{1/4} y \tag{3.45}$$

with the boundary condition:

$$p = p_{wf} \quad \text{at} \quad r = \left(x^2 + y^2\right)^{1/2} = r_w$$

Equation (3.44) may be transformed:

$$\frac{\delta^2 p}{\delta u^2} + \frac{\delta^2 p}{\delta v^2} = 0 \tag{3.46}$$

with the boundary condition

$$p = p_{wf} \quad \text{at} \quad \left(k_x / k_y\right)^{1/2} u^2 + \left(k_y / k_x\right)^{1/2} v^2 = r_w^2$$

$$\frac{\delta^2 p}{\delta u^2}+\frac{\delta^2 p}{\delta v^2}=0 \tag{3.47}$$

It appears that the effect of anisotropy in the permeability is equivalent to a shrinking or expansion of the coordinates.

The boundary condition is specified on an ellipse. The solution of Eq. (3.47) is not radial but isobars are a family of concentric ellipses.

Similarly to Eq. (3.40), the well flow rate in the rectangular mesh is:

$$\frac{k_x h\Delta y}{\mu B\Delta x}\left(p_3-2p_B+p_1\right)+\frac{k_y h\Delta x}{\mu B\Delta y}\left(p_2-2p_B+p_4\right)=Q$$

from transforms Eq. (3.45)

$$k_x\frac{\Delta y}{\Delta x}=(k_xk_y)^{1/2}\frac{\Delta v}{\Delta u} \quad \text{and} \quad k_y\frac{\Delta x}{\Delta y}=(k_xk_y)^{1/2}\frac{\Delta u}{\Delta v} \quad \text{then}$$

$$\frac{(k_xk_y)^{1/2}h\Delta v}{\mu B\Delta u}\left(p_3-2p_B+p_1\right)+\frac{\left(k_xk_y\right)^{1/2}h\Delta u}{\mu B\Delta v}\left(p_2-2p_B+p_4\right)=Q$$

$$r_0^{uv}=0.14\left(\Delta u^2+\Delta v^2\right)^{1/2} \quad \textit{(Deducted from mathematical calculation and numerical simulation)}$$

$$p_B-p_{wf}=\frac{q\mu}{2\pi\left(k_xk_y\right)^{1/2}}\text{Ln}\left(\frac{r_0}{r_w}\right) \qquad p_B-p_{wf}=\frac{q\mu}{2\pi\left(k_xk_y\right)^{1/2}}\text{Ln}\left(\frac{r_0^{uv}}{\hat{r}_w}\right)$$

So

$$r_0=\left(\frac{r_w}{\hat{r}_w}\right)r_0^{uv}$$

$$r_0=0.28\frac{\left[\left(k_y/k_x\right)^{1/2}\Delta x^2+\left(k_x/k_y\right)^{1/2}\Delta y^2\right]^{1/2}}{\left(k_y/k_x\right)^{1/4}+\left(k_x/k_y\right)^{1/4}} \quad \textit{(SI or Darcy units)}$$

Remark:
The formula was built for an areal flow with k_x different to k_y. The same formulation can be used for a horizontal well when flow occurs in plane x, z or y, z,. where k_z replaces k_x or k_y.

Consequently for numerical reservoir simulations, using square or non square grid blocks, the pressure calculated for a well block is the same as the flowing pressure at an equivalent radius, r_0, the well block pressure P_B, is related to the bottom-hole pressure by:

$$p_B-p_{wf}=\frac{q\mu}{2\pi kh}\text{Ln}\frac{r_0}{r_w}$$

The equivalent well-block radius r_o for isotropic system and aspect ration $\Delta y/\Delta x$ is:

$$r_0 = 0.14\left(\Delta x^2 + \Delta y^2\right)^{1/2} \quad \textit{(SI or Darcy units)} \tag{3.48}$$

For anisotropic medium, the equivalent well-block radius is:

$$r_0 = 0.28\frac{\left[\left(k_y/k_x\right)^{1/2}\Delta x^2 + \left(k_x/k_y\right)^{1/2}\Delta y^2\right]^{1/2}}{\left(k_y/k_x\right)^{1/4} + \left(k_x/k_y\right)^{1/4}} \quad \textit{(SI or Darcy units)} \tag{3.49}$$

Note:

Assuming a square grid mesh, r_0 from Eq. (3.48) gives:

$$r_0 = 0.14 \times \sqrt{2\Delta x^2} = 0.198\Delta x$$

Result slightly different to the one obtained in Eq. (3.37).

3.10 LAMINAR FLOW IN CAPILLARY TUBES POISEUILLE'S LAW

It is convenient and instructive to treat the pore spaces as if they were composed of bundles of parallel capillary tubes of various diameters [18, 79].

Considering a capillary tube of length L and inside radius r_0 (Fig. 3.12) in which an incompressible fluid of viscosity μ poises is flowing in a laminar or viscous regime under a pressure gradient $(p_A - p_B)$. If the fluid wets the capillary walls, the velocity is zero at the wall and rises to a maximum at the centre.

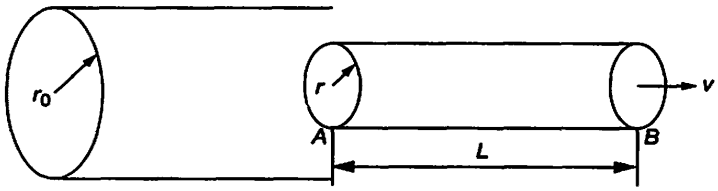

Figure 3.12 Capillary tube.

Assuming a steady-state flow regime, a fluid particle velocity is uniform along the tube length but depends on the radius within the fluid stream. The pressure driving force is equal and opposite to the viscous forces.

$$\pi r^2 (p_A - p_B) = \mu \frac{dv}{dr} dS$$

dS: lateral cylindrical area $2\pi rL$

$$dv = -\frac{1}{2\mu}\frac{\Delta p}{L} r dr \qquad v = -\frac{1}{4\mu}\frac{\Delta p}{L} r^2 + \text{Cte}$$

$v = 0$ at the wall r_0 then

$$v = \frac{(r_0^2 - r^2)}{4\mu L}\Delta p \tag{3.50}$$

Eq. (3.50) gives the velocity of any shell of radius r, and indicates that the velocity profile has a parabolic shape from a maximum at the centre to zero at the walls.

The volume rate of flow through an element dr in thickness is:

$$dq = v dS = \frac{1}{4\mu}\frac{\Delta p}{L}(r_0^2 - r^2) \times 2\pi r dr$$

$$q = \frac{\pi \Delta p}{2\mu L}\left[r_0^2 \int_0^{r_0} r dr - \int_0^{r_0} r^3 dr \right]$$

$$q = \frac{\pi r_0^4}{8\mu L}\Delta p \tag{3.51}$$

CGS

q: cm^3/s
r: cm
μ: poise
L: cm
Δp: $dynes/cm^2$

This is the Poiseuille's law for viscous flow of liquids through capillary tubes.

A similar equation has been derived for gas assuming a finite gas-slippage velocity at the capillary wall since gas is a non wetting fluid.

Darcy's law for linear liquid flow in permeable beds, Eq. (3.1) and Poiseuille's law Eq. (3.51) for capillary flow are similar.

Darcy's law:

$$q = k\frac{P_1 - P_2}{\mu L} A \tag{3.52}$$

q: cm^3/s
A: cm^2
μ: centipoises
k: Darcy
P: atm

Poiseuille's law:

$$q = \frac{\pi r_0^4}{8\mu L}\Delta p \tag{3.53}$$

q: cm^3/s
r: cm
μ: poise
L: cm
p: $dynes/cm^2$

Darcy's law expressed in terms of $dynes/cm^2$ and poise becomes:

$$q = \frac{k}{1.01325\times10^8}\frac{A(P_1 - P_2)}{\mu L} \tag{3.54}$$

with $A = \pi r_0^2$ in Eq. (3.54) and equating with Eq. (3.53) gives:

$$k = 12.67\times10^6 r_0^2 \tag{3.55}$$

k: darcys
r_0: cm

Considering a porous system made of a bundle of capillary tubes, the permeability of the medium depends on the pore throat size distribution and porosity. A flow network of tubes would be similar to layers of different permeabilities in parallel such that the average permeability can be calculated from the equation

$$k_{avg} = \frac{\sum_{j=1}^{m} k_j A_j}{\sum_{j=1}^{m} A_j} \tag{3.56}$$

k_j: permeability of one capillary tube
A_j: area of flow represented by one tube of permeability k_j
A_j can be expressed in terms of the capillary tube radius r_j

$$A_j = n_j \pi r_j^2$$

n_j: number of tubes of radius r_j

from Eq. (3.55) $$k_j = 12.67\times10^6 r_j^2$$

The permeability of a rock composed of closely packed capillaries of $1.25\ 10^{-4}$ cm radiuses is about 0.20 darcy. If only 25 per cent of the rock is pore channels, that is 0.25 porosity, the permeability becomes about 0.050 darcy or 50 mD.

Remark:
The permeability of a rock is a function not only of the pore size but of the arrangement or porosity of the media.

3.11 INTERFERENCE PHENOMENA STEADY-STATE SMALL GROUP OF WELLS [88]

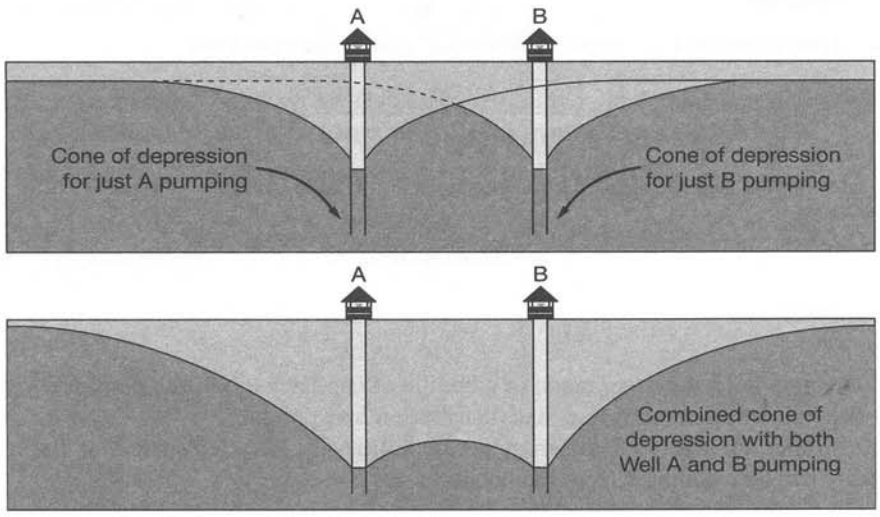

Figure 3.13 Pressure profile between two producing wells.

Assuming two producing wells draining a large radius R in comparison to the distance d between the two wells, the total production is not the addition of the individual well capacity. Well 1 creates a circular pressure sink, therefore well 2 is not submitted to the virgin reservoir pressure p_e (Fig. 3.13).

The well flowing pressure of well 1 can be expressed as:

$$p_{w1} = p_e - \left[\frac{q_1\mu}{2\pi kh}\mathrm{Ln}\left(\frac{R}{r_{w1}}\right) + \frac{q_2\mu}{2\pi kh}\mathrm{Ln}\left(\frac{R}{d}\right)\right] \tag{3.57}$$

p_e is the average reservoir pressure in the production vicinity
q_1, q_2: production rates

well 1 in addition to its production, drains fluid (well 2) in the total drainage area as if its radius r_w was equal to d.

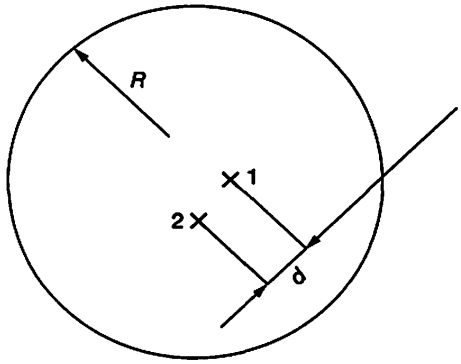

Figure 3.14 Two producing wells in the same drainage area.

For two identical wells (1 and 2 Fig. 3.14), the production rate is:

$$q_1 = q_2 = \frac{2\pi kh}{\mu} \frac{(p_e - p_w)}{\mathrm{Ln}\left(\frac{R^2}{d_2 r_w}\right)}$$

The production rate is reduced.

For example with $R = 1\ 500$ m, $r_w = 0.1$ m $d = 100$ m

$$\mathrm{Ln}(R/r_w) = 9.6 \qquad \mathrm{Ln}(R^2/dr_w) = 12.3$$

The individual production rate with interference is 78% of the production rate without interference.

Case of three wells in an equilateral triangular pattern of mutual distance d_3 (Fig. 3.15).

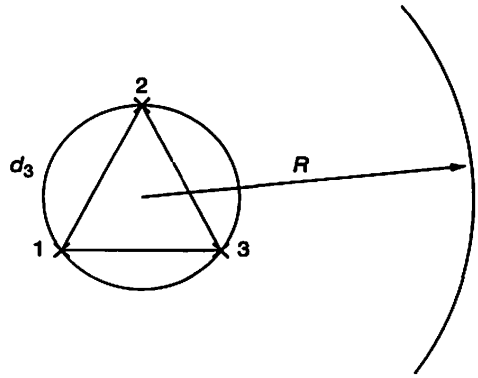

Figure 3.15 Three regularly located wells.

$$p_{w1} = p_e - \frac{q\mu}{2\pi kh}\left[\text{Ln}\frac{R}{r_{w1}} + \text{Ln}\frac{R}{d_3} + \text{Ln}\frac{R}{d_3}\right]$$

$$q_1 = q_2 = q_3 = \frac{2\pi kh}{\mu}\frac{(p_e - p_w)}{\text{Ln}\left(\dfrac{R^3}{r_w d_3^2}\right)}$$

Case of four wells in a square pattern of mutual distance d_4 (Fig. 3.16).

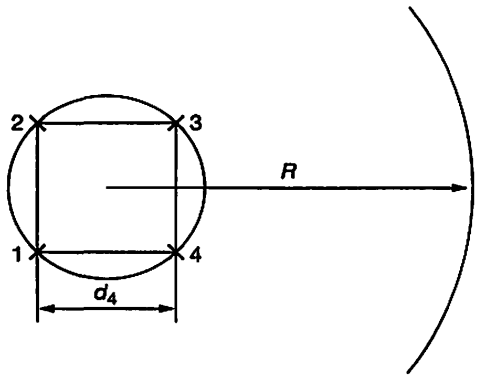

Figure 3.16 Four wells.

$$p_{w1} = p_e - \frac{q\mu}{2\pi kh}\left[\text{Ln}\frac{R}{r_{w1}} + \text{Ln}\frac{R}{d_4} + \text{Ln}\frac{R}{d_4} + \text{Ln}\frac{R}{d_4\sqrt{2}}\right]$$

$$q_1 = q_2 = q_3 = q_4 = \frac{2\pi kh}{\mu}\frac{(p_e - p_w)}{\text{Ln}\left(\dfrac{R^4}{r_w d_4^3\sqrt{2}}\right)} \quad \textit{(SI or Darcy units)} \qquad (3.60)$$

For example with $R = 1\,500$ m, $r_w = 0.1$ m $d_4 = 100$ m

The ratio of productivity with interference and productivity without is: 9.6/17.4 = 0.55

Considering a small group of steady-state production (or injection) wells acting in a circular area of radius R the well flowing pressure of well I may be expressed as:

$$p_{wi} = p_e - \frac{\mu}{2\pi kh}\left[q_i \text{Ln}\left(\frac{R}{r_{wi}}\right) + \sum_j q_j \text{Ln}\left(\frac{R}{r_{i,j}}\right)\right]$$

$r_{i,j}$: well distance between well I and all others.

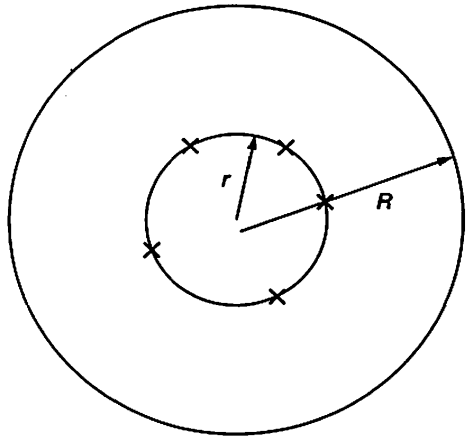

Figure 3.17 n wells on a circle.

If n wells are distributed uniformly over a circular ring of radius r (Fig. 3.17), the productivity of the group of wells becomes: (see Appendix K)

$$Q_n = \frac{2\pi kh}{\mu B} \frac{(p_e - p_w)}{\mathrm{Ln}\left(\frac{R}{r}\right) + \frac{1}{n}\mathrm{Ln}\left(\frac{r}{nr_w}\right)}$$

The maximum rate corresponds to a single well with a radius r.

The individual well productivity from the group compared to the one of an isolated well is

$$\frac{q_n}{q} = \frac{1}{n} \frac{\mathrm{Ln}\left(\frac{R}{r_w}\right)}{\mathrm{Ln}\left(\frac{R}{r}\right) + \frac{1}{n}\mathrm{Ln}\left(\frac{r}{nr_w}\right)} \tag{3.58}$$

The result shows the limitation of adding production wells in the same area since the pressure sink created by one producer have an impact on the productivity of the other wells. The effect can be important for offshore fields in particular where producers are distributed on a circle in which the centre is the production platform.

It must be noted that the phenomenon is automatically taken into account in a reservoir simulation model with sufficient grid cells between wells; but not in material balance software.

3.12 COMBINED BEDS

3.12.1 Linear Beds in Series

Considering several beds of equal cross sections but of different lengths and permeabilities in which the same linear flow rate q occurs (Fig. 3.18). Assuming an incompressible fluid, the pressure drops are additive then:

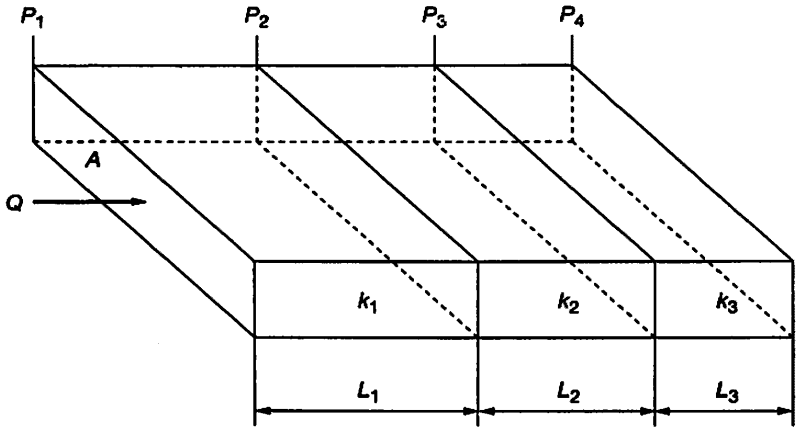

Figure 3.18 Linear Beds in series.

$$(p_1 - p_4) = (p_1 - p_2) + (p_2 - p_3) + (p_3 - p_4)$$

$$\frac{Q\mu \sum L_i}{k_{avg} A} = \frac{Q\mu L_1}{k_1 A} + \frac{Q\mu L_2}{k_2 A} + \frac{Q\mu L_3}{k_3 A}$$

$$\frac{\sum L_i}{k_{avg}} = \frac{L_1}{k_1} + \frac{L_2}{k_2} + \frac{L_3}{k_3}$$

$$k_{avg} = \frac{\sum L_i}{\sum \frac{L_i}{k_i}} \tag{3.59}$$

The average permeability defined above is an equivalent permeability necessary to obtain the same flow rate under the same total pressure drop. This calculation is used to define an average permeability in an upscaling procedure.

3.12.2 Linear Beds in Parallel

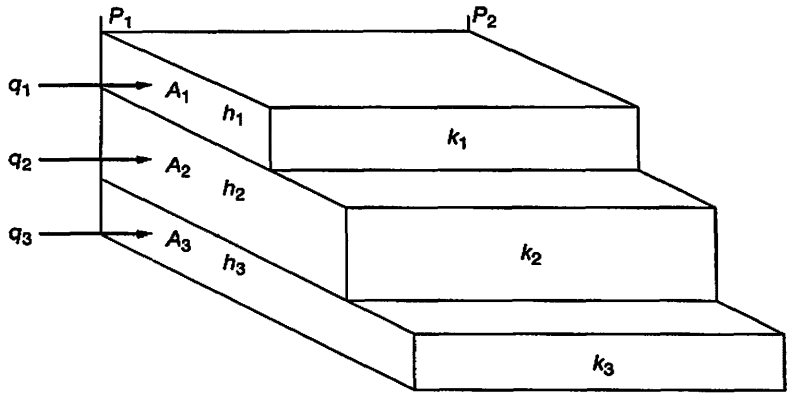

Figure 3.19 Linear Beds in parallel.

The total flow rate q_t (Fig. 3.19) is:

$$q_t = q_1 + q_2 + q_3$$

$$\frac{k_{avg}\sum A_i(p_1 - p_2)}{\mu L} = \frac{k_1 A_1(p_1 - p_2)}{\mu L} + \frac{k_2 A_2(p_1 - p_2)}{\mu L}$$

$$k_{avg}\sum A_i = k_1 A_1 + k_2 A_2 + k_3 A_3$$

with all beds of the same width, so areas are proportional to their thickness.

$$k_{avg} = \frac{\sum k_i h_i}{\sum h_i} \tag{3.60}$$

3.12.3 Radial Flow, parallel beds

$$\frac{2\pi k_{avg}\sum h_i(p_e - p_w)}{\mu B_0 \mathrm{Ln}(r_e / r_w)} = \frac{2\pi k_1 h_1(p_e - p_w)}{\mu B_0 \mathrm{Ln}(r_e / r_w)} + \frac{2\pi k_2 h_2(p_e - p_w)}{\mu B_0 \mathrm{Ln}(r_e / r_w)} + \frac{2\pi k_3 h_3(p_e - p_w)}{\mu B_0 \mathrm{Ln}(r_e / r_w)}$$

$$k_{avg}\sum h_i = k_1 h_1 + k_2 h_2 + k_3 h_3$$

$$k_{avg} = \frac{\sum k_i h_i}{\sum h_i} \tag{3.61}$$

3.12.4 Grid Block Transmissibility

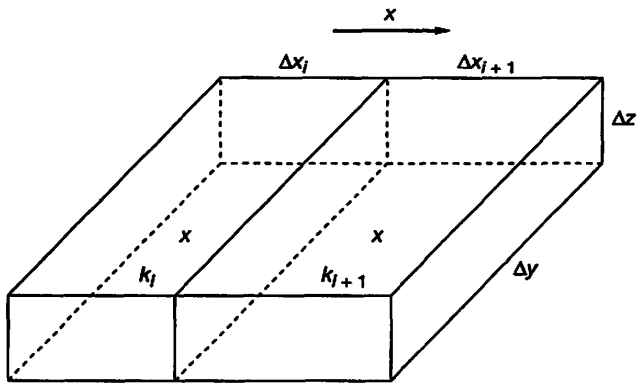

Figure 3.20 Two neighbor grid blocks.

Considering two rectangular grid blocks (Fig. 3.20) having permeabilities k_i, k_{i+1} and constant cross-section $\Delta y \times \Delta z$. By convention the flow occurs from the centre of block i to the centre of block $i + 1$.

Writing Darcy's law for the fluid movement from the centre of block i to the interface and from the interface to block centre $i + 1$ leads to:

$$q = \frac{k}{\mu}\frac{\Delta y \times \Delta z}{\Delta x_i / 2}\Delta p_1 \qquad q = \frac{k}{\mu}\frac{\Delta y \times \Delta z}{\Delta x_{i+1} / 2}\Delta p_2 \qquad \textit{(SI or Darcy units)}$$

Half connections may be defined as:

$$T_i = k_i \frac{\Delta y \times \Delta z}{\Delta x_i / 2} \qquad T_{i+1} = k_i \frac{\Delta y \times \Delta z}{\Delta x_{i+1} / 2}$$

$$\Delta p_1 = q/T_i \qquad \Delta p_2 = q/T_{i+1}$$

$$\Delta p_1 + \Delta p_2 = \Delta p = q\left(\frac{1}{T_i} + \frac{1}{T_{i+1}}\right)$$

The two half connections are combined to define a transmissibility factor between the adjacent block centers as:

$$\frac{1}{T_{i,i+1}} = \frac{1}{T_i} + \frac{1}{T_{i+1}} \quad \text{or} \quad T_{i,i+1} = \frac{T_i \times T_{i+1}}{T_i + T_{i+1}} \tag{3.61}$$

The result is similar to the calculation of an average permeability for beds in series.

This calculation is performed in all reservoir simulators in the block centre transmissibility calculation option.

$$T_i = \text{Cte} \times k_i \frac{\Delta y \times \Delta z}{\Delta x_i / 2}$$

Units	metric	field	lab
	m^3/d	bbl/d	cm^3/hr
$T = \text{Cte} \times k_x \frac{\Delta y \times \Delta z}{\Delta x / 2}$	mD	mD	mD
(half block connection)	m	ft	cm
	Cte = $8.527\ 10^{-3}$	$1.127\ 10^{-3}$	3.6

Units:

$$|T| \text{ or } |W_k| = \frac{cp \times rm^3/d}{\text{bar}} \qquad |T| \text{ or } |W_k| = \frac{cp \times rbbl/d}{\text{psi}} \qquad |T| \text{ or } |W_k| = \frac{cp \times rcm^3/hr}{\text{atm}}$$

For a well connection factor: $W_k = \text{Cte} \dfrac{\theta k_o h}{\text{Ln}\left(\dfrac{r_o}{r_w}\right) + S}$

θ: angle of the segment connecting with the well, in radians = 2π for a Cartesian grid.
k_o: effective permeability.
h: net thickness.
S: skin factor.
r_o: pressure equivalent radius defined by Eq. (3.49).

Remark:
Transmissibility has a dimension of a permeability multiplied by a length: mD . ft or mD . m.

$$q = k \frac{\Delta p}{\mu L} A \quad or \quad |kL| = \frac{q\mu}{\Delta p}$$

The corresponding units for transmissibility are:

Metric units:	*cp . rm^3/d per bar*	*(rm^3/d: reservoir m^3/d)*
Field units:	*cp . rbbl/d per psi*	*(rbbl/d: reservoir bbl/d)*
Lab units:	*cp . rcm^3/hr per atm*	*(rcm^3/hr: reservoir cm^3/hr)*

Permeability has a dimension of an area; therefore the transmissibility has a dimension of a volume.
Ratio of transmissibility expressed in metric units and field units:

$$\textit{Ratio:} \quad \frac{cp \times rm^3/d/\text{bar}}{cp \times rbbl/d/\text{psi}} = \frac{rm^3/\text{bar}}{rbbl/\text{psi}} = 0.1589873 \times 14.503 = 2.3058$$

To convert from mDft to mDm, multiply mDft by 2.3058

3.13 NON-DARCY FLOW

3.13.1 Flow Equation

On the macroscopic scale, flow in a porous media is generally described by Darcy's law, which is valid only for very low velocities. At higher velocities, in addition to the viscous force component represented by Darcy's equation, there is also an inertial force acting to convective accelerations of the fluid particles in passing through the pore spaces. Deviations from Darcy's law, observed at high velocities, can be added in mathematical terms in several ways. The most widely accepted model is the Forchheimer's equation (1901) [2, 63]:

$$-\frac{dp}{dx}=\frac{\mu}{k}u+\beta\rho u^2 \tag{3.62}$$

The first term on the right hand side of Eq. (3.62) is the Darcy or viscous component while the second is the non-Darcy component. In the last term, β is the coefficient of inertial resistance.

Dimensional analysis shows:

$$-\frac{dp}{dx}\left[\frac{ML}{T^2L^2}\right]\left[\frac{1}{L}\right]=[\beta]\rho\left[\frac{M}{L^3}\right]u^2\left[\frac{L^2}{T^2}\right]$$

Therefore

$$[\beta]=\left[L^{-1}\right]$$

Darcy units:

β = turbulence factor, atm-sec^2/gram
p = pressure, atm
x = length, cm
μ = viscosity, cp
ρ = density, g/cc
u = velocity, cm/s
k = permeability, Darcy

The non-Darcy component is negligible at low flow velocities and is generally omitted from liquid equations. For a given pressure drawdown, the velocity of gas is at least an order of magnitude greater than for oil, due to the low viscosity of the former, and the non-Darcy component is therefore often included in equations describing the flow of a real gas through porous medium.

For gases, the equation is best expressed in terms of mass velocity $W/A = \rho u$, because the mass velocity is constant when the cross section is constant.

with W = mass flow rate, g/sec A = Flow area, cm^2

Eq. (3.62) can be written:

$$\rho\frac{-dp}{dx}=\frac{\rho\mu u}{k}+\beta\rho^2u^2=\frac{\mu W}{kA}+\beta\left(\frac{W}{A}\right)^2 \qquad \text{since } \rho=\frac{M_w p}{zRT}$$

$$-\frac{M_w}{zRT}\int_1^2 pdp=\left[\frac{\mu W}{kA}+\beta\left(\frac{W}{A}\right)^2\right]\int_1^2 dx$$

With

M_w = Molecular mass
z = gas compressibility factor
T = absolute temperature

Integrating between points 1 and 2 in the flow path, one obtains:

$$\frac{M_w(P_1^2-P_2^2)}{2zRT\mu L(W/A)}=\frac{W}{A}\frac{\beta}{\mu}+\frac{1}{k} \tag{3.63}$$

Experimental data from core flow can be plotted (Fig. 3.21) as [2]

$$\frac{M_w(P_1^2-P_2^2)}{2zRT\mu L(W/A)} \quad \text{versus} \quad \frac{W}{A}\mu$$

The slope of the curve is the turbulence factor β and the intercept of the line is $1/k$ (Fig. 3.21).

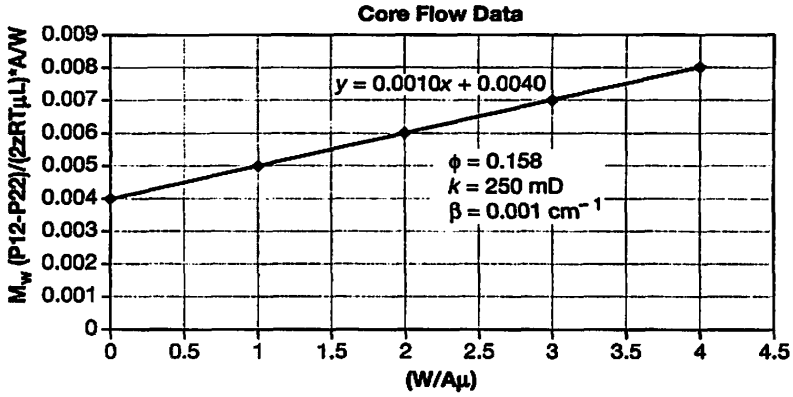

Figure 3.21 Experimental data plot.

Correlations of high-velocity flow in porous media, including the permeability range on which each correlation is based, were built.

A common correlation is presented in the form of:

$$\beta = \frac{b}{k^a} \tag{3.64}$$

Values of a and b depend on the formation properties.

Janicek and Katz [2, 89] presented a correlation of turbulence factors with permeability and porosity.

$$\beta = \frac{b}{k^a \phi^c}$$

Katz and Cornell [63] proposed the simple relationship of β to k for sandstones, limestones and dolomites:

$$\beta = \frac{13.25 \times 10^{10}}{k^{4/3}} \tag{3.65}$$

β: turbulence factor, m^{-1}

The estimate of the Inertial-Turbulent flow factor D (within the subject of gas well testing theory) is:

$$D = \frac{2.216 \times 10^{-16} \beta k M_w P_{st}}{h \mu r_w T_{st}} \tag{3.66}$$

D: IT flow factor, $(m^3/d)^{-1}$
β: turbulence factor, m^{-1}
k: reservoir permeability, mD
M_w: gas molecular mass, g/mol
P_{st}, T_{st}: standard conditions pressure and temperature (101.325 kPa, 288.15 K)
h: net pay thickness, m
μ: gas viscosity, μPa.s
r_w: wellbore radius, m

Eq. (3.62) can be rewritten as:

$$-\frac{dp}{dx} = (1 + F_0)\frac{\mu}{k} u$$

where F_0 is the Forchheimer number, which is similar to the

Reynolds number

$$F_0 = \frac{\beta \rho k u}{\mu} \tag{3.67}$$

At low flow rates, (e.g., $F_0 < 0.01$), the pressure drop is linearly proportional to the flow rate. At high flow rates (e.g., $F_0 > 0.1$), the pressure drop exceeds the one predicted by Darcy's law.

The Reynolds number is given by Eq. (3.68) [2]

$$R_e = \frac{\beta k \rho u}{6.33 \times 10^{10} \mu} \tag{3.68}$$

k = permeability, mD
μ = fluid viscosity, cp

To compare flow data for porous media with velocities into the turbulent regime, they may be plotted as friction factor versus Reynolds number.

The friction factor is defined by:

$$f = \frac{64 g_c \rho (P_1 - P_2) A^2}{\beta L W} \tag{3.69}$$

f = friction factor, dimensionless
g_c = 32.17 conversion factor, lb mass-ft/(lb force) (sec^2)
ρ = fluid density, lb mass/cu. ft
P = pressure, lb force/sqft
A = area of flow, sqft
β = turbulence factor, ft^{-1}
L = length of flow, ft
W = mass flow rate, lb mass/sec

Eq. (3.63) can be solved for ΔP^2:

$$P_1^2 - P_2^2 = \frac{2zRTL\mu}{M_w A k} W + \frac{2zRTL}{M_w A^2} \beta W^2 \tag{3.70}$$

or

$$P_1^2 - P_2^2 = AQ_m + BQ_m^2 \tag{3.71}$$

Q_m: mass gas rate in the reservoir along a constant section

$P_1^2 - P_2^2 = (\Delta P^2)$: ~ loss of head in the reservoir between locations 1 and 2.

3.13.2 Gas Well Flow Rate Expressions

Eq. (3.62) represents both laminar and inertial-turbulent (IT) flow effects. It is referred as the generalized Laminar-Inertial-Turbulent (LIT) momentum balance equation for steady-state flow.

3.13.2.1 Empirical Deliverability Equation

From a large number of observations, the deliverability of a gas well is expressed in the form:

$$Q_g = C\left(P_R^2 - P_{wf}^2\right)^n = C\left(\Delta P^2\right)^n \tag{3.72}$$

Q_g = gas flow rate at std conditions m^3/d or Mscf/d (10^3 scf/d)
C = coefficient which describes the position of the stabilized deliverability line
P_R = average reservoir shut in pressure bars or psia
P_{wf} = bottom hole flowing pressure bars or psia
n = exponent which characterizes the flow turbulence.

P_{wf} is the stabilized sand face pressure resulting from the surface constant flow rate Q_g. If the pressure is not stabilized, C decreases with time but eventually becomes constant at stabilization.

Remarks:
for n = 1, the flow is laminar
for n = 0.5, the flow is fully turbulent in the formation
n is kept to vary between 0.5 to 1

From Eq. (3.72) one can write:

$$\log(Q_g) = \log(C) + n \log(\Delta P^2) \tag{3.73}$$

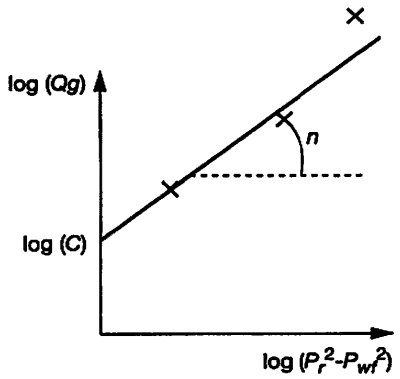

Figure 3.22 Three gas flow rates.

Plotting $\log(Q_g)$ versus $\log(\Delta P^2)$ (Fig. 3.22) for at least three different rates, allows to determine $\log(C)$ and n. n is the slope of the curve.

C and n depend on gas properties, such as viscosity, temperature, compressibility and reservoir properties such as permeability, net pay thickness, well bore radius and damage.

3.13.2.2 Quadratic Deliverability Equation [84]

The equation is derived from Eq. (3.71) expressed in volume rates instead of mass rate.

$$P_R^2 - P_{wf}^2 = AQ_g + BQ_g^2 \tag{3.74}$$

AQ_g = pressure-squared drop due to laminar flow and well bore effects
BQ_g^2 = pressure-squared drop due to inertial-turbulent flow effects

The derivation of equation Eq. (3.74) assumes ideal conditions for the well and reservoir. Sometimes anomalous results may be explained in terms of deviations from the idealized situations.

Assumptions are summarized below:

- Isothermal conditions through the reservoir
- Gravitational effects negligible
- Single fluid flow
- Homogenous and isotropic medium, constant porosity
- Permeability independent of pressure
- Constant fluid viscosity and compressibility factor
- Small pressure gradient
- Radial-cylindrical flow model applicable

Eq. (3.74) can be written:

$$\frac{P_R^2 - P_{wf}^2}{Q_g} = A + BQ_g \tag{3.75}$$

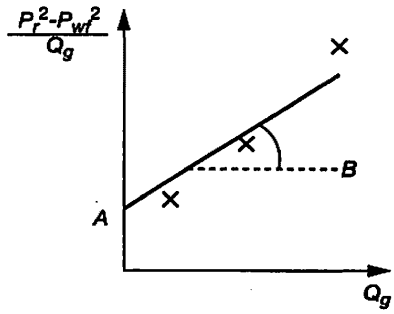

Figure 3.23 Three gas flow rates.

The plot Figure 3.23 $(P_R^2 - P_{wf}^2)/Q_g$ versus Q_g is a straight line.

Intersect with vertical axis is A, and the slope defines B.

With at least three different stabilized rates, the well deliverability equation can be deducted. The validity of the equation is based on many constraints, so that in practice a negative B value may be obtained. In such a case, the method can't be used; a negative B value has no physical meaning.

3.14 SUPERPOSITION PRINCIPLE

The solution of complex differential equations can be broken down into relatively simple solutions if the physical phenomenon is linear and the boundary conditions independent of time.

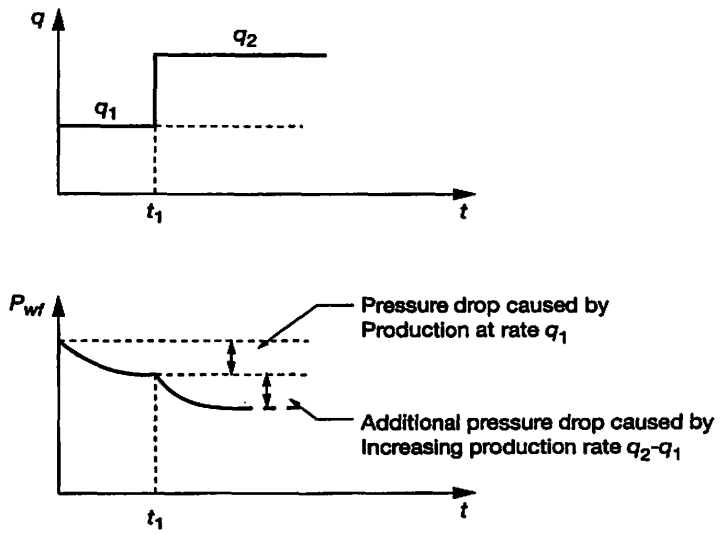

Figure 3.24 Superposition Principle.

he example depicted in Figure 3.24, at time 0 a constant rate q_1 is imposed at the well. ll pressure change is governed by the solution of the diffusivity equation. At time t_1, q_1) increment rate change is imposed. This rate increment creates a new pressure disturbance at the well. The pressure behavior from t_1 onward can be calculated by adding the pressure change due to q_1 and the pressure change generated by the rate increment $(q_2 - q_1)$. In other words we continue the pre t_1 solution forward in time past t_1 and add to it (or superpose) the solution generated by the rate increment.

The principle is also available if a pressure change is imposed at the well instead of a rate change.

CHAPTER 4

Multiphase Flow in Reservoirs

4.1 INTRODUCTION

Let's consider a cross section of a reservoir shown below with an initial gas cap and an aquifer (Fig. 4.1).

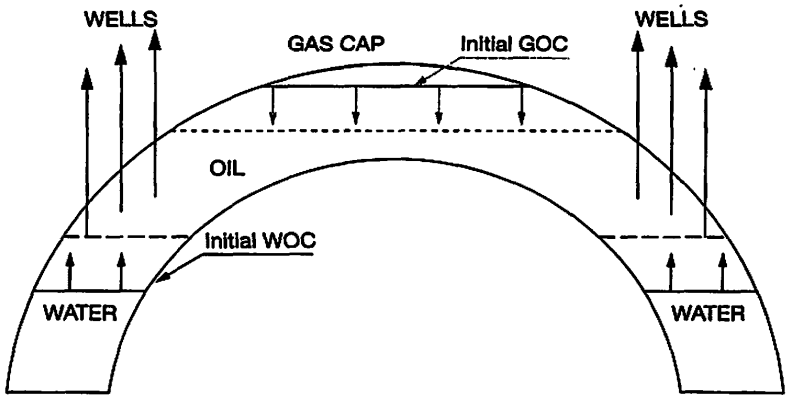

Figure 4.1 Reservoir Cross-section.

The depletion occurring in the oil zone due to oil production affects the initial equilibrium in the reservoir. The consequences are:

- The expansion of the initial gas cap
- The rise of the initial Water Oil Contact.

Therefore at the top of the reservoir, oil and gas move simultaneously. Similarly at the initial water oil contact, a movement of oil and water takes place.

In the case of a gas reservoir associated with an aquifer, gas and water move simultaneously around the initial gas water contact.

This is a description of the diphasic flow (oil, water), or (gas, oil), or (gas, water).

Oil, water and gas phases mobile simultaneously occur in particular configuration like during a WAG (Water Alternate Gas) process. This is the triphasic flow case.

4.2 MULTIPHASE FLOW AT PORE SCALE

Two Phase System:

When a wetting and a non wetting phase flow together in a porous rock, each phase follows separate and distinct paths. At any saturation of the two phases, a certain number of pores are available for passage of the wetting phase while the remainder is able to pass only the non wetting phase. Pores passing the non wetting phase also contain some wetting phase (usually the connate water). The changing effect of saturation of one fluid is to open more pores to flow of the phase whose saturation is increased and, conversely to decrease the number of pores available for passage of the second phase. When two fluids flow simultaneously, they interfere. The consequence is the decrease of the sum of the two effective permeabilities to a value less than the absolute permeability. In other words, the sum of the two relative permeabilities is always less than unity.

The ease with which a phase can flow depends on:

- The size of the pore throats
- The number of pores which are occupied by the phase
- The probability that these pores are hydraulically interconnected.

The first two factors depend on the pore throat size distribution and the wetting ability of the phase with respect to the rock surface. The last factor is governed by the extent to which the phase saturates the porous media. There are two limits. The one occurs when the non wetting phase saturation is so high that the wetting phase is reduced to an irreducible saturation. At this point, the probability of finding interconnected pores able to pass the wetting phase is negligible. Thus the hydraulic conductivity is lost and the relative permeability to the phase becomes zero. The second limit is analogous to the first and occurs when the non wetting phase saturation is so small that relatively few pores will be interconnected becomes negligible, no flow of the non wetting fluid can occur and the relative permeability to the phase is zero. In the case of the gas oil system, the non wetting fluid gas is at *critical gas saturation* (S_{gc}).

Three Phase Flow:

Behavior when three phases are present is similar to the two phase system behavior. In a case of a water wet rock with three phases (oil, water and gas) present during a drainage process, the fluid distribution is the following:

- *Water*: fills completely the smallest pores, wets all grains and is present as pendular rings at grain contacts and other interstices in pores able to pass only oil or gas.
- *Oil*: uses the available space in a range of pore sizes of which the smallest just exceeds the maximum size completely filled with water.
- *Gas*: like oil, it occupies the available space in a range of pore sizes. The range encompassed lies between the maximum size completely filled with oil and the largest pores present in the media.

Gas, like water, is restricted to a particular range of pore sizes and its flow is not influenced by the nature of the other fluids that fill the other pores. The number of pores filled with oil depends upon the particular size distribution of the pores in which the three phases coexist and upon the oil saturation.

4.3 MULTIPHASE FLOW AT MACROSCOPIC SCALE (CORE, BLOCK)

All the theories concerning porous media phenomenon, lead to macroscopic laws that are applicable to large dimension blocks. So reasoning on porous media is similar to reasoning on continuous media characterized by local parameters which individual value is defined at any point in space.

Immiscible Fluid Equilibrium:

An average saturation of fluid 1 in a block is defined as the ratio of the pore volume occupied by the fluid to the total pore volume.

Very often the concept of average saturation is used for cores or simulation blocks although it is known that a saturation profile is present. This concept is also used in the up scaling process when the reservoir engineer converts a geological model into a reservoir simulation model.

Assuming a reservoir fluid system at equilibrium in the gravity field, hydrostatic laws apply to determine the pressure of each fluid which depends on height. This is why a pressure data alone is meaningless if it is not associated with the corresponding depth.

Pressure in each phase is then determined as:

$p_o = p_{0ref} + (\rho_o \times g \times \Delta h)$	P_o: pressure in oil	ρ_o: oil density
$p_g = p_{gref} + (\rho_g \times g \times \Delta h)$	P_g: pressure in gas	ρ_g: gas density
$p_w = p_{wref} + (\rho_w \times g \times \Delta h)$	P_w: pressure in water	ρ_w: water density

The capillary pressure is defined as the difference between pressures in the two fluids at the same height.

$$P_{cog} = P_g - P_o \qquad P_{cow} = P_o - P_w$$

P_{cog}: capillary pressure between oil and gas
P_{cow}: capillary pressure between oil and water

4.4 DARCY'S LAW APPLIED TO MULTIPHASE FLOW

The permeability of two or three phases flowing through a porous sample can be computed from laboratory experimental data by assuming that Darcy's law applies to each phase. The permeability of the phase varies with its saturation. The computed permeability is called effective permeability of that phase at such saturation.

$$u_o = -\frac{k_o \rho_o}{\mu_o}\frac{\delta \Phi_o}{\delta x} \qquad u_w = -\frac{k_w \rho_w}{\mu_w}\frac{\delta \Phi_w}{\delta x} \qquad u_g = -\frac{k_g \rho_g}{\mu_g}\frac{\delta \Phi_g}{\delta x} \tag{4.1}$$

u_o, u_w, u_g: Darcy (superficial) velocity of oil, water, gas
k_o, k_w, k_g: effective permeabilities of oil, water, gas
Φ_o, Φ_w, Φ_g: potentials of oil, water, gas

Φ_o is defined for the oil phase: $\Phi_o = \int_{p_{od}}^{p_o} \frac{dp_o}{\rho_o} + g(Z - Z_d)$

ρ_o: oil density
p_{od}: oil phase pressure at reference datum
Z: elevation above horizontal datum
Z_d: elevation of the reference datum (*usually the Mean Sea Level*)
g: acceleration

If we assume ρ_o constant over the interval of interest, the oil potential becomes:

$$\Phi_o = p_o + \rho_o g \times \Delta h$$

Eqs. (4.1) become in the x direction:

$$u_o = -\frac{k_o}{\mu_o}\frac{\delta p_o}{\delta x} \qquad u_w = -\frac{k_w}{\mu_w}\frac{\delta p_w}{\delta x} \qquad u_g = -\frac{k_g}{\mu_g}\frac{\delta p_g}{\delta x} \tag{4.2}$$

Darcy's Law for a linear horizontal sample (one dimension)

$$q_o = \frac{k_o}{\mu_o L} A(P_{o1} - P_{o2})$$

q_o: oil rate; μ_o: oil viscosity; P_o: oil pressure

$$q_g = \frac{k_g}{\mu_g L} A(P_{g1} - P_{g2})$$

q_g: gas rate; μ_g: gas viscosity; P_g: gas pressure

$$q_w = \frac{k_w}{\mu_w L} A(P_{w1} - P_{w2})$$

q_w: water rate; μ_g: water viscosity; P_w: water pressure

A: sample section area
L: sample length

k_o, k_g, k_w are effective permeabilities of oil, gas and water function of saturations varying from zero to a maximum when the other phase or phases are at their residual saturations.

Phase pressures are related through capillary pressures. *(oil pressure = main pressure)*

$$P_g = P_o + P_{cog}$$
$$P_w = P_o - P_{cow}$$

P_{cog}: capillary pressure oil, gas
P_{cow}: capillary pressure oil, water

4.5 RELATIVE PERMEABILITY [1, 9, 15, 81]

The relative permeability of a phase is defined as the ratio of the effective permeability to the absolute permeability.

Remark: the absolute permeability is an intrinsic property of the rock, independent of the filling fluid.

$$k_{ro} = \frac{k_o}{k} \qquad k_{rw} = \frac{k_w}{k} \qquad k_{rg} = \frac{k_g}{k} \tag{4.3}$$

k_{ro}, k_{rw}, k_{rg}: relative permeability of oil, water and gas respectively
k: absolute rock permeability

Relative permeability is a concept without any scientific background; it is based on observation and laboratory experiments, used to describe multiphase flow regimes.

Oil-water System

Relative permeability is an empirical method of correlating multiphase flow in porous media with the saturation of the phases and the path followed in reaching a particular saturation.

Label 1 of Figure 4.2, represents 100% water saturation formation before the oil migration took place. The curve from label 1 to 2 is the path followed (drainage) when oil saturation increases until the wetting phase is minimum ($S_{wc} = 0.2$) where $k_{rw} = 0$. Curve 2 to 3 is the path of an imbibition process when the wetting phase (water) increases until the maximum value $S_w = (1 - S_{orw})$

The oil permeability curve varies between $S_w = S_{wc}$ where k_{ro} is maximum to $S_w = (1 - S_{orw})$.

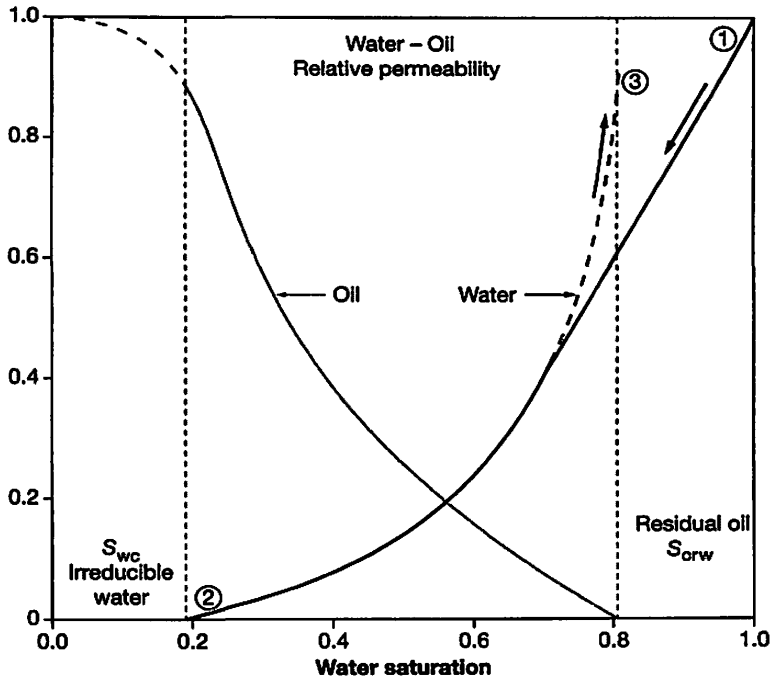

Figure 4.2 Oil Water-Relative Permeability versus Water Saturation.

Gas-oil System

Gas-oil Relative Permeabilities:

Two plots are commonly used:

- k_{rg}, k_{ro} versus S_g
- or k_{rg}, k_{ro} versus S_L (liquid saturation: oil + water).

A minimum gas saturation is necessary for the gas to be mobile. This is defined as the critical gas saturation S_{gc} (Fig. 4.3) when the gas bubbles form a continuous phase. Generally the S_{gc} value is not known; 5% is a first approach commonly admitted.

The maximum gas saturation possible in the rock must leave room for the connate water saturation and the residual oil existing after gas flood.

Thus $S_{gmax} = 1 - S_{wc} - S_{org}$.

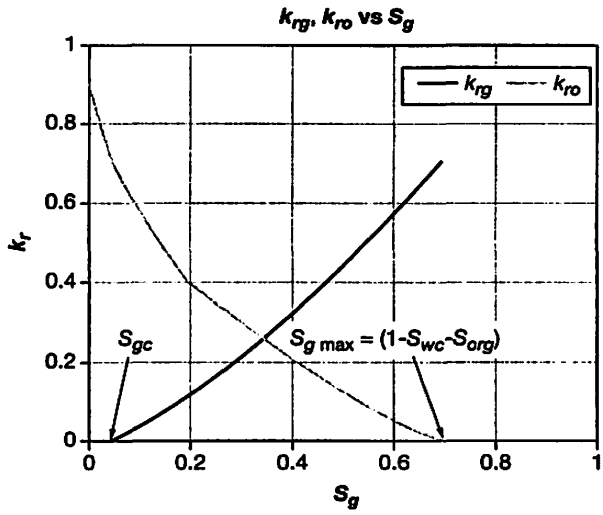

Figure 4.3 Plot k_{rg}, k_{ro} versus S_g Gas oil relative permeability.

4.5.1 Factors Influencing Relative Permeabilities

Wettability:

Wettability is the most important factor influencing relative permeability curves. It is also difficult to reproduce in the laboratory the reservoir condition wettability. In a strong water wet rock, the irreducible water saturation may be as high as 45% and the k_{rwmax} quite low.

Water flow through the porous media is difficult due to the high rock affinity for the water.

Oil relative permeability decreases quickly as water saturation increases.

An oil wet rock may exhibit a very low irreducible water saturation (as low as 5%) associated with a high k_{rwmax}. The rock does not retain the water in the porous media.

Inter Facial Tension (IFT):

Water oil, or water gas, or oil gas displacements occur with IFT in the range of 10 to 40 dynes/cm. Changes of IFT over this interval have little effect on relative permeability. One of the enhance oil recovery processes consists of 'killing' the interfacial tension to very low values; the net effect is an increase of relative permeability of each phase.

As miscibility nears, the physical properties of the two phases converge to critical conditions. As a result there is no more interfacial tension, no capillary pressure and the total hydrocarbon is displaced.

Heterogeneity of Core:

Laboratory measured water oil imbibition relative permeability data are carried out on selected core samples. Cores are visually selected and submitted to a linear X ray survey in order to avoid fractures or heterogeneity that would disturb the displacement. Sandstone rocks in many depositional environments show significant small-scale laminations. Micro fractures may provoke a displacement process with bypassing. All these anomalies affect the measured relative permeabilities.

4.5.2 Oil Water Capillary Pressure

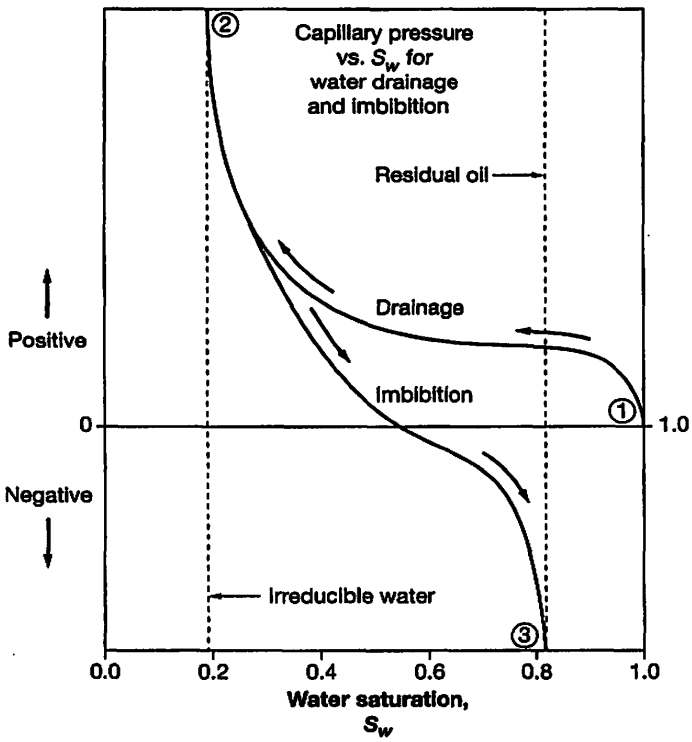

Figure 4.4 Capillary pressure versus saturation in a water wet rock.

A water wet rock capillary pressure is depicted on Figure 4.4. End point label 1 represents the 100% water saturation at initial reservoir status, before the oil migration had taken place. The drainage curve (S_w decreasing from 1) represents the path followed when oil migrates into the reservoir. Therefore, drainage capillary pressure data are used to estimate connate water saturation (S_{wc} or S_{wirr}) at end point label 2, the initial oil saturation. The irreducible

water saturation is the water volume that allows electricity to flow when a resistivity or induction logging device is used to survey the formation. According to the water salinity and the formation porosity, the value of S_{wc} is deducted by the Archie's formula.

The vertical axis can be scaled in height above the free water level or in pressure which is:

$$P_{cow} = \Delta\rho \times g \times h \tag{4.4}$$

$\Delta\rho$: density difference between water and oil ($\rho_w - \rho_o$)
g: acceleration
h: height above free water level
units: SI P_w: Pa ρ: kg/m^3 h: m

Remarks:
Tight carbonate reservoirs may not exhibit final constant connate water saturation as above, but a continuous water saturation decreasing upwards. The reservoir may exhibit a transition zone over the whole thickness. Then the calculated water saturation from log analysis decreases continuously upwards.
Some reservoirs may exhibit connate water saturation plus a certain amount of mobile water. This may be explained by the fact that the hydrocarbon migration process has not been complete and was interrupted by tectonic movement which isolated the reservoir trap from its "kitchen". The production test in such conditions will give oil plus water even if it had been interpreted as an oil bearing zone.

The second curve between labels 2 and 3 (Fig. 4.4) is the imbibition curve. The water saturation increases and displaces the oil. This process is observed in the field when the oil water contact is moving upwards into the initial oil bearing zone (active bottom aquifer) or in the case of an active edge aquifer. The curve crosses the horizontal axis at water saturation much less than 1. Between the point labeled 2 and that point, the imbibition curve is defined as natural or spontaneous imbibition process. The curve is continued to negative capillary pressures to represent the saturation change of the reservoir when it is submitted to a "forced" water flood. This process is occurring at the laboratory when a water flood is carried out on a core. It is then observed that continuous water injection generates oil production even after several injected pore volumes. The asymptote represents the trapped oil or the residual oil saturation after water flood (S_{orw}). In the field, a water injection scheme is the application. The graph shows that the water saturation can be increased to about 80% by increasing the water-phase pressure and simultaneously displacing oil from the pore space.

In summary, capillary pressure curves are a measure of fluid distribution, saturations, wettability, and connectedness in a porous rock. They represent also an experimental correlation of the pressure difference between two phases at equilibrium in the rock.

4.5.3 Normalized Saturations (or Reduced)

Relative permeability data are usually obtained from laboratory investigations on suitable cores. However, this source may be lacking and some suitable approximations must be derived.

Stone defines normalized saturations as:

$$S_o^* = \frac{S_o - S_{om}}{1 - S_{wc} - S_{om}} \text{ with } S_o \geq S_{om} \qquad S_w^* = \frac{S_w - S_{wc}}{1 - S_{wc} - S_{om}} \quad S_w \geq S_{wc}$$

$$S_g^* = \frac{S_g}{1 - S_{wc} - S_{om}} \tag{4.5}$$

S_{om}: minimum oil saturation

4.5.4 Corey Relative Permeability functions [90, 91]

For homogenous media, Corey proposed relative permeability as follows:

$$k_{rw}(S_w) = k_{rw\max} \times \left[\frac{S_w - S_{wc}}{1 - S_{wc} - S_{orw}}\right]^{n_w} \tag{4.6}$$

$$k_{ro}(S_w) = k_{ro\max} \times \left[\frac{1 - S_w - S_{orw}}{1 - S_{wc} - S_{orw}}\right]^{n_o} \tag{4.7}$$

k_{rwmax} and k_{romax}: end point water, oil relative permeabilities
S_{wc}: connate water saturation
S_{orw}: residual oil saturation behind the water front
n_w and n_o: Corey exponent for water and oil

For a water wet system:

S_{orw} may be 30% or higher Corey exponent n_o = 2 to 3 n_w = 4 to 6 k_{romax} = 0.6 to 0.8.

For an intermediate wet case

k_{rwmax} = 0.1 to 0.4 n_w = 4 to 6

The most extensive published data is that of Braun and Holland [94].

4.5.5 History-dependent Saturation Functions [92, 93, 94]

The relative permeability of a phase usually depends on the path that was followed to reach the saturation. This is termed hysteresis.

Relative permeability hysteresis has been considered of significance only between the primary drainage and the imbibition curves. Many experiments have been carried out of these processes. Hysteresis between secondary drainage and imbibition curves has also been recognized by several authors, but there are few published data on relative permeability scanning curves. The most extensive published data is that of Braun and Holland [94]. They found that the relative permeability scanning curves to be reversible. The saturation intervals of the scanning loops are so small, however, that hysteresis, if present, would experimentally be difficult to detect.

Water oil relative permeabilities in a mixed wet system show similar hysteretic behavior. The oil relative permeability in an oil wet system exhibits negligible hysteresis, as does water relative permeability in water wet system.

The impact of such behavior is well known in the underground gas storing operations. The injected gas volume is perfectly known but the recovered gas volume is definitively less due to high pressure trapped gas saturation.

Different authors studied hysteresis and proposed algorithms to predict the capillary pressure and relative permeability to use following a saturation history.

4.5.6 Three Phase Relative Permeabilities [95, 96, 97]

Leverett, in 1941[95] reported results of steady-state flow through unconsolidated sand of oil, water and gas. From this work, the basic concepts of three-phase flow were established.

It was found that the relative permeability to the wetting phase was a function only of the wetting phase saturation. Usually water, the wetting phase occupies the smaller pores. At any wetting-phase saturation, the same portion of the pores is occupied by the wetting phase, irrespective of the two other phases.

When gas is in the pore system, it is the fluid which is least likely to wet the rock; therefore the relative permeability is dependent upon the total liquid saturation. Some authors indicate that the relative permeability to gas is only function of gas saturation.

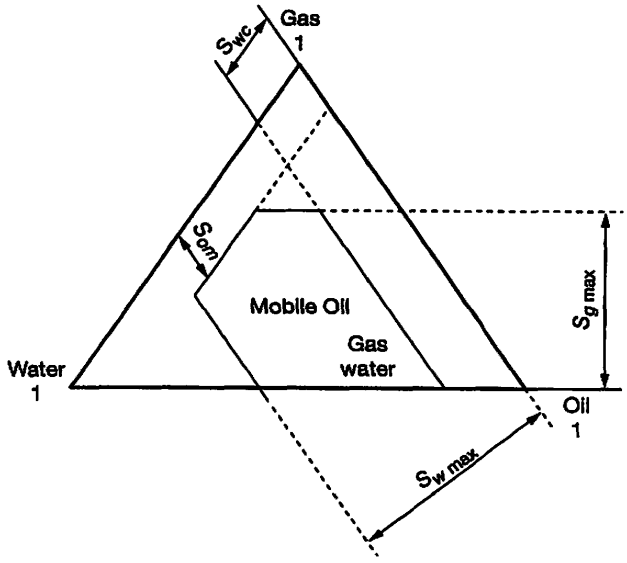

Figure 4.5 Mobile oil Saturation Interval.

Figure 4.5 shows the saturation domain where the three phases are mobile simultaneously.

Three-phase relative permeability data is rarely available thus approximations must be used. Industry practice is to assume the relative permeabilities of water and gas are the same as two-phase relative permeabilities. Only oil relative permeability is treated as a function of both water and gas saturations.

$$k_{rw} = f(S_w) \qquad k_{rg} = f(S_g) \qquad k_{ro} = f(S_w, S_g) \tag{4.8}$$

The k_{ro} is rarely known. It can be deducted from interpretation of time consuming laboratory measurements.

Stone (1973) [98, 99, 100] established a formulation to predict k_{ro} with two models.

First Stone's Model:

$$k_{ro} = S_o^* \beta_w \beta_g \tag{4.9}$$

β_w and β_g are determined from the condition that Equation (4.9) reduces to two phase-system at limit points.

$$S_g = S_g^* = 0 \text{ and } S_w = S_{wc}$$

Therefore:

$$\beta_w = \frac{k_{row}(S_w)}{1 - S_w^*} \qquad \text{and} \qquad \beta_g = \frac{k_{rog}(S_g)}{1 - S_g^*}$$

S_o^*, S_w^*, S_g^* defined by Eq. (4.5)

Second Stone's model:

The equation is a combination of two-phase relative permeabilities derived from channel flow considerations:

$$k_{ro} = \left(k_{row} + k_{rw}\right)\left(k_{rog} + k_{rg}\right) - \left(k_{rw} + k_{rg}\right) \tag{4.10}$$

k_{ro} must be ≥ 0; negative k_{ro} implies immobile oil

It is noted that both models reduce to two-phase system if the relative permeabilities at end points are equal to 1.

$$k_{row}(S_{wc}) = k_{rog}(S_g = 0) = 1$$

The model is valid when gas oil relative permeabilities are measured in the presence of irreducible water.

For reservoir calculations, the models need modifications for consistency with the definition of relative permeabilities.

Other models were proposed by different authors and compared [101].

4.6 POTENTIAL

The velocity vector of a fluid element is normal to the equipotential surfaces and the magnitudes of these vectors are proportional to the gradients of the potentials. The distribution of potential within a fluid determines the macroscopic velocity of the fluid and also the overall flow.

An opened production well creates within the reservoir pressure gradients in all directions (vertical and horizontal). To describe fluid movement within the reservoir, it is necessary to refer all element fluid pressures to a common datum. This concept is the fluid potential defined as:

$$\Phi_f = P_f + (\rho_f \times g \times \Delta z) \tag{4.11}$$

Φ_f: potential of (oil, gas, water)
P_f: local fluid pressure
ρ_f: fluid density
Δz: height difference between the reported point and the reservoir datum
g: acceleration

For reservoir engineering calculations, the three fluid pressures are never carried through the study. Only one pressure is used: pressure in the oil. If no oil is present then gas pressure is used. The other fluid pressures are deducted from the capillary pressure relationships. This methodology is used in all reservoir simulators.

4.7 FRACTURED RESERVOIRS

Fractured reservoirs are often associated with carbonate lithologies.

A fractured reservoir is made of fractures and matrix. The fractures may be characterized as micro fractures in which case they represent a sort of macro heterogeneities, and then the reservoir can be studied as a single porosity system. Other cases are described as a two porosity system (Fig. 4.6):

- Matrix which stores most of the hydrocarbon.
- Fracture network with a low fluid volume capacity.

Usually the matrix has a poor porosity and permeability, whereas fractures represent a low porosity associated with high permeabilities. The first basic descriptions of the reservoir behavior were reported by Warren and Root [102], also by Mattax and Kyte [103]. Other studies were carried out from laboratory experiments [104, 105].

Two media mean two porosities, two permeabilities and two sets of relative permeabilities.

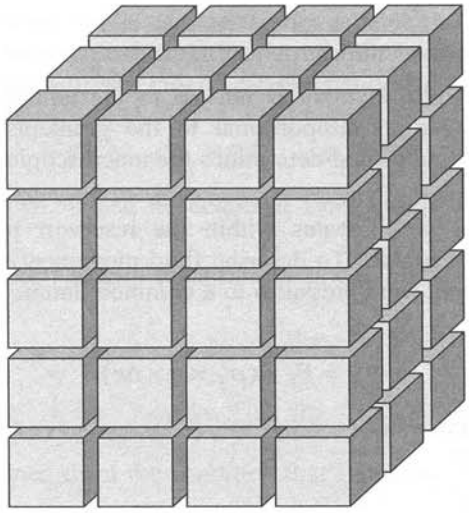

Figure 4.6 Representation of a fractured reservoir.

4.7.1 Counter-Current Flow

The multiphase flow concept up to now assumed that both fluids flow in the same direction (co-current flow).

Counter-current flow is different from co-current in that fluids flow in opposite directions. This may occur in many reservoir processes, such as primary and secondary hydrocarbon migration, gas storage in an aquifer, steam assisted gravity drainage (SAGD) and some secondary and tertiary recovery processes. Counter-current flow driven by spontaneous imbibition has been of interest in fractured reservoirs during water flooding. Several investigators studied this subject [104, 105].

Counter-current flow is associated with gravity drainage recovery process, in which gravity is the dominating driving force. The recovery is effective under favorable conditions: high vertical permeability, a favorable oil relative permeability, high vertical continuity, a large density difference, low oil viscosity, and long oil drainage times after the region has been invaded. Such conditions are present particularly in a fractured system where gravity segregation occurs.

4.7.2 Gas Diffusion Through Oil Saturated Matrix

An oil saturated block surrounded by gas filled fractures creates an unbalanced system.

Large component concentration contrasts exist between the two phases. Therefore a process consisting of exchanging compositions between the two phases occurs that is called gas diffusion. The physical phenomenon has been described by the diffusion Fick's laws.

4.7.3 Convection in Matrix Blocks

Gas diffusion through the matrix modifies locally the hydrocarbon density. If in addition a temperature gradient exists between top and bottom (large reservoir thickness), then conditions are met to create a convection fluid movement through the block.

4.8 LABORATORY MEASUREMENTS

Two main families of experiments are performed:

- Experiments run under laboratory conditions.
- Experiments run under reservoir conditions.

To be representative of the reservoir flow, core plugs must be selected with care following the dip angle and avoiding heterogeneities.

4.8.1 Relative Permeabilities at Laboratory Conditions

Cores are cut, cleaned, dried and resaturated with water and refined oil. The key issue in the process is to restore the initial wettability. Wettability has a large impact on the relative permeability curves.

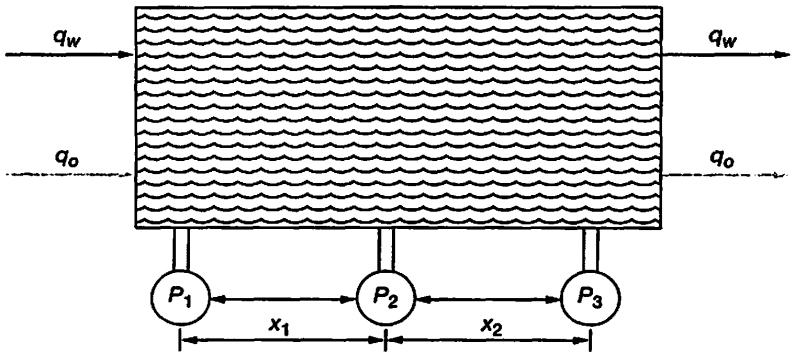

Figure 4.7

Steady State Technique:

The use of the technique, allows one to calculate relative permeability of water, oil and gas directly using Darcy's law. The process consists in injecting two different fluids at one end at different ratios and measure fluid volumes produced at the other end (Fig. 4.7). Average fluid saturation is calculated from the rate ratios.

The steady-state regime implies constant input and output rates and stabilized pressure gradient across the core. Low permeability cores may not allow reaching steady-state regime within a "reasonable" time delay. Therefore unsteady-state flow regime is used.

One must make sure that results are not influenced by the "saturation end effect".

Unsteady-state Technique:

The core preparation is the same as previously but the measurements necessitate an interpretation with software to deduct the relative permeabilities [15, 106].

4.8.2 Experiments at Reservoir Conditions

This is the state of the art when it comes to relative permeability measurements. The measurement is generally made on composite cores. Composite cores are made of several core plugs butted end to end. The total length of the composite core may be about 0.6 up to 3 meter long. Reservoir conditions are reproduced (temperature) in a high pressure cylinder concentric to the core holder.

Complex apparatus and operations are required to perform the survey which implies time consuming then high cost. Such experiments are carried out with field reservoir fluids or laboratory recombined fluids.

A two or three phase flow may be performed in reservoir conditions.

Water flood experiment, is carried out with the core is the horizontal position. A gas flood experiment is carried out with the core in the vertical position and gas injection head at the top. The recorded experimental data (pressures, flow rates) are used for tuning a simulation model of the flood. The objective is to create the appropriate relative permeabilitiy curves to match the core flood performance.

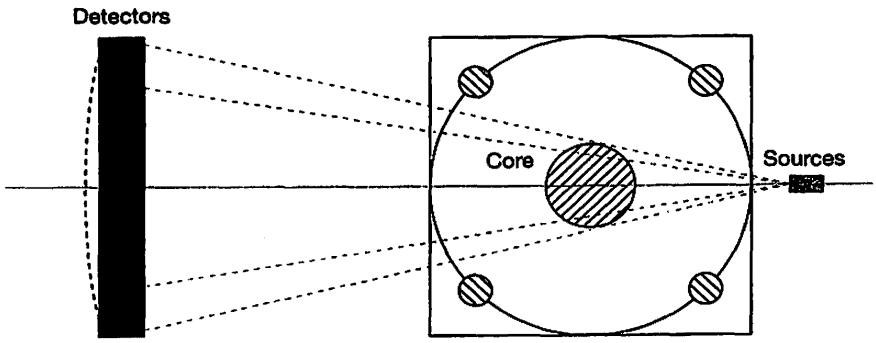

Figure 4.8 X-ray rig for saturation monitoring.

Additional data may be collected for fine simulation tuning with an in-situ saturation monitoring apparatus. The principle consists of submitting the flooded core to X-ray survey at different steps during the flood. The interpretation of the survey gives the saturation profile in the core at different times of the experiment.

WAG (Water Alternate Gas) experiment can be carried out at reservoir conditions to generate an experimental three-phase relative permeability curves. In that case the three phases are simultaneously present in the core therefore additional data is necessary to distinguish oil phase and gas phase. This is given by a two energy level X-ray that influence differently the detectors according to the fluid density encountered and the energy level of the emitted-ray (Fig. 4.8).

4.9 FRONTAL DISPLACEMENT THEORY, BUCKLEY-LEVERETT EQUATION

Immiscible Fluid Displacement:

The objective is to calculate the oil recovery resulting from displacement by an immiscible fluid like water. Several basic assumptions are necessary, then mathematical development conduct to the Buckley-Leverett displacement theory.

It must be said that before the use of sophisticated computing facilities, the application of this theory was the only way for the reservoir engineer to predict saturation, water breakthrough time and water cut evolution versus time.

Assumptions:

Displacement occurs through a horizontal core where gravity effects are ignored.

Displacement occurs under vertical equilibrium conditions.

The vertical equilibrium implies a good vertical permeability.

Flowing fluids are incompressible (no compressibility is considered for oil and water).

Displacement is considered linear.

Displacement in 1 D (dimension) means that fluid saturations at any point in the linear path are uniformly distributed with respect to thickness.

Displacement occurs at a high injection rate, so that capillary end effect and gravity forces are negligible.

4.9.1 Equation of Continuity or Conservation Mass Law [59, 79]

Considering an element of a reservoir through which a single phase is flowing in the x direction (Fig. 4.9). Then at any instant:

Mass rate in – Mass rate out = Mass rate of accumulation

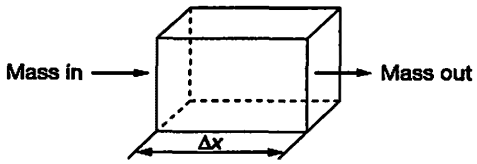

Figure 4.9 Mass Balance on Element.

$$(\rho_x v_x \Delta y \Delta z) - (\rho_{x+\Delta x} v_{x+\Delta x} \Delta y \Delta z) = (\Delta x \Delta y \Delta z)\,\phi \frac{(\rho_{t+\Delta t} - \rho_t)}{\Delta t}$$

introducing reservoir volume rate for water

water flowing through element $A\varphi dx$

A: cross section area

φ: porosity

$$q_w \rho_w\big|_x - q_w \rho_w\big|_{x+dx} = A\phi dx \frac{\delta}{\delta t}(\rho_w S_w)$$

or

$$q_w \rho_w\big|_x - \left(q_w \rho_w\big|_x + \frac{\delta}{\delta x}(q_w \rho_w)dx\right) = A\phi dx \frac{\delta}{\delta t}(\rho_w S_w)$$

can be reduced to:

$$\frac{\delta}{\delta x}(q_w \rho_w) = -A\phi \frac{\delta}{\delta t}(\rho_w S_w)$$

It is assumed an incompressible flow ($\rho_w \approx$ constant) then:

$$\left[\frac{\delta q_w}{\delta x}\right]_t = -A\phi \left[\frac{\delta S_w}{\delta t}\right]_x \tag{4.12}$$

the full differential of the water saturation is:

$$dS_w = \left[\frac{\delta S_w}{\delta x}\right]_t dx + \left[\frac{\delta S_w}{\delta t}\right]_x dt$$

the plane movement study of constant water saturation implies: $dS_w = 0$ then:

$$\left[\frac{\delta S_w}{\delta t}\right]_x = -\left[\frac{\delta S_w}{\delta x}\right]_t \left[\frac{dx}{dt}\right]_{S_w} \text{ in addition } \left[\frac{\delta q_w}{\delta x}\right]_t = \left[\frac{\delta q_w}{\delta S_w}\frac{\delta S_w}{\delta x}\right]_t \tag{4.13}$$

Substituting Eqs. (4.13) into Eq. (4.12) gives:

$$\left[\frac{\delta q_w}{\delta S_w}\right]_t = A\phi\left[\frac{dx}{dt}\right]_{S_w} \tag{4.14}$$

total rate q_t is constant then $q_w = f_w q_t$

The fractional flow of water, at any point in the reservoir, is defined as:

$$f_w = \frac{q_w}{q_o + q_w} \qquad q_t = q_o + q_w \ \textit{(reservoir conditions)} \tag{4.15}$$

Therefore Equation (4.14) can be written: plane velocity of constant water saturation

$$v_{S_w} = \left[\frac{dx}{dt}\right]_{S_w} = \frac{q_t}{A\varphi}\left[\frac{\delta f_w}{\delta S_w}\right]_{S_w} \tag{4.16}$$

This is the Buckley-Leverett equation (also called the frontal advance equation) which implies that, for a constant water injection rate, ($q_i = q_t$), the constant water saturation plane velocity is proportional to the derivative of the fractional flow evaluated for that saturation.

Other way to say, the equation states that in a linear displacement process, each water saturation plane moves through the porous media at a velocity that can be computed from the derivative of the fractional flow with respect to water saturation.

As the total flow rate q_t increases, the velocity of the plane of saturation correspondingly increases.

Eq. (4.16) can be integrated to yield:

$$[x]_{S_w} = \frac{W_i}{A\phi}\left[\frac{df_w}{dS_w}\right]_{S_w} \tag{4.17}$$

x is the total distance that the plane of given water saturation moves, W_i is the cumulative water injected with initial condition $W_i = 0$ at $t = 0$. Therefore at a given time, (W_i = Cte), the position of different water saturation planes can be plotted from Eq. (4.17).

4.9.2 Fractional Flow Equation

For a horizontal flow and neglecting capillary forces, the fractional flow for water is:

$$f_w = \frac{q_w}{q_o + q_w} = \frac{\dfrac{k_{rw}}{\mu_w}}{\dfrac{k_{ro}}{\mu_o} + \dfrac{k_{rw}}{\mu_w}} = \frac{1}{1 + \dfrac{k_{ro}}{k_{rw}}\dfrac{\mu_w}{\mu_o}} \tag{4.18}$$

q_w:	water rate	k_{rw}:	water relative permeability	μ_w:	water viscosity
q_o:	oil rate	k_{ro}:	oil relative permeability	μ_o:	oil viscosity

Application

Considering the following relative permeability data, the fractional water flow f_w (calculated for $\mu_w/\mu_o = 0.666$) corresponding and the calculated derivative df_w/dS_w

Table 4.1 Fractional Flow Calculation

Sw	krw	kro	fw	dfw/dSw
0.20	0.000	0.920		
0.25	0.009	0.750	0.0177	0.522
0.30	0.030	0.600	0.0698	1.197
0.35	0.050	0.450	0.1430	1.732
0.40	0.070	0.350	0.2309	2.126
0.45	0.100	0.280	0.3491	2.381
0.50	0.130	0.230	0.4591	2.495
0.55	0.180	0.180	0.6002	2.469
0.60	0.230	0.130	0.7265	2.303
0.65	0.280	0.099	0.8094	1.997
0.70	0.350	0.050	0.9131	1.550
0.75	0.430	0.020	0.9700	0.964
0.85	0.600	0.000	1	

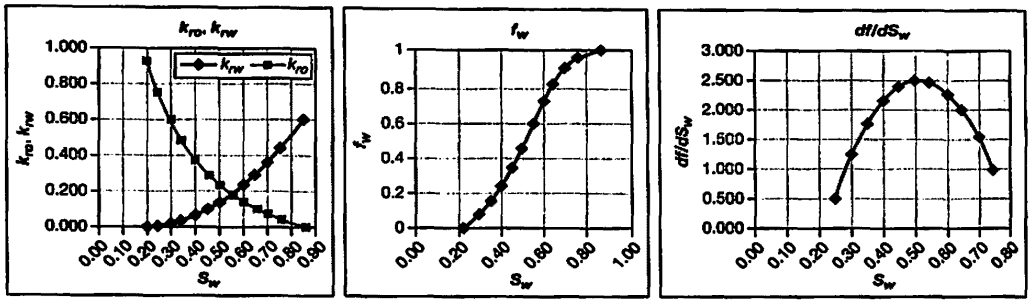

Figure 4.10 Fractional Flow Graphs.

Figure 4.10 shows the fractional water cut, f_w and the derivative (df_w/dS_w) plotted against water saturation from the data of Table 4.1.

Assuming a channel type reservoir under very active water drive, the water will replace the total fluid withdrawal.

Total reservoir oil production rate; 500 m^3/d *(reservoir conditions)*
Formation thickness: 20 m
Formation width: 400 m

The water front will travel at a distance from the initial water oil contact after 60, 120, 240 days:

At 60 days at 120 days at 240 days

$$[x]_{S_w} = 15\left[\frac{\delta f_w}{\delta S_w}\right]_{S_w} \qquad [x]_{S_w} = 30\left[\frac{\delta f_w}{\delta S_w}\right]_{S_w} \qquad [x]_{S_w} = 60\left[\frac{\delta f_w}{\delta S_w}\right]_{S_w}$$

For $S_w = 40\%$ from the plot, $df_w/dS_w = 2.126$

At 60 days, the 40% water saturation front is at a distance of

$$[x]_{S_w=40\%} = 15 \times 2.126 = 31.9 \text{ m}$$

At 120 days:

$$[x]_{S_w=40\%} = 30 \times 2.126 = 63.8 \text{ m}$$

At 240 days:

$$[x]_{S_w=40\%} = 60 \times 2.126 = 127.6 \text{ m}$$

From Figure 4.10c it can be seen that for a value of df_w/dS_w corresponds two water saturation values.

Most fractional flow curves exhibit two water saturations having the same value of df_w/dS_w. The consequence of that is according to Eq. (4.17), two different saturations would have the same velocity; that is would exist at the same point in the formation at the same time.

4.10 APPLICATIONS

Relative permeabilities measured in the laboratory are dependent on the rock sample wettability and experimental conditions (fluids, pressure gradients, laboratory conditions or reservoir conditions).

Relative permeabilities are used to describe the multiphase flow occurring in reservoirs.

The technique, mathematically simple is used in all reservoir simulators.

The important points of the curves are the limit point values:

- Minimum and maximum saturations.
- Maximum values of relative permeabilities.

4.10.1 Water Oil System

Minimum Saturations

The minimum water saturation or irreducible water saturation has a direct impact on the initial hydrocarbon in place calculation. Different techniques are available to assess the values:

- Open hole logging survey interpretation.
- Petrophysical laboratory experiments (capillary pressure curve, flood experiments).

Usually different values are obtained from each technique for the same rock type. The maximum water saturation corresponding to the residual oil saturation (S_{orw}) is difficult to estimate. Usually the value is deducted from the water oil relative permeability measurements carried out in the laboratory (at laboratory or reservoir conditions). As mentioned before the result is dependent on the operating conditions and the rock wettability restitution.

In the field, the cased hole survey technique like the residual oil saturation survey or the Thermal Decay Tool can be used to deduct S_{orw} in flooded areas.

S_{orw} can also be estimated from a local correlation based on mature basin field performance observation.

Maximum Relative Permeability Values

k_{romax} must always be < 1 due to the presence of irreducible water saturation. The k_{rwmax} is very dependent on the rock wettability. For a water wet rock k_{rwmax} may be as low as 0.1. For a mixed wet rock k_{rw} max may be equal to 0.7. The maximum k_{rw} value has a direct impact on the amount of produced water volumes; as a consequence it is often used as a tuning parameter for simulation history matching.

4.10.2 Gas-oil System

The minimum gas saturation also called the critical gas saturation (S_{gc}) is not known. It can be deducted from the interpretation of a gas flood experiment carried out at reservoir conditions. Practically, 5% is used for usual reservoir engineering hand calculations and simulation studies.

The maximum gas saturation is:

$$S_{gmax} = 1 - S_{org} - S_{wi}$$

S_{org} is the oil saturation left behind a gas flood. It has been observed that S_{org} is smaller than S_{orw}. The final value depends mainly on the rock heterogeneity, the amount of pore volume injected and experimental conditions.

For engineering consistency, the oil relative permeability k_{romax} must be the same in the water oil system and in the gas oil system.

4.10.3 Three-phase Relative Permeabilities

Three-phase relative permeabilities are necessary for reservoir simulation implying a Water Alternate Gas process (WAG). All commercial simulators offer different algorithms based on known correlations (Stone 1 and 2) and others found in published papers [101]. Ideally a reservoir study should be based on curves deduced from a laboratory WAG experiment performed at reservoir conditions.

4.10.4 Frontal Displacement Theory, Buckley-Leverett Equation

At time of the slide rule reservoir hand calculations, the theory was used by engineers to predict water flood performance with simple analytical relationships. The calculation was carried out for different sections of the reservoir. The summation of the results was performed to give a global field performance prediction.

Nowadays the use of a reservoir simulation model is the rule to match and predict the reservoir performance.

CHAPTER 5

Natural Drainage Mechanisms of Hydrocarbon Reservoirs

5.1 INTRODUCTION

In this chapter, only the reservoir fluid movements associated with reservoir pressure changes are considered. Cases of water or gas injection are treated in the chapter "Enhanced oil recovery".

A reservoir is defined as a porous matrix system filled up with water, oil, and/or gas. In all cases, some non-movable water called "irreducible water or connate water" is present in the porous media characterized by its saturation S_{wir} or S_{wc}.

In general, the reservoir thickness is thin compared to the area, so the reservoir temperature can be assumed constant over the entire thickness.

To produce hydrocarbon at surface, fluid movement must take place in the reservoir under a pressure gradient. The pressure gradient is obtained by creating a communication between the reservoir and the surface facilities through the production wells.

Before any human interference occurs, the system consisting of a porous rock with hydrocarbon and eventually an associated aquifer is in equilibrium. The producing well opened at surface unbalances the whole system:

Hopefully hydrocarbon is produced, fluid pressure changes, and the aquifer may be triggered to move along the created pressure gradient.

In the case of an oil reservoir with an initial gas cap, the gas always expands due to its high compressibility. Consequently, the gas oil contact tends to move down into the initial oil zone. In addition, the aquifer tries to compensate the voidage created by the fluid withdrawal and invade the initial oil zone.

The natural drainage mechanisms is studied and illustrated by what is called the material balance equation. The method was extensively used when engineers had only a pencil, a sheet of paper and a slide rule to work with. The calculations are based only on bottom condition volumes.

The material balance equation is the basic tool for the reservoir engineer to analyze the reservoir performance and behavior. The final objective being:

- To check the production data consistency.
- To understand the production mechanisms.
- To predict future production profile.
- To prepare the use of a more sophisticated tool that is a reservoir simulator.

Material-Balance-Equations:

In 1935, D.L. Katz of the U of Michigan proposed a tabular method of obtaining a material balance for a closed reservoir. Basically, a material-balance equation is a statement that accounts for the volumes and quantities of fluids that are initially present in, produced from, injected into, and that remain in a reservoir at any state of its depletion.

Also, that same year, Schilthuis published a material-balance equation that included the same terms of fluid volumes and changes with time as Katz's method. The application of Katz's method required the experimental determination of phase equilibrium data; the Schilthuis method represented a simplification in that the requisite terms were reduced to simpler expressions.

Later, Schilthuis proposed a method to calculate water encroachment using the material-balance equation, but his method required accurate production-history data. Several years later, William Hurst developed a method for determining the rate of water influx that was independent of the material-balance equation and production history; only data on pressure history and rock and fluid properties were required.

For practical reasons and simplification, the natural drainage is studied in three steps according to initial and final reservoir conditions:

- Undersaturated oil reservoir.
- Dissolved gas expansion.
- Reservoir with an initial gas cap.

Water entry calculations are explained into details to proceed to the 'history match' procedure.

Finally dry gas reservoir drainage is treated with the production well loss of head interaction.

The material balance calculation consists of evaluating at different dates the reservoir condition status, in comparison with the initial conditions. Between the two dates some reservoir fluid has been produced and or injected. Production rates and conditions that occurred have no impact on the calculation. Similarly to the thermodynamic theory, the material balance is focused on a system (the reservoir) at initial conditions and the same system after some processes (production and or injection) occurred; the transformation path followed by the process being irrelevant.

Production data are measured and reported at surface conditions. The symbols used are usually written in capital letters. To evaluate data at reservoir conditions, the PVT properties are needed. Needless to say the accuracy of the PVT functions has a large impact on the calculations. Those properties must be selected with great care.

Traditionally the material balance calculations are performed and termed in volumes associated with PVT functions (B_o, B_g, B_w, R_s). The method is appropriate when the "black oil" concept is valid. In case of volatile oil or gas-condensate, an EOS (Equation of State) is needed.

5.2 UNDERSATURATED OIL RESERVOIR

Initial state: reservoir pressure well above the oil bubble point pressure.

Final state: reservoir pressure above bubble point pressure.

The reservoir oil is produced in a monophasic regime the reservoir pressure declines. The drainage mechanism is also called: "monophasic fluid expansion".

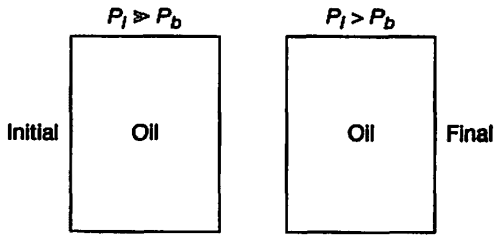

Figure 5.1 Oil reservoir Initial State and Final State.

Assumptions:

- Undersaturated oil reservoir.
- Closed reservoir.
- Formation and connate water compressibilities neglected.

The volumetric material balance indicates that the container volume does not change between initial time and final time after having produced N_p.

Or volume occupied by remaining oil = volume occupied by initial oil at reservoir conditions

$$(N - N_p) \times B_o = N \times B_{oi}$$

N: initial oil in place
N_p: cumulative oil produced at standard conditions
B_o: oil FVF at final pressure
B_{oi} initial oil FVF

Then

$$N_p = \frac{B_o - B_{oi}}{B_o} \times N \tag{5.1}$$

The recovery factor is expressed as the ratio of the cumulative oil produced divided by the initial oil in place, both at stock tank conditions.

$$R = \frac{N_p}{N} = \frac{B_o - B_{oi}}{B_o} \tag{5.2}$$

The recovery factor is determined from the oil formation volume factor change between initial and final pressures.

The above assumptions can be applied to a laboratory experiment when no water is present and the container being a stainless steel Hassler cell. A geological reservoir is made of a porous rock, associated with connate water and oil. All components react to a depletion according to its respective compressibility.

Compressibility:

Any material submitted to a pressure drop induces a volume change. The compressibility of a material is defined as the fractional change in volume of the material volume with a unit change in pressure.

$$c = -\frac{1}{V}\left(\frac{\partial V}{\partial p}\right) \tag{5.3}$$

c:	compressibility	
V:	initial material volume	(the negative sign is used to keep
δV:	volume change	the compressibility positive)
δp:	pressure change	

The reservoir is made of oil, connate water and pores

For a pressure drop *DP* applied to the reservoir,
The oil volume in the reservoir increases by: $c_o \times V_p \times S_o \times DP$
The connate water volume increases by: $c_w \times V_p \times S_w \times DP$
The pore volume shrinks by: $c_p \times V_p \times DP$

All these volume changes contribute to the production; therefore

$$N_p \times B_o = V_p(c_o S_o + c_w S_w + c_p) \times DP$$

The production (at reservoir conditions) is the sum of all volume changes

$$N_p \times B_o = V_p S_o \frac{(c_o S_o + c_w S_w + c_p)}{S_o} \times DP$$

An equivalent compressibility is defined as

$$c_e = \frac{(c_o S_o + c_w S_w + c_p)}{S_o} \tag{5.4}$$

Instead of having a complex system made of pores, oil, plus connate water, it can be imagined a system, made of oil only with an equivalent compressibility c_e.

$$V_p S_o = N \times B_{oi}$$

Oil produced is:

$$N_p \times B_o = N \times B_{oi} c_e \times DP \tag{5.5}$$

To evaluate the equivalent compressibility, c_o is needed.

By definition the oil compressibility is:

$$c_o = -\frac{1}{V_{oi}} \frac{dV_o}{dP} = -\frac{1}{B_{oi}} \frac{B_o - B_{oi}}{P_f - P_i} \tag{5.6}$$

V_{oi}: initial oil volume
dVo: oil volume change
$P_f - P_i$: final – initial pressure

Remarks
c_o: *obtained from the PVT laboratory measurements*
c_w: *can be found in the literature.*
c_p: *can be measured in the laboratory but more often deducted from the Hall correlation. Figure 1.10.*
Order of magnitude:

$$c_w \cong c_p \cong 0.5\ 10^{-4}\ \text{bar}^{-1} \text{ or } 3 \text{ to } 4\ 10^{-6}\ \text{psi}^{-1}$$

Usually the recovery due to the monophasic expansion only is very low a few %.
If the reservoir is associated with a connected aquifer some water will invade the initial oil zone to compensate the oil production. The water volume changes must be taken into account:

$$N_p \times B_o = N \times B_{oi} \times c_e \times DP + W_e - W_p \tag{5.7}$$

W_e: *cumulative water entry in the initial oil zone*
W_p: *cumulative water produced*
Finally if the reservoir depletion is small then $B_o \# B_{oi}$ *and*

$$N_p \approx N \times c_e \times DP$$

5.3 DISSOLVED GAS EXPANSION

For all the following calculations, the reservoir oil is assumed to be at bubble point pressure at initial time in a closed reservoir without gas cap and no aquifer.

As soon as production starts, the reservoir pressure decreases and solution gas comes out of solution to build gas saturation up in the reservoir. In a first step the gas bubbles are dispersed over the whole oil zone until the time comes when a created continuous gas phase becomes mobile and accumulates to the top of the reservoir, creating what is called a secondary gas cap (Fig. 5.2).

In this calculation, the water and pore compressibilities are neglected since the gas compressibility is so high, that influence of pore and water compressibilities are completely masked.

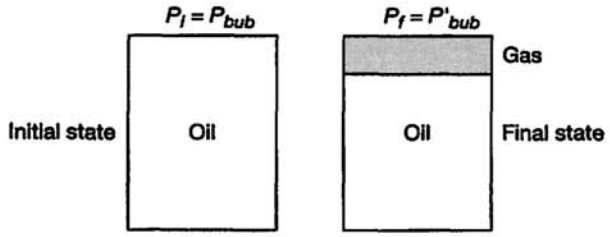

Figure 5.2 Oil Reservoir Initial and Final Conditions.

The volumetric material balance is written at reservoir conditions as:

Initial reservoir fluid volume = final fluid volume

Table 5.1 Initial and Final Reservoir Conditions

At initial pressure P_i		At final pressure P_f	
Surface conditions			
initial oil volume std: gas volume std:	N NR_{si}	remaining oil std: remaining gas std:	$N - N_p$ $NR_{si} - G_p$
Reservoir conditions			
reservoir oil volume: free gas reservoir volume:	NB_{oi} 0	remaining oil res: free gas res: $[NR_{si} - G_p - \underbrace{(N - N_p) R_s}_{\text{gas in solution}}] B_g$	$(N - N_p) B_o$

Table 5.1 depicts the reservoir data at initial time (pressure $P_i = P_b$) and final time (pressure P_f).

NR_{si}: total gas in solution within the reservoir initially (std)
G_p: cumulative produced gas at surface
B_g: gas FVF at final pressure P_f

at reservoir conditions $$NB_{oi} = (N - N_p) B_o + [NR_{si} - G_p - (N - N_p) R_s] B_g \quad (5.4)$$

Eq. (5.4) expresses the reservoir fluid volume occupied at initial time is equal to the fluid volumes at final time. Some free gas appears in the reservoir.

Introducing the diphasic (oil + gas) formation factor: B_t at pressure P

$$B_t = B_o + (R_{si} - R_s)\, B_g \tag{5.5}$$

And the average cumulative *GOR*: $R_p = G_p/N_p$

The material balance Eq. (5.4) can be written:

$$N_p[B_o + (R_p - R_s)\, B_g] = N(B_t - B_{ti}) \tag{5.6}$$

Recovery factor at pressure P:

$$R = \frac{N_p}{N} = \frac{B_t - B_{ti}}{B_o + (R_p - R_s)B_g} \tag{5.7}$$

Eq. (5.7) shows at pressure P that the maximum recovery factor R is obtained when R_p is minimum. Reservoir gas is 'energy'; therefore surface gas production must be limited to the solution gas. In the field the operator monitors and limits the *GOR*.

Other way to express Eq. (5.6):

$$N = \Phi_N N_p + \Phi_g G_p \tag{5.8}$$

$$\Phi_N(P) = \frac{B_o - R_s B_g}{(B_o - R_s B_g) - (B_{oi} - R_{si} B_g)} \tag{5.9}$$

$$\Phi_g(P) = \frac{B_g}{(B_o - R_s B_g) - (B_{oi} - R_{si} B_g)} \tag{5.10}$$

Φ_N and Φ_g are functions of oil and gas PVT properties.

Eq. (5.8) can be used in two ways:

1) known parameters: N from geology and N_p, G_p production data:
Then reservoir pressure P can be calculated

2) Np, Gp, and P are measured
N can be deduced and checked with the geologist's evaluation

Remark:
Formation and connate water compressibility have been omitted in the equations. This is because as soon as free gas is present, the water and rock compressibilities become negligible compared to the one of gas. For hand calculation the omission is admitted but in commercial software those are taken into account.

5.4 PRODUCTION FORECAST

The production *GOR* is function of the relative permeabilities and, through the DarcyLaw, function of oil saturation

$$\text{GOR} = \frac{dG_p}{dN_p} = R_s + \frac{k_{rg}}{k_{ro}} \times \frac{\mu_o B_o}{\mu_g B_g} \tag{5.11}$$

$$V_p = \frac{NB_{oi}}{S_{oi}} \qquad S_o = \frac{(N - N_p)}{V_p} = \frac{(N - N_p)B_o}{NB_{oi}} S_{oi}$$

$$S_{oi} = 1 - S_{wi}$$

Knowing N and $k_{rg}/k_{ro}(S_o)$, production forecast is calculated by solving the two equations by pressure steps:

$$N = \Phi_N N_p + \Phi_g G_p \qquad \frac{dG_p}{dN_p} = R_s + \frac{k_{rg}}{k_{ro}} \times \frac{\mu_o B_o}{\mu_g B_g}$$

It can be found in the literature curves giving $\log(k_{rg}/k_{ro})$ function of gas saturation S_g.

Tracy Calculation Method:

The production forecast method is based on an iterative calculation with limitations:

- Production is assumed to occur only by dissolved gas expansion.
- The reservoir is closed (no water entry).
- The liberated gas in the reservoir is assumed to remain dispersed in the oil zone; no migration occurs, no secondary gas cap.

If a well *GOR* is constant when producing below the bubble point pressure, liberated gas segregation most probably is taking place and a secondary gas cap is created.

The calculation is conducted by pressure steps from the two equations:

$$N = N_{p(i-1)} \times \Phi_N + G_{p(i-1)} \times \Phi_g + \Delta N_p \times \Phi_N + \Delta G_p \times \Phi_g \tag{5.12}$$

$$\Delta G_p = \frac{GOR_{(i-1)} + GOR_i}{2} \times \Delta N_p$$

$GOR_{(i-1)}$ is known; GOR_i is assumed, and ΔG_p calculated.

knowing ΔN_p, N_p is deduced

knowing N_p, $S_o = \frac{(N - N_p)B_o}{NB_{oi}} S_{oi}$ can be calculated

with S_o, k_{rg}/k_{ro} is deduced

then the *GOR* at step *i*

$$GOR_i = R_s + \frac{k_{rg}}{k_{ro}} \times \frac{\mu_o B_o}{\mu_g B_g}$$

The last calculated GOR_i is compared to the assumed GOR_i at start; an iterative process is performed until the two *GOR* are equal.

Conclusion:

The recovery factor expected from a dissolved gas expansion process is between 5 and 25%.

The process is often abandoned when the *GOR* highly increases.

The recovery factor at a reservoir pressure is sensitive to R_p: the cumulative production *GOR*. This is why in some producing countries, it is forbidden to produce oil at a *GOR* above the solution gas oil ratio (R_s).

The critical gas saturation S_{gc} is an important parameter; it retains the free gas in the reservoir more or less. The higher S_{gc} is, the better the recovery factor will be.

Water and rock compressibilities can be neglected for hand calculations since free gas compressibility is very high.

5.5 NATURAL DRAINAGE MECHANISM OF AN OPENED RESERVOIR

Up to now, two drainage mechanisms have been discussed:

- Monophasic expansion above bubble point pressure.
- And dissolved gas expansion below bubble point pressure.

An oil zone may be submitted at its boundaries to:

- A gas entry by an initial gas cap expansion.
- Or water entry by an aquifer expansion.
- Or both simultaneously.

Volumetric Material Balance for an opened reservoir (Fig. 5.3).

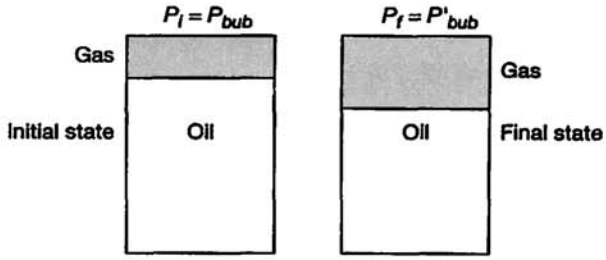

Figure 5.3 Initial and Final Conditions of a Reservoir with an initial Gas cap.

Assumptions: Initial gas cap
Pore and connate water compressibilities neglected

Initial oil in place: NB_{oi}

Initial gas in place in the gas cap: GB_{gi}

G: gas volume in the gas cap at surface conditions

B_{oi}, B_{gi}: oil and gas FVF at initial conditions

The size of the initial gas cap is expressed relative to the size of the oil zone by the factor m:

m = Initial reservoir free gas volume/Initial reservoir oil volume $m = \dfrac{GB_{gi}}{NB_{oi}}$

$$\text{so: } G = \frac{mNB_{oi}}{B_{gi}}$$

After some oil production, the reservoir pressure drops to P.
The initial gas cap has expanded. Its final reservoir volume is

$$GB_g = \frac{mNB_{oi}}{B_{gi}} B_g$$

The reservoir gas cap expansion is:

final volume – initial volume

$$\frac{mNB_{oi}}{B_{gi}} B_g - mNB_{oi} = mNB_{oi}\left(\frac{B_g}{B_{gi}} - 1\right)$$

The volumetric material balance expressed at reservoir conditions [79] is:
Initial volume occupied by the oil =

oil volume left in the reservoir with its dissolved gas
+ liberated gas from oil and staying in the reservoir
+ gas volume from the initial gas cap invading the oil zone
+ water entry from aquifer – produced water

$$NB_{oi} = (N - N_p)B_o \qquad \textit{oil volume left in the reservoir with its dissolved gas}$$
$$+ [NR_{si} - G_p - (N - N_p)R_s]\, B_g \qquad \textit{liberated gas from oil, staying in the reservoir}$$
$$+ mNB_{oi}\left(\frac{B_g}{B_{gi}} - 1\right) \qquad \textit{gas cap expansion}$$
$$+ W_e - W_p B_w \qquad \textit{water entry from aquifer – produced water}$$

Introducing $R_p = G_p/N_p$:

$$N_p[B_o + (R_p - R_s)\, B_g] = N[(B_o - B_{oi}) + (R_{si} - R_s)\, B_g] + mNB_{oi}\left(\frac{B_g}{B_{gi}} - 1\right) + (W_e - W_p B_w) \tag{5.13}$$

with $B_t = B_o + (R_{si} - R_s)\, B_g$

$$N_p\left[B_o + \left(R_p - R_s\right) B_g\right] = N_p\left[B_t + \left(R_p - R_{si}\right) B_g\right]$$

$$N_p[B_t+(R_p-R_{si})B_g]=N(B_t-B_{ti})+mNB_{oi}\left(\frac{B_g}{B_{gi}}-1\right)+(W_e-W_pB_w) \qquad (5.14)$$

Dividing Eq. (5.14) by D: $D=N_p[B_t+(R_p-R_{si})B_g]$

then
$$1=\underbrace{\frac{N(B_t-B_{ti})}{D}}_{DDI}+\underbrace{\frac{mNB_{oi}\left(\frac{B_g}{B_{gi}}-1\right)}{D}}_{SDI}+\underbrace{\frac{W_e-W_pB_w}{D}}_{WDI} \qquad (5.15)$$

Numerators of these fractions are the expansions of the initial oil zone; the expansion of the initial gas cap; and the net water influx, respectively. The denominator is the volume of hydrocarbon produced expressed at present reservoir pressure conditions.

DDI: Depletion Drive Index
SDI: Segregation (gas cap) Drive Index
WDI: Water Drive Index

Those three parameters characterize the production mechanism of the reservoir and will guide the operator in his choice for future development: (natural depletion, water or gas injection).

In Eq. (5.13) the left side term is the total fluid underground withdrawal. Adding terms relative to water injection W_i and gas injection G_i, plus compressibility terms for rock and connate water, the generalized material balance equation is obtained; the one which is used in all material balance software.

5.6 GENERALIZED MATERIAL BALANCE EQUATION [59]

Including gas injection and water injection terms

$$N_p(B_o-B_gR_s)+B_g(G_p-G_i)+(W_p-W_i)B_w$$
$$=N\left\{(B_o-B_{oi})+(R_{si}-R_s)B_g+mB_{oi}\left(\frac{B_g}{B_{gi}}-1\right)+(1+m)B_{oi}\left(\frac{S_{wc}c_w+c_f}{1-S_{wc}}\right)(P_i-P)\right\}+W_e$$

or
$$F=N\times E+W_e \qquad (5.16)$$

F: total underground fluid withdrawal
N: Initial oil in place volume at standard conditions
E: Expansion of oil and dissolved gas, connate water, pore volume shrinkage (oil zone + gas cap)
W_e: reservoir cumulative water entry at pressure P
G_i: cumulative injected gas
W_i: cumulative injected water

$$F = N_p(B_o - B_g R_s) + B_g(G_p - G_i) + (W_p - W_i)\,B_w$$

$$E = (B_o - B_{oi}) + (R_{si} - R_s)\,B_g + mB_{oi}\left(\frac{B_g}{B_{gi}} - 1\right) + (1+m)\,B_{oi}\left(\frac{S_{wc}c_w + c_f}{1 - S_{wc}}\right)(P_i - P)$$

5.7 OIL SATURATION CALCULATION IN THE OIL ZONE

At initial time, the initial oil in place is expressed as:

$N \times B_{oi} = V_p \times S_{oi}$ with $S_{oi} = 1 - S_{wc}$ initial oil saturation

Pore volume is: $V_p = \dfrac{NB_{oi}}{1 - S_{wc}}$

A fraction of the pore volume x, has been invaded by the gas cap due to its expansion. Residual oil saturation in the oil invaded zone by gas is defined as S_{org}.

A fraction of the pore volume y, has been invaded by water. We assume that residual oil and gas saturations are known in that invaded zone as: S_{orw} and S_{gt}.

S_{org}, and S_{orw} are the residual oil saturations behind the gas and water fronts respectively.

S_{gt} is the trapped gas saturation.

Assuming that the gas created by the depletion does not migrate to the top of the reservoir, water, gas and oil volumes can be expressed as saturation functions:

Water volume:

$$\frac{NB_{oi}}{1 - S_{wc}}\,y\left(1 - S_{orw} - S_{gt} - S_{wc}\right) = W_e - W_p B_w \tag{5.17}$$

Gas volume:

$$\frac{NB_{oi}}{1 - S_{wc}}\left[x(1 - S_{wc} - S_{org}) + (1 - x - y)(1 - S_{wc} - S_o) + yS_{gt}\right] = mNB_{oi}\left(\frac{B_g}{B_{gi}} - 1\right) + \left[(NR_{si} - G_p) - (N - N_p)\,R_s\right]B_g \tag{5.18}$$

Oil volume:

$$\frac{NB_{oi}}{1 - S_{wc}}\left[xS_{org} + (1 - x - y)\,S_o + yS_{orw}\right] = (N - N_p)\,B_o \tag{5.19}$$

The system of three equations and three unknowns (x, y, S_o) can be solved to evaluate the oil saturation in the producing oil zone.

5.8 USE OF THE GENERALIZED VOLUMETRIC MATERIAL BALANCE EQUATION

The material balance equation allows the engineer to check production data history consistency. Missing production data can be computed from the equation. Starting with m and N obtained by planimetry, crosscheck between geological values (static) and production history (dynamic) can be performed. It must be emphasized that the material balance procedure works only for the connected oil; it is not influenced by isolated oil pools.

From the production history, the field relationship k_{rg}/k_{ro} versus S_o can be calculated.

The combination material balance, GOR equation permits to run production forecast in the same way that has been shown for the dissolved gas expansion drive reservoir.

5.9 PVT PROPERTIES FOR MATERIAL BALANCE EQUATION

5.9.1 PVT Properties

It has been seen in the different material balance formulas, that PVT properties are a key parameter for the accuracy of the calculation. Therefore, the properties must be selected with great care.

If no laboratory experiment is available, the engineer is conducted to use correlations adapted as near as possible to the present study case.

The laboratory reports results of different experiments that have been ordered by the operator:

Usually the results are:

- Constant mass study to define the bubble point pressure.
- Flash liberation of bubble point oil to standard conditions.
- Flash liberation of bubble point oil through separators and to stock tank.
- Differential vaporization liberation.

For each process, values of formation volume factor B_o and dissolved gas R_s ratios are reported. The difficulty is that none of these processes simulate properly the field operation.

The differential vaporization process is an approximation of what is taking place far away from the production well in the reservoir. Gas being highly mobile, under a small pressure gradient it moves quickly to the production well.

Flash liberation is considered to occur between the reservoir and the surface separators. There are some differences between the process simulated in the laboratory and the field operations. In the field, the oil and gas traveling through the tubing are submitted to a progressive pressure and temperature changes. The result is gas comes out of solution

gradually in the tubing. In addition to this, the two phases gas and oil travel at different velocities in the tubing. The complex process is not reproducible in the laboratory.

From the two laboratory experiments, a composite PVT is built for material balance calculations.

5.9.2 Correction of Oil Formation Volume Factor [1]

$$\text{Composite FVF } B_o = B_{od}\frac{B_{ofb}}{B_{odb}} \tag{5.20}$$

B_{od} oil FVF obtained during the differential process function of pressure f(P)
B_{ofb} oil FVF obtained from the flash liberation through separators of the oil at its bubble point pressure
B_{odb} oil FVF measured during the differential process of the oil at its bubble point pressure

Interpretation: using the FVF differential as a reference, it is corrected by a constant valueB_{ofb}/B_{odb} (<1) over the pressure range.

The relationship between the two FVF (flash and differential) is assumed to be constant over the entire pressure range of interest.

5.9.3 Correction of Solution Gas-oil Ratios

$$R_s \text{ composite } R_s = R_{sfb} - (R_{sid} - R_{sd}) \times \frac{B_{ofb}}{B_{obd}} \tag{5.21}$$

R_{sfb} solution gas oil ratio obtained from bubble point oil during flash liberation through separators
R_{sid} solution gas oil ratio calculated during differential process of the oil at its bubble point pressure
R_{sd} gas in solution calculated during differential process $f(P)$
$(R_{sid} - R_{sd})$ represents the amount of liberated gas during the differential process at each pressure step.

Interpretation: the flash liberation through separators (R_{sfb}) is used as a reference.

The composite solution gas is computed as equal to the total liberated gas during the flash through separators, minus the calculated liberated gas during the differential process at each pressure step; corrected by the FVF ratio. (*The liberated gas during the differential process is considered too high*).

The undersaturated oil formation volume factors are deducted from the constant mass study where the relative volumes are reported.

$$B_o = \frac{V_{ores}}{V_{ostd}} = \frac{V_{ores}}{V_{ob}} \times \frac{V_{ob}}{V_{ostd}} \tag{5.22}$$

V_{ores} oil volume at reservoir conditions
V_{ob} oil volume at saturation pressure *(bubble point pressure)*
V_{ostd} oil volume at standard conditions
$\frac{V_{ores}}{V_{ob}} = V_r$ relative volume reported in the constant mass study
$\frac{V_{ob}}{V_{ostd}} =$ oil FVF at bubble point pressure

5.9.4 Conclusion

The composite B_o and R_s above commonly used for the material balance studies honor the reservoir gas volumes. Nevertheless, at low pressures, the composite dissolved gas-oil ratio may become negative.

5.9.5 Reservoir Pressure for Material Balance

As previously mentioned, the Material Balance study is based on a production history analysis. Pressure history is needed simultaneously with the cumulative fluid volume produced. In the modern terminology a material balance study is also called a zero dimension model or a tank model since no reservoir geometry is considered. Therefore only one pressure value characterizes the reservoir behavior versus time and cumulative fluid production.

All reservoir pressure data are deduced from well pressure build-up and RFT surveys. All values must be corrected and reported to the same datum for consistency.

The material balance study assumes that all the reservoir oil contribute to the fluid expansion and production. Therefore if some oil is isolated or is badly connected, areally or vertically to the main pool, it is difficult to use this technique.

The choice of the datum is important so that pressures referenced to that datum represent an average reservoir pressure. The ideal situation is to define the datum as a horizontal plane dividing vertically the oil pool into two equivalent oil volumes.

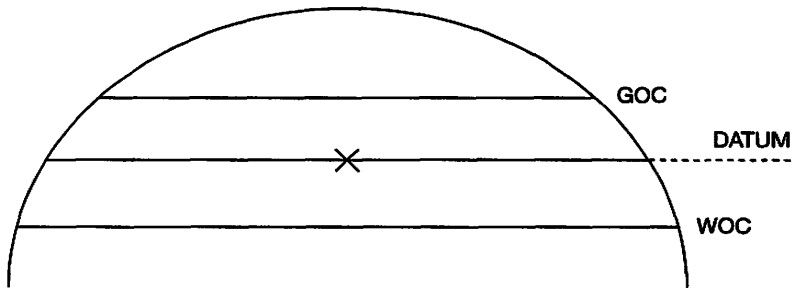

Figure 5.4 Reservoir Cross section.

The datum must also be defined in reference to a fix horizontal plane. Usually the Mean Sea Level is used (MSL).

5.10 WATER ENTRIES

5.10.1 Introduction

The generalized material balance equation contains the term: W_e (reservoir cumulative water entry in the oil zone) Eq. (5.16).

$$F = N \times E + W_e$$

No one can have access to the reservoir water entry value. Nevertheless, a separate evaluation of W_e can be performed with the help of some assumptions.

5.10.2 Aquifer Configurations

Infinite Aquifer:

Usually most of hydrocarbon accumulations are hydraulically linked with an aquifer, which is very often much bigger than the trapped hydrocarbon volume.

It is common to have aquifer volumes 10 to 100 folds the hydrocarbon volume.

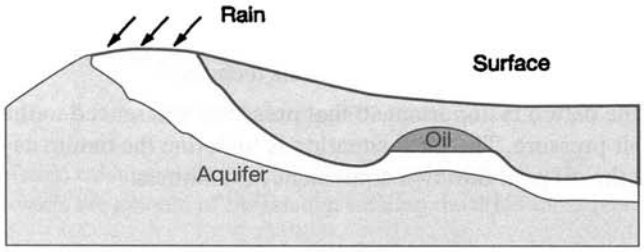

Figure 5.5 Infinite Aquifer.

Some reservoirs are submitted to constant water loading through an aquifer extending up to surface. It is considered as an infinite aquifer (Fig. 5.5).

Bottom Water Drive:

The aquifer is in contact with the entire hydrocarbon area. Water invasion occurring vertically is governed by the reservoir vertical permeability (Fig. 5.6).

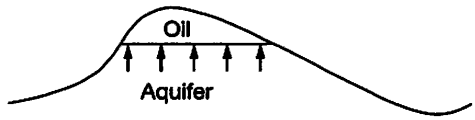

Figure 5.6 Bottom aquifer.

The associated model is approximated by a cylinder whose section equals the oil water contact area.

Edge Water Drive:

The aquifer surrounds the hydrocarbon reservoir. The water entries take place laterally. Horizontal permeability is governing the water movement.

The associated model is approximated by a radial circular flow taking place, limited by an external radius r_e and internal r_o. r_o represents the radius of the oil pool similarly to r_w the well radius in the well radial flow equation.

Linear Water Drive:

This is a typical aquifer shape encountered in fluvio-deltaic deposition reservoirs. Those reservoirs are channels (Fig. 5.7).

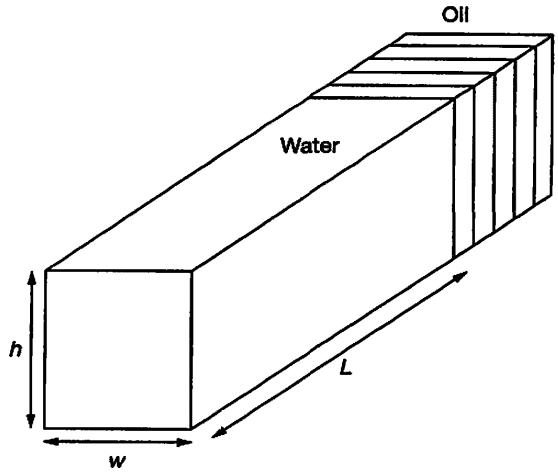

Figure 5.7 Linear aquifer.

5.10.3 Determination of Water Influx Independent of Material Balance Calculation

In response to a pressure drop in the oil zone, the aquifer reacts to offset or delay pressure decline by providing water, called water influx or encroachment. The aquifer may be considered as an independent unit which supplies water to the reservoir in response to a pressure change at its boundary.

It is possible to calculate water influx from the reservoir pressure history at the boundary (oil water contact), with knowledge of the aquifer dimensions and its characteristics, independently of the material balance calculations.

5.10.3.1 Small Pot Model

This the simplest model where the aquifer volume is known and reacts instantly to a pressure drop applied at the oil water boundary. The aquifer expands into the oil zone of an amount function of the water volume and the total compressibility (aquifer plus rock).

$$W_e = W \times c_t \times (P_i - P) \tag{5.23}$$

W_e	cumulative water entry	c_p	pore compressibility
W	aquifer volume	P_i	initial reservoir pressure at oil water contact
c_t	total aquifer compressibility = $(c_w + c_p)$	P	current reservoir pressure at oil water contact
c_w	water compressibility		

The equation is a re-statement of the compressibility definition applied to an aquifer. It can be only used for small aquifers when it can be assumed that under a pressure drop at the boundary, the entire aquifer volume is mobilized to expand instantaneously noting that the equation is independent of time.

5.10.3.2 Hurst Van Everdingen Model (Unsteady State Water Influx)

The small pot water influx model has the great advantage of simplicity but is limited for field applications since aquifers usually do not respond instantaneously to a pressure drop at the oil water boundary.

Hurst and Van Everdingen [59, 79, 85] referred to the diffusivity equation to elaborate a solution for the constant terminal pressure and constant terminal rate cases. The model consists of a cylindrical aquifer surrounding a cylindrical oil reservoir. See Appendix M for more details. The solution being complex, H.V.E. compiled tables for finite and infinite aquifers.

$$\frac{dW_e}{dt} = \frac{A(P_i - P)}{\log(\alpha \times t)}$$

5.10.4 Methodology for the Hurst Van Everdingen (HVE) Water Influx Calculation

The basic reservoir study is to fit the calculated reservoir pressure with the observed reservoir pressure; it is the history match procedure. The known fluid produced volumes are

used for input into a model (zero dimension for the tank model or multi dimensions for the numerical reservoir simulator); the reservoir pressure is calculated and compared with the field measured reservoir pressure. The reservoir pressure history at the oil water contact can be approximated by a series of pressure steps versus time. Each pressure step generates a water influx calculated by the HVE solution versus time. The linearity of diffusivity equation allows the application of the superposition principle. Therefore the total water influx into the oil zone at time t is equal to the sum of all contributions of the previous perturbations. To reproduce the smooth curve relationship pressure versus time, the pressure plateaus can be taken very small. For hand calculations, one year time intervals are chosen.

5.10.5 Example of a Pressure History for Water Entry Calculation

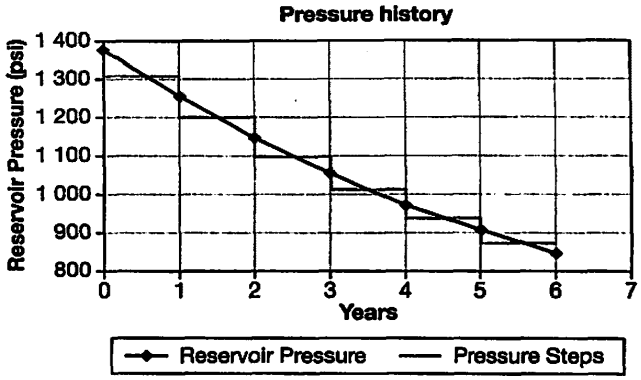

Figure 5.8 Reservoir Pressure History.

Figure 5.8 depicts a reservoir pressure history. The continuous pressure decline is modified into a series of pressure step drops. An average pressure is calculated (plateau pressure).

Table 5.2 Example of a Reservoir Pressure History

Reservoir Pressure	
Year	**History**
0	1 370
1	1 250
2	1 145
3	1 054.5
4	974.5
5	909
6	851

time interval 0 to 1 year average pressure: $P = {}^1/_2(1\,370 + 1\,250) = 1\,310$
pressure step 1 for HVE calculation: from 1 370 to 1 310
plateau pressure in the period year 1 to 2: $P = {}^1/_2(1\,250 + 1\,145) = 1\,197.5$
pressure step 2: for HVE calculation: from 1 310 to 1 197.5
and so on.

The pressure steps to use for the calculation are:

Step 1: from 1 370 to 1 310

Step 2: from 1 310 to 1 197.5

etc.

Remark

If no reservoir pressure decline is observed during production, it means that the voidage created by the production is completely compensated by the cumulative water entry. In terms of rate:

$$q_{voidage} = Q_o B_o + Q_g B_g - Q_o R_s B_g + Q_w B_w$$

$$q_{voidage} = Q_o B_o + (Q_g - Q_o R_s) B_g + Q_w B_w$$

In terms of cumulative:

$$F = N_p B_o + (G_p B_g - N_p R_s B_g) + W_p B_w$$

$$\text{or} \quad F = N_p B_o + \left(R_p - R_s\right) B_g + W_p B_w \tag{5.24}$$

5.10.6 Application to the Radial and Linear Water Drive

The subject was treated in chapter 3 section 7.6. The solution methodology is illustrated in Table 5.3.

Radial aquifer model

$$t_D = \text{Cte} \times \frac{kt}{\varphi \mu c r_o^2}$$

Field units:

Cte =	0.000264 for	(t in hours)
	0.00634	(t in days)
	2.309	(t in years)

(5.25)

$$U = 1.119 \times f \times \phi \times h \times c_t \times r_0^2 \ \text{(bbl/psi)} \tag{5.26}$$

U: constant for aquifer characteristics
t_D: Dimensionless time
f: circle fraction
φ: aquifer porosity (fraction)
h: aquifer thickness
$c_t = c_w + c_p$: total compressibility
r_0: boundary oil water radii

Linear aquifer model Field units:

$$t_D = \text{Cte} \frac{kt}{\varphi \mu c_t L^2} \tag{5.27}$$

$$U = 0.1781 \times W \times L \times h \times \varphi \times c_t \text{ (bbls/psi)} \quad (5.28)$$

W: channel width
L: aquifer length
h: aquifer thickness
φ: aquifer porosity (fraction)
$c_t = c_w + c_p c_w$: water compressibility
c_p: pore compressibility

5.10.7 Example of Water Entry Calculation

1) Calculation of the U constant

$$U = 1.119 \times f \times phi \times h \times c \times r_0^2$$

2)Dimensionless time calculation

$$t_D = 2.309 \times k \times t/(phi \times \mu \times c \times r_0^2)$$

t in years

3) Depletion steps determination

4) Determination r_{eD} radii ratio r_e/r_o (aquifer/oil)

5) Calculation W_D (HVE tables) cumulative water influx during time interval $T_d - t_{Dj}$ for which the depletion is acting (Appendix N)

6) Total cumulative water entry is the sum of the cumultaives due to each pressure step

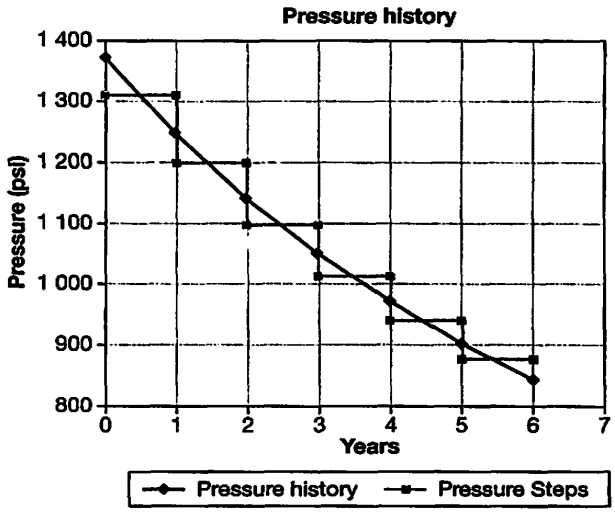

Table 5.3a Hurst Van Everdingen Calculation Methodology

EXAMPLE							
Time (an)	t_D	Pressure	Pressure steps	Delta P	Delta P	From the table	
						t_D	W_d for $r_{eD} = 5$
0	0	1 370	1 310	1 370-1 310	60	0	
1	5.67	1 250	1 197.5	1 310-1 197.5	112.5	5.67	4.89
2	11.34	1 145	1 100	1 197.5-1 100	97.5	11.34	7.47
3	17.01	1 054.5	1 014.5	1 100-1 014.5	85.5	17.01	9.11
4	22.68	974.5	942	1 014.5-942	72.5	22.68	10.17
5	28.35	909	880	942-880	62	28.35	10.83
6		851					

Table 5.3b Hurst Van Everdingen Calculation Methodology

time (year)	Water entry
1	$U \times (60 \times 4.89)$
2	$U \times (60 \times 7.47 + 112.5 \times 4.89)$
3	$U \times (60 \times 9.11 + 112.5 \times 7.47 + 97.5 \times 4.89)$
4	$U \times (60 \times 10.17 + 112.5 \times 9.11 + 97.5 \times 7.47 + 85.5 \times 4.89)$
5	$U \times (60 \times 10.83 + 112.5 \times 10.17 + 97.5 \times 9.11 + 85.5 \times 7.47 + 72.5 \times 4.89)$

At time 1 year, 60 psi pressure drop occurred so $W_e = U \times 60 \times 4.89$.

At time 2 year, the first perturbation continues to generate water at a higher rate (7.47) and a second pressure step (112.5 psi) generates a water flow at the initial rate 4.89.

At any time, the total cumulative water entry is equal to the sum of the individual contribution of each pressure drop.

4.89, 7.47, 9.11, 10.83 are found in the HVE table Appendix N.

Remark:
The calculation is performed independently of the oil reservoir performance except for the pressure history at the oil water contact that is an input for the model.

The reservoir water entry volume at any time is equal to the sum of the contribution of each pressure step.

5.10.8 Empirical Water-Encroachment Equations [107]

5.10.8.1 Schilthuis Steady State

The model assumes a time dependent flow rate in a steady state process. The water influx equation is approximated by:

$$\frac{dW_e}{dt} = A(P_i - P)$$

A: aquifer productivity constant

$$W_e(t) = A\int_0^t (P_i - P)\,dt \tag{5.29}$$

5.10.8.2 Hurst Steady State

Other empirical model the water influx is defined as:

$$\frac{dW_e}{dt} = \frac{A(P_i - P)}{\log(\alpha \times t)}$$

$$W_e = \int_0^t \frac{A(P_i - P)}{\log(\alpha \times t)}\,dt \tag{5.30}$$

A and α: constants

These empirical models are based on the assumption that the pressure disturbance at oil water contact travels instantaneously throughout the aquifer and reservoir system.

5.10.9 History Match

The generalized material balance equation is:

$$F = N \times E_t + W_e$$

F: Total underground fluid withdrawal
N: Initial oil in place volume at standard conditions
E_t: Total Expansion
W_e: reservoir cumulative water entry at pressure P

The independently calculated cumulative water influx history W_e is substituted into the material balance equation. Different cross check methods allow the user to verify the validity of the aquifer model parameters that have been chosen to estimate the water influx. The history match process consists of modifying the aquifer parameters until an acceptable match is obtained within engineering accuracy. There is not a unique solution to the problem but the retained parameters must look sound to the reservoir engineer and the geologist.

The equation can be written:

$$\frac{F - W_e}{E_t} = N \tag{5.31}$$

$(F - We)/E_t$ is constant $= N$

Therefore by plotting $(F - We)/E_t$ versus F is an horizontal line. This is the Campbell plot.

Other way to write the equation:

$$\frac{F}{E_t} = N + \frac{W_e}{E_t}$$

Points are expected to fit a straight line with a unit slope and an intersection with the Y axis equal to N, in a plot representing F/E_t versus W_e/E_t

Pressure Versus Reservoir Voidage Plot:

The method consists of plotting the reservoir pressure versus underground fluid withdrawal. Only one point location (pressure) exists for a defined reservoir voidage.

Reservoir voidage is defined as the total effective cumulative fluid produced from the reservoir at bottom conditions. The relationship between reservoir pressure and total reservoir voidage is unique even after a complex production history. The plot is an excellent tool to check production data consistency (Fig. 5.9).

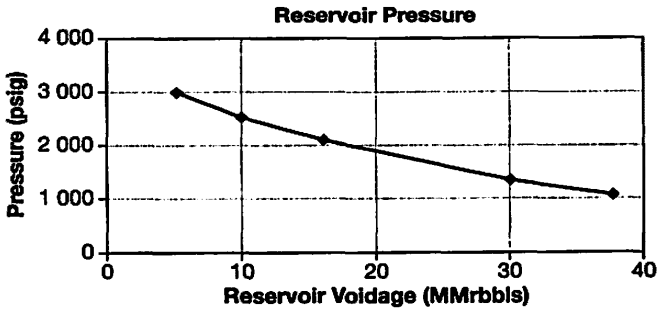

Figure 5.9 Reservoir pressure versus reservoir voidage.

5.10.9.1 History Match Procedure

Once an aquifer model is selected, the water influx is calculated with the HVE method. The Campbell and pressure versus voidage plots are drawn to check the data consistency within the material balance equation. The user modifies one or several aquifer parameters and rerun the calculations until a satisfactory match is obtained. Software manufacturers have built a

regression algorithm to perform an automatic match. The user needs to specify the parameters to regress on, and their limits.

MBAL program [107] uses the tank pressure plus production data as input for the model, and calculates the the main fluid production.

	Oil reservoir	**Gas reservoir**
Input	tank pressure	tank pressure
	G_p, G_{inj}	W_p
	W_p, W_{inj}	
Calculations	N_p	G_p equivalent
	W_e	W_e

For an oil reservoir, N_p is calculated from the generalized material balance equation assuming no water entry ($W_e = 0$) but using the field measured reservoir pressures, and G_p, W_p, G_i, W_{inj}. The calculation underestimates the cumulative oil produced on the plot reservoir pressure versus N_p. The plot is a PVT consistency check (Fig. 5.10).

Solving Equation (5.16) for N_p gives:

$$N_p = \frac{N\left\{(B_o - B_{oi}) + (R_{si} - R_s)\,B_g + mB_{oi}\left(\frac{B_g}{B_{gi}} - 1\right) + (1+m)\,B_{oi}\left(\frac{S_{wc}c_w + c_f}{1 - S_{wc}}\right)(P_i - P)\right\}}{(B_o - B_g R_s)} - \frac{(G_p - G_i)\,B_g + (W_p - W_i)\,B_w}{(B - B_g R_s)} \quad (5.32)$$

Analytical Method Example:

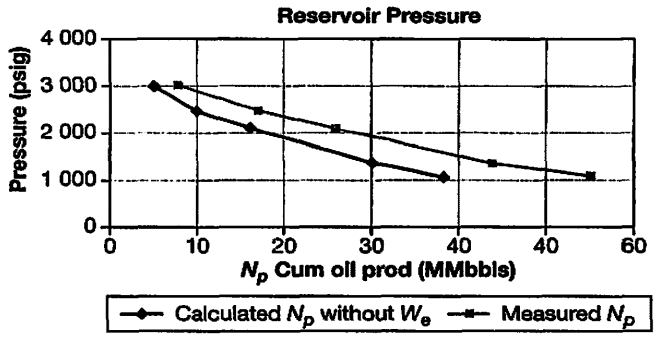

Figure 5.10 N_p Calculation.

Figure 5.10 shows calculated N_p below the measured N_p, proving the presence of an active aquifer. The history match consists of calculating a W_e history, and deduct N_p. History match is obtained when the calculated N_p overlays the measured N_p.

5.11 GAS RESERVOIR DRAINAGE

5.11.1 Generalities

A gas accumulation is often associated with an oil rim. It may happen that the gas oil contact is encountered a long time after the accumulation discovery.

The different gas definitions refer to the PVT behavior of the gas which depends on the initial reservoir gas composition, initial reservoir pressure and temperature.

It must be noted that it is very important for the operator to know the initial hydrocarbon nature (vapor or critical fluid) in the reservoir and its behavior during the production process.

The hydrocarbon properties are a key factor for the development decisions. The objective is to recover the maximum hydrocarbon mass under sound economical conditions.

The difficulty with gas reservoirs is storage and transport. Both are very expensive compared with oil. Therefore before developing a gas reservoir, the company negotiators must find a client to buy the gas and agree on a long term contract before starting any field development works. Usually negotiations and field evaluation studies are carried out simultaneously. Contract terms are also continuously updated with the latest reservoir evaluations.

5.11.2 Gas Types (Fig. 5.11)

Dry Gas Reservoir:

A reservoir gas is qualified as dry when two conditions prevail:

- The gas in the reservoir is always monophasic whatever the reservoir pressure.
- At surface conditions, the produced well stream is also monophasic (no liquid condensation occurs in the separator).

Wet Gas Reservoir:

A reservoir gas is qualified as wet when the two conditions are fulfilled:

- The gas in the reservoir is always monophasic whatever the reservoir pressure.
- At surface conditions, associated liquid is produced simultaneously with gas.

Gas Condensate Reservoir:

A reservoir gas is qualified as gas condensate when the two conditions are fulfilled:

- Liquid deposition in the reservoir occurs with reservoir pressure decline.
- At surface conditions, associated liquid is produced simultaneously with gas.

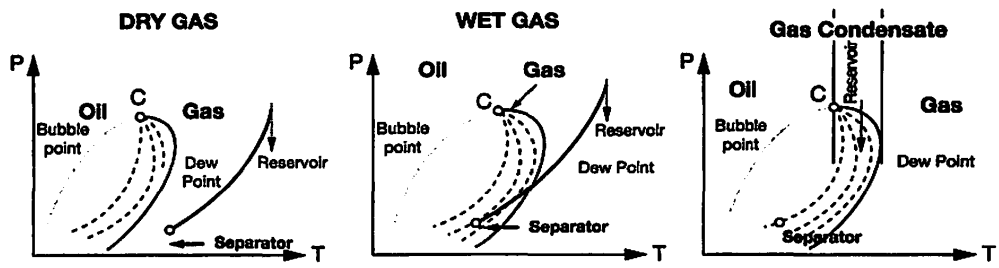

Figure 5.11 Dry gas, Wet gas and Gas Condensate.

5.11.3 Definition Review

The gas formation volume factor is defined as: $B_g = \frac{V_{res}}{V_{std}}$

gas FVF = gas volume ratio at reservoir conditions to standard conditions.

The real gas equation of state is: $pv = ZRT$

p:	gas absolute pressure	psia	bars(a)	Pa(a)
v:	gas volume	cu. ft	m^3	m^3
R:	gas constant			
Z:	gas compressibility (gas deviation factor)			
T:	absolute gas temperature	°Rankine	K	K

Writing the equation for the same gas at two conditions: reservoir and standard conditions gives:

$P_{res} \times V_{res} = Z_{res} R T_{res}$

$P_{std} \times V_{std} = Z_{std} R T_{std}$

At low pressure, real gases behave like ideal gas. Then $Z_{std} = 1$

The B_g definition becomes:

$$B_g = \frac{V_{res}}{V_{std}} = \frac{P_{std}}{T_{std}} Z \frac{T_{res}}{P_{res}} \tag{5.33}$$

B_g depends on the standard conditions chosen, gas composition (Z), and reservoir conditions (pressure, temperature).

Standard conditions used in the industry:

	Field units	**metric**	**SI**
P_{std} = (1 atm)	14.7 psia	1.01325 bars	101 325 Pa
T_{std} =	520°R (60°F + 460)	288 K (15°C + 273)	288 K

Remark: the standard pressure may also be considered as P_{std} = 100 kPa.

B_g is then $B_g = \text{Cte}\frac{ZT}{P}$

Cte = 0.028269 for field units
0.00352 metric units
351.8 SI

At standard conditions, 1 gas mole occupies 23.645 dm^3.

Following the definitions above, all gas reservoir studies must be conducted with absolute reservoir pressures.

5.11.4 Material Balance

Only a dry gas reservoir case is discussed in this chapter. Rock and connate water compressibilities are neglected.

Considering an initial gas volume G, and G_p cumulative gas produced at time t_p the material balance principle consists of writing that the container volume does not change between the initial and final time t_p.

Assumptions:

Dry gas

Closed reservoir (no water influx)

At reservoir conditions.

Initial gas in place at Pi = gas volume left in reservoir at P

$$GB_{gi} = (G - G_p)\, B_g$$

B_{gi}: gas FVF at initial pressure
B_g: gas FVF at pressure P
P_i: initial reservoir pressure
G: initial gas in place
G_p: cumulative gas produced

Therefore

$$G_p = G\left(1 - \frac{B_{gi}}{B_g}\right) \tag{5.34}$$

$$B_{gi} = \frac{P_{std}}{P_i}\frac{Z_i T}{T_{std}} \qquad B_g = \frac{P_{std}}{P}\frac{ZT}{T_{std}}$$

Then

$$G_p = G\left(1 - \frac{Z_i}{P_i}\frac{P}{Z}\right) \tag{5.35}$$

The cumulative gas produced is a linear function of P/Z

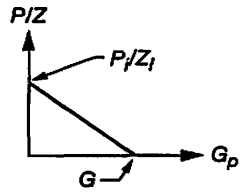

Figure 5.12 P/Z versus Cumulative Gas Produced.

The intersection with the horizontal axis gives the initial gas in place G (Fig. 5.12).

The reservoir monitoring activity consists of plotting P/Z versus the cumulative gas produced G_p and cross check the "dynamic initial gas in place" value, seen by the material balance calculation, with the "static" gas in place evaluation performed by the geologist.

Case of a dry gas reservoir with water influx.

The previous material balance equation is modified as:

$$GB_{gi} = (G - G_p)\, B_g + W_e$$

$$G_p = G\left(1 - \frac{B_{gi}}{B_g}\right) + \frac{W_e}{B_g} \qquad G_p = G\left(1 - \frac{Z_i}{P_i}\frac{P}{Z}\right) + \frac{W_e}{B_g} \tag{5,36}$$

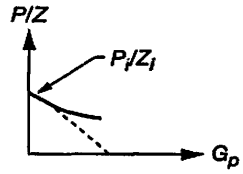

Figure 5.13 P/Z plot versus Gp with an aquifer.

The reservoir pressure is maintained at a higher level than in the previous case due to the water influx (Fig. 5.13).

5.11.5 Recovery Factor for Gas Reservoirs

Recovery factor is defined as G_p/G.

5.11.5.1 No water influx

$$\frac{G_p}{G} = \left(1 - \frac{Z_i}{P_i}\frac{P_a}{Z_a}\right) \tag{5.37}$$

At abandonment reservoir pressure P_a, G_p is the cumulative gas produced (reserves)
Z_i: initial gas compressibility at P_i
Z_a: final gas compressibility at P_a

when $Z_i \approx Z_a$ then

$$\frac{G_p}{G} = \left(1 - \frac{P_a}{P_i}\right) \tag{5.38}$$

Consequently a simple calculation of the recovery factor (then reserves) can be performed when initial and abandonment reservoir pressures are known.

Reservoir depletion is only due to the gas expansion. The recovery factor is independent of rate. Recovery factor may be as high as 80 to 95%.

5.11.5.2 With water influx

Recovery factor

$$\frac{G_p}{G} = \left(1 - \frac{Z_i}{P_i}\frac{P_a}{Z_a}\right) + \frac{W_e}{GB_{ga}} \tag{5.39}$$

The recovery factor is more difficult to estimate since the water entry term is not known. In addition, the fact of having an aquifer invading the initial gas zone, water will trap high pressure reservoir gas in the porous media which in turn will jeopardize the recovery factor. Free water moving in the reservoir means also production wells invaded by water and killed. Watered-out wells will have to be abandoned and replaced by new wells drilled higher up in the structure. The consequence of such a scenario is difficult to forecast; the recovery factor may fall as low as 50 to 60%.

The recommendation when the problem occurs is to produce the gas at a very high rate, then depleting the reservoir quickly and hoping that the aquifer will react slowly. The ultimate recovery factor (so reserves) is dependent on the field production rate.

With a production history, W_e can be estimated in the same way as for oil reservoirs by using the Hurst Van Everdingen method.

5.11.6 Wet Gas Reservoir

In of such reservoir, there is no phase change in the reservoir; therefore the reservoir hydrocarbon composition is constant. At surface, liquid and gas quantities produced will depend on the separator conditions (pressure and temperature) and on the reservoir pressure.

A table giving the liquid and vapor fractions as a function of reservoir pressure can be built from a PVT package. The table is used to predict the gas and liquid production rates.

5.11.7 Gas Condensate Reservoir

The hydrocarbon system is characterized by a high dew point pressure and a low dew point pressure.

Usually such reservoir is at an initial pressure equal to the hydrocarbon dew point pressure. As soon as production starts, heavy hydrocarbon components deposit in the porous media. This liquid being at low saturation is never recovered under practical reservoir conditions. To study such reservoirs, it is necessary to use a PVT package and a compositional reservoir simulator.

5.11.8 Development of Gas Reservoirs

Before developing a gas reservoir, a long term contract between the operator and the gas buyer must be concluded. Specific terms are used in the contract which must be known by all those who participate in the project.

DCQ Delivered Contract Quantity:

This is the average gas rate to be delivered to the client at a particular location at a specified pressure during the plateau duration required (15 to 20 years usually).

Swing or Peak Rate

At any time, the operator must be able to deliver a higher rate than the DCQ during a short period. This can be expressed as a gas rate (peak rate) or as a percentage of the DCQ (swing). For example in winter gas demand is higher than in summer. Practically, the field potential must match the peak rate permanently.

Well Potential:

The well potential is the maximum gas rate possible produced by the well with all the production constraints honored.

Constraints are:

- Minimum well head flowing pressure.
- Maximum gas velocity through tubing and surface facilities < Vmax.

Field Potential:

The field potential is the maximum gas rate possible produced by the field when all producers flow at their potential.

5.11.9 Gas well Productivity or IPR *(Inflow Performance Relationship)*

Gas has a very low viscosity, therefore when submitted to a pressure gradient; gas flows at high velocity through the porous media compared to liquid. Similarly to the theory of fluid mechanics, two flow regimes may occur laminar or turbulent. The highest gas velocity takes place in the vicinity of the well bore. In the laminar regime, only the viscous forces generate a loss of head through the porous media. High velocity and tortuous porous media may provoke a turbulent regime. In that case, an additional pressure drop due to the turbulence appears.

5.11.9.1 Quadratic Deliverability Relationship (see chapter 3, paragraph 13)

Based on the fluid mechanics, an expression was developed to quantify the loss of head of a gas well. It is called the quadratic equation.

$$P_r^2 - P_{wf}^2 = AQ_g + BQ_g^2 \tag{5.40}$$

P_r:	average reservoir pressure	psia	bar or kPa
P_{wf}:	stabilized bottom hole flowing pressure	psia	bar or kPa
Q_g:	stabilized gas flow rate at std conditions	Mscfd	m^3/d

A&B: constants determined from well testing
AQ_g: laminar component of the pressure drop
BQ_g^2: turbulent component of the pressure drop

The deliverability equation can be written as: $\dfrac{P_r^2 - P_{wf}^2}{Q} = A + BQ$

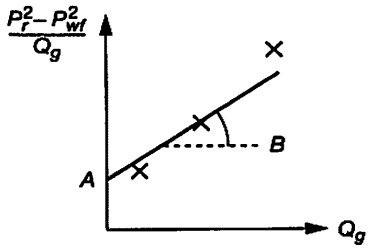

Figure 5.14 Deliverability Plot.

The plot $(P_r^2 - P_{wf}^2)/Q_g$ versus Q_g is a straight line (Fig. 5.14).

In the field a back pressure test is carried out at three different stabilized rates. From the plot, A and B are deducted.

In practice the plot may show a negative slope. This would mean a negative turbulent component which is nonsense. In such a case, the quadratic equation cannot be used.

5.11.9.2 Empirical Deliverability Relationship

From a large number of observations, an empirical deliverability relationship is expressed in the form as:

$$Q_g = C\left(P_r^2 - P_{wf}^2\right)^n \tag{5.41}$$

Q_g:	stabilized gas flow rate at std conditions	Mscfd	m^3/d
P_r:	average reservoir pressure	psia	bar or kPa
P_{wf}:	stabilized bottom hole flowing pressure	psia	bar or kPa
C:	coefficient which describes the position of the deliverability line		
n:	exponent which describes the inverse of the slope of the deliverability line		

n varies from 1 for a completely laminar flow, to 0.5 for fully turbulent flow. It can be considered as a measurement of the degree of turbulence.

C and n may be considered to be constant for a limited range of flow rates.

Eq. (5.41) can be written as:

$$\log(Q_g) = \log C + n\log(P_r^2 - P_{wf}^2)$$
$$y = b + ax$$

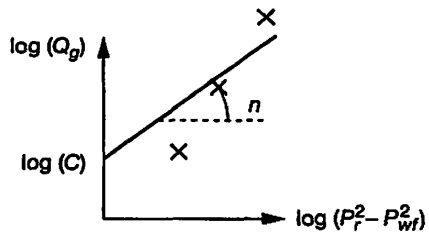

Figure 5.15 Deliverability Plot.

Conducting a production test at three stabilized rates, plot on Figure 5.15 can be drawn.

Plot on Figure 5.15 gives the C and n parameters characterizing the reservoir deliverability equation.

The Absolute Open Flow (AOF) potential of a well is defined as the rate at which the well would produce if it was possible to set the atmospheric pressure at the sand face. In the deliverability equation, $P_{wf} = 1$ atmosphere. This parameter is a criterion used by the regulatory authorities to compare well capacities, and define the allowable producing rates.

For a laminar flow regime ($n = 1$), C is determined from the radial flow of gas theory [2]:

$$C = \frac{0.000703 k_g h}{zT\mu Ln\left(\frac{r_d}{r_w}\right)} \quad \text{(Field units)} \tag{5.42}$$

k_g: permeability to gas mD
μ: gas viscosity cp
h: sand thickness ft
z: compressibility factor
Q_g: gas flow rate at std conditions Mcf/d
P: absolute pressure psia
T: absolute flowing temperature °R

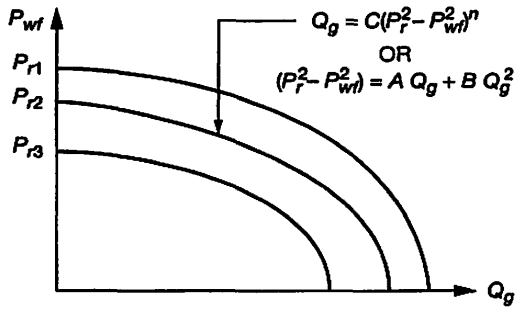

Figure 5.16 Deliverability Equation.

Figure 5.16 shows the deliverability curve for different reservoir pressures $P_{r1} > P_{r2} > P_{r3}$.

5.11.10 Well Operating Conditions, Determination of Well Quantity

Several production wells are necessary to honor the field rate. The number of wells depends on the formation deliverability capacity, on the well configuration (depth, tubing internal diameter) and other constraints like the flowing pressure at the delivery location. The project engineer must make sure that no bottle neck exists in the production line from the well completion to the delivery point.

From a selected well configuration, a calculation called Vertical Lift Performance (VLP) is carried out. Considering the production tubing plus some surface equipment, the calculation consists of determining the bottom hole flowing pressure when a fixed well head flowing pressure has been selected for different gas flow rates. This is also called the loss of head calculation.

Remark: the gas rates must cover the whole range of expected flow rates.

Figure 5.17 exhibits the bottom hole flowing versus gas rate for different fixed well head flowing pressures (1 000, 500, 250 psia).

The calculation results are presented in the form of tables associating a list of gas flow rates, a list of well head flowing pressures and a matrix of corresponding to the bottom hole flowing pressures.

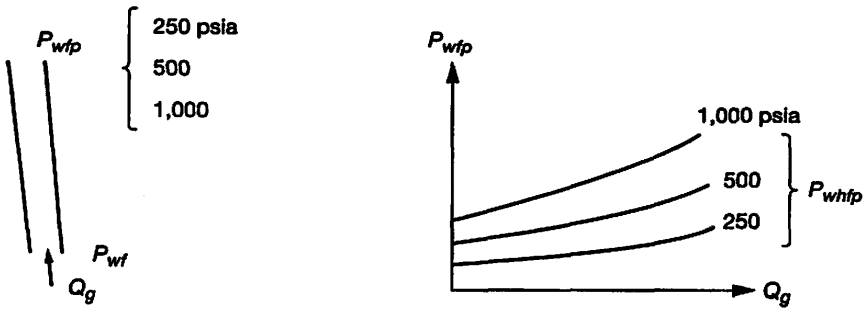

Figure 5.17 Tubing Performance Curves.

Finally by combining the deliverability curve and the vertical lift performance on the same plot, the intersect of the two curves gives the proper gas rate and bottom hole flowing pressure for the selected conditions (static reservoir pressure, and well head flowing pressure).

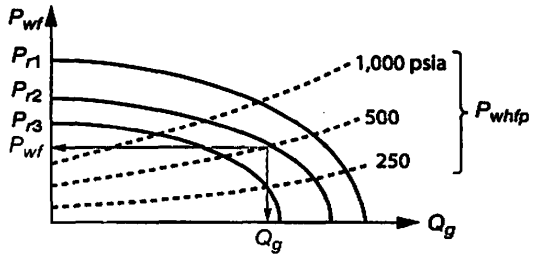

Figure 5.18 Well Operating Point Determination.

The necessary number of wells to honor the field rate is equal to the field rate divided by the individual well rate. It has to be noted that the production tubing internal diameter has a large impact on the loss of head then on the necessary number of wells. When the reservoir pressure declines, the individual rate decreases. The solution to honor the field rate is to drill new wells. At a certain point, it is useless to increase the number of wells because the reservoir pressure is too low. It is then necessary to accept a lower well head flowing pressure and compensate the flowing pressure loss by installing compressor units.

5.11.11 Development, Conclusion

Gas is not easily cheaply stored and transported like oil. A gas reservoir development plan is carried out in parallel to the necessary negotiations with one or several clients. Data gathered

in the appraisal wells have a direct impact on the terms of the contract. For example, the DCQ to deliver and the contract duration are dependent on the initial gas in place estimation. Also the gas characteristics defined in the contract are dependent on the actual field gas properties. Delivery conditions (rate and pressure) are dependent on the loss of head in the production tubing, and in surface facilities up to the delivery location. Planning compression units may be necessary to keep honoring the contract terms after some depletion has taken place.

Similarly to oil reservoirs, the development approach is different when the project is offshore or on land.

An accurate monitoring is necessary for allocation determination when the revenues must be shared by several owners.

Building a development plan is a team work including many specialists that must to work together.

5.12 SUMMARY

The drainage mechanisms are:

Compaction drive	*page 27*
Monophasic expansion	*page 249*
Solution gas drive	*page 251*
Gas cap expansion	*page 255*
Water drive	*page 255*
Diffusion	*page 236*
Imbibition (fractured reservoirs)	*page 230*
Gravity drainage	*page 236*

CHAPTER 6

Reservoir Simulation

6.1 GENERALITIES

The goal of the chapter is to demystify the tool "reservoir simulator" and to emphasize that simulation associated with material balance study are the basic techniques necessary for an engineer to be familiar with.

During the last 30 years, the numerical techniques and data management used in simulators improved with the continuous increasing performances offered by the computer industry. Many of them have been abandoned and new more sophisticated were developed to simulate complex geology, complex well design and fluid behavior.

The use of a reservoir simulator is a difficult task and necessitates from the engineer a minimum of investment into the techniques that are used in simulation. The objective is to understand and to master the software possibilities and limits.

Very often the engineer's energy is focused on 'how to get the software running' losing the practical reservoir engineering field common sense, and order of magnitude of results.

Reservoir engineering and reservoir simulation are not exact sciences. Input data are results obtained from geophysics, geology, petrophysics, fluid behavior studies and production engineering techniques. Each of these techniques has their weaknesses due to necessary interpretation methods based on physical indirect measurements.

The primary objective of a reservoir study is to predict future performance of a reservoir and to improve economically the ultimate recovery.

Before investing into a development plan, the corporate management needs to evaluate the economical aspect of the project. To achieve this goal, a reservoir study must be carried out, taking into account all the available data from the reservoir and technical experience gathered from analogous reservoir behavior.

A reservoir simulator is a computer programme which offers multiple possibilities and translates the basic physical laws that govern fluid flow through porous media, the conservation mass law and the diffusivity equation in addition to the fluid behavior.

The reservoir simulator associated with a data set relative to a reservoir, constitutes what is called a reservoir model. The model concentrates all the knowledge that has been gathered by the geophysicist, the geologist, petrophysicist, reservoir engineer and production engineer. The consequence is that a reservoir study must be conducted as a team work in which all the specialists must communicate, react to correct and improve the reservoir model. The key factor for the organization is the data management. Software manufacturers offer now data bases that allow manipulation of large amount of data very efficiently.

The complexity of the programme has its origin in the large amount of data involved to characterize a reservoir and the numerous options available needed to conduct a reservoir study.

The formula GI = GO Garbage In = Garbage Out is always valid.

This chapter is organized in the following way:

- General concepts used in all simulators.
- Data from a general simulation data set (static data, recurrent data) are reviewed.
- Special topics used in simulation are explained.

The theoretical aspects of the reservoir simulation developed in this chapter are limited to the one used in the most popular commercial simulators: ECLIPSE (Schlumberger) and VIP (Halliburton Landmark).

6.2 INTRODUCTION TO RESERVOIR SIMULATION

The reservoir simulation technique has been dependent on the computer industry development of hardware and software.

Simulation is based on the discretization of space and time. The objective is to convert the diffusivity equation into data that can be treated numerically by a computer.

The first reservoir simulators appeared in the 1960's when a series of so called scientific computers were available. The discretization of space and time is a materialization of the finite difference technique to solve the diffusivity equation.

Different algorithms were developed. Each algorithm, or so called numerical scheme is characterized by its accuracy, its application limits and hardware requirements (CPU work, main memory, extended and virtual memory, disk capacity). The maximum problem size that can be treated is limited by the computer performances, storage and the software result handling facilities.

Figure 6.1 illustrates the evolution of the hardware used for reservoir simulation from the 1960's to present days.

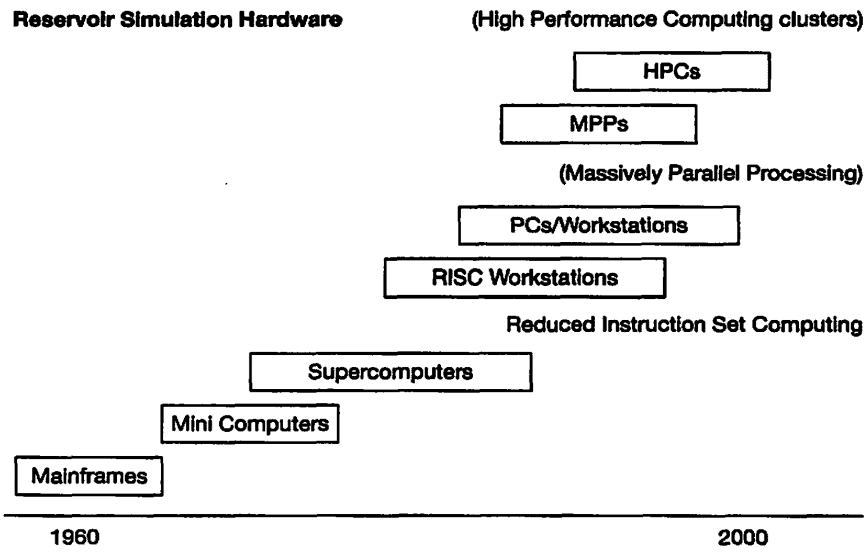

Figure 6.1 Reservoir Simulation Hardware.

6.3 TRANSMISSIVITY, PERMEABILITY, MOBILITY, TRANSMISSIBILITY

Some confusion exists in the vocabulary used by ground water engineers and reservoir engineers. Even in the world of reservoir simulation, the same word may have different meanings when employed by different authors.

6.3.1 Transmissivity, Permeability

Darcy's Law is a generalized relationship for flow in porous media. It shows the volumetric rate is a function of the flow area, elevation, fluid pressure and to proportionality constant. It may be stated in different forms depending on the flow conditions.

One dimensional flow column filled with water at surface is shown on Figure 6.2.

For a finite 1-D flow, it may be stated:

$$Q = KA\frac{\Delta h}{L} \text{ or in differential form: } Q = KA\left(\frac{dh}{dl}\right) \tag{6.1}$$

Q: discharge (volume of water per unit time) m^3/s or ft^3/s
K: hydraulic conductivity (dependent upon size and arrangement of pores, fluid dynamics such as viscosity, density and gravitational effects)
A: cross-sectional area (at a right angle to ground water flow direction) m^2 or ft^2
dh/dl hydraulic gradient (this is the common notation for a change in head per unit distance)

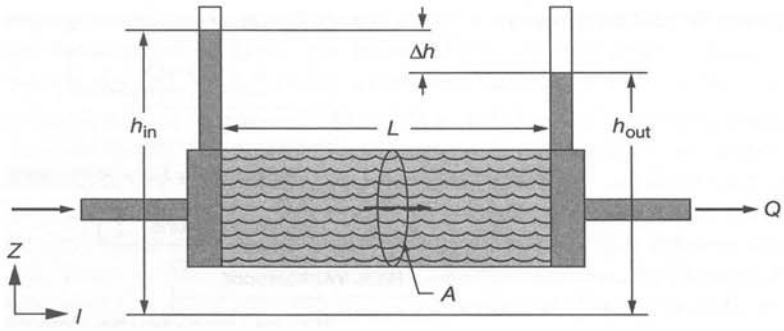

Figure 6.2 Horizontal Core Sample.

The hydraulic head at a specific point h, is the sum of the pressure head and the elevation correction or:

$$h = \frac{p}{\rho g} + z \quad \text{or} \quad h = \frac{p}{\gamma} + z \tag{6.2}$$

	SI units:	English units
p = water pressure	Pa	lb/ft^2
ρ = water density	kg/m^3	–
z = elevation	m	ft
γ = water specific weight	–	lb/ft^3
g = acceleration	m/s/s	

The flow is a function of the hydraulic head change.

Eq. (6.1) can be written:

$$K = \frac{Qdl}{Adh} \tag{6.3}$$

Dimensional analysis gives: $$|K| = \frac{L^3T^{-1}L}{L^2L} = LT^{-1}$$

Combining Eqs. (6.1) and (6.2):

$$Q = KA\frac{\Delta p}{\rho g L} \tag{6.4}$$

K: hydraulic conductivity has a dimension of a velocity ft/d or m/s

The Darcy flux is defined as the volumetric flow per unit area:

$$q = Q/A \quad \text{m/s or ft/s} \tag{6.5}$$

The Darcy flux is not the velocity of the water in the pores. The solid matrix takes up some of the flow area. The average pore water velocity is termed the seepage velocity, v, is given by:

$$v = Q/A = q/\varphi \tag{6.6}$$

φ: porosity of the media

Transmissivity:

In saturated groundwater analysis with nearly horizontal flow, it is common practice to combine the hydraulic conductivity with the aquifer thickness, b into a single variable:

$$T = K \times b \tag{6.7}$$

T: Transmissivity m^2/s ft^2/d

Transmissivity T (m^2/sec, or ft^2/d) is a hydraulic property, which measures the ability of the aquifer to transmit ground water throughout its entire saturated thickness. It is defined as the product of the hydraulic conductivity K (m/sec) and the saturated thickness b (m), in the direction normal to the base of the aquifer.

Permeability:

When the fluid is other than water at standard conditions, the conductivity is replaced by the permeability of the media.

The Darcy law to define permeability was expressed in chapter 3 as:

$$Q = k\frac{\Delta P}{\mu L}A \tag{6.8}$$

k: absolute permeability of the media with 100% fluid saturation
μ: fluid viscosity
ΔP: pressure gradient

Comparing Eq. (6.4) and (6.8) the relationship between hydraulic conductivity and absolute permeability is deducted.

$$K = \frac{k\rho g}{\mu} \text{ or } K = \frac{kg}{\nu} \tag{6.9}$$

μ is the dynamic viscosity of water (Pascal seconds Pa.s, poise or ldf.s/ft^2)
ν is fluid kinematic viscosity, (m^2/s or ft^2/s)

Remark
Hydraulic conductivity and Transmissivity are properties used in hydrogeology and ground water techniques but not used in reservoir engineering.

6.3.2 Mobility, Transmissibility

Mobility of phase l is defined as:

$$\lambda_l = \frac{k \times k_{rl}}{\mu_l} \tag{6.10}$$

λ_l: fluid mobility
k: absolute permeability
k_{rl}: relative permeability of phase l
μ_l: fluid viscosity

Transmissibility from Darcy's law expressed between centers of block i and block $i+1$ is: (see Chapter 3, paragraph 12)

$$q = k_i \times A_i \frac{p_i - p_{\text{int}}}{\Delta x_i / 2} = k_{i+1} \times A_{i+1} \frac{p_{i+1} - p_{\text{int}}}{\Delta x_{i+1} / 2} \tag{6.11}$$

(p_{int}: pressure at interface)

Eq. (6.11) can be written *(off the grid system)*

$$q = \lambda \times (P_i - P_{i+1})$$

Transmissibility of phase l is defined as:

$$T_l = \frac{k \times k_{rl}}{\mu_l \times B_l} \tag{6.12}$$

"Transmissibility" includes the formation volume factor term, while "mobility" does not.

There are several possible mobilities:

- *Upstream*: fluid mobility based on relative permeability and viscosity computed from fluid saturations and pressures in the upstream cell i.
- *Downstream*: fluid mobility based on relative permeability and viscosity computed from fluid saturations and pressures in the downstream cell $i+1$.
- *Average*: a weighted average in which the mobility is a function of both i and $i+1$ cells.
- *Harmonic*: a harmonic average value where the mobilities are averaged as series resistances.

The corresponding flow equations are [81]:

$q = \lambda_i (P_i - P_{i+1})$	Upstream
$q = \lambda_{i+1} (P_i - P_{i+1})$	Downstream
$q = \left[w\lambda_i + (1-w)\lambda_{i+1} \right] \times (P_i - P_{i+1})$	Weighted
$q = \frac{\lambda_i \lambda_{i+1}}{(\lambda_i + \lambda_{i+1})} (P_i - P_{i+1})$	Harmonic

w is a weighting parameter. If $w = 1$, the equation reverts to the upstream, and for $w = 0$, the equation reverts to the downstream value.

In practice the downstream mobility is not used. The harmonic average may lead to erroneous results. Software manufacturers use upstream mobilities.

The value of absolute permeability is assigned to the centre of the block and the pressure dependent properties are evaluated from the block pressure p_i. The mobility λ_i is assumed to be constant within the block, and is used to compute lambda $i+$ or $-^1/_2$. The approximation is satisfactory if the properties do not change too much between two adjacent blocks. When a large permeability contrast and uncertain data exists between two blocks, large errors may result.

Remark:
The word "transmissibility" is often used in reservoir simulation technique as the constant value characterizing the connection between two adjacent blocks. The value is calculated from the block geometry and the absolute block permeability.

6.3.3 Transmissibility in reservoir simulation [108, 109]

The term "inter block transmissibility factor" is often used in simulation technique

The transmissibility factor was calculated for a regular grid mesh in the chapter 3 "Fluid Flow in Reservoirs" from the half connection concept.

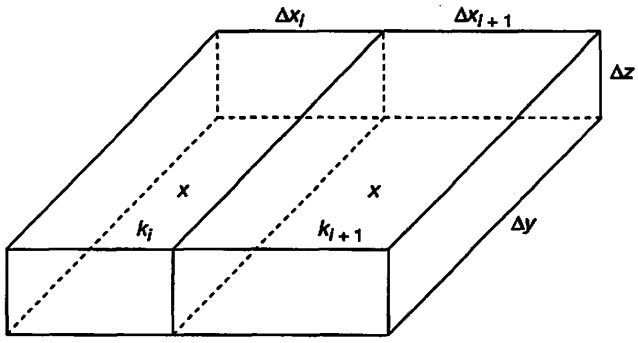

Figure 6.3 Two neighbor blocks.

To calculate the transmissibility between two block centers (Fig. 6.3), Darcy's law is used from the block centre to the interface and from the interface to the adjacent block centre. The block permeabilities used are the absolute permeability of each block so the transmissibility value is independent of the filling fluids.

$$T_i = k_i \frac{\Delta y \times \Delta z}{\Delta x_i / 2} \qquad T_{i+1} = k_i \frac{\Delta y \times \Delta z}{\Delta x_{i+1} / 2}$$

And:

Resistance to flow

$$\frac{1}{T_{i,i+1}} = \frac{1}{T_i} + \frac{1}{T_{i+1}} \qquad T_{i,i+1} = \frac{T_i \times T_{i+1}}{T_i + T_{i+1}} \tag{6.13}$$

Where

T_i: half connection of bock i from centre to interface
T_{i+1}: half connection in block $i + 1$ from interface to block centre
$T_{i,\,i+1}$: inter-block connection between the two block centers
$1/T_i$: flow resistance in block i

These relationships need modification in the following cases:

- Presence of a non regular grid.
- Presence of a depth difference between adjacent blocks.
- Net over gross thickness different of 1.

$$T_i = k_i \frac{\Delta y_i \times \Delta z_i}{\Delta x_i / 2} \times NTG_i \times DIPC \qquad T_{i+1} = k_{i+1} \frac{\Delta y_{i+1} \times \Delta z_{i+1}}{\Delta x_{i+1} / 2} \times NTG_{i+1} \times DIPC \quad (6.14)$$

NTG_i: net to gross in block i
$DIPC$: dip correction

In the case of a net to gross thickness < 1, the net thickness is concentrated symmetrically at the centre of the block in the vertical direction.

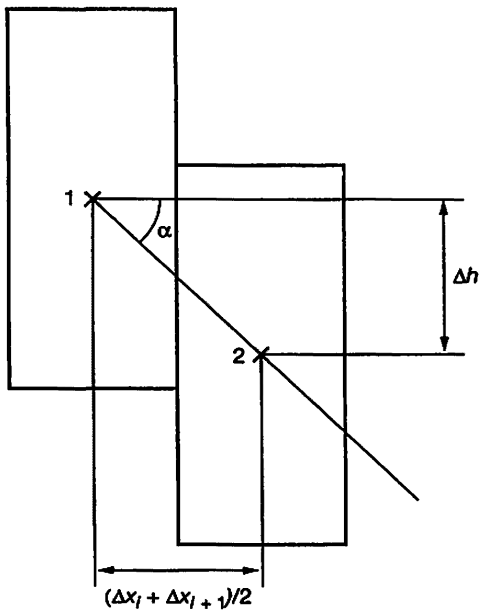

Figure 6.4 Dipping neighbor blocks.

In this context, transmissibility depends only on block geometry and absolute permeability.

Considering two neighbor blocks simulating a formation dipping bed (Fig. 6.4), the resistance to flow is higher than in the previous case by the factor 1/cos α.

$$\text{Resistance to flow } r = \frac{1}{T\cos\alpha}$$

Therefore the inter-block transmissibility between block i and $i+1$, becomes:

$$T_{i,i+1} = \frac{T_i \times T_{i+1}}{T_i + T_{i+1}} \times \cos^2\alpha \tag{6.15}$$

dip correction is calculated as:

$$\text{Dip correction} = \cos^2\alpha = \frac{\left[\frac{\Delta X_i + \Delta X_{i+1}}{2}\right]^2}{\left[\frac{\Delta X_i + \Delta X_{i+1}}{2}\right]^2 + (\Delta h)^2} \tag{6.16}$$

Eqs. (6.15, 6.16) are used in ECLIPSE to calculate the inter-block transmissibility (in x and y directions) in the option called 'OLDTRANR'.

'OLDTRANR' in ECLIPSE, calculates transmissibility between two adjacent cells based on the harmonic average intern transmissibility of each cell.

'OLDTRAN' in ECLIPSE, calculates transmissibility between two adjacent cells from the harmonic average permeability of each block weighted by the respective effective block thicknesses.

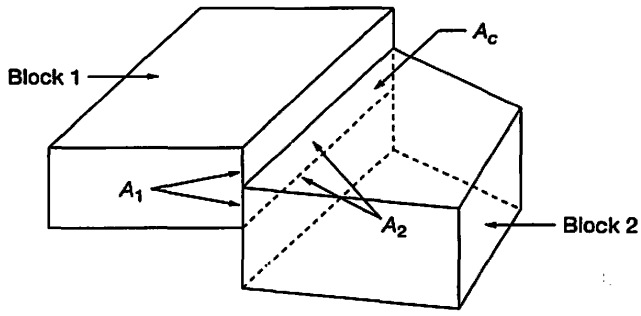

Figure 6.5 Irregular grid blocks.

Considering two irregular neighbor grid blocks Figure 6.5.

The integration of differential equations in the divergent form demands the calculation of fluxes in the control volume interfaces. As the domain may be heterogeneous, sometimes with great differences in terms of permeability in adjacent grid-blocks, the definition of

average properties in the interface may result in errors in the flux calculation. The appropriate procedure is to calculate transmissibility as the inverse of the resistance in each control volume.

Resistance to flow from block centre 1 to interface is: $r_1 = \frac{A_1}{T_1}$

Resistance to flow between the interfaces to block centre 2 is: $r_2 = \frac{A_2}{T_2}$

The two blocks exchange fluid through the common area A_c.

The effective resistance to flow from block 1 to block 2, taking into account the contact area A_c between the blocks is:

$$r_{1,2} = r_1 + r_2 = \frac{A_1}{A_c T_1} + \frac{A_2}{A_c T_2} \quad \text{then} \quad T_{1,2} = \frac{A_c}{\frac{A_1}{T_1} + \frac{A_2}{T_2}} \tag{6.17}$$

A_c: contact surface
A_1, A_2: complete surface of each neighbor
T_1, T_2: inner transmissibilities

If the adjacent blocks are in full contact the interface areas, $A_1 = A_2 = A_c$.

Transmissibility calculation becomes:

$$T_{1,2} = \frac{A_c}{\frac{A_1}{T_1} + \frac{A_2}{T_2}} = \frac{T_1 \times T_2}{T_1 + T_2}$$

For orthogonal grids with fully coincident interfaces, this procedure leads to the exact flux determination. On the other hand, for non-orthogonal grids, grids with partial contact between the grid-blocks or local refinement, the flux surfaces need to be defined.

If $A_1 \neq A_2 \neq A_c$ and locally non-orthogonal, there is the need of not only a surface multiplier but also of some type of projection of the surface. In this case, the transmissibility will not tend to the exact value with grid refinement, which would be expected in any numerical solution. Thus, when non-orthogonal grids and/or grids with partial contact are used, the flux calculation cannot be exactly calculated if only two grid points are used.

6.3.4 Corner point geometry [110]

The use of rectangular grids associated with the standard finite difference method does not allow a perfect representation of reservoir geological features and reservoir description in particular for faults. Flexible grid such as corner point geometry is used to improve accuracy.

The corner point geometry can represent complex reservoir geometries by specifying the corners of each grid block in grid building (Fig. 6.8). It is then possible to simulate non neighbor connecting flow across a fault.

The simulator determines for each grid volume the distance between the two opposite face barycentres, the transversal area in the flux direction and the transmissibilities. The transversal area in the flux direction is calculated by contact area of adjacent volumes.

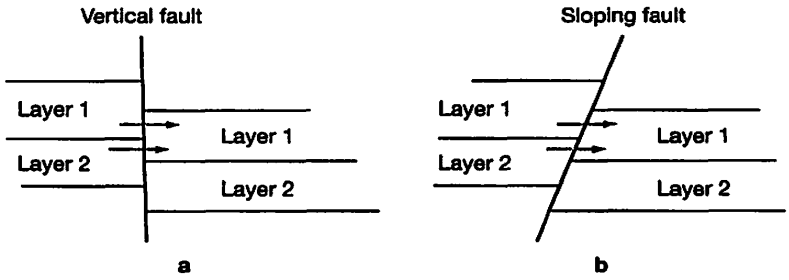

Figure 6.6 Non neighbor connections.

Figures 6.6a and b illustrate the occurance of non neighbor connections in the case of a vertical or a sloping fault. In the case of non sealing fault, fluid flow takes place from layer 2 on the left of the fault into layer 1 on the right side of the fault. The user has a direct control on the possibility to allow flow or not with the use of a specific keyword.

To calculate the transmissibility between two blocks, the coordinates of the centroid of the two blocks are first determined. Then half connection from the centroid to the right face is calculated. The area considered is the perpendicular area to the flow between the two centroids. Consequently, the dip correction is automatically taken into account.

Finally the full transmissibility between adjacent grid blocks is equal to the harmonic average of the two half transmissibilities. The described procedure is called 'NEWTRAN' in ECLIPSE.

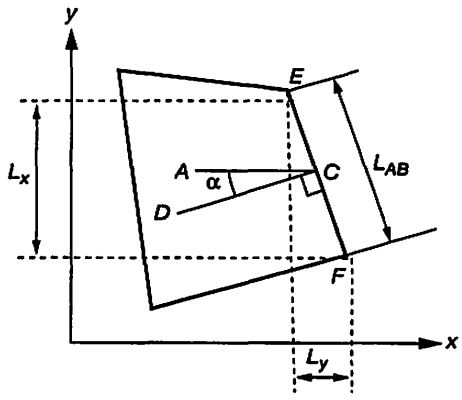

Figure 6.7 Non regular grid block.

Considering the non regular grid block shown in Figure 6.7. The right face is the interface between block A and block B (not shown). Point A is the centroid of block A. AC is the vector from A to C (center of EF). CD is a vector normal to the right edge, whose length is equal to the right edge.

$$\left|\overline{CD}\right| = L_{AB} \qquad \left|\overline{AC}\right| = L_A$$

α is the angle between $\overline{AC}$ and $\overline{CD}$.

The half block transmissibility between the centroid and the right face of the block is:

$$T_A = k_A \frac{\Delta z \times L_{AB} \cos\alpha}{L_A} = k_A \frac{\Delta z \times L_A L_{AB} \cos\alpha}{(L_A)^2}$$

The half-block transmissibility can be written as:

$$T_A = k_A \frac{\Delta z \times \left|\overline{AC}\right| \left|\overline{CD}\right| \cos\alpha}{\left|\overline{AC}\right|^2}$$

The scalar product of two vectors a and b having an angle α between them is expressed as:

$$a \cdot b = |a||b|\cos\alpha \quad \text{or} \quad a \cdot b = a_x b_x + a_y b_y$$

where a_x and a_y are the x and y components of the vector a, and b_x and b_y are the x and y components of the vector b, respectively. Therefore the half block transmissibility can be expressed as:

$$T_A = k_A \Delta z \frac{(x_C - x_A)(x_C - x_D) + (y_C - y_A)(y_C - y_D)}{(x_C - x_A)^2 + (y_C - y_A)^2}$$

since vectors $\overline{EF}$ and $\overline{CD}$ are perpendicular,

$$(x_C - x_D) = (y_E - y_F) = L_x \text{ and } (y_C - y_D) = (x_F - x_E) = L_y \text{ then}$$

$$T_A = k_A \Delta z \frac{L_x(x_C - x_A) + L_y(y_C - y_A)}{(x_C - x_A)^2 + (y_C - y_A)^2} \tag{6.18}$$

The half block transmissibility of the adjacent block B is calculated, then the two values are combined to calculate the inter block transmissibility between A and B:

$$T_{AB} = \frac{T_A \times T_B}{T_A + T_B} \tag{6.19}$$

The above calculation is performed in ECLIPSE as the NEWTRAN option which is automatically activated when the corner point grid option is used. It is noticeable that the dip correction is taken into account.

Note:

VIP [109] *offers two options for calculating the transmissibility between adjacent grid block:*

- *Standard option "HARINT" (harmonic integration) and*
- *NEWTRAN (similar to ECLIPSE).*

In the "HARINT" option, the eventual irregular shape grid block is mapped to a unit cube. The grid block volume is obtained by integration by summing up the elemental tube volumes across the block.

Corner point option generates a voluminous amount of data; therefore a preprocessor software to create the data file is necessary.

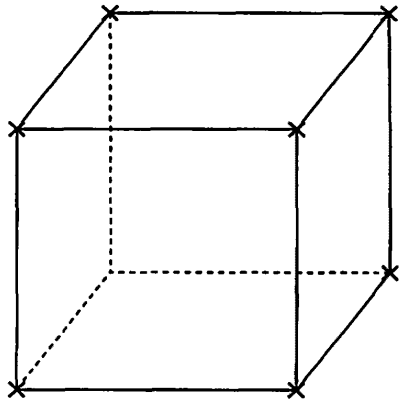

Figure 6.8 Corner point geometry; 8 data point per block.

6.3.5 Modeling Highly Faulted Reservoirs

Faults are common features in oil and gas reservoirs. Large faults, which exceed the layer thickness lead to compartmentalization and thus have strong effect on reservoir performance. Faults can either form reservoir boundaries or reside within the reservoir itself. Good indications of the presence of an unidentified fault within a reservoir include a sudden increase or decrease in water production; areas of a field being left undrained; wells drilled into a non-prospective down-thrown block; or a premature decrease in a well's production. In general, non-sealing faults can break up extensive horizontal barriers and thus improve the vertical sweep and sealing faults will act as barriers to flow and reduce communication in the reservoir. Today, the significance of faults is becoming far more apparent and greater efforts than ever before are being undertaken to produce accurate maps of these subterranean features. To produce high quality models for geologic horizons, the gridding process should

take into consideration the existence of faults. Finite difference numerical reservoir simulators generally assume that cells in any one-model layer are contiguous. From assigned depths, cell sizes and permeabilities, the simulator then determines the transmissibility between adjacent cells. To assist the efficient solution of the equations, connections are restricted to those between adjacent blocks in one model layer. This fact imposes severe limitations in representing faulted reservoirs in three dimensions because the fault throws juxtapose blocks from different layers.

The PEBI (Perpendicular Bisection) grid introduced by Heinemann regards the fault as inner boundaries. The flow equation is not used to calculate the fluid transfer through surfaces, but the faults are handled by boundary conditions in the equations.

6.4 MATRIX OF CONNECTION VALUES

Considering a linear model made of five grid blocks as shown on Figure 6.9. The problem is materialized by a matrix of 5 by 5 elements in Figure 6.9.

A cross in the matrix depicts non zero elements showing fluid exchanges possibilities between blocks.

Particularly block 1 communicates with block 2. Block 2 communicates with block 1 and 3. No communication occurs between block 1 and 3. The same process is repeated for all blocks. The result is a sparse matrix showing a symmetrical triangular structure for a **linear model** (1 dimension).

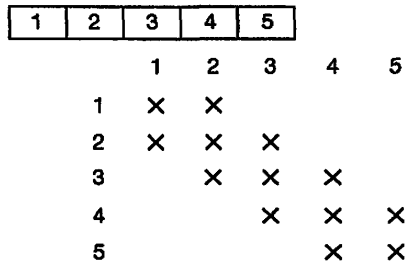

Figure 6.9 1D model.

Two-dimension reservoir model ($i = 4; j = 3$):

4 grid blocks in the x direction and 3 in the y direction (Fig. 6.10).

Block 1 communicates with 2 and 5.

Block 6 communicates with blocks 2, 5, 7 and 10.

The resulting matrix structure is a symmetrical pentadiagonal matrix.

3D model ($i = 4, y = 3, z = 2$) (Fig. 6.11)

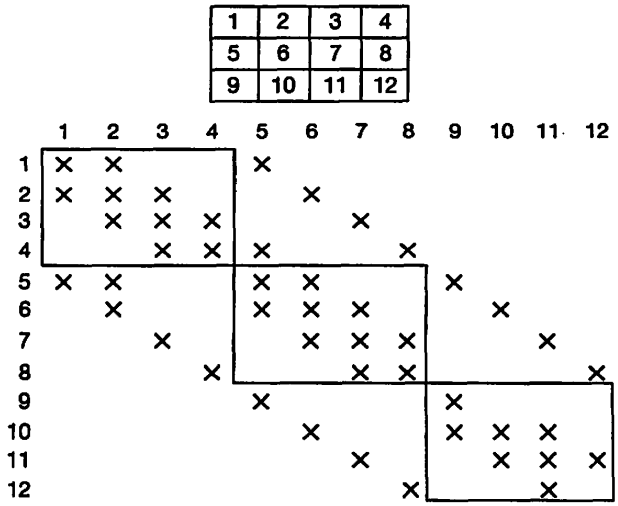

Figure 6.10 2D model.

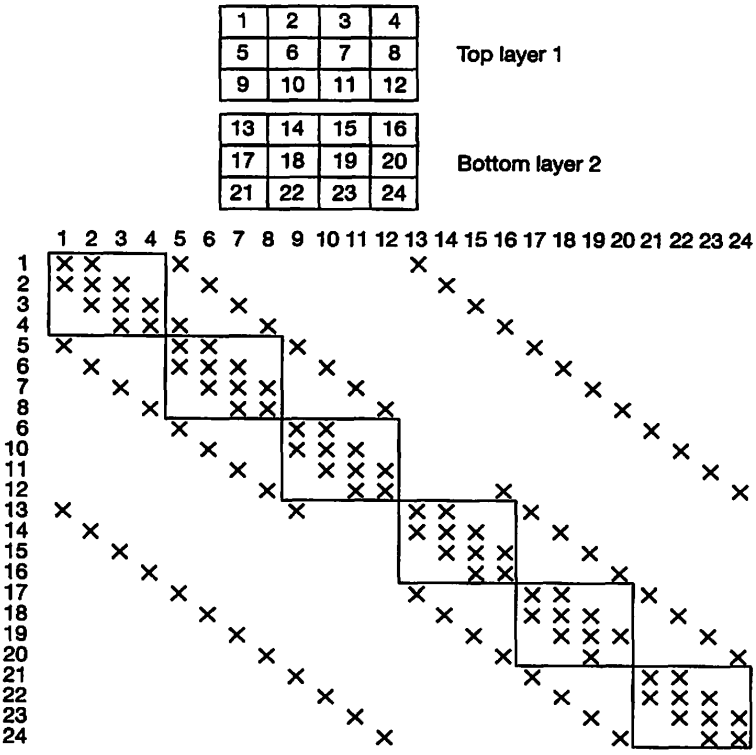

Figure 6.11 Three Dimension model; heptadiagonal matrix.

The matrix is 4 * 3 * 2 = 24 by 24 elements.

Block number 6 communicates with blocks 2, 5, 7, 10 and 18 etc.

The resulting matrix structure is a symmetrical heptadiagonal matrix.

The presence of non-neighbor connections (due to faults), creates additional elements in the matrix system that breaks the symmetrical character.

6.5 FINITE DIFFERENCE EQUATIONS [111]

Only a few problems involving partial differential equations can be solved analytically. The others can be approximated with the finite difference technique and treated numerically with a computer program. This is the case of the diffusivity equation which is similar to the diffusion of heat.

The partial differential equation is replaced by its finite-difference equivalent. The finite-difference equations can be derived by making a Taylor series expansion of the function at a given point and then solve for the required derivative.

The first order partial derivative of function f is:

$$\frac{\delta f}{\delta x} = \lim_{h \to o} \frac{f(x+h) - f(x)}{h} \tag{6.20}$$

The Taylor's series expansion gives:

$$f(x+h) = f(x) + h\frac{df}{dx} + \frac{h^2}{2!}\frac{d^2 f}{dx^2} + \ldots\ldots \qquad \frac{df}{dx} = \frac{f(x+h) - f(x)}{h} - \frac{h}{2!}\frac{d^2 f}{dx^2} \tag{6.21}$$

By neglecting the second term, a truncation error is introduced of the order of h

$\Delta f = f(x+h) - f(x)$ is forward difference

$\Delta f = f(x) - f(x-h)$ is backward difference

$\Delta f = f\left(x + \frac{h}{2}\right) - f\left(x - \frac{h}{2}\right)$ is central difference

Taylor's development for $f(x + h)$ and $f(x - h)$ is:

$$f(x+h) = f(x) + \frac{h}{1!}\frac{df}{dx} + \frac{h^2}{2!}\frac{d^2 f}{dx^2} + \frac{h^3}{3!}\frac{d^3 f}{dx^3} + \ldots\ldots \tag{6.22}$$

$$f(x-h) = f(x) - \frac{h}{1!}\frac{df}{dx} + \frac{h^2}{2!}\frac{d^2 f}{dx^2} - \frac{h^3}{3!}\frac{d^3 f}{dx^3} + \ldots\ldots \tag{6.23}$$

Therefore $$f(x+h) - f(x-h) = 2h\frac{df}{dx} + 2\frac{h^3}{3!}\frac{d^3 f}{dx^3} + \ldots\ldots \tag{6.24}$$

The second derivative can be obtained from

$$f(x+h)+f(x-h)=2f(x)+h^2\frac{d^2f}{dx^2}+2\frac{h^4}{4!}\frac{d^4f}{dx^4}+\ldots.. \tag{6.25}$$

Therefore $$\frac{d^2f}{dx^2}=\frac{f(x+h)-2f(x)+f(x-h)}{h^2}+0\times h^2-2\frac{h^4}{4!}\frac{d^4f}{dx^4} \tag{6.26}$$

The errors associated with the approximations are different; the forward and backward schemes have errors of the order of h, while the central form and the second derivative are of the order of h^2. The error is called the truncation error.

For application of reservoir simulation, let's replace function f by P (pressure), and h by Δx, the grid block length.

$$\frac{\delta P}{\delta x}=\frac{P_{i+1}-P_i}{\Delta x} \qquad \frac{\delta P}{\delta x}=\frac{P_i-P_{i-1}}{\Delta x}$$

$$\frac{\delta P}{\delta x}=\frac{P_{i+1}-P_{i-1}}{2\Delta x} \qquad \frac{\delta^2 P}{\delta x^2}=\frac{P_{i+1}-2P_i+P_{i-1}}{\Delta x^2} \tag{6.27}$$

Space intervals Δx, Δy, Δz as well as the sequence Δt_m in the model are arbitrary and are chosen sufficiently small to limit the truncation error.

6.6 BLACK OIL MODEL

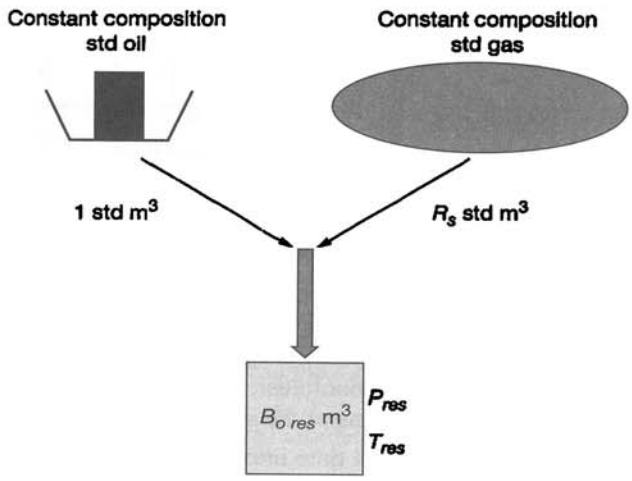

Figure 6.12 Black oil concept.

The black oil option is made of two pseudo-components (Fig. 6.12):

- Pseudo surface dead oil component of fixed composition.
- Pseudo surface gas component of fixed composition.

Undersaturated oil is made of dead oil with some amount of pseudo gas component in solution.

Diphasic hydrocarbon system is made of dead oil with some amount of pseudo gas component in solution plus some free gas.

For each reservoir grid block, the material balance equation is written between the start and end of the time step as (Fig. 6.13):

Mass rate in – mass rate out = accumulation mass rate

Gas reservoirs can also be treated with the black-oil option if the fluid produced composition (liquid and vapor) are constant (independent of pressure). The option considers some liquid dissolved in gas with ratio CGR (Condensate Gas Ratio) defined as R_v.

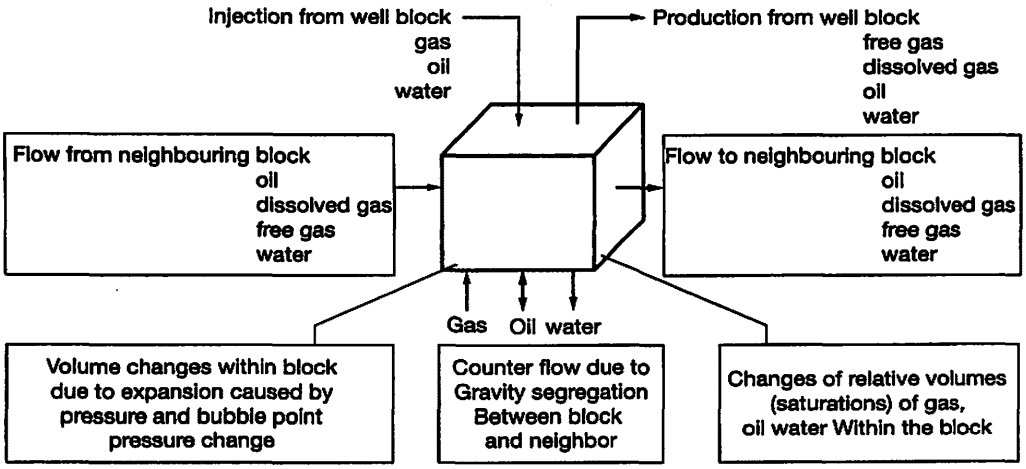

Figure 6.13 Material balance in a grid block.

6.6.1 Semi-discretized Equations for Black-oil [112, 113]

The difference equations can be regarded as one of the discretized forms of the governing differential equations.

Whenever the differential equation is nonlinear, the transmissibilities and/or coefficient of the time-derivative term will be functions of the solution (i.e., the dependent variable).

Space is discretized into grid cells, and time into time steps. The discretized form of the equations is obtained directly by writing the mass conservation equation for each cell and each pseudo component at every time step.

In a three dimensional problem, cell i has six adjacent cells except for the border cells. ('*i*' stands for internal; '*e*' for external).

Water equation: mass balance

$$\sum_e T_{i,e}\left(\frac{k_{rw}}{\mu_w}\rho_w\right)\left(\Phi_{we}-\Phi_{wi}\right)+\delta(i)q_w=\frac{\Delta m_w}{\Delta t} \tag{6.28}$$

mass exchange between blocks + production or injection = accumulation mass rate

$T_{i,e}$: connection value for block *i* (includes geometry and absolute permeability) with its neighbors
k_{rw}, μ_w: water relative permeability and viscosity
ρ_w: water density
$\Phi_{we}-\Phi_{wi}$: water potential difference between exterior block *e* and *i*
$\delta(i)$: Dirac delta function = 0, or 1 production or injection water rate from a well perforation
Δm_w: water mass change during time step Δt in cell *i* (function of φ, ρ_w and S_w)

Dead oil equation:

$$\sum_e T_{i,e}\left(\frac{k_{rL}}{\mu_L}\rho_o\right)(\Phi_{Le}-\Phi_{Li})+\delta(i)q_o=\frac{\Delta m_o}{\Delta t} \tag{6.29}$$

k_{rL}, μ_L: hydrocarbon liquid phase relative permeability and viscosity
ρ_o: contribution of pseudo-component to the hydrocarbon liquid phase density

Gas pseudo component:

$$\sum_e T_{i,e}\left(\frac{k_{rL}}{\mu_L}\rho_{DG}\right)(\Phi_{Le}-\Phi_{Li})+\frac{k_{rG}}{\mu_G}\rho_G\left(\Phi_{Ge}-\Phi_{Gi}\right)+\delta(i)\left(q_{DG}+q_G\right)=\frac{\Delta m_{DG}+\Delta m_G}{\Delta t} \tag{6.30}$$

ρ_{DG}: contribution of dissolved gas to the hydrocarbon liquid phase density
ρ_G: free gas density

Additional equations:

$$S_w+S_L+S_G=1$$
$$P_w=P_L-P_{cw} \tag{6.31}$$
$$P_G=P_L+P_{cG}$$

The water phase pressure is deducted from the hydrocarbon liquid phase through the capillary pressure relationship. The same applies for the gas phase.

Remarks:
The saturation dependent term and the transmissibility connection value used are the one affected to the upstream block.
Φ_L refers to the oil phase potential. The oil phase is made of dead oil plus some solution gas. Subscript (L) is used to avoid confusion with the dead oil subscript (o).

Variables:

In the black oil model, there are:

- three basis equations:
  - water, oil component and gas component
- three independent variables:
  - pressure (generally oil phase or gas phase pressure)
  - saturation S_w
  - bubble point pressure P_b (or R_s) if the grid block is undersaturated or:
  - gas saturation S_g if the grid block is diphasic

For black oil gas reservoir studies, dissolved condensate R_v is used symmetrically to the solution gas R_s for oil reservoirs.

6.6.2 Fully implicit Algorithm [108, 112, 113]

The discretized equations describing the flow of oil, water and gas can be formulated in terms of errors associated with each phase in each cell of the reservoir.

$$R_o = \frac{\Delta m_o}{\Delta t} - \delta(i)\, q_o - \sum_e T_{i,e}\left(\frac{k_{rL}}{\mu_L}\rho_o\right)(\Phi_{Le} - \Phi_{Li}) \tag{6.32}$$

For simplification let us write:

$$R_i = \frac{\Delta m_i}{\Delta t} - q_i - \sum_n f_{ni} \tag{6.33}$$

Δm_i: mass change accumulated during the current time step Δt
$\Sigma f_{ni} = F$: net flow rate exchange with neighboring grid blocks
q_i: net flow rate exchange between perforation and block
R_i: error defined for each cell and each component

The residual or error R_i is a three component vector $\begin{bmatrix} R_o \\ R_w \\ R_g \end{bmatrix}_i$ for each cell (6.34)

$\sum_n f_{ni}$: is the summation of the flow terms extending over all cells neighboring cell *i*.

The constituent terms of Eq. (6.32) are pressure and saturation dependent. The fully implicit scheme implies that all terms of Eq. (6.32 or 6.33) are evaluated at the end of the time step.

The equations in terms of P_o, S_w, S_g or R_s must be solved simultaneously for each cell. Referring to the connection matrix Figure 6.11, each element of the matrix "*x*" is a 3 by 3 sub matrix.

The solution is obtained when

$$R(X) = 0. \tag{6.35}$$

Each element of the solution vector X has three components:

error on oil, water and gas

$$R = \begin{bmatrix} R_o \\ R_w \\ R_g \end{bmatrix} \tag{6.36}$$

the solution for each cell is:

$$X = \begin{bmatrix} P_o \\ S_w \\ S_g \text{ or } R_s \text{ or } R_v \end{bmatrix} \tag{6.37}$$

Newton-Raphson iteration is used to solve the non-linear Eq. (6.35). At each iteration, the linear equation must be solved:

$$R(X+x) = R(X) + \frac{\delta R}{\delta X} x = 0 \tag{6.38}$$

The Jacobian $\frac{\delta R}{\delta X}$ is:

$$\frac{\delta R_i}{\delta X_j} = \begin{bmatrix} \frac{\delta R_o}{\delta P_o} & \frac{\delta R_o}{\delta S_w} & \frac{\delta R_o}{\delta S_g} \\ \frac{\delta R_w}{\delta P_o} & \frac{\delta R_w}{\delta S_w} & \frac{\delta R_w}{\delta S_g} \\ \frac{\delta R_g}{\delta P_o} & \frac{\delta R_g}{\delta S_w} & \frac{\delta R_g}{\delta S_g} \end{bmatrix}_{ij} \tag{6.39}$$

To do this, the linear equations need to be solved:

$$J \times x = R(X) \quad \text{or} \quad x = J^{-1} R(X) \tag{6.40}$$

each Newton iteration procedure consists of:

- solving Eq. (6.40)
- update the solution vector: $X \rightarrow X + x$
- compute the new residual $R(X)$
- when $R(X)$ is sufficiently small, then proceed to the next time step
- otherwise, update the Jacobian and repeat the iteration.

The mass change during the time step Δt is:

$$\Delta M = M_{t+\Delta t} - M_t \tag{6.41}$$

M: mass vector per unit fluid surface density

with

$$M = V_p \begin{bmatrix} \dfrac{S_o}{B_o} + \dfrac{R_v S_g}{B_g} \\ \dfrac{S_w}{B_w} \\ \dfrac{S_g}{B_g} + \dfrac{R_s S_o}{B_o} \end{bmatrix} \tag{6.42}$$

V_p: pore volume S_o: oil saturation B_o: oil FVF R_v: condensate gas ratio
S_g: gas saturation B_g: gas FVF S_w: water saturation B_w: water FVF
R_s: solution gas oil ratio

When S_g is zero, the solution variable becomes R_s^*. The oil is undersaturated. When S_o is zero, the solution variable becomes R_v. The gas is undersaturated.

** some authors use P_b instead of R_s*

6.6.3 IMPES Algorithm

The IMPES (Implicit Pressures Explicit Saturations) residual is similar to the fully implicit residual calculation Eq. (6.35), except that all flow and well terms are computed using pressure and saturation dependent terms, obtained at the end of the previous time step. The result for flow terms in matrix Eq. (6.40) is that each element becomes a scalar instead of a sub matrix (3 by 3). The computer work to solve the system is decreased.

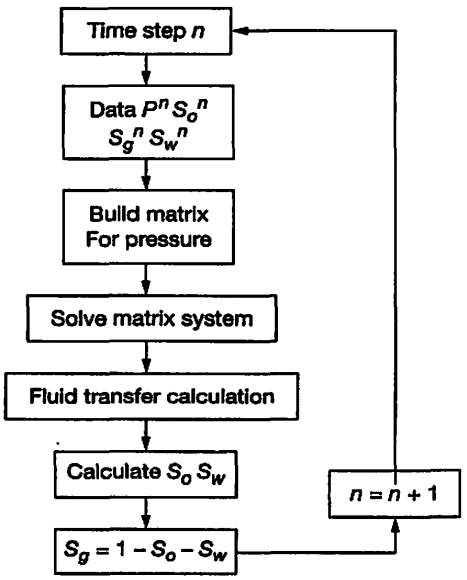

Figure 6.14 IMPES Algorithm.

The new matrix system expressed in terms of pressure is build with mobility terms prevailing at the end of the previous time step.

Solving the matrix system is carried out with an iterative method.

Fluid transfer calculations are made by using the Darcy's law.

New saturations are calculated. Figure 6.14 shows the corresponding work flow.

6.7 COMPOSITIONAL MODEL

6.7.1 Basic Definitions

The *mole* (abbreviation, mol) is the Standard International (SI) unit of material quantity. One mole is the number of atoms in precisely 12 thousandths of a kilogram (0.012 kg) of C-12, the most common naturally-occurring isotope of the element carbon. This number is equal to approximately 6.022169×10^{23}, called the Avogadro constant.

Molar mass is the mass of one mole of a chemical element or chemical compound

The unit is g/mol, or in the International System kg/mol; symbol used: M_w

Molar volume: volume occupied by one mole of material. (m^3/mol)

Molar density: mass of material expressed in moles per unit volume; it is the inverse of the molar volume (mol/m^3)

Total hydrocarbon component *i*:

$$z_i = Lx_i + Vy_i$$

L: liquid fraction
V: vapor fraction $L + V = 1$

Equilibrium constant for component *i*: $k_i = y_i/x_i$

y_i: component fraction in the vapor phase;
x_i: component fraction in the liquid phase.

6.7.2 Formulation

The formulation models the flow of two hydrocarbon phases: oil and gas and a water phase.

Each hydrocarbon phase is a mixture of N_c hydrocarbon components which may include non-hydrocarbons such as CO_2, N_2, or H_2S.

Similarly to the black oil formulation, the semi-discretized equations are written for each component fluid that is: water and hydrocarbon components.

Water Equation:

$T_{i,e}$: connection value for block i (includes geometry and absolute permeability) with its neighbors

$$\sum_e T_{i,e}\left(\frac{k_{rw}}{\mu_w}\rho_w\right)(\Phi_{we}-\Phi_{wi})+\delta(i)\,q_w=\frac{\Delta m_w}{\Delta t} \tag{6.43}$$

k_{rw}, μ_w: water relative permeability and viscosity
ρ_w: water density
$\Phi_{we}-\Phi_{wi}$: water potential difference between exterior block e and i
$\delta(i)$: Dirac delta function = 0, or 1 production or injection water rate from a well perforation
Δm_w: water mass change during time step Δt in cell i (function of φ, ρ_w and S_w)

Hydrocarbon Component Balance for Element *k* and Cell *i*:

$$\sum_e T_{ie}\left(\frac{k_{rL}}{\mu_L}\frac{x_k M_{wk}}{M_{wL}}\rho_L\right)(\Phi_{Le}-\Phi_{Li})+\sum_e T_{ie}\left(\frac{k_{rG}}{\mu_G}\frac{y_k M_{wk}}{M_{wG}}\rho_G\right)(\Phi_{Ge}-\Phi_{Gi})$$

Liquid hydrocarbon — vapor hydrocarbon

$$+\delta(i)\left[\frac{x_k M_{wk}}{M_{wL}}q_L+\frac{y_k M_{wk}}{M_{wG}}q_G\right]=\frac{\Delta m_k}{\Delta t}$$

producing or injecting perfo (6.44)

k_{rL}: liquid relative permeability (oil)
M_{wk}: molecular mass of component k
M_{wL}: molecular mass of liquid (oil)
k_{rG}: gas relative permeability
M_{wG}: molecular mass of gas phase
q_L: oil mass rate
Δm_k: mass change of component k
Φ_{Le}: oil potential of exterior block
Φ_{Ge}: gas potential of exterior block
Δm_T: total hydrocarbon mass change of component k
μ_L: viscosity of liquid (oil)
x_k: liquid mole fraction
ρ_L: liquid density
μ_G: viscosity of gas
y_k: vapor mole fraction
ρ_G: gas density
q_G: gas mass rate
Δt: time step length
Φ_{Li}: oil potential at block i
Φ_{Gi}: gas potential at block i

Total Hydrocarbon Mixture:

$$\sum_e T_{ie}\left[\frac{k_{rL}}{\mu_L}\rho_L(\Phi_{Le}-\Phi_{Li})+\frac{k_{rG}}{\mu_G}\rho_G(\Phi_{Ge}-\Phi_{Gi})\right]+\delta(i)\,(q_L+q_G)=\frac{\Delta m_T}{\Delta t} \tag{6.45}$$

Variables:

N_c: number of components, there is:

- one balance equation per component:
- one equation for water
- one equation for the total hydrocarbon mixture.

In the fully implicit mode, other solution variables are:

$$S_o, S_g, S_w$$

The associated constraints on compositions are:

$$\sum_{i=1}^{N_c} x_i = 1 \qquad \sum_{i=1}^{N_c} y_i = 1 \tag{6.46}$$

Constraint on fluid saturations is interpreted as volume balance.

The volume balance consists of having the total fluid volume to fit the pore volume for each block.

Error or residual on volume: $R_v = V_p - V_F = 0$ (6.47)

V_p: cell volume
V_F: total fluid volume

Fluid volume can be expressed as:

$$V_F = \left(\frac{m_T L}{b_o^m} + \frac{m_T V}{b_g^m} + \frac{m_w}{b_w^m} \right) \tag{6.48}$$

With $$m_T = \sum_{N_c} m_c \tag{6.49}$$

L and V are the liquid and vapor mole fractions: b_o^m, b_g^m and b_w^m are the molar densities of oil, gas and water.

The phase compositions are obtained with an Equation of State in addition to the Vapor Liquid Equilibrium calculation to determine V and L.

The form of the Jacobian matrix condition is: $$J = \frac{dR_{fl}}{dX} \tag{6.50}$$

expressed in terms of solution variables:

- pressure, water saturation, molar density of each component and
- residual equations R_w, R_c, R_m.

The flow rate of component k embedded in the liquid phase oil into cell i from neighboring cell n is:

$$F_{\mathrm{Ln}\,i}^k = T_{ni} x_L^k k_{rL}(S_L) \frac{b_L^m}{\mu_L} \tag{6.51}$$

6.7.3 Fully Implicit Algorithm

The fully implicit calculation consists of solving all unknowns simultaneously in terms of:

- Oil pressure
- Vapor liquid equilibrium
- Inter block fluid movements
- Hydrocarbon molar composition of mixture at end of time step
- Pressure and saturation function terms evaluated at end of time step
- S_o, S_w, and S_g at end of time step
- Well flow terms evaluated at end of time step conditions.

The fully implicit mode requires heavy computing work, since at each iteration, equilibrium (L and V determination) and flash calculation are necessary for each cell. This is why it is recommended to limit the number of components and to use the IMPEC (Implicit Pressure Explicit Composition) mode.

6.7.4 IMPEC Scheme

The IMPEC (or called IMPEM Implicit Pressure Explicit in Mobility) mode is similar to the IMPES scheme for the Black oil model. Similarly to the IMPES black-oil option, the transmissibilities are treated explicitly. After solving the pressure equation, the mass change of each component is calculated from the conservation mass equation.

The mass terms M_{t+dt} are evaluated at the end of the time step. Flow terms between cells are calculated assuming saturations, fluid mobility and reservoir density terms present at the end of the previous time step.

Newton's iteration method is used to solve the non-linear residual equations $R(X) = 0$.

6.7.5 AIM (Adaptive Implicit Method) Scheme

Typically a reservoir simulation does not need a fully implicit treatment of all grid blocks. For example in the aquifer grid blocks, no saturation changes occur during the simulation. On the other hand a well block and some blocks close to the well may be submitted to large saturation changes during simulation.

The saturation change during a time step depends on:

- Time step length.
- Grid block pore volume.
- Pressure gradient therefore fluid velocity.

Usually to improve the pressure profile and saturation changes around the well, the grid block size is decreased. This configuration is used typically in coning studies which necessitate fully implicit treatment.

Thomas and Thurnau (1981) [114, 115] introduced the Adaptive Implicit Method procedure for black-oil simulators. It was noted that for most reservoir simulation problems,

a fully implicit treatment is usually not required and that if a fraction of the computational cells are treated implicitly, sufficient computational stability is provided to allow for large time steps of a size comparable to a fully implicit simulation. The concept has been extended to compositional models. The option is recommended to be used when running a compositional model with ECLIPSE 300.

Typically, a reservoir simulation begins with IMPES treatment for most blocks in the reservoir, except for the well blocks and perhaps their nearest neighbors. Usually the initial timestep and those after a well constraint change are small to resolve the pressure transient. As the timestep length increases, more cells require an implicit treatment in order to maintain numerical stability and convergence within a reasonable number of Newtonian iterations. The aim of the application of AIM is to be able to use large timesteps comparable to those of a fully implicit treatment, with similar accuracy, but at a reduced computing time and storage. The difficulty is to define a criterion for the switching of the appropriate cells to be treated explicitly or implicitly [116].

ECLIPSE 300's option is based on the paper written by K.H. Coats [117].

6.8 FULLY IMPLICIT VERSUS IMPES OR IMPEC

The IMPES scheme involves the pressure equation alone to be solved, and then the deduced calculated pressures are used to evaluate fluid transfers, and saturation. The approach assumes saturation dependent parameters, constant during the current timestep.

The algorithm is stable under the following condition:

Slow saturation changes which imply:

- Large grid block pore volumes compared to fluid throughputs.
- Small pressure gradients within the reservoir.
- Limited timestep length.

Conditions for compositional models are similar to the one above, pointing that saturation calculations are the results of component mass transfers followed by a VLE (Vapor Liquid Equilibrium) calculation.

When the above conditions are not fulfilled, diverging oscillations occur.

The fully implicit mode, involves the simultaneous solution of the flow equations of oil, water, gas and fluid saturations. The process requires heavy computer work.

The fully implicit mode being very stable, larger timestep lengths than in the IMPES scheme are allowed.

6.8.1 Stability

Stability is concerned with the growth of error amplitude from timestep to timestep.

6.8.1.1 Fully Implicit

The fully implicit algorithm treats all primary variables implicitly which results in an unconditional stability.

6.8.1.2 IMPES

In IMPES mode, there are two possible instability sources:

The first comes from the explicit treatment of primary variables. The IMPES algorithm treats capillary pressure explicitly, and has therefore a stability limit depending on the magnitude of dP_c/dS. Capillary pressure can be considered as a correction applied to the primary variable oil pressure to calculate the gas and water pressures. In IMPES mode, the correction must have a limited magnitude (P_{cmax}) compared to the main variable; otherwise the correction may be too high and introduce an unstable behavior like an oscillating response. It is then recommended to limit the maximum capillary pressure value obtained from the laboratory to a 'reasonable' value.

The second limit results from the explicit treatment of the calculated matrix coefficients which are strongly non linear elements. To be valid, the calculation in the IMPES mode implies a slow saturation change (since it was assumed to be constant during the timestep) between beginning and end of the timestep. This condition has a direct impact on the choice of the timestep length. Experience dictates a tolerated maximum saturation variation of about 3% in any grid cell of the model.

6.8.1.3 Gas Percolation [100]

The gas percolation problem may occur in the IMPES mode. As mentioned, the matrix pressure is solved; and the transport equation is used to calculate fluid transfers between cells with the new potentials. It is noted that the vertical transmissibility is large due to the important vertical interface area between cells even with a low vertical permeability. As a result the calculated vertical gas transfer quantity may be very large even greater than the mobile gas present in the upsteam cell. The instability is essentially due to the explicit treatment of the matrix elements and is accentuated by the large difference in densities of oil and gas and the low viscosity of gas. If a built in control to limit the phenomenon in the simulator does not exist, the user needs to decrease the vertical transmissibilities. The computation accuracy is not affected. It is noted that in the fully implicit mode, the problem cannot occur.

6.8.2 Numerical Dispersion or Numerical Diffusion

Reservoir simulators use standard first order differencing methods. One of the problems with these methods is that they do not accurately model the movement of phase discontinuities. For tertiary recovery, the accurate tracking of phase discontinuities is essential in determining the efficiency of the process.

The extensive use of the fully implicit simulator is motivated principally by the much greater stability and robustness of fully implicit methods when applied to problems involving gravity segregation, high permeability contrasts, coning, bubble point crossing, etc. The strong stability of the method allows the simulator to take much longer time steps than would be possible with the IMPES method. The main drawback is the increased numerical dispersion arising from time truncation errors (as distinct from space truncation errors) resulting in additional smearing of flood fronts. ECLIPSE proposes a flux limiting scheme option to prevent unphysical oscillations near sharp fronts [118].

6.9 TREATMENT OF WELLS

A well constitutes a boundary condition (source or sink) for the model that is the communication between the reservoir and surface. Wells may have different geometries, vertical, deviated, or horizontal. The communication between the grid block and the well is the perforation which is represented by a virtual point located in the centroid of the grid block. The perforation can be opened or closed and is characterized by its connection value W_k similarly to the transmissibility concept between grid blocks.

The relationship between the block pressure and the well flowing pressure has been treated in the chapter 3 "Fluid flow in Reservoirs".

A well may be constituted of a single perforation or of several perforations having a common flowing pressure. The result is that for a producing well, it may happen that a perforation absorbs fluid instead of producing. This phenomenon is called cross-flow.

The flow rate from cell i into a production perforation is:

$$q_i = W_k \times \left(\frac{k_{ro}}{\mu_o B_o} + \frac{k_{rw}}{\mu_w B_w} + \frac{k_{rg}}{\mu_g B_g} + R_s \frac{k_{ro}}{\mu_o B_o} \right) \Delta P \tag{6.52}$$

Summing dead oil rate
\+ water rate
\+ free gas rate
\+ solution gas rate

In matrix form and adding the condensate rate option for gas reservoirs:

$$q_i = W_k \times \Delta P \times \begin{bmatrix} \frac{k_{ro}}{\mu_o B_o} + R_v \frac{k_{rg}}{\mu_g B_g} \\ \frac{k_{rw}}{\mu_w B_w} \\ \frac{k_{rg}}{\mu_g B_g} + R_s \frac{k_{ro}}{\mu_o B_o} \end{bmatrix} \tag{6.53}$$

W_k: perforation connection factor in block i
ΔP: perforation drawdown at block centre i

For an oil well operating at a fixed flow rate Q_o, the bottom hole flowing pressure P_{wf} is obtained from the conditions:

$$\Sigma q_{oi} = Q_o \tag{6.54}$$

The summation is taken over all cells in which the perforation is opened.

The bottom hole flowing pressure is algebraically eliminated in Eq. (6.53). For wells operating at fixed tubing head pressure, well lift curves must be supplied in tabular form. A target flow rate is obtained by finding a simultaneous solution to the well lift curve and the inflow performance relationship obtained by summing Eq. (6.52) over all layers. The well is then treated as if it were rate controlled.

Multiple Connections:

A well can be completed in one or several layers. The connections belonging to a particular well may not be in the same vertical column of grid blocks. So it is possible to simulate deviated or horizontal wells. Multiphase flow from a perforation is governed by two phase or three phase relative permeabilities. Usually by default, the relative permeability functions used by the simulator are the one that belong to the perforated block. For some problems, it is possible to define special functions dedicated to the well called pseudo-relative permeabilities.

6.10 SOLVER

6.10.1 Non-linear Iteration

The Newton-Raphson iteration expressed by Eq. (6.38) is also called non-linear iteration or outer-iteration. The goal is to minimize the errors on material balance. Water residual, hydrocarbon residual, pressure, saturation vapor fraction and mole fraction changes are calculated for a compositional model. Grid blocks experiencing these maximum changes are also pinpointed.

A convergence criterion is defined to stop the iterating process and validate the solution.

Each Newton-Raphson iteration, Eq. (6.40) consists of a set of linear equations that need solving. Generally an iterative calculation method is used due to the large system size. This calculation is called linear iteration or inner iteration. An appropriate convergence criterion is also defined to stop the iteration and validate the result.

At each Newton-Raphson iteration, (outer iteration), Eq. (6.40) needs to be solved.

$$J \times x = R(X)$$

x: variable increment
J: Jacobian
$R(X)$: matrix of errors

or
$$A \times x = b \tag{6.55}$$

A is the Jacobian matrix $dR(X)/dX$, and b is the non-linear residual of the prior Newton iteration. For small problems, the system (linear equations) may be solved by Gaussian elimination.

$$x = J^{-1}R(X)$$

However, this is not practical for large studies. In such a case an iterative method is used.

After m iteration, the residual can be written:

$$r_m = b - A \times x_m \tag{6.56}$$

$$B \times x_m = r_m \tag{6.57}$$

Where B is an approximation matrix to A chosen so that the solution of Eq. (6.57) may be obtained efficiently.

To update the solution x_m, the "Orthomin procedure" is used for non-symmetric matrix A, or the "Conjugate Gradient method" for symmetric A matrices.

The effectiveness of the method depends critically on how closely the preconditioning matrix B approximates to A. The method called Nested Factorization is widely used by software manufacturers.

The linear convergence (inner iteration) being validated, with an outer iteration failing to converge in the allowed outer iteration number, the timestep size is cut by a factor of two and the calculation repeated. Timestep cuts can occur for a converged timestep if a timestep maximum change value is exceeded by more the allowed limit.

6.10.2 Solution of Linear System of Equations (inner iteration)

6.10.2.1 Direct Method

$$A \times x = b \tag{6.58}$$

Direct methods are used for small models. The insurance of getting a solution is the advantage, but drawbacks are:

- Heavy computer work necessary.
- Large storage capacity required.

Gaussian elimination [119] with the grid blocks ordered by D4 ordering (alternate diagonal) is used. The D4 ordering assuming a symmetrical matrix eliminates the presence of non neighbor connections created by faults. The solver requiring a large computer work limits the size of the problem that can be treated.

6.10.2.2 Iterative Method

With the increasing number of cells, iterative methods are used.

The requirements of an iterative nonlinear equation solver can be summarized by:

- The iterative method should lead to the desired root of the equation; possibly the equation should be formulated to yield only one root.
- The iterative method should be stable, avoiding oscillating behavior.
- The iterative method should lead rapidly to solution.
- The iterative method should avoid numerical instability.

A variety of iterative methods are available to solve large sparse matrices; some of them take advantage of the symmetrical character of the matrix.

The solution of the linear equations: $A \times x = b$

depends on the existence of an approximation, B, to the coefficient matrix A such that $B \times \varphi^{-1}$ is easily calculated for any vector φ. The rate of convergence of the iteration depends primarily on how well B approximates to A.

Consequently to the common use of the corner point geometry technique, non-neighbor connections may occur and cancel the symmetrical character of the matrix.

During the 1980's, researchers worked on iterative methods to satisfy the increasing needs of robust and efficient methods. Preconditioning is designed to obtain a fast inversion with minimal storage and to ensure that material is conserved at each iteration.

One way to approximate matrix A is the nested factorization [120]. This approximation is used as a preconditioning matrix for a truncated conjugate gradient algorithm "Orthomin" described by Vinsome [121].

Several variations of the Nested Factorization method were tested and implemented in reservoir simulators [122, 123, 124, 125].

6.10.3 Concluding Remarks

Figure 6.15 depicts the solver flow chart with an iterative method to solve the linear equations and the outer iteration or so called the Newton Raphson iteration. For small model the inner iteration can be replaced by the Gaussian elimination with the D4 ordering.

The Orthomin procedure is an accelerator for convergence. The iterative calculation is based on the LSOR (Line Successive Over Relaxation) iterative method [126]. The relaxation technique is applied to a group of cells along a line (a row or a column). The unknown values are solved simultaneously assuming that those values on the previous line are known. The calculation is performed on all columns or rows, sweeping all the planes of the model until convergence is obtained.

6.10.4 Convergence

Convergence is concerned with the growth or damping of error from iteration to iteration at a fixed timestep

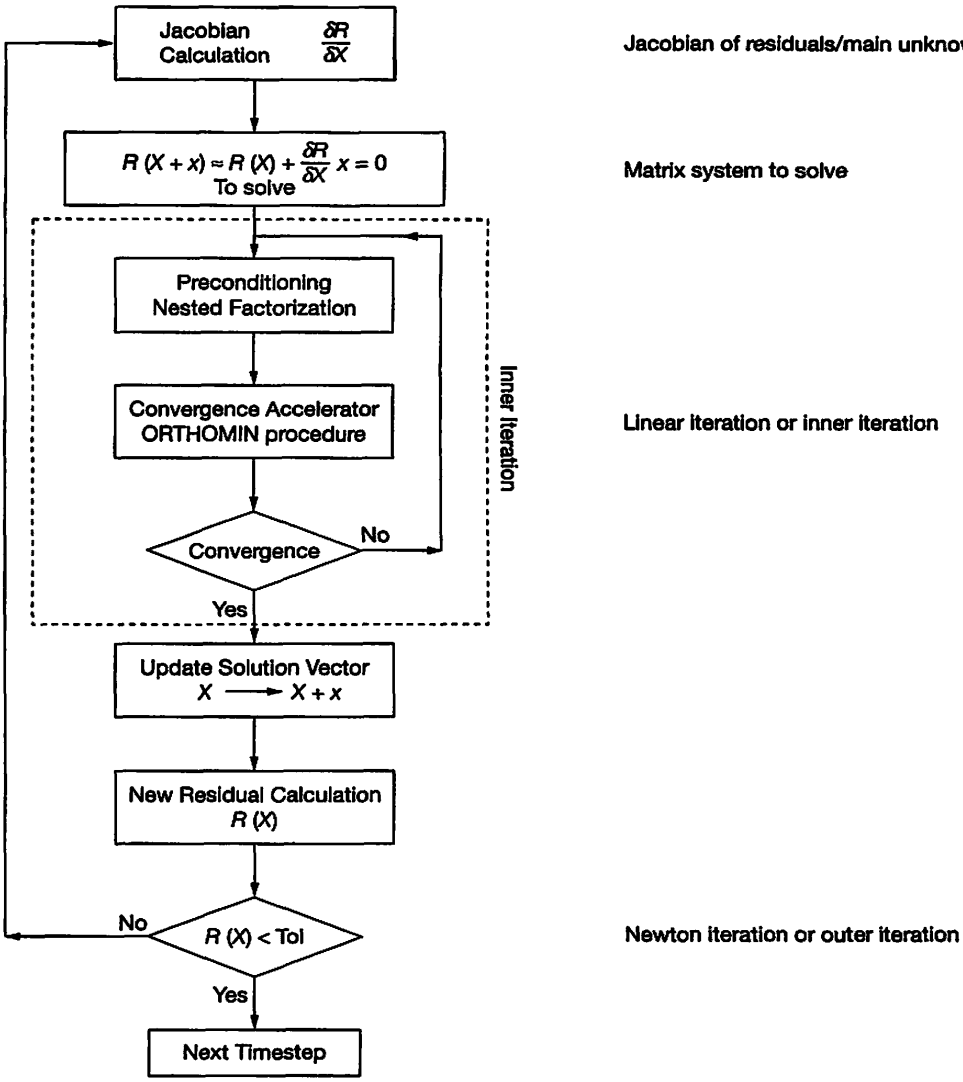

Figure 6.15 Solver Work Flow.

Difficulties may appear with iterative methods from the absence of convergence in some problems. Convergence may take too many iterative loops or diverge. A problem is qualified difficult when large permeability contrasts are present, which has an impact on the connection matrix elements.

6.10.4.1 Convergence of Non-linear System (Outer Iteration)

VIP gives the possibility to monitor the convergence of the non-linear iteration with the "PRINT" keyword. Residuals in hydrocarbon balance and the water balance equations are compared with the material balance error tolerances "TOLHC" for hydrocarbons, and "TOLRW" for water. When residuals are less than tolerances, the iterating process is stopped.

Convergence criterion for the outer iteration in ECLIPSE 100 is based on material balance and maximum residual checks on R. The criterion may be changed by the use of the "TUNING" keyword.

The convergence criterion in ECLIPSE 300 is based on solution change targets.

Pressure and saturation changes being small enough, these targets "SCONVP" and SCONVS" in the "CVCRIT" keyword can be used to tighten down the convergence.

6.10.4.2 Convergence of Linear Systems (inner iteration)

The more powerful the preconditioning the fewer iterations are required for convergence.

Linear iterations in VIP are monitored with the "BLITZ" keyword. Many parameters can be changed by the user to improve the convergence rate of the solver:

- JLU1: preconditioning option for IMPES or Constrained Pressure Residual [123].
- JLUN: preconditioning option for fully implicit formulation.
- JCOR, JOPT and JCPR.

In ECLIPSE 100, the convergence of the linear solver is monitored by setting the 7^{th} parameter of the keyword "DEBUG" greater than 0.

The maximum saturation normalized residual is used [108] to define the convergence criterion for the linear iteration. The default settings can be changed in the "TUNING" keyword.

The line of blocks chosen is the one corresponding to the direction of highest transmissibilities (usually the Z direction). The selected direction may be changed by the user with the "SOLVDIRS" keyword in ECLIPSE in case of convergence difficulties.

6.11 SATURATION FUNCTIONS

Saturation dependent functions include capillary pressures and relative permeabilities. Most of research work was based on two-phase systems. The functions are defined for the oil gas and the oil water systems.

6.11.1 Capillary Curve

Drainage curve is used to calculate the initial reservoir conditions. Imbibition capillary pressure curve is necessary for fractured reservoirs. Usually imbibition curves are used during the dynamic simulation run.

The value of S_w at which water starts to flow is called the critical water saturation S_{wc}.

The slope of capillary pressure curve at irreducible saturations must be finite in numerical models. It is recommended to avoid an asymptotical shape associated with high P_c values near the critical saturation.

Within the model, only one pressure is considered: oil pressure. Pressure in the gas and water are deducted from the oil pressure through the capillary pressure relationships.

The capillary pressure may be considered as a pressure correction to the main phase pressure to compute the associated phase movement. In the gas water system, the main unknown is the gas pressure.

$$P_g = P_o + P_{cog} \qquad P_w = P_o - P_{cow} \tag{6.59}$$

Consequently if the correction level is much higher than the main phase pressure change, the model may be destabilized in particular in the IMPES numerical scheme where saturation functions used are the one obtained at the end of the previous timestep.

6.11.2 Relative Permeabilities

Relative permeability curves must be consistent. The maximum oil relative permeability in the oil water system must be the same value as the one in the gas oil system. It is recommended to use smooth curves instead of sharp variation curves. It is remembered that the derivative of the k_r functions versus saturation are necessary in the iterative calculation process.

Three phase relative permeabilities are determined from the two-phase k_r with different formulations offered by the programme.

6.11.3 Saturation Keys

The conclusion of a rock typing study leads the engineer to define families of saturation functions. Each set needs to be assigned to a particular group of grid blocks. Therefore it is necessary to enter several sets of saturation functions and assign the proper set to each grid block. This is done through the use of a saturation key (an integer for each grid cell).

6.11.4 End-Point Scaling

Geomodels provide for each cell a value of water saturation. The option end-point scaling allows the user to model spatial differences in relative permeability and capillary pressure end points from a single set of generic saturation functions.

From a set of saturation functions, the programme calculates normalized functions versus reduced saturations. For each block end point values are assigned and the corresponding functions are deducted.

The calculation is divided into two steps: saturation end-point scaling, then end-point relative permeability scaling.

Normalized relative permeabilities are calculated as [100]:

$$S_o^* = \frac{S_o - S_{om}}{(1 - S_{wc} - S_{om})} \qquad S_w^* = \frac{S_w - S_{wc}}{(1 - S_{wc} - S_{om})} \qquad S_g^* = \frac{S_g}{(1 - S_{wc} - S_{om})}$$

with $S_o \geq S_{om} \qquad S_w \geq S_{wc}$

S_o^*, S_w^*, S_g^*: reduced oil, water, gas saturations
S_o, S_w, S_g: current oil, water, gas saturations
S_{om}: minimum oil saturation
S_{wc}: minimum water saturation

6.12 PRESSURE FUNCTIONS

6.12.1 Fluid Properties

Pressure functions include the hydrocarbon PVT properties when the "black-oil" option is used. That is the oil and gas FVF with the solution gas versus the saturation pressure.

The saturation pressure functions must be fully described over the total anticipated useful pressure interval. One undersaturated line is defined for R_s, B_o and μ_o. The programme generates a parallel line when necessary crossing the proper bubble point pressure to simulate a variable bubble point pressure.

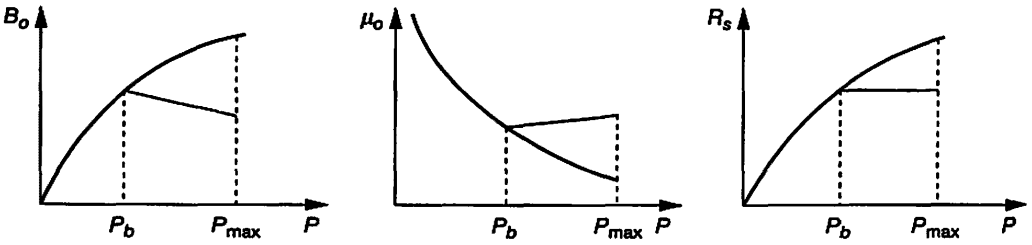

Figure 6.16 Oil PVT functions.

Gas formation volume factor B_g plus eventually the condensate concentration versus pressure are necessary.

Fluid properties for a compositional model are governed by a tuned equation of state.

6.13 EQUILIBRATION

Equilibration includes the static reservoir calculations at initial time. That is the determination of each block pressure and saturations from the basic data. Three cases need to be considered:

- Black-oil model
- Compositional model
- Supercritical initialization.

6.13.1 Black-Oil Model

The option assumes surface oil and gas of constant compositions and densities.

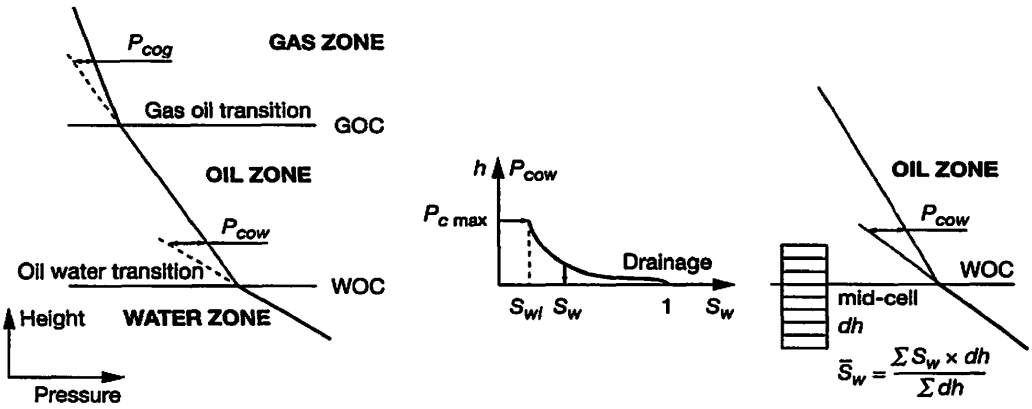

Figure 6.17 Model Initialization.

Two conditions are possible:

- Constant bubble point pressure and dew point versus depth
- or variable bubble point pressure and dew point versus depth.

6.13.1.1 Constant R_s and R_v Versus Depth

With a constant dissolved gas R_s in the oil, reservoir oil density is calculated as:

$$\rho_o = \frac{\rho_{ostd} + (\rho_g \times R_s)}{B_o} \tag{6.59}$$

ρ_o: reservoir oil density
ρ_{ostd}: stock tank oil density
ρ_g: surface gas density
R_s: standard solution gas ratio
B_o: oil formation volume factor

Oil density is converted into pressure gradient (Fig. 6.17). Knowing the initial reservoir pressure at datum, pressure for each grid block center is determined.

By definition at the GOC, gas pressure is equal to the oil pressure = oil bubble point pressure = reservoir pressure ($P_{cog} = 0$).

At WOC oil pressure is equal to water pressure ($P_{cow} = 0$)

For the gas zone, a similar calculation is carried out. Reservoir gas density is:

$$\rho_g = \frac{\rho_{gstd} + (\rho_{cond} \times R_v)}{B_g^*} \tag{6.60}$$

ρ_g: reservoir gas density
ρ_{gstd}: standard gas density
ρ_{cond}: surface condensate density
R_v: standard condensate gas ratio (CGR)
B_g^*: gas formation volume factor (two phase)

An average gas pressure is assigned to each grid block.

Saturation Determination:

In the oil water transition zone the difference between oil pressure and water pressure is the capillary pressure P_{cow}. For each grid cell center, P_{cow} is determined from the pressure gradients and through the capillary pressure curve P_c versus S_w, the water saturation is evaluated (Fig. 6.17). For capillary pressures above P_{cowmax}, the water saturation is equal to S_{wc}.

Some grid blocks are crossed by the WOC. By convention, the block is designed to belong to the oil zone or the water zone according to the respective location of its center with the WOC.

If the block center is above the WOC, the block is included in the oil zone, otherwise in the water zone.

The average water saturation is calculated for those blocks by dividing the total height of the block into 10 equal sub layers. Water saturation is determined for each sub layer with the P_c curve. The average saturation is then calculated as:

average saturation:

$$\bar{S}_w = \frac{\sum S_{wi} \times dh}{\sum dh} \tag{6.61}$$

6.13.1.2 Variable R_s and R_v Versus Depth

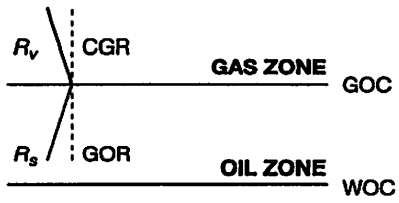

Figure 6.18 Variable Condensate Gas Ratio and R_s versus depth.

In the gas zone, R_v is maximum at the GOC.

In the oil zone, R_s is maximum at the GOC.

Oil zone: (Fig. 6.18)

Oil and water phase pressures versus depth are calculated from:

$$\frac{dP_o}{dh} = \rho_o(P_o, R_s) \times g \qquad \frac{dP_w}{dh} = \rho_w(P_o) \times g \tag{6.62}$$

with

$$P_w = P_o - P_{cow}$$

$\rho_o(P_o, R_s)$: oil density function of oil pressure and solution gas ratio
g: gravitational constant

Gas zone:

Gas phase pressure versus depth is calculated from:

$$\frac{dP_g}{dh} = \rho_g(P_o, R_v) \times g \tag{6.63}$$

with

$$P_g = P_o + P_{cog}$$

$\rho_g(P_o, R_v)$: gas density function of oil pressure and condensate gas ratio

The proper phase pressures are assigned to each grid block.

The saturation initialization is the same as the previous case.

6.13.2 Compositional Model

A gas or oil composition versus depth is entered. Intermediate compositions are determined by interpolation. At the GOC, a dew point or bubble point pressure calculation (depending on the known phase composition) is carried out. The calculated unknown phase composition in equilibrium is used to define the missing phase composition versus depth.

Supercritical initialization [109]

Deep and thick hydrocarbon reservoirs may contain a supercritical fluid. It means there is no gas oil contact in the hydrocarbon column. In the top section of the reservoir, the hydrocarbon is a gas condensate. The heavy component concentration increases with depth, so the fluid is qualified as a volatile oil at the bottom of the reservoir. In-situ hydrocarbon density increases smoothly with depth. The phenomenon is highlighted with an RFT survey. The fluid compositions are always at temperature and pressures that do not cross the equilibrium two-phase envelope. At some depth in the reservoir, the change of classification from gas to oil occurs without any classical change marked by a gas oil contact. The user needs to input an estimated GOC. The simulator performs a bubble point pressure and dew point pressure calculations using the input compositions as a function of depth. The fluids are sorted using the k values of the heaviest component to determine whether the reservoir fluid is oil or gas. The criterion to detect the pseudo gas oil contact is based on the heavy component k value when it switches to a value less than one.

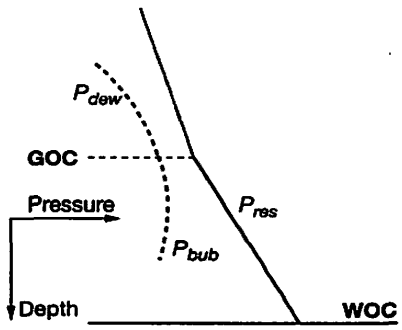

Figure 6.19 Supercritical fluid.

6.14 WELLS

The well ensures the communication between the reservoir and the surface facilities. A well is constituted of one perforation or a group of perforations sharing the same pressure regime.

The production or injection well may have a vertical, deviated or horizontal profile.

The relationship between the grid block and the bore hole is called the connection factor W_k or the well index W_i, function of the geometry and the absolute grid block permeability.

For the perforation j, the inflow performance of phase p in volumetric terms is written

$$Q_p = W_k \frac{k_{rp}}{\mu_p B_p} \Delta p \tag{6.64}$$

Q_p: volumetric flow rate of phase p from perfo j
W_k: perforation connection value
k_{rp}: phase relative permeability at the perforation
B_p: phase formation volume factor
Δp: block pressure – corrected for height bottom hole flowing pressure

For compositional simulation, the relationship becomes for component i:

$$q_{i,j} = x_{i,j} b^m_{o,j} q_{o,j} + y_{i,j} b^m_{g,j} q_{g,j} \tag{6.65}$$

$q_{i,j}$: molar rate of component i from perfo j
$x_{i,j}$: liquid mole fraction of component i from perfo j
$b^m_{o,j}$: liquid reservoir molar density
$q_{o,j}$: volumetric oil rate from perfo j
$y_{i,j}$: vapor mole fraction of component i from perfo j
$b^m_{g,j}$: vapor reservoir molar density
$q_{g,j}$ volumetric vapor rate from perfo j

The perforation connection value W_k was defined in the chapter "Fluid flow in Reservoirs" according to the Placeman's theory:

$$W_k = \frac{Ckh}{\mathrm{Ln}\left(\frac{r_o}{r_w}\right) + S} \tag{6.66}$$

C: unit conversion factor
k: perforated block absolute permeability
h: effective opened block thickness
r_o: equivalent radius
r_w: well radius
S: skin factor
r_o: in a Cartesian grid is expressed as:

$$r_0 = 0.28 \frac{\left[(k_y/k_x)^{1/2} \Delta x^2 + (k_x/k_y)^{1/2} \Delta y^2\right]^{1/2}}{(k_y/k_x)^{1/4} + (k_x/k_y)^{1/4}} \tag{6.67}$$

6.14.1 Well Controls and Limits

Wells can be controlled with the following options:

- Oil or gas or water surface rate.
- Fixed bottom hole flowing pressure.
- Total withdrawal flow rate (oil plus gas plus water) at reservoir conditions.
- Minimum well head flowing pressure.

When running a reservoir pressure history match, it is recommended to control all producers with the option total flow rate also called reservoir voidage. Production wells withdraw the total amount of material out of the reservoir, so the aquifer size and activity can be adjusted to honor the reservoir pressure behavior independently of GOR and water cut performances. Usually calculated oil, gas and water rates are wrong. Once the pressure match is acceptable, the simulation is rerun with the oil rates specified to the producing wells. The simulator computes gas and water rates, consequently the production GOR and water cut. These parameters need to be matched with history. This is the second part of the history match.

To run predictions, it is usual to control the production wells with a nominal oil rate and a minimum well head flowing pressure. The constraint corresponds to the minimum manifold or separator pressure expected during production. When the reservoir cannot produce the rate at the minimum well head flowing pressure, rate decline is admitted.

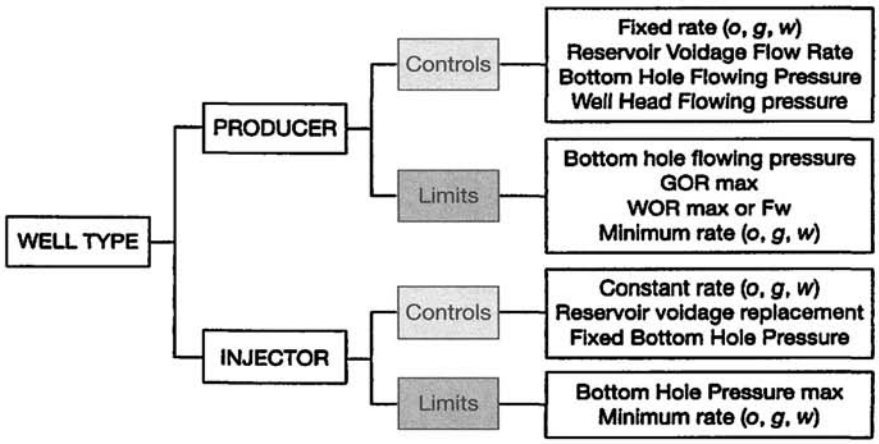

Figure 6.20 Controls and limits for each well type.

Any well must be given a limit flowing pressure:

- For a producer: minimum flowing pressure P_{wf}.
- For an injector: maximum flowing pressure P_{wmax}.

Usually the maximum flowing pressure is less or equal to the formation fracturing pressure.

If, for a production well controlled by a fixed phase rate, the calculated flowing pressure falls below the defined limit pressure, the well control switches automatically to bottom hole flowing pressure. Consequently, the phase rate declines.

Controls and limits are illustrated in Figure 6.20.

6.14.2 Field Production Facilities

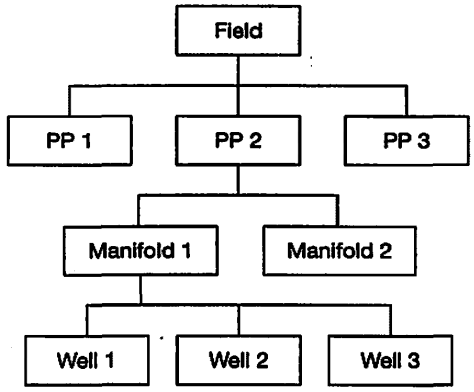

Figure 6.21 Offshore Facilities.

Different words are used to describe the production facilities. An example of offshore and one for land facilities are illustrated on Figures 6.21 and 6.22

PP: Production Platform

Manifold: large collector where several well production fluids from wells are mixed

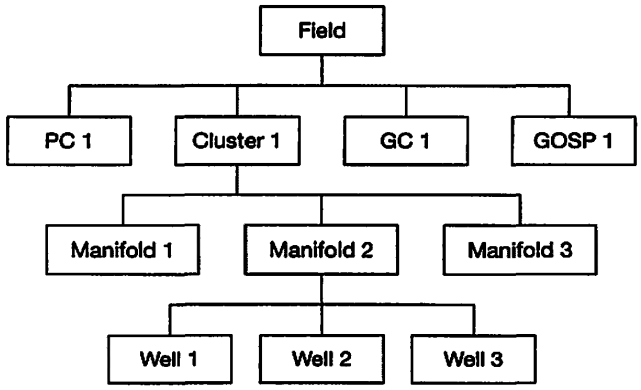

Figure 6.22 Land Facilities.

PC:	Production centre
or	
Cluster:	group of well heads located on a small area
or	
GC:	Gathering Centre
or	
GOSP:	Gas Oil Separating Plant

Software manufacturers, simulate the hierarchy of the production facilities. Controls and limits can be specified independently at each level.

6.14.3 Well Head Flowing Pressure Control

The well head flowing pressure control is usually used for predictions. The control involves the reservoir deliverability (Inflow Performance Relationship) and the completion flowing capacity simultaneously (Vertical Lift Performance or *Vertical Flow Performance*). The curve intersect (Fig. 6.23) represents the operating condition where both conditions are satisfied.

The vertical flow performance is included in the simulation data set, as tables. The table gives the bottom hole flowing pressure. For an oil well the table is defined in terms of oil rate, Gas Oil Ratio, and water cut, but can also be defined in terms of liquid rate, gas liquid ratio and water cut.

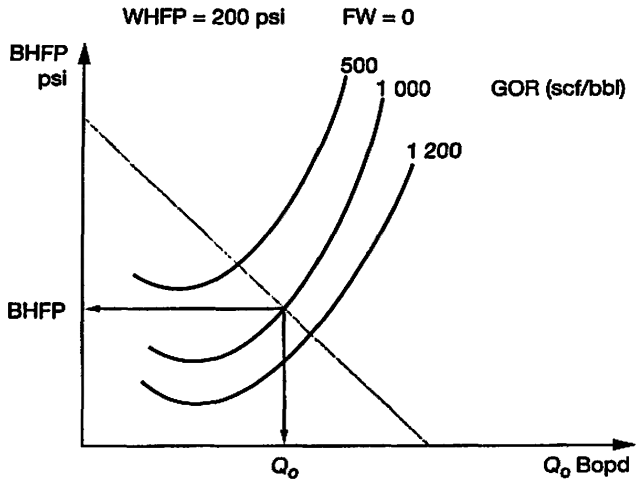

Figure 6.23 Vertical Lift Performance and PI curves.

Loss of head table example

Wellhead pressure 200

Oil rates 300 500 800 1 000 1 500 2 500 3 500

Gas oil ratios 300 700 1 500 2 500 3 500

Water cuts: 0 0.2 0.5 0.8 0.95

corresponding table

	W_{hfp}	200						(psi)
	Q_o	300	500	800	1 000	1 500	2 500	(bopd)
	GOR	300		700	1 500	2 500	3 500	(scf/bbl)
	F_w	0	0.5	0.8	0.95			
	GOR Q_o							
$F_w = 0$	300	P_{wf1}	P_{wf2}	P_{wf3}	P_{wf4}	P_{wf5}	P_{wf6}	
	700	P_{wf7}	P_{wf8}	P_{wf9}	P_{wf10}	P_{wf11}	P_{wf12}	
	1 500	P_{wf13}	P_{wf14}	P_{wf15}	P_{wf16}	P_{wf17}	P_{wf18}	
	2 500	P_{wf19}	P_{wf20}	P_{wf21}	P_{wf22}	P_{wf23}	P_{wf24}	
	3 500	P_{wf25}	P_{wf26}	P_{wf27}	P_{wf28}	P_{wf29}	P_{wf30}	
$F_w = 0.5$								
$F_w = 0.8$								
$F_w = 0.95$								

P_{wf1}, P_{wf2}... are the bottom hole flowing pressures to ensure the corresponding oil rate with the minimum well head flowing pressure 200 psi.

Remark:
Table formats are specific to each simulator. The loss of head calculation programme offers an export file directly compatible with the input simulator format.

In this option, the user specifies a nominal oil rate for the well. The simulator calculates the operating conditions (Q_o, P_{wf}) with the IPR and VLP curves. If the nominal rate is less than the operating rate, the simulator applies the nominal rate. Conversely if the nominal rate is higher than the operating rate, the simulator applies the operating rate.

6.14.4 Concluding Remark

The relationship between the block pressure and the well flow rate is based on steady-state flow theory. To simulate transient flow around the well, small grid mesh description is necessary around the well block.

6.15 AQUIFER MODELING

A reservoir model to be representative of the field needs to include the associated aquifer properly dimensioned. That is the first priority of a reservoir engineer. The basic associated parameters are: volume of the aquifer and its activity (energy).

6.15.1 Block Aquifer

One method to model the aquifer is to extend the model in the aquifer by several blocks with large pore volumes which are connected to the reservoir blocks around the edges of the oil zone. The aquifer volume is adjusted by setting very high porosities (higher than 1) and the water entries (activity) are adjusted by modifying the transmissibility between the aquifer blocks and the hydrocarbon bearing blocks. The main drawback to the procedure is the addition of a large amount of grid blocks. The simulator takes care of transient aquifer response automatically.

6.15.2 Injection Wells

An other way to model an aquifer is to set "pseudo water injection wells" at the oil water contact; then adjust the water injection rate by setting a fixed bottom hole flowing pressure and monitor the cumulative water entries.

6.15.3 Analytical Aquifers

All simulators offer the option to use "analytical aquifers".

6.15.3.1 Carter-Tracy Aquifer

The Carter-Tracy aquifer model is a simplified approximation to a fully transient model, derived from the standard Van Everdingen and Hurst theory.

Two main parameters govern the behavior of the aquifer:

The time constant

$$T_c = \frac{\varphi \mu_w c_t r_0^2}{k}$$

φ: aquifer porosity
μ_w: water viscosity in the aquifer
c_t: total compressibility (rock + water $c_f + c_w$)
r_0: outer radius of oil zone
k: aquifer permeability

and the aquifer constant:

$$B = r_0^2 h \phi c_t f$$

h: aquifer thickness
f: circle fraction

The time constant is used to convert time t into dimensionless time t_D through:

$$t_D = \frac{t}{T_c}$$

The dimensionless time, is used to evaluate the unit water influx from the Hurst Van Everdingen solution table. Usually, simulators include a default table corresponding to an infinite reservoir.

The aquifer calculated influx rates contribute to the residual in implicit equations. The cumulative aquifer influx W_e is updated explicitly at the end of the timestep.

6.15.3.2 Fetkovich Aquifer

The model assumes that the aquifer pressure response is felt throughout the entire aquifer. The model is best suited for limited aquifers where transient response can be considered negligible. In this approach, the aquifer flow into the hydrocarbon zone is modeled in the same way as the flow of oil from a reservoir into a well.

The inflow equation is:

$$\frac{dW_e}{dt} = J(p_a - p)$$

J: aquifer productivity index
p_a: average pressure in the aquifer
p: pressure at the oil or gas contact

The aquifer influx We is evaluated using the aquifer material balance based on the rock and water expansion.

$$W_e = c_t W (p_i - p_a)$$

c_t: total compressibility
W: initial aquifer water in place
$p_i - p_a$: pressure drop between aquifer and hydrocarbon zone

6.16 TIMESTEP MANAGEMENT

The user needs results at regular time intervals or at fixed dates. For example in a long simulation run, one may require a solution every month or quarter. The results are stored in binary form on the disk, ready to be read and analyzed with the appropriate post-processing programme. It must be noted that the stored results are instantaneous values at the recorded dates. It is often necessary to calculate average rates between two dates based on cumulative

changes divided by the elapsed time length. Between two "storing dates", the simulator carries out several calculation timesteps.

All simulators include an automatic timestep control. Control is based on the maximum calculated parameter changes during a calculation timestep. The faster the changes, the smaller the calculation timestep should be.

6.16.1 IMPES Algorithm

In the IMPES algorithm, using large stable timesteps gives the smallest truncation errors [100]. After completion of a calculation timestep, the programme detects the grid blocks where the maximum pressure and saturation changes occurred during the timestep. Practically the maximum saturation change over the grid is kept below a given limit "DSLIM" for every timestep. Typically a value of 5 to 10% is used depending on the problem. A target value for the ΔS change is used to trigger the automatic timestep control. Usually 3% is used for saturation. The same principle is applied for the pressure changes during the simulation.

The actual changes are nonlinear and the limiting values may be considerably exceeded with the predicted Δt (Fig. 6.24).

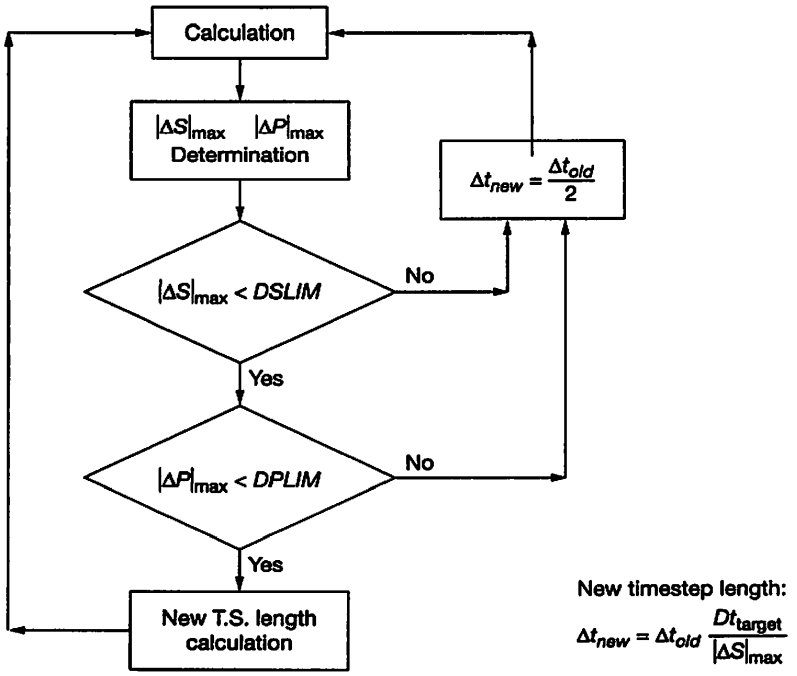

Figure 6.24 Timestep management Flow Chart.

6.16.2 Fully Implicit or AIM Algorithms

As mentioned before, these algorithms are very stable and allow much larger calculation timestep lengths than IMPES does. Acceptable saturation changes may be as high as 30% with high throughputs across the grid cells. A reservoir simulation may be run with one month calculation timestep length during history match.

Remarks:
Figure 6.24 illustrates the timestep management flow chart. The timestep length is cut by 2 when the maximum pressure or saturation changes exceed the limit. The timestep cut may be also activated when the solver inner or outer iteration process fails to converge.

6.17 SPECIAL TOPICS

6.17.1 Local Grid Refinement [127, 128, 129]

The Local Grid Refinement (LGR) option is a special feature (Fig. 6.25) which enables the user to improve the resolution and detail in a particular area of a reservoir study, without increasing the resolution everywhere. The domain of applications includes:

- Coning effects in field wide models
- Horizontal wells
- Interference between multiple reservoirs
- Unconfined pattern
- Delineation of faults.

To increase the calculation efficiency, some simulators offer an option, for each local grid to be solved individually using "local time stepping". This allows the local grids to have shorter timesteps than the global grid without holding up the progress of the global grid simulation. Each local grid may require several calculation timesteps to reach the end of a global timestep. The local timesteps are chosen to synchronize with the end of each global timestep.

Flows between the local and global systems are computed as boundary conditions to each local simulation. The process includes updating well rates and material balance in host cells of the global model to be consistent with the local models.

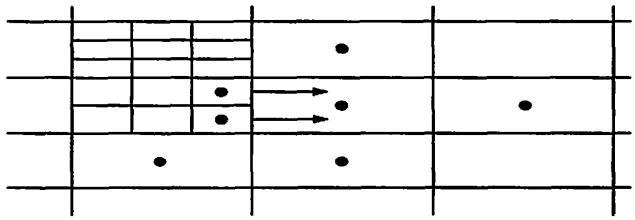

Figure 6.25 Local Grid Refinement example.

Figure 6.25 illustrates a grid refinement of 3 × 3 small grids in a main block.

6.17.2 Parallel Processing [108, 109, 130]

The need of large simulation has been a continuous request by users. Software manufacturers and users were limited by the by computer capacities (CPU speed, main memory, disk storage). During the 1980's, the industry turned to costly super computers associated with the vectorization techniques to work on large scale problems (Fig. 6.1). With the continuous technology improvements, the industry offered similar performances on so called RISC (Reduced Instruction Set Computing) workstations. Parallel techniques were developed by having several CPU working simultaneously, associated with a proper software and hardware to ensure communications between them. From a single data set, the technique consists of distributing across different processors in parallel the computing work necessary to complete the simulation. The main advantage is the low cost hardware involved.

To improve the computing performance, it is necessary to "parallelize" the code.

With the development of the micro computer industry in the 2000's, the use of Personal Computers is possible to run simulations.

The software divides the reservoir into domains with approximately equal number of active cells. The drawback is for the linear solver algorithm requiring more iterations than the purely serial solver. The effect is very model dependent.

6.18 CONDUCTING A RESERVOIR SIMULATION STUDY

6.18.1 Data management

It has been estimated that Exploration Production (E&P) professionals can spend up to a third of their time looking for data and another third checking its source and reliability and making it usable [131]. That leaves only a third for doing any work. It certainly happens that the wrong data gets used or for the wrong purpose or that mistakes creep in during conversion or formatting. Sometimes, companies reacquire data they already possess although, in the extreme, if it takes so long to find and check for errors, starting again may be more cost-effective than setting out to look for what exists.

Often the same data is stored more than once and it is not obvious which is the best or more recent version.

Data are stored on different supports:

– paper for old data, films, specialized data base, digitized old data and so on.

To perform a reservoir study, all participants express the same requirements:

– Quick, complete and reliable access to the information at their disposal.

- Improve capacity for the organization to "learn" i.e. to share experience, to solve.
- Problems once and avoid to make the same mistake twice.
- Good, secure links with colleagues, partners, suppliers, contractors.
- As a result, cheaper, faster, and more profitable activities.

A reservoir study starts from a geological model that has been built with a commercial programme. The geomodel is created with data that have been stored in a "working data base". Ideally the working data base is being filled from a corporate data base. The corporate data base has been filled up with validated data that have been checked by experts of all disciplines.

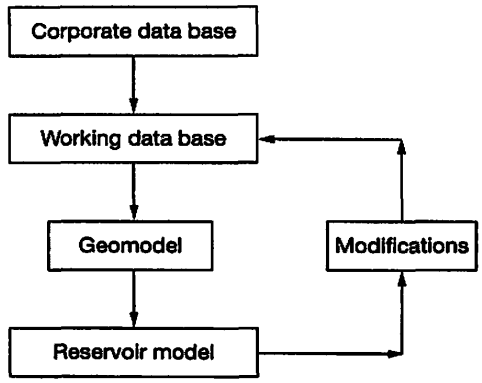

Figure 6.26 Reservoir model Building work flow.

The reservoir model is deducted from the geomodel.

During the reservoir study, adjustments and modifications are initiated by the geologist and the reservoir engineer. The modifications are made on the working data base contents so consistency between the base and the reservoir model is preserved.

Figure 6.26 illustrates the work flow.

6.18.2 Building a Reservoir Model

Building a reservoir model is a long process involving geophysicist, geologist and reservoir engineer skills.

From the working data base (Fig. 6.27), the geologist and geophysicist use the appropriate software to create the structure. The reservoir volume is divided into grid blocks. All the geological model grid blocks are populated with basic data such as porosity, permeability and water saturation. Finally, the initial hydrocarbon in place is calculated.

Often the model built by the geologist can't be handled by the reservoir simulator.

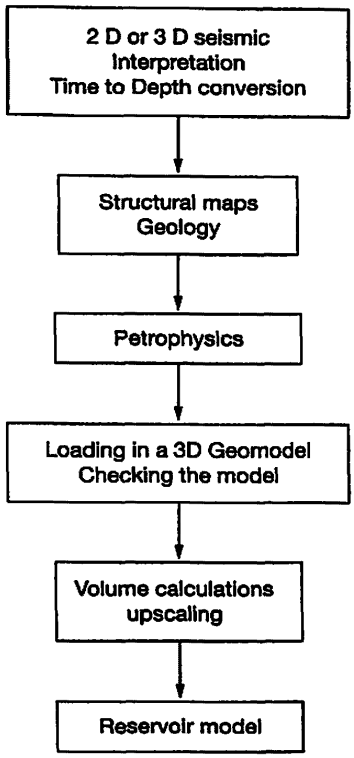

Figure 6.27 Reservoir Modeling Workflow.

Decreasing the number of cells is necessary. This is accomplished by the "upscaling" procedure.

During the "upscaling" process, some features of the model are lost. The difficulty is to make sure that the loss has a negligible impact on the model performance. The last requirement is to obtain the same reservoir volumes in both models: the detailed geological and the reservoir models.

6.18.3 History Match

Before running any predictions, it is necessary to "calculate" the production history. This is a tedious task of the "history match" The procedure is divided into three steps:

- Aquifer dimensioning with material balance calculation.
- Reservoir pressure match.
- Phase rate match.

Aquifer Dimensioning:

A preliminary study with material balance software is necessary to run the aquifer match as explained in chapter 5. The expected result is the aquifer volume plus its permeability.

Reservoir pressure match:

The aquifer volume is to be reproduced in the reservoir model with aquifer cells or analytical functions. The reservoir model production history is run with all the producing wells governed by the "reservoir voidage" option. The user needs to adjust the aquifer volume and activity to reproduce the field observed reservoir pressure history. Aquifer activity can be adjusted by modifying aquifer permeability or using transmissibility multipliers between aquifer grid cells and hydrocarbon bearing cells.

Reservoir pressure history must be prepared with great care. The data origin is mainly from build-up tests and or from RFT's (Repeat Formation Tester) surveys run in new wells. Some simulators accept direct RFT pressure measurements to be compared with the calculated cell pressures. Reservoir pressure deducted from DST (Drill Stem Test) need to be compared with an average pressure calculated from the well surrounding cells and the well block. It is usual to calculate an average pressure from 5 grid cells (areal model) weighed by the respective pore volumes.

$$\overline{P} = \frac{\sum P_i V_{ip}}{\sum V_{ip}}$$

Given Q_o, Q_g and Q_w, surface oil, gas and water rates, the total fluid withdrawal at reservoir conditions is:

$$q_T = Q_o B_o + Q_g B_g - Q_o R_s B_g + Q_w B_w$$

Pressure match is an adjustment of the reservoir energy balance between:

- Initial hydrocarbon volume in place.
- Rock and connate water compressibilities.
- Aquifer activity.

The solution to the problem is not unique but must look sound to the geologist and to the reservoir engineer.

Phase rate match:

During the pressure match procedure, production phase rates are not honored. Simulation is rerun by setting the oil rate (or gas rate for gas reservoir) for producers so bottom hole flowing pressure, gas and water rates are calculated by the simulator. The phase rate matching consists of adjusting the calculated GOR and water cuts to the field measured values.

To honor the relationship between reservoir pressure, bottom hole flowing pressure and phase rates, productivity indexes need to be adjusted. This is accomplished by applying multiplication factors to the well perforation connection values.

Tuning parameters used for history match:

- Hydraulic flow units (permeability).
- Permeability barriers (vertical and or horizontal).
- Grid block relative permeabilities (shape and end points).

Simulators by default use the block assigned relative permeability to govern the well phase rates. Nevertheless it is possible to design specific relative permeability curves for the well phase calculation.

The general rule in manual history matching is to change the parameters which have the largest uncertainty and also the largest influence on the calculation. Often sensitivity runs to some of the parameters are carried out to evaluate the impact on the calculation. Matching breakthrough times is a difficult task. Breakthrough times are sensitive to truncation errors (numerical dispersion) and the accurate matching requires finer grid than normally necessary. Using a "Local Grid Refinement" is a possibility or the use of "pseudo-relative permeabilities" can help. An unsuccessful attempt for a match indicates that some of the basic assumptions of the model (geology, structure, volumes, extensions, PVT behavior, energy balance between initial hydrocarbon in place and aquifer activity) may have to be revised. Inaccuracy in production data particularly for old reservoirs (gas productions) may be the source of difficulties. All model modifications should be applied in the "working data base" so that the data base is always consistent with the reservoir model.

The process of history matching is time consuming and frustrating. It represents a large portion of the cost of a study.

There has been during the last thirty years, a large research effort devoted to automating the process by using "inverse simulation". In the procedure, equations are solved for the values of selected reservoir parameters, so that the differences between the computed results and observed behavior are minimized.

History matching techniques are also used to interpret laboratory experiments like water flood, WAG (Water Alternate Gas) flood, gas injection, tertiary experiment or in situ combustion.

6.18.4 Predictions

This is the final goal of a reservoir study. Before running any predictions, a good understanding of the reservoir production mechanisms is necessary that is an acceptable "within engineering accuracy" history match available. The reliability of the predictions for future performance depends on the amount of data available for the match. Even with a good history match, the reliability of predictions decreases as we look farther and farther ahead. It is therefore necessary to update the model with new historical data.

To predict reservoir performance, usually production wells are controlled with a minimum well head flowing pressure option according to the field practices. Different scenarios may be envisaged like:

- New drilling, workovers.
- Enhanced oil recovery with water or gas injection.

6.18.5 Restart Facility

A result restart file is a file that contains all elements necessary for a simulation to run from any date after the initial time. The file is stored on the disc in binary form at dates that are decided by the user. A restart input data file may be short and contain only the recurrent data. Its use can save a lot of computing time by avoiding starting from the initial time for all simulating scenarios following a production history match.

6.19 CONCLUDING REMARKS

Large experience in reservoir engineering is necessary to take full advantage of the technology offered in reservoir simulation. A minimum investment in the technology is required to understand and master the "tool". Many assumptions are necessary to build a reservoir model therefore calculations are only approximate and a good engineering judgment is required to evaluate input data and interpret calculation results.

Appendices

APPENDIX A Conversion Factors

To convert from	to	Multiply by
Length		
foot	meter (m)	0.3048
foot	inches	12
mile (US)	meter	1 609.344
Area, Permeability		
acre	metre^2 (m^2)	4 046.856
foot^2	metre^2 (m^2)	$9.290 * 10^{-2}$
hectare	metre^2 (m^2)	10 000
darcy	millidarcy (mD)	1 000
darcy	metre^2 (m^2)	$9.869\,230 * 10^{-13}$
millidarcy	metre^2 (m^2)	$9.869\,230 * 10^{-16}$
Volume		
acre-foot	metre^3 (m^3)	$1.233\,482 * 10^{3}$
acre-foot	ft^3 (cuft)	$4.356 * 10^{4}$
acre-foot	barrel (bbls)	$7.758\,368 * 10^{3}$
barrel	metre^3 (m^3)	0.158 987
barrel	ft^3 (cuft)	5.614 583
barrel	gallon (US)	42.0
cubic-foot	metre^3 (m^3)	$28.31685 * 10^{-3}$
Mass		
pound-mass	kilogram (kg)	0.453 5923

To convert from	to	Multiply by
Force		
dyne	newton (N)	$1.000 * 10^{-5}$
kilogram-force	newton (N)	9.806 650
pound-force	newton (N)	4.448 222
Pressure		
atmosphere	bar	1.0132 500
atmosphere	pascal (Pa)	$1.0132\ 500 * 10^{5}$
atmosphere	psi	14.696
bar	pascal (Pa)	$1.0 * 10^{5}$
bar	psi	14.503
Viscosity		
centipoise	pascal-second (Pa.s)	$1.0*10^{-3}$
Temperature		
°C	°Farenheit	(multiply by 1.8 + 32)
°F	°Rankine	°R = °F + 460
°C	Kelvin	K = °C + 273

APPENDIX B Multiples

	US	Metric	power	Examples
Thousand	M	k	10^{3}	Mscf, kPa
Million	MM	M	10^{6}	MMscfd, Mm^3
Billion	B	G	10^{9}	Bcf, Gm^3
Trillion	T	T	10^{12}	Tcf

APPENDIX C Darcy's Law for Gas

For a constant mass rate, the volumetric flow rate is constant for liquids, because the density does not change significantly during the flow through the core sample [2].

$$q = \frac{k}{\mu} A \frac{P_1 - P_2}{L} \tag{C.1}$$

q: volumetric flow rate, cm^3/s
μ: gas viscosity, cp
A: core section area, cm^2
P_1, P_2: upstream and downstream pressures, atm
L: core length, cm

For gases, the volumetric flow q varies with pressure, the value for q at the average pressure in the core must be used in Eq. (C.1).

To convert gas volumes at the mean pressure to gas volumes at 1 atm, the term Q is used for gas flows in cm^3/s at pressure P_b according to Eq. (C.2).

P_b is the absolute base pressure for gas measurements.

$$Q = q\frac{P_1 + P_2}{2P_b} \tag{C.2}$$

Combining Eqs. (C.2) Eq. (C.1), the Darcy's law for gases becomes:

$$Q = \frac{k}{2\mu LP_b}A(P_1^2 - P_2^2) \quad \textit{(Darcy units)} \tag{C.3}$$

With Q: *gas volumetric flow rate at atmospheric pressure* P_b.

APPENDIX D Gas $m(p)$ Property Calculation

Calculation example of gas pseudo-function $m(p)$							
P(bar)	μ	Z	$2p/\mu z$	average	delta P	aver * DP	$m(p)$
20	0.012244	0.964	3 388	1 694	20	33 878	3.388E+04
40	0.013246	0.910	6 634	5 011	20	100 214	1.341E+05
60	0.014269	0.866	9 710	8 172	20	163 435	2.975E+05
80	0.015314	0.831	12 577	11 143	20	222 868	5.204E+05
100	0.016379	0.804	15 189	13 883	20	277 657	7.981E+05
120	0.017465	0.785	17 502	16 345	20	326 909	1.125E+06
140	0.018572	0.774	19 481	18 492	20	369 836	1.495E+06
160	0.019700	0.770	21 105	20 293	20	405 869	1.901E+06
180	0.020850	0.772	22 369	21 737	20	434 745	2.335E+06
200	0.022020	0.780	23 284	22 826	20	456 528	2.792E+06
220	0.023211	0.794	23 875	23 580	20	471 591	3.264E+06
240	0.024423	0.813	24 180	24 028	20	480 554	3.744E+06
260	0.025657	0.836	24 240	24 210	20	484 200	4.228E+06
280	0.026911	0.863	24 100	24 170	20	483 397	4.712E+06
300	0.028186	0.894	23 802	23 951	20	479 017	5.191E+06
320	0.029483	0.928	23 387	23 594	20	471 887	5.663E+06

Parameters μ and Z, functions of pressure are obtained from the PVT analysis of the gas or from standard gas correlations at the reservoir temperature.

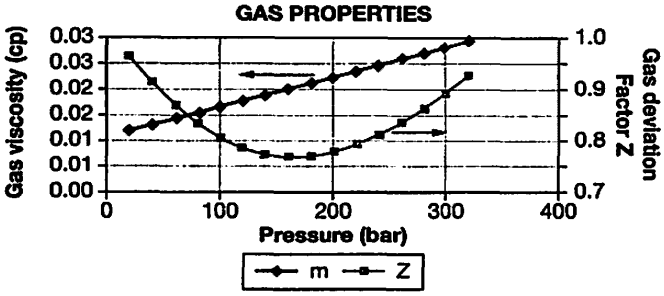

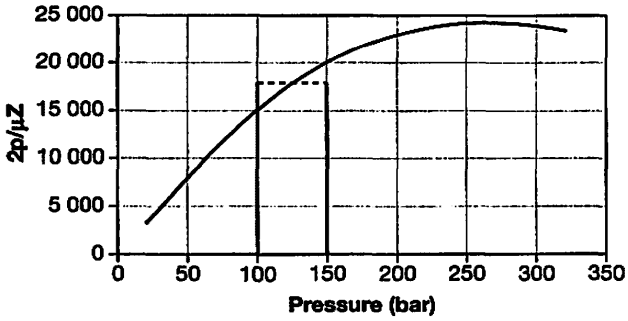

Using a simple graphical method for numerical integration, (trapezoidal rule), a table m(p) function of the actual pressure is obtained.

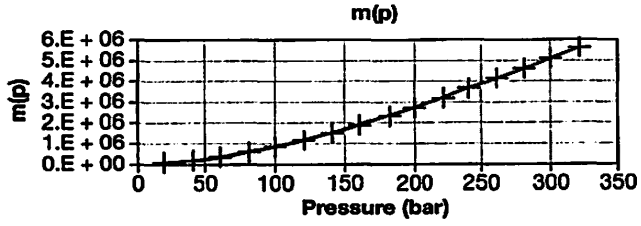

APPENDIX E Applied Mathematics

E.1 Compressibility

Definition:

$$c = -\frac{1}{V}\left(\frac{\delta V}{\delta P}\right)_T = \frac{1}{\rho}\left(\frac{\delta \rho}{\delta P}\right)$$

c: compressibility at constant temperature T
V: initial volume
δV: volume change
δP: pressure change
ρ: fluid density
$\delta\rho$ density change

Physically, compressibility has to be a positive value. Therefore when c is defined from volume or density variations, the sign is changed to keep $c > 0$.

For liquids, compressibility can be considered constant in the pressure range of interest.

$$c = \frac{1}{\rho}\frac{d\rho}{dp} \qquad \int \frac{d\rho}{\rho} = c\int dp \qquad \mathrm{Ln}\frac{\rho}{\rho_0} = c(p - p_0)$$

so $$\rho = \rho_0 e^{c(p-p_0)} \qquad e^x = 1 + x + x^2/2! + x^3/3! + \ldots$$

$$e^{c(p-p_0)} = 1 + c(p-p_0) + \left[\frac{c(p-p_0)}{2!}\right]^2 + \ldots$$

since c is very small, higher order terms can be neglected.

$$e^{c(p-p_0)} = 1 + c(p-p_0) \text{ then } \rho = \rho_0[1 + c(p-p_0)]$$

This formulation is applied to most reservoir oils and reservoir waters. For gases, the approximation is not valid, and the complete equation is used.

E.2 Derivative of a function u^2

$$\frac{\delta(p^2)}{\delta x} = 2p\frac{\delta p}{\delta x} \qquad \frac{\delta^2(p^2)}{\delta x^2} = 2\frac{\delta}{\delta x}\left(p\frac{\delta p}{\delta x}\right) = 2\left[\left(\frac{\delta p}{\delta x}\right)^2 + p\frac{\delta^2 p}{\delta x^2}\right]$$

E.3 Calculation of the real gas compressibility

$$c = -\frac{1}{V}\left(\frac{\delta V}{\delta P}\right)_T \text{ with } pv = znRT \qquad v = \frac{1}{p}nzRT$$

$$\frac{\delta v}{\delta p} = nRT\frac{\delta}{\delta p}\left(\frac{z}{p}\right) = \frac{nzRT}{p}\left[\frac{1}{z}\frac{\delta z}{\delta p} - \frac{1}{p}\right]$$

substituting into the compressibility definition c:

$$c_g = -\frac{1}{v}\frac{nRTz}{p}\left[\frac{1}{z}\frac{\delta z}{\delta p} - \frac{1}{p}\right] = \frac{1}{p} - \frac{1}{z}\frac{\delta z}{\delta p} \equiv \frac{1}{p}$$

if z changes are small, the compressibility of gas can be approximated to $1/p$.

Gas compressibility is very pressure dependent.

APPENDIX F Density, Pressure Gradient

Pressure Gradient	Units	DENSITY			
		g/cm^3	kg/m^3	Lbs/cu. ft	Lbs/gal
0.100	kgf/cm^2/m	1.000	1 000.0	62.428	8.345
0.098	Bars/m	1.000	1 000.0	62.428	8.345
1.422	psi/m	1.000	1 000.0	62.428	8.345
0.434	psi/ft	1.000	1 000.0	62.428	8.345

Relative Density (/water)

1

DENSITY		PRESSURE GRADIENT	
1.000	g/cm^3	0.100	kgf/cm^2/m
1 000.0	kg/m^3	0.098	Bars/m
62.428	Lbs/cu. ft	1.422	psi/m
8.345	Lbs/gal	0.434	psi/ft

Oil density

$$\rho_o = \frac{141.5}{131.5 + °API} \qquad °API = \frac{141.5}{\rho_o} - 131.5$$

°API = 42 0.8156 g/cc

Rho o = 0.8156 g/cc 42.0 °API

Oil density at reservoir

Rho air at SC = 0.001225 g/cc

Rho oil = (Rho oil Std + 0.001225 * gas relative dens * Rs)/Bo

Rho oil S	0.837	g/cc
gas relative density:	0.8	/air
Rs:	552.1	vol/vol
Bo:	2.8	

Rho oil = 0.492 g/cc or 0.213 psi/ft

or

Rho oil = (Rho oil Std + Rhog * Rs)/Bo

Rho oil Std	0.837	g/cc
Rho g Std	0.0009784	g/cc
Rs:	552.09	vol/vol
Bo:	2.8	

Rho oil = 0.492 g/cc

APPENDIX G

Prediction of minimum gas flow rate required for liquid removal from gas wells (Ref. trans. AIME (1969) Vol 246 – Page 1475)

Compressibility factor Z applied, for tubing pressures above 5 000 psi, use the 5 000 psi point on the pressure scale.

The purpose of this chart is to estimate the minimum flow rate required to remove either condensate or water through a given diameter of the tubing or a given area of the annulus at well head conditions. Calculations show that, for typical field conditions, it is in fact at this point that the highest flow rate is required.

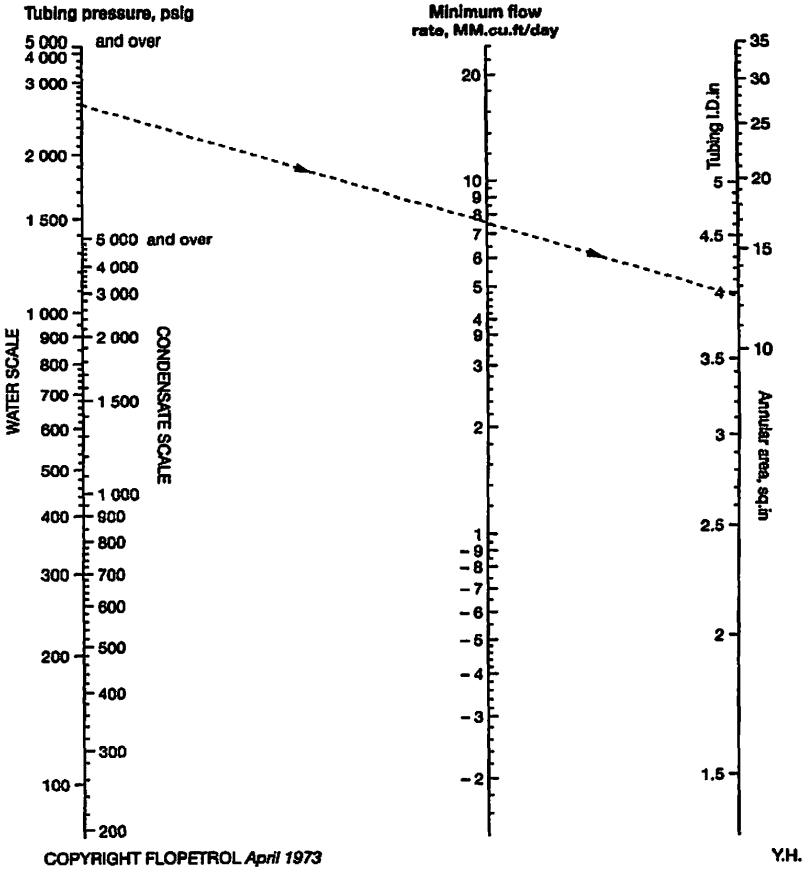

APPENDIX H Thermodynamic Review [70]

Thermodynamics is a branch of sciences which deals with energy and work of a system.

H.1 Internal Energy

The concept term defines the energy possessed by a mass other than potential or kinetic. The symbol "U" is commonly used to represent internal energy. Some authors use "E".
Internal energy is the sum of all forms of energy possessed by a mass other than kinetic and potential.

Total Energy is therefore = U + PE + KE.

PE: potential energy KE: kinetic energy

Internal energy of a fluid is a state variable, that is, a variable which depends only on the state of the fluid and not on any process that produced that state.

It is possible to define additional state variables which are combinations of existing state variables. For a gas a useful state variable is the enthalpy which is defined to be the sum of internal energy U plus the product of the pressure p and volume V.

H.2 Enthalpy

Enthalpy, also called the heat content, of a closed system having a volume V and a uniform pressure p is defined by

$$H = U + pV \tag{H.1}$$

The enthalpy of a heterogeneous system is the sum of the enthalpies of the individual phases.

A system can exchange energy with exterior in four ways:

- Energy associated with mass entering.
- Energy associated with loss of mass.
- Heat exchange.
- Work exchange.

Heat (Q) is defined as all energy crossing the boundary of the system that is not associated with mass transfer, solely as a result of a temperature difference between the system and the surroundings. Heat gained by the system is by convention positive; heat lost by the system is negative.

Work (W) is defined as all energy crossing the boundary of the system that is not associated with mass transfer, and no temperature difference. Work delivered by the system (leaving it) is by convention positive. Work done on the system (entering it) is negative. This convention is the one adopted in the English system. The French convention differs for the work by saying that work delivered by the system (leaving it) is negative and work received is positive.

For a system with heat transfer Q and work W, the change in internal energy from state 1 to state 2 is equal to the difference in the heat transfer into the system and the work done by the system:

first law of thermodynamics

$$U_2 - U_1 = Q - W \text{ (}\textit{english convention}\text{)} \quad \text{(H.2)}$$

$$U_2 - U_1 = Q + W \text{ (}\textit{french convention}\text{)}$$

For an adiabatic process, (Q = 0; no heat exchange), the law becomes:

$$U_2 - U_1 = -W \text{ (}\textit{english convention}\text{)}$$

$$U_2 - U_1 = W \text{ (}\textit{french convention}\text{)}$$

In the absence of energy transfer other than the work generated by pressure forces, the compression work is equal to the internal energy change.

The work and heat transfer depend on the process used to change the state.

In a case of a constant pressure process, the work done by gas is given as the constant pressure p times the volume change:

$$W = p \times (V2 - V1) \quad \text{(H.3)}$$

Substituting (H.3) into equation (H.2)

$$U2 - U1 = Q - p \times (V2 - V1)$$

or

$$(U2 + p \times V2) - (E1 + p \times V1) = Q \quad \text{(H.4)}$$

$$H2 - H1 = Q$$

H.3 Second Law of Thermodynamics Entropy

The first law of thermodynamics deals with the system property changes between the system and its surroundings with no distinction between the different energy types: heat and work. It is not possible to determine between two states which one is the most stable.

The second law allows to calculate the work amount obtained during a determined process and to evaluate its efficiency in comparison to an ideal chosen reference process. The second law introduces the concept of reversible and irreversible process.

A process is defined reversible when it is made of continuous successive states at equilibrium. In practice, energy dissipation like viscous forces, electrical heat dissipation, induce real irreversible processes.

H.4 Clausius's Postulate

Heat does not move from a cold system to a hot one on its own.

Entropy measures the spontaneous dispersal of energy: how much energy is spread out during a process, or how widely spread out it becomes as a function of temperature.

Entropy change = "energy dispersed"/ T

$q_{reversible}/T$, like in a phase change process (melting or vaporization, where $\Delta S = \Delta H_{fusion}/T$ or $\Delta H_{vaporization}/T$, respectively.)

For a closed thermodynamic system, symbol S is used to quantify the amount of thermal energy not available to do work. It can be considered to be a measure of the system's disorder and that is a property of the system's state.

The entropy change of a system is the sum of entropy changes due to its interaction with exterior plus the entropy changes due to internal modifications.

$$dS = dS_e + dS_i$$

dS_e is a function of heat exchanges with exterior: $dS_e = \frac{\delta Q}{T}$

dS_i relative to the intern transformations is considered positive for the spontaneous transformations and nil for reversible transformations.

Therefore $$dS \geq \frac{\delta Q}{T} \qquad \text{(H.5)}$$

The entropy change is always positive.

H.5 Relationship Between First and Second Law

first law: second law:

$$dU = \delta Q + \delta W \qquad dS \geq \frac{\delta Q}{T}$$

Eliminating the term δQ for an isotherm process, it can be written:

$$dU - TdS \leq W_T$$

The work given to the system during the process is at least equal to the increase of the function $U - TS$. The limit value is reached for a reversible process.

The function $F = U - TS$ is the Helmotz's free energy.

Free enthalpy or Gibbs energy is defined by:

$$G = F + PV \text{ or } G = H - TS$$

Remark:
U, H, S, F are derived properties of a system which are not measurable directly. They may be expressed in terms of measurable properties: P, V, T

In the Gibbs equation, $\Delta G = \Delta H - T\Delta S$, each term describes an aspect of the energy that is dispersed because of a chemical reaction occurring in a system:

- ΔG is the total energy that is spread out in the universe (system plus surroundings) due to the reaction that has taken place in the system.
- ΔH is the energy from the reaction that is dispersed from the system to the surroundings.
- $T\Delta S$ is the energy that is dispersed in the system.

If each term divided by T, the Gibbs can be seen as an "all entropy" equation.

H.6 Equilibrium of an Isolated System

When a system is isolated (no exchange of matter, work or heat), its internal energy and volume are constants.

From Eq. (H.5) it can be deducted:

$$dS \geq 0$$

Entropy of an isolated system in equilibrium, submitted only to reversible processes, is constant. If the system is submitted to irreversible processes, its entropy increases.

For a system at constant mass changes from equilibrium conditions T, p, to $T + dT$, $p + dp$, the internal energy variation is:

$$dU = TdS - pdv$$

and $$dG = dH - TdS - SdT = dU + pdv + vdp - Tds - SdT$$

so $$dG = vdp - SdT$$

therefore $$v = \left(\frac{\delta G}{\delta p}\right)_T \text{ and } S = -\left(\frac{\delta G}{\delta T}\right)_p \qquad \text{(H.6)}$$

H.7 Chemical Potential

Considering a complex system made of several components like a hydrocarbon mixture, where the mass of an individual component can vary independently of the others, the changes will induce a variation of the internal energy. The total differential of internal energy can be written:

$$dU = TdS - pdv + \frac{\delta U}{\delta m_1} dm_1 + \ldots\ldots\ldots + \frac{\delta U}{\delta m_n}$$

m_1, m_2, $\ldots\ldots m_n$ are the masses of each component; free energy and free enthalpy are expressed as:

$$dG = -SdT + vdp + \frac{\delta G}{\delta m_1} dm_1 + \ldots\ldots\ldots + \frac{\delta G}{\delta m_n}$$

$$dF = -SdT - pdv + \frac{\delta F}{\delta m_1} dm_1 + \ldots\ldots\ldots + \frac{\delta F}{\delta m_n}$$

As $G = U + pv - TS$ and $F = U - TS$

$dG + SdT - vdp = dU - TdS + pdv$ therefore:

$$\left(\frac{\delta U}{\delta m_i}\right)_{S,v} = \left(\frac{\delta G}{\delta m_i}\right)_{T,p}$$

$dF + SdT = dU - TdS$ then:

$$\left(\frac{\delta U}{\delta m_i}\right)_{S,v} = \left(\frac{\delta G}{\delta m_i}\right)_{T,p} = \left(\frac{\delta F}{\delta m_i}\right)_{v,T}$$

Gibbs called these quantities chemical potentials μ_i.

State functions are usually reported to one mole of complex solution. Designing n_1, n_2, ...n_n the number of moles of each component, the molar chemical potential is:

$$\left(\frac{\delta U}{\delta n_i}\right)_{S,v} = \left(\frac{\delta G}{\delta n_i}\right)_{T,p} = \left(\frac{\delta F}{\delta n_i}\right)_{v,T}$$

Assuming a system made of one hydrocarbon component in vapour phase and liquid phase at pressure P and temperature T. When a liquid mole migrates into vapour, the free Gibbs enthalpy G varies:

$$\Delta G = gl - gv$$

gl: free enthalpy of a liquid mole
gv: free enthalpy of vapour
Since the system is at equilibrium, $\Delta G = 0$ then $gl = gv$

If the system is out of equilibrium, the component will tend to migrate from the state where the free enthalpy is high to the phase where the enthalpy is low.

Free enthalpy is somehow a measure of the escaping tendency of a component to move from one phase to the other.

The pressure dependent Gibbs free energy in a closed system is given by the combined first and second laws as:

$$dG = Vdp - SdT \tag{H.7}$$

At constant temperature, the equation becomes:

$$dG = Vdp$$

The free enthalpy change during a process from pressure p_1 to pressure p_2 is:

$$G(p_2) = G(p_1) + \int_{p1}^{p2} Vdp$$

The equation is general and applies to all isotropic substance: solids, liquids, ideal gases, and real gases.

H.8 Fugacity

Considering the free enthalpy of a perfect gas mole during the process at constant temperature from pressure p_1 to p_2.

According to Eq. (H.7)

$$\left(\frac{\delta G}{\delta p}\right)_T = V \text{ then } G_2 - G_1 = \int_{p1}^{p2} V dp \text{ with } V = \frac{RT}{p} \text{ (perfect gas)}$$

$$\Delta G = G_2 - G_1 = RT \int_{p1}^{p2} \frac{dp}{p} = RT \log \frac{p_2}{p_1}$$

$$\Delta G = RT \log \frac{p_2}{p_1} \tag{H.8}$$

The Avogadro-Ampere law states that different gas masses equal to their molecular mass, occupy the same volume at the same conditions (pressure, temperature).

Eq. (H.8) cant' be used for a real gas. A new state function is used called fugacity taking the value f_1 for p_1 and f_2 at pressure p_2.

In an isothermal process at temperature T for a real gas:

Similarly to Eq. (H.8) $$\Delta G' = RT \text{ Ln} \frac{f_1}{f_2} \tag{H.9}$$

The fugacity tends to pressure p when p decreases to 0 since a real gas behaves like a perfect gas when pressure decreases to 0.

From Eqs. (H.8 and H.9)

$$\Delta G' - \Delta G = RT \text{ Ln} \frac{f_2}{f_1} - RT \text{ Ln} \frac{p_2}{p_1} = RT \text{ Ln} \frac{f_2}{p_2} - RT \text{ Ln} \frac{f_1}{p_1}$$

For an isothermal process in the case of a perfect gas

$$dG = Vdp - SdT = Vdp = \frac{RT}{p} dp$$

For a real gas $$dG' = V'dp$$

V': real gas molar volume

$$\Delta G' = \int_{p_1}^{p_2} V' dp$$

For a perfect gas $$\Delta G = \int_{p_1}^{p_2} V dp = \int_{p_1}^{p_2} RT \frac{dp}{p}$$

$$\Delta G' - \Delta G = \int_{p_1}^{p_2} \left(V' - \frac{RT}{p} \right) dp = RT \left[\text{Ln} \frac{f_2}{p_2} - \text{Ln} \frac{f_1}{p_1} \right]$$

When p decreases to 0 then f tends to p; Ln(f/p) tends to 0

Therefore

$$\int_0^{p_2}\left(V'-\frac{RT}{p}\right)dp = RT\,\mathrm{Ln}\frac{f_2}{p_2}$$

or

$$\mathrm{Ln}\frac{f}{p} = \int_0^{p}\left(\frac{V}{RT}-\frac{1}{p}\right)dp$$

For a real gas of free enthalpy G at pressure P, the fugacity of the gas is the virtual pressure f at which it should be if it behaved as a perfect gas.

It is also sometimes useful to think of the fugacity as a "corrected partial pressure." Recall that the partial pressure is the mole fraction of a component times the total pressure. For an ideal gas, the fugacity is identical to the partial pressure (a quantity called the fugacity coefficient is the ratio of the fugacity to the partial pressure; it is one for an ideal gas). So fugacity can be thought as a correction to the partial pressure, accounting for the fact that real substances are not ideal gases.

APPENDIX I Application of the *Ei(x)* Function

The direct application of the *Ei* function is the interference test. The practical method to run an interference test between wells, consists of flowing one well at a constant rate and monitor the reservoir pressure changes in a closed well at some distance R from the producer. The pressure wave generated by the producing well will reach the closed in well after some time delay following the production start. The elapsed time is dependent on the rate level and on the fluid and reservoir properties:

- Thickness
- Porosity
- Permeability
- Fluid viscosity, compressibility.

Example:

- Fluid production rate: 0.864 m^3/d
- Observed pressure drop at closed in well: 0.2 atm
- Distance between wells: 100 m
- Fluid viscosity: 1 cp
- Fluid compressibility: 1.52 10^{-4} atm^{-1}
- Reservoir thickness: 1 m
- Reservoir porosity: 0.1
- Reservoir permeability: 1 mD

Determine the time when the 0.2 atm pressure occurs at the observation well?

Solution:

The general solution to the diffusivity equation for the constant rate well and infinite reservoir is given by the equation called the exponential integral solution:

$$p_i - p(r,t) = \frac{q\mu}{2\pi kh}\left[-\frac{1}{2}E_i\left(-\frac{\phi\mu c r^2}{4kt}\right)\right]$$

p_i:	initial pressure	ϕ:	reservoir porosity
$p(r, t)$:	pressure at distance r, and time t	c:	fluid compressibility
q:	fluid flow rate at reservoir conditions	h:	reservoir thickness
μ:	fluid viscosity	k:	reservoir permeability
r:	distance between wells		

It can be written:

$$\frac{4\pi kh\Delta P}{q\mu} = Ei\left(-\frac{\phi\mu c r^2}{4kt}\right) \quad \textit{(Darcy units)}$$

$$y = Ei(x)$$

All data must be converted into Darcy units

$q = 10\ cm^3/s$ $\mu = 1\ cp$ $k = 0.001$ Darcy $h = 100$ cm

$r = 10\,000$ cm $c = 1.52\ 10^{-4}\ atm^{-1}$ $\Delta P = 0.2$ atm

$$y = \frac{4\pi \times 0.001 \times 100 \times 0.2}{10 \times 1} = 0.0251$$

From the $Ei(x)$ table Appendix J, it is found: $x = 2.5$

Therefore:

$$t = \frac{\phi\mu c r^2}{4kx} \qquad t = \frac{0.1 \times 1 \times 1.52 \times 10^{-4} \times 10\,000^2}{4 \times 0.001 \times 2.5} = 1.52 \times 10^5 \text{ seconds or } 42 \text{ hours}$$

conclusion:

After producing 42 hours, a 0.2 atm pressure change is measured at the observation well.

Other units:

$$\frac{4\pi kh\Delta P}{q\mu} = Ei\left(-\frac{\phi\mu c r^2}{4kt}\right) \quad \textit{(Darcy units)}$$

$$y = \beta\frac{kh\Delta P}{q\mu} \qquad x = \alpha\frac{\phi\mu c r^2}{kt}$$

		α	β
Darcy units		1/4	4π
Oilfield units	t: hours	948.385	0.0141587
	t: days	39.516	
	t:years	0.108	
European Metric (mD, bar)	t: hours	703.646	0.1071536
	t: days	29.319	
	t:years	0.080	
Canadian Metric (mD, kPa)	t: hours	70365	0.001071536
	t: days	2931.9	
	t:years	8.032	
SI		1/4	4π

Remark: if q is expressed at surface conditions, q × Bo must be used in the equation.

APPENDIX J Exponential Integral Table

	$0 < x < 10.9$	Table $f(x) = -Ei(-x)$ *The Petroleum Engineer August 1956*								
x	0	1	2	3	4	5	6	7	8	9
0.00	∞	6.332	5.639	5.235	4.948	4.726	4.545	4.392	4.259	4.142
0.01	4.038	3.944	3.858	3.779	3.705	3.637	3.574	3.514	3.458	3.405
0.02	3.355	3.307	3.261	3.218	3.176	3.137	3.098	3.062	3.026	2.992
0.03	2.959	2.927	2.897	2.867	2.838	2.810	2.783	2.756	2.731	2.706
0.04	2.681	2.658	2.634	2.612	2.590	2.568	2.547	2.527	2.507	2.487
0.05	2.468	2.449	2.431	2.413	2.395	2.377	2.360	2.344	2.327	2.311
0.06	2.295	2.279	2.264	2.249	2.235	2.220	2.206	2.192	2.178	2.164
0.07	2.151	2.138	2.125	2.112	2.099	2.087	2.074	2.062	2.050	2.039
0.08	2.027	2.015	2.004	1.993	1.982	1.971	1.960	1.950	1.939	1.929
0.09	1.919	1.909	1.899	1.889	1.879	1.869	1.860	1.850	1.841	1.832
0.10	1.823	1.814	1.805	1.796	1.788	1.779	1.770	1.762	1.754	1.745
0.11	1.737	1.729	1.721	1.713	1.705	1.697	1.689	1.682	1.674	1.667
0.12	1.660	1.652	1.645	1.638	1.631	1.623	1.616	1.609	1.603	1.596
0.13	1.589	1.582	1.576	1.569	1.562	1.556	1.549	1.543	1.537	1.530
0.14	1.524	1.518	1.512	1.506	1.500	1.494	1.488	1.482	1.476	1.470
0.15	1.464	1.459	1.453	1.447	1.442	1.436	1.431	1.425	1.420	1.415
0.16	1.409	1.404	1.399	1.393	1.388	1.383	1.378	1.373	1.368	1.363
0.17	1.358	1.353	1.348	1.343	1.338	1.333	1.329	1.324	1.319	1.314
0.18	1.310	1.305	1.301	1.296	1.291	1.287	1.282	1.278	1.274	1.269
0.19	1.265	1.261	1.256	1.252	1.248	1.243	1.239	1.235	1.231	1.227
0.20	1.223	1.219	1.215	1.210	1.206	1.202	1.198	1.195	1.191	1.187
x	0	1	2	3	4	5	6	7	8	9
0.0	∞	4.0380	3.3550	2.9590	2.6810	2.4680	2.2950	2.1510	2.0270	1.9190
0.1	1.8230	1.7370	1.6600	1.5890	1.5240	1.4640	1.4090	1.3580	1.3090	1.2650
0.2	1.2230	1.1830	1.1450	1.1100	1.0760	1.0440	1.0140	0.9850	0.9570	0.9310
0.3	0.9060	0.8820	0.8580	0.8360	0.8150	0.7940	0.7740	0.7550	0.7370	0.7190
0.4	0.7020	0.6860	0.6700	0.6550	0.6400	0.6250	0.6110	0.5980	0.5850	0.5720
0.5	0.5600	0.5480	0.5360	0.5250	0.5140	0.5030	0.4930	0.4830	0.4730	0.4640
0.6	0.4540	0.4450	0.4370	0.4280	0.4200	0.4120	0.4040	0.3960	0.3880	0.3810
0.7	0.3740	0.3670	0.3600	0.3530	0.3470	0.3400	0.3340	0.3280	0.3220	0.3160
0.8	0.3110	0.3050	0.3000	0.2950	0.2890	0.2840	0.2790	0.2740	0.2690	0.2650
0.9	0.2600	0.2560	0.2510	0.2470	0.2430	0.2390	0.2350	0.2310	0.2270	0.2230
1.0	0.2190	0.2160	0.2120	0.2090	0.2050	0.2020	0.1980	0.1950	0.1920	0.1890
1.1	0.1860	0.1830	0.1800	0.1770	0.1740	0.1720	0.1690	0.1660	0.1640	0.1610
1.2	0.1580	0.1560	0.1530	0.1510	0.1490	0.1460	0.1440	0.1420	0.1400	0.1380
1.3	0.1350	0.1330	0.1310	0.1290	0.1270	0.1250	0.1240	0.1220	0.1200	0.1180
1.4	0.1160	0.1140	0.1130	0.1110	0.1090	0.1080	0.1060	0.1050	0.1030	0.1020
1.5	0.1000	0.0985	0.0971	0.0957	0.0943	0.0929	0.0915	0.0902	0.0889	0.0876
1.6	0.0863	0.0851	0.0838	0.0826	0.0814	0.0802	0.0791	0.0780	0.0768	0.0757
1.7	0.0747	0.0736	0.0725	0.0715	0.0705	0.0695	0.0685	0.0675	0.0666	0.0656
1.8	0.0647	0.0638	0.0629	0.0620	0.0612	0.0603	0.0595	0.0586	0.0578	0.0570
1.9	0.0562	0.0554	0.0546	0.0539	0.0531	0.0524	0.0517	0.0510	0.0503	0.0496
2.0	0.0489	0.0482	0.0476	0.0469	0.0463	0.0456	0.0450	0.0444	0.0438	0.0432
x	0	1	2	3	4	5	6	7	8	9
2	4.89E-02	4.26E-02	3.72E-02	3.25E-02	2.84E-02	2.49E-02	2.19E-02	1.92E-02	1.69E-02	1.48E-02
3	1.30E-02	1.15E-02	1.01E-02	8.94E-03	7.89E-03	6.87E-03	6.16E-03	5.45E-03	4.82E-03	4.27E-03
4	3.78E-03	3.35E-03	2.97E-03	2.64E-03	2.34E-03	2.07E-03	1.84E-03	1.64E-03	1.45E-03	1.29E-03
5	1.15E-03	1.02E-03	9.08E-04	8.09E-04	7.19E-04	6.41E-04	5.71E-04	5.09E-04	4.53E-04	4.04E-04
6	3.60E-04	3.21E-04	2.86E-04	2.55E-04	2.28E-04	2.03E-04	1.82E-04	1.62E-04	1.45E-04	1.29E-04
7	1.15E-04	1.03E-04	9.22E-05	8.24E-05	7.36E-05	6.58E-05	5.89E-05	5.26E-05	4.71E-05	4.21E-05
8	3.77E-05	3.37E-05	3.02E-05	2.70E-05	2.42E-05	2.16E-05	1.94E-05	1.73E-05	1.55E-05	1.39E-05
9	1.24E-05	1.11E-05	9.99E-06	8.95E-06	8.02E-06	7.18E-06	6.44E-06	5.77E-06	5.17E-06	4.64E-06
10	4.15E-06	3.73E-06	3.34E-06	3.00E-06	2.68E-06	2.41E-06	2.16E-06	1.94E-06	1.74E-06	1.56E-06

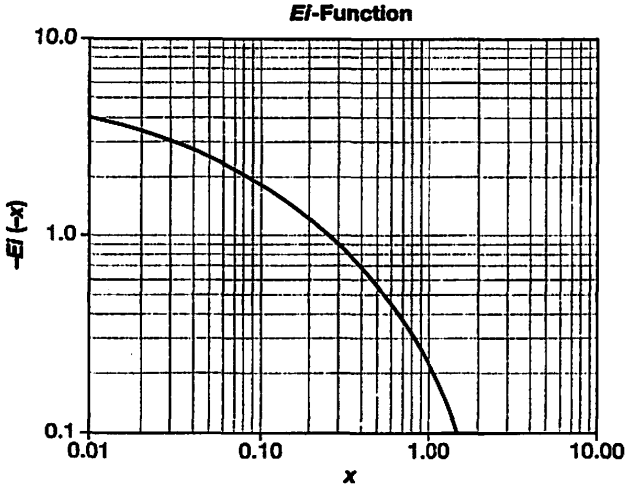

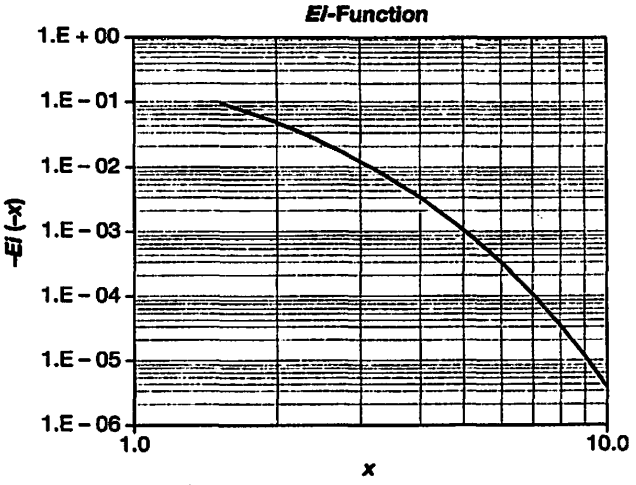

APPENDIX K

Interference between wells distributed uniformly over a circular ring of radius r

K.1 Case of two identical wells distributed uniformly over a circle of radius *r*

The well flowing pressure of well 1 is determined as following:
d is the distance between the wells

$$p_{w1} = p_e - \left[\frac{q_1 \mu B}{2\pi kh} \mathrm{Ln}\left(\frac{R}{r_{w1}}\right) + \frac{q_2 \mu B}{2\pi kh} \mathrm{Ln}\left(\frac{R}{d}\right)\right] \tag{K.1}$$

$$q_1 = q_2 = \frac{2\pi kh}{\mu B} \frac{(p_e - p_w)}{\mathrm{Ln}\left(\frac{R^2}{d_2 r_w}\right)} \tag{K.2}$$

The well flow rate ratio between the well submitted to interference and the isolated well is:

$$\frac{q_2}{q} = \frac{\mathrm{Ln}\left(\frac{R}{r_w}\right)}{\mathrm{Ln}\left(\frac{R^2}{d_2 r_w}\right)} \tag{K.3}$$

Distance between the wells is: $d_2 = 2r$
The denominator becomes:

$$D = \mathrm{Ln}\left(\frac{R^2}{2r_w r}\right) \text{ or } D = 2\,\mathrm{Ln}(R) - \mathrm{Ln}(r) - \mathrm{Ln}(2r_w)$$

$$D = 2\,\mathrm{Ln}(R) - 2\,\mathrm{Ln}(r) + \mathrm{Ln}(r) - \mathrm{Ln}(2r_w) = 2\left[\mathrm{Ln}(R) - \mathrm{Ln}(r) + \frac{1}{2}\mathrm{Ln}(r) - \frac{1}{2}\mathrm{Ln}(2r_w)\right]$$

$$D = 2\left[\mathrm{Ln}\left(\frac{R}{r}\right) + \frac{1}{2}\mathrm{Ln}\left(\frac{r}{2r_w}\right)\right] \tag{K.4}$$

K.2 Case of three wells

individual rates and the ratio are similar to Eq. (K.2):

$$q_1 = q_2 = q_3 = \frac{2\pi kh}{\mu B} \frac{(p_e - p_w)}{\mathrm{Ln}\left(\frac{R^3}{r_w d_3^2}\right)} \qquad \frac{q_3}{q} = \frac{\mathrm{Ln}\left(\frac{R}{r_w}\right)}{\mathrm{Ln}\left(\frac{R^3}{r_w d_3^2}\right)}$$

The distance d between two wells is: $d = r\sqrt{3}$

The denominator becomes: $$D = \mathrm{Ln}\left(\frac{R^3}{3r_w r^2}\right)$$

$$D = 3\,\mathrm{Ln}(R) - 2\,\mathrm{Ln}(r) - \log(3r_w) = 3\,\mathrm{Ln}(R) - 3\,\mathrm{Ln}(r) + \ln(r) - \log(3r_w)$$

$$D = 3\left[\mathrm{Ln}\left(\frac{R}{r}\right) + \frac{1}{3}\mathrm{Ln}\left(\frac{r}{3r_w}\right)\right] \qquad \text{(K.5)}$$

K.3 Case of n = 4 wells uniformly on a circle

From Eq. (K.3), the denominator is

$$D = \mathrm{Ln}\left(\frac{R^4}{r_w d_4^3\sqrt{2}}\right) \qquad d = r\sqrt{2} \qquad d^3 = 2r^3\sqrt{2}$$

$$D = \mathrm{Ln}\left(\frac{R^4}{4r_w r^3}\right)$$

$$D = \mathrm{Ln}(R^4) - 3\,\mathrm{Ln}(r^3) - \mathrm{Ln}(4r_w) = 4\,\mathrm{Ln}(R) - 4\,\mathrm{Ln}(r) + \mathrm{Ln}(r) - \mathrm{Ln}(4r_w)$$

$$D = 4\left[\mathrm{Ln}\left(\frac{R}{r}\right) + \frac{1}{4}\mathrm{Ln}\left(\frac{r}{4r_w}\right)\right] \qquad \text{(K.6)}$$

From Eqs. (K.4, K.5, K.6), a general form is deducted for the denominator as:

$$D = n\left[\mathrm{Ln}\left(\frac{R}{r}\right) + \frac{1}{n}\mathrm{Ln}\left(\frac{r}{nr_w}\right)\right]$$

Finally the general formula giving the flow rate ratio between a well submitted to interference in a uniformly distributed well configuration over a circular ring of radius r; and an isolated well is:

$$\frac{q_n}{q} = \frac{1}{n}\frac{\mathrm{Ln}\left(\frac{R}{r_w}\right)}{\left[\mathrm{Ln}\left(\frac{R}{r}\right) + \frac{1}{n}\mathrm{Ln}\left(\frac{r}{nr_w}\right)\right]}$$

n: number of wells
R: drainage radius
r: radius of the circle

APPENDIX L Well Formulas

$$Q_o = \frac{2 \times \pi \times k \times k_{ro} \times h \times (P_r - P_{wf})}{\mu_o \times B_o \times \left[\mathrm{Ln}\left(\frac{r_e}{r_w}\right) + S \right]}$$

	SI units	Darcy units
q_o	m^3/s	cm^3/s
k	m^2	Darcy
k_{ro}	ratio	ratio
h	m	cm
P	Pa	atm
μ_o	Pa.s	cp

$$Q_o = \frac{0.00708 \times k \times k_{ro} \times h \times (P_r - P_{wf})}{\mu_o \times B_o \times \left[\mathrm{Ln}\left(\frac{r_e}{r_w}\right) + S \right]}$$

	Field Units
q_o	Bopd
k	mD
k_{ro}	ratio
h	ft
P	psi
μ_o	cp (mPa.s)

$$Q_o = \frac{0.053577 \times k \times k_{ro} \times h \times (P_r - P_{wf})}{\mu_o \times B_o \times \left[\mathrm{Ln}\left(\frac{r_e}{r_w}\right) + S \right]}$$

	Metric Units
q_o	m^3/d
k	mD
k_{ro}	ratio
h	m
P	bar
μ_o	cp (mPa.s)

APPENDIX M Hurst van Everdingen Water Influx Model

Assumptions:

- Radial monophasic flow
- Infinite homogenous and isotropic porous medium
- Small and constant fluid compressibility, constant fluid viscosity
- Gravity forces are neglected.

The combination of the mass conservation law with the Darcy law and fluid equation of state lead to the diffusivity equation:

Equation of state $$\rho = \rho_0 e^{c(p-p_o)}$$

Diffusivity $$\frac{\delta^2 p}{\delta r^2} + \frac{1}{r}\frac{\delta p}{\delta r} = \frac{\phi \mu c}{k}\frac{\delta p}{\delta t}$$

ρ: fluid density
c: fluid compressibility
p: pressure
r: radius
φ: porosity
μ: fluid viscosity
k: permeability
t: time

$\frac{k}{\phi \mu c}$ is the hydraulic diffusivity

The diffusivity equation is a partial differential equation of second order in pressure. Historically, this equation first arose in the study of heat conduction.

Solutions of the diffusivity equation depend on the boundary conditions used.

HVE (Hurst Van Everdingen) have computed solutions for two cases:

M.1 Constant terminal rate case

a unit production rate is made to flow across the boundary (at r_o) from time zero onward and the resulting pressure drop is computed versus time.

This procedure conducts to the expression of the well flow rate used for the well pressure buildup analysis.

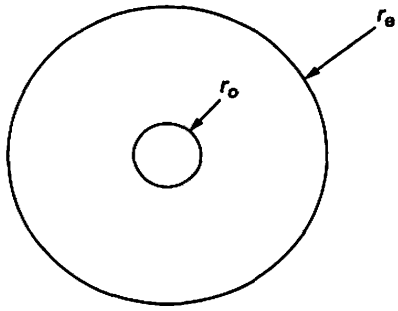

Radial aquifer model.

r_o: radius of the oil water boundary
r_e: external aquifer radius

for an infinite aquifer case:

$$p \to p_e \text{ as } r \to \infty$$

$$p(r,t) = p_e - \frac{q\mu}{2\pi kh}\left\{-\frac{1}{2}Ei\left(-\frac{\phi\mu c r^2}{4kt}\right)\right\}$$

for a bounded circular aquifer the solution is a combination of Bessel functions.

r_D is used to characterize the aquifer volume in comparison with the reservoir oil volume.

Dimensionless radius:

$$r_D = \frac{r_e}{r_o}$$

Dimensionless time:

$$t_D = \frac{kt}{\phi\mu c r_o^2}$$

M.2 Constant terminal pressure case

Circular aquifer geometry

A unity pressure drop at the boundary (r_o) is applied at time zero and pressure is kept constant thereafter. The amount of fluid influx is computed versus time.

The dimensionless influx rate evaluated at $r_D = 1$ evaluates the change in rate from 0 to q due to a Δp pressure drop applied at reservoir boundary r_o at time $t = 0$.

$$q_D(t_D) = \frac{q\mu}{2\pi kh\Delta p}$$

the cumulative influx is: $\frac{\mu}{2\pi kh\Delta p}\int_0^{t_D} q\,dt = \int_0^{t_D} q_D(t_D)\frac{dt}{dt_D}dt_D$

which gives: $$\frac{W_e\mu}{2\pi kh\Delta p} = W_D(t_D)\frac{\phi\mu c_t r_o^2}{k}$$

Therefore $$W_e = 2\pi\phi hc_t r_o^2 \Delta p W_D(t_D) \text{ (Darcy units)}$$

W_e: cumulative water influx (cm^3) due to a pressure drop Δp (atm) applied at r_o at $t = 0$
φ: aquifer porosity
h: aquifer thickness (cm)
c_t: total aquifer compressibility ($c_w + c_p$) (atm^{-1})
r_o: oil pool radius (cm)
k: aquifer permeability (Darcy)
μ: water viscosity (cp)
$W_D(t_D)$: dimensionless cumulative water influx per unit pressure drop applied at r_o at time $t = 0$

The equation can be expressed as:

$$W_e = U\Delta p W_D(t_D) \text{ with } U = 2\pi f\phi hc_t r_o^2$$

f is the fraction of the circle where contact between oil zone and aquifer occurs

U is the aquifer constant for radial geometry.

All terms of the equations are in the unit system associated with Darcy's Law.

q: cm^3/s
p: atm
L: cm
k: Darcy
μ: cp

Darcy Units

$$t_D = \frac{kt}{\phi\mu c_t r_o^2} \text{ (t sec)} \qquad t_D = \text{const} \times \frac{kt}{\phi\mu c_t r_o^2}$$

Field Units

const = 0.000264 (t hours)
= 0.00634 (t days)
= 2.309 (t years)

μ: cp
c: psi^{-1}
r: ft
k: mD

$U = 2\pi f\varphi\, hc_t r_o^2$ (cm^3/atm)

$U = 1.119 f\varphi\, hc_t r_o^2$ (bbl/psi)

Linear aquifer geometry

The flow is essentially linear in an oil reservoir with an adjoining aquifer contained between two parallel sealing planes (channel). The constant terminal pressure case is also applied.

The diffusivity equation is given by:

$$\frac{\delta^2 p}{\delta x^2} = \frac{\phi \mu c}{k} \frac{\delta p}{\delta t}$$

x: absolute distance measured from the plane of influx extending out into aquifer.

The cumulative water influx is similar to the radial case except for the definition of t_D constant and U.

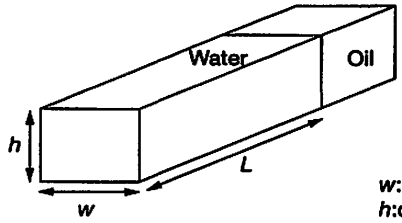

w:channel width
h:channel height

Darcy Units

$$t_D = \frac{kt}{\phi \mu c_t r_o^2} \quad \text{(t sec)} \qquad t_D = \text{const} \times \frac{kt}{\phi \mu c_t L^2}$$

Field Units

const = 0.000264 (t hours)
= 0.00634 (t days)
= 2.309 (t years)

μ: cp
c: psi^{-1}
r: ft
k: mD

$$U = w\,Lhf\varphi\, c_t\, r_o^2 \ (\text{cm}^3/\text{atm}) \qquad U = 0.1781 wLh\varphi\, c_t \ (\text{bbl/psi})$$

Remark:
In the case of infinite aquifer, the water influx is always governed by transient flow conditions.

APPENDIX N Dimensionless Water Influx W_d for Values of Dimensionless Time

Infinite aquifer		$r_e/r_w = 1.5$		$r_e/r_w = 2.0$	
Dimensionless time t_D	Fluid influx $W_D(t_D)$	Dimensionless time t_D	Fluid influx $W_D(t_D)$	Dimensionless time t_D	Fluid influx $W_D(t_D)$
0.00	0	5.0E-02	0.276	5.0E-02	0.278
0.01	0.112	6.0E-02	0.304	7.5E-02	0.345
0.05	0.278	7.0E-02	0.33	1.0E-01	0.404
0.10	0.404	8.0E-02	0.354	1.3E-01	0.458
0.15	0.52	9.0E-02	0.375	1.5E-01	0.507
0.20	0.606	1.0E-01	0.395	1.8E-01	0.553
0.25	0.689	1.1E-01	0.414	2.0E-01	0.597
0.30	0.758	1.2E-01	0.431	2.3E-01	0.638
0.40	0.898	1.3E-01	0.446	2.5E-01	0.678
0.50	1.02	1.4E-01	0.461	2.8E-01	0.715
0.60	1.14	1.5E-01	0.474	3.0E-01	0.751
0.70	1.251	1.6E-01	0.486	3.3E-01	0.785
0.80	1.359	1.7E-01	0.497	3.5E-01	0.817
0.90	1.469	1.8E-01	0.507	3.8E-01	0.848
1	1.569	1.9E-01	0.517	4.0E-01	0.877
2	2.447	2.0E-01	0.525	4.3E-01	0.905
3	3.202	2.1E-01	0.533	4.5E-01	0.932
4	3.893	2.2E-01	0.541	4.8E-01	0.958
5	4.539	2.3E-01	0.548	5.0E-01	0.983
6	5.153	2.4E-01	0.554	5.5E-01	1.028
7	5.743	2.5E-01	0.559	6.0E-01	1.070
8	6.314	2.6E-01	0.565	6.5E-01	1.108
9	6.869	2.8E-01	0.574	7.0E-01	1.143
10	7.411	3.0E-01	0.582	7.5E-01	1.174
11	7.94	3.2E-01	0.588	8.0E-01	1.203
12	8.457	3.4E-01	0.594	9.0E-01	1.253
13	8.964	3.6E-01	0.599	1.0	1.295
14	9.561	3.8E-01	0.603	1.1	1.330
15	9.949	4.0E-01	0.606	1.2	1.358
16	10.434	4.5E-01	0.613	1.3	1.382
17	10.913	5.0E-01	0.617	1.4	1.402
18	11.386	6.0E-01	0.621	1.6	1.432
19	11.855	7.0E-01	0.623	1.7	1.444
20	12.319	8.0E-01	0.624	1.8	1.453
21	12.778			2.0	1.468
22	13.233			2.5	1.487
23	13.684			3.0	1.495
24	14.131			4.0	1.499
25	14.573			5.0	1.500
26	15.013				
27	15.45				
28	15.883				
29	16.313				
30	16.742				
31	17.167				
32	17.59				
33	18.011				
34	18.429				
35	18.845				
36	19.259				

$r_e/r_w = 2.5$		$r_e/r_w = 3.0$		$r_e/r_w = 3.5$	
Dimensionless time t_D	**Fluid influx $W_D(t_D)$**	**Dimensionless time t_D**	**Fluid influx $W_D(t_D)$**	**Dimensionless time t_D**	**Fluid influx $W_D(t_D)$**
1.0E-01	0.408	3.0E-01	0.755	1.00	1.571
1.5E-01	0.509	4.0E-01	0.895	1.20	1.761
2.0E-01	0.599	5.0E-01	1.023	1.40	1.94
2.5E-01	0.681	6.0E-01	1.143	1.60	2.111
3.0E-01	0.758	7.0E-01	1.256	1.80	2.273
3.5E-01	0.829	8.0E-01	1.363	2.00	2.427
4.0E-01	0.897	9.0E-01	1.465	2.20	2.574
4.5E-01	0.962	1.00	1.563	2.40	2.715
5.0E-01	1.024	1.25	1.791	2.60	2.849
5.5E-01	1.083	1.50	1.997	2.80	2.976
6.0E-01	1.140	1.75	2.184	3.00	3.098
6.5E-01	1.195	2.00	2.353	3.25	3.242
7.0E-01	1.248	2.25	2.507	3.50	3.379
7.5E-01	1.299	2.50	2.646	3.75	3.507
8.0E-01	1.348	2.75	2.772	4.00	3.628
8.5E-01	1.395	3.00	2.886	4.25	3.742
9.0E-01	1.440	3.25	2.990	4.50	3.85
9.5E-01	1.484	3.50	3.084	4.75	3.951
1.0	1.526	3.75	3.170	5.00	4.047
1.1	1.605	4.00	3.247	5.50	4.222
1.2	1.679	4.25	3.317	6.00	4.378
1.3	1.747	4.50	3.381	6.50	4.516
1.4	1.811	4.75	3.439	7.00	4.639
1.5	1.870	5.00	3.491	7.50	4.749
1.6	1.924	5.50	3.581	8.00	4.846
1.7	1.975	6.00	3.656	8.50	4.932
1.8	2.022	6.50	3.717	9.00	5.009
2.0	2.106	7.00	3.767	9.50	5.078
2.2	2.178	7.50	3.809	10	5.138
2.4	2.241	8.00	3.843	11	5.241
2.6	2.294	9.00	3.894	12	5.321
2.8	2.340	10.00	3.928	13	5.385
3.0	2.380	11.00	3.951	14	5.435
3.4	2.444	12.00	3.967	15	5.476
3.8	2.491	14.00	3.985	16	5.506
4.2	2.525	16.00	3.993	17	5.531
4.6	2.551	18.00	3.997	18	5.551
5.0	2.570	20.00	3.999	20	5.579
6.0	2.599	22.00	3.999	25	5.611
7.0	2.613	24.00	4.000	30	5.621
8.0	2.619			35	5.624
9.0	2.622			40	5.625
10.0	2.624				

$r_e/r_w = 4.0$		$r_e/r_w = 4.5$		$r_e/r_w = 5.0$	
Dimensionless time t_D	**Fluid influx $W_D(t_D)$**	**Dimensionless time t_D**	**Fluid influx $W_D(t_D)$**	**Dimensionless time t_D**	**Fluid influx $W_D(t_D)$**
2.00	2.442	2.5	2.835	3.0	3.195
2.20	2.598	3.0	3.196	3.5	3.542
2.40	2.748	3.5	3.537	4.0	3.875
2.60	2.893	4.0	3.859	4.5	4.193
2.80	3.034	4.5	4.165	5.0	4.499
3.00	3.170	5.0	4.454	5.5	4.792
3.25	3.334	5.5	4.727	6.0	5.074
3.50	3.493	6.0	4.986	6.5	5.345
3.75	3.645	6.5	5.231	7.0	5.605
4.00	3.792	7.0	5.464	7.5	5.854
4.25	3.932	7.5	5.684	8.0	6.094
4.50	4.068	8.0	5.892	8.5	6.325
4.75	4.198	8.5	6.089	9.0	6.547
5.00	4.323	9.0	6.276	9.5	6.760
5.50	4.560	9.5	6.453	10	6.965
6.00	4.779	10	6.621	11	7.350
6.50	4.982	11	6.930	12	7.706
7.00	5.169	12	7.208	13	8.035
7.50	5.343	13	7.457	14	8.339
8.00	5.504	14	7.680	15	8.620
8.50	5.653	15	7.880	16	8.879
9.00	5.790	16	8.060	18	9.338
9.50	5.917	18	8.365	20	9.731
10	6.035	20	8.611	22	10.07
11	6.246	22	8.809	24	10.35
12	6.425	24	8.968	26	10.59
13	6.580	26	9.097	28	10.80
14	6.712	28	9.200	30	10.98
15	6.825	30	9.283	34	11.26
16	6.922	34	9.404	38	11.46
17	7.004	38	9.481	42	11.61
18	7.076	42	9.532	46	11.71
20	7.189	46	9.565	50	11.79
22	7.272	50	9.586	60	11.91
24	7.332	60	9.612	70	11.96
26	7.377	70	9.621	80	11.98
30	7.434	80	9.623	90	11.99
34	7.464	90	9.624	100	12.00
38	7.481	100	9.625	120	12.00
42	7.490				
46	7.494				
50	7.497				

$r_e/r_w = 6.0$		$r_e/r_w = 7.0$		$r_e/r_w = 8.0$	
Dimensionless time t_D	**Fluid influx $W_D(t_D)$**	**Dimensionless time t_D**	**Fluid influx $W_D(t_D)$**	**Dimensionless time t_D**	**Fluid influx $W_D(t_D)$**
6.0	5.148	9.0	6.861	9	6.861
6.5	5.440	9.5	7.127	10	7.398
7.0	5.724	10	7.389	11	7.920
7.5	6.002	11	7.902	12	8.431
8.0	6.273	12	8.397	13	8.930
8.5	6.537	13	8.876	14	9.418
9.0	6.795	14	9.341	15	9.895
9.5	7.047	15	9.791	16	10.361
10.0	7.293	16	10.23	17	10.82
10.5	7.533	17	10.65	18	11.26
11	7.767	18	11.06	19	11.70
12	8.220	19	11.46	20	12.13
13	8.651	20	11.85	22	12.95
14	9.063	22	12.58	24	13.74
15	9.456	24	13.27	26	14.50
16	9.829	26	13.92	28	15.23
17	10.19	28	14.53	30	15.92
18	10.53	30	15.11	34	17.22
19	10.85	35	16.39	38	18.41
20	11.16	40	17.49	40	18.97
22	11.74	45	18.43	45	20.26
24	12.26	50	19.24	50	21.42
25	12.50	60	20.51	55	22.46
31	13.74	70	21.45	60	23.40
35	14.40	80	22.13	70	24.98
39	14.93	90	22.63	80	26.26
51	16.05	100	23.00	90	27.28
60	16.56	120	23.47	100	28.11
70	16.91	140	23.71	120	29.31
80	17.14	160	23.85	140	30.08
90	17.27	180	23.92	160	30.58
100	17.36	200	23.96	180	30.91
110	17.41	500	24.00	200	31.12
120	17.45			240	31.34
130	17.46			280	31.43
140	17.48			320	31.47
150	17.49			360	31.49
160	17.49			400	31.50
180	17.50			500	31.50
200	17.50				
220	17.50				

$r_e/r_w = 9.0$		$r_e/r_w = 10.0$	
Dimensionless time t_D	**Fluid influx $W_D(t_D)$**	**Dimensionless time t_D**	**Fluid influx $W_D(t_D)$**
10	7.417	15	9.965
15	9.945	20	12.32
20	12.26	22	13.22
22	13.13	24	14.09
24	13.98	26	14.95
26	14.79	28	15.78
28	15.59	30	16.59
30	16.35	32	17.38
32	17.10	34	18.16
34	17.82	36	18.91
36	18.52	38	19.65
38	19.19	40	20.37
40	19.85	42	21.07
42	20.48	44	21.76
44	21.09	46	22.42
46	21.69	48	23.07
48	22.26	50	23.71
50	22.82	52	24.33
52	23.36	54	24.94
54	23.89	56	25.53
56	24.39	58	26.11
58	24.88	60	26.67
60	25.36	65	28.02
65	26.48	70	29.29
70	27.52	75	30.49
75	28.48	80	31.61
80	29.36	85	32.67
82	30.18	90	33.66
90	30.93	95	34.60
95	31.63	100	35.48
100	32.27	120	38.51
120	34.39	140	40.89
140	35.92	160	42.75
160	37.04	180	44.21
180	37.85	200	45.36
200	38.44	240	46.95
240	39.17	280	47.94
280	39.56	320	48.54
320	39.77	360	48.91
360	39.88	400	49.14
400	39.94	440	49.28
440	39.97	480	49.36
480	39.98		

Plot for $r_e/r_w = 5$ and 10

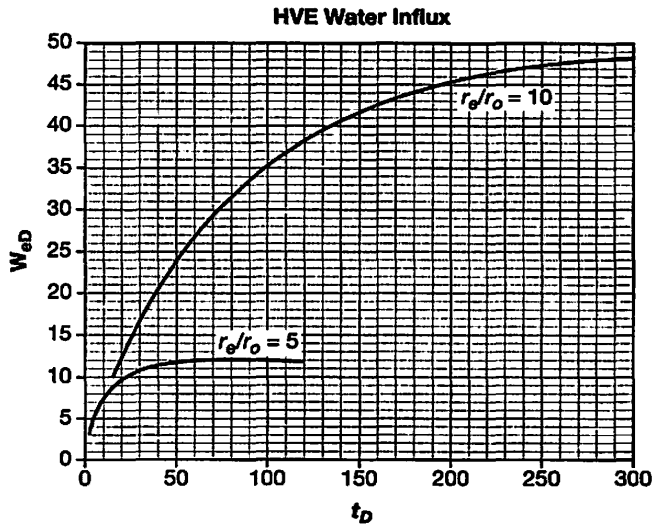

References

[1] Petroleum Reservoir Engineering Physical Properties. J.W. Amyx, D.M. Bass, R.L. Whiting, Mc Graw-Hill, 1960.

[2] Handbook of Natural Gas Engineering. Donald L. Katz, Mc Graw-Hill, 1959.

[3] The Permeability of porous media to liquids and gases. L.J. Klinkenberg presented at Eleventh Mid-Year Meeting, Tulsa, Oklahoma, May 1941.

[4] Klinkernberg Permeability Measurements: Problems and Practical Solutions. Colin A. McPhee and Kevin G. Arthur. Edinburgh Petroleum Services Limited, UK.

[5] Cours de Production, tome 1 : Caractéristiques des roches réservoirs. Analyse des carottes. R. Monicard, Editions Technip, 1975.

[6] Degradation of Reservoir Quality by Clay Content, Unayzah Formation, Central Saudi Arabia. George R. Polkowski Saudi Aramco. GeoArabia Middle East Petroleum Geosciences Volume 2, Number 1, March 1997.

[7] Wettability Literature Survey – W.G. Anderson.
Part 1 Rock/oil/brine interactions and the effects of core handling on wettability, JPT (Oct. 1986).
Part 2 Wettability measurement, JPT (nov. 1986).
Part 3 The effects of wettability on the electrical properties of porous media, JPT (Dec.1986).
Part 4 The effects of wettability on capillary pressure, JPT (Oct. 1987).
Part 5 The effects of wettability on relative permeability, JPT (Nov. 1987).
Part 6 The effects of wettability on waterflooding, JPT (Dec. 1987).

[8] Fundamentals of Reservoir Engineering. Calhoun, J.C. Jr., U. of Oklahoma Press, Norman, OK, 1947.

[9] Waterflooding. G. Paul Whillite, SPE Textbook Series vol. 3, SPE, 1986.

[10] Effects of Crude oil Components on Rock Wettability. Denekas, M.O., Mattax, C.C and Davis G.T., Trans AIME 1959, 216.

[11] Measurement of Fractional Wettability of Oil Field Rocks by Nuclear Magnetic Resonance. Brown, R.J.S. and Fatt, I., Trans. AIME, 207, 1956.

[12] Role of capillary Forces in Determining Microscopic Displacement Efficiency for Oil Recovery by Water Flooding. Melrose, J.C. and C.F. Bradner, J. Can. Pet. Tech., 13, 42, 1974.

[13] Fundamental Study of Imbibition in Fissured Oil fields. Iffly R., Rousselet D.C. and Vermeulen J.L., SPE N° 4102, 1972.

[14] Gravity and Capillary effects on the Matrix Imbibition in Fissured Reservoirs. Lefebure du Prey, E., SPEJ, pp. 195-205, June 1978.

[15] Petroleum Engineering Handbook. H.B. Bradley, SPE, 1992.

[16] The Reservoir Engineering Aspects of Waterflooding. Forrest F. Craig, JR, Monograph Vol. 3 of The Henry L. Doherty Series, 1971.

[17] Theory and Application of Capillary Pressure. By C.E. Evans and E.T. Guerrero, University of Tulsa, SPWLA Twentieth Annual Logging Symposium, June 1979.

[18] Computation and Interpretation of Capillary Pressure from a Centrifuge. Brian Skuse, Stanford U., Abbas Firoozabadi, Henry J. Ramey Jr., SPE Formation Evaluation, March 1992.

[19] Role of Capillary Forces in Determining Microscopic Displacement Efficiency for Oil Recovery by Waterflooding. Melrose, J.C. and Brandner, C.F., J. Cdn. Pet. Tech., Oct.-Dec. 1974.

[20] Dynamic and Static Forces Required To Remove a Discontinuous Oil Phase from Porous Media Containing Both Oil and Water. J.J. Taber, SPE Reprint Series N° 24.

[21] The Effect of Fluid Pressure Decline Oil Volumetric Changes of Porous Rocks. Geertsma, J., Trans. AIME, vol. 210, 1957. Non-linear Elastic Behavior of porous Media. W. van der Knaap, presented at SPE, October 1958, Houston. Pore Volume Compressibilities of Sandstone Reservoir Rocks. Fatt, I., JPT March, 1958. Compressibility of Reservoir Rocks. Hall, Howard N., Trans. AIME, p. 309, 1953.

[22] Compressibility of Reservoir Rocks. Hall, Howard N., Trans. AIME, 1953.

[23] The Bachaquero Study- A Composite Analysis of the Behavior of a Compaction Drive/Solution Gas Drive Reservoir. Merle, H.A., Kentie, C.J.P., Van Opstal, G.H.C., Schneider, G.M.G., Shell Internationale Petroleum Mij.; Kentie, C.J.P.

[24] Reservoir compaction and surface subsidence in the north sea Ekofisk field. By Musharraf M. Zaman, Abdulazeez Abdulraheem and Jean Claude Roegiers. Subsidence due to fluid withdrawal. Developments in Petroleum Sciences, 41 edited by G.V. Chilingarian, EC. Donaldson and T.F. Yen, Elsevier Sciences B.B., 1995.

[25] Capillary pressures, their measurement using mercury and the calculation of permeability. Purcell, W. R., From: AIME, Petroleum Transactions, Feb. p. 39-48, 1949.

[26] The Electrical Resistivity Log as an Aid in Determining Some Reservoir Characteristics. Archie, G.E., Pet. Tech., Vol. 5, N°. 1, Jan., 1942.

[27] Log Interpretation Principles/Application Schlumberger 1987.

[28] Society of Core Analysts. Laboratory Measurements of Cementation Factor and Saturation Exponent Under Reservoir Conditions on Assab Rock Samples by Daniel G. Longeron, IFP Rueil-Malmaison, and Fathi A. Yahya Abu Dhabi, National Oil Company. Fifth Annual Technical Conference San Antonio, Texas, August, 1991.

[29] Introduction to Schlumberger Well Logging Number 8. Schlumberger Well Surveying Corporation, 1958.

[30] Natural Gamma Ray Spectrometry. Essentials of N.G.S. Interpretation Schlumberger, 1982.

[31] Oilfield Review (Schlumberger), Elsevier USA, January, 1994.

[32] Schlumberger Technical Review. Volume 17, Number 2, April, 1969.

[33] Some Theoritical Considerations Related to Quantitative Evaluation of the Physical Characteristics of Reservoir Rock from Electrical Log Data. Wyllie, M.R.J. and Rose, W.D., J.P.T., April, 1950.

[34] Using Log-Derived Values of Water Saturation and Porosity, by R.L. Morris and W.P. Biggs. Transactions of the SPWLA eight Annual Logging Symposium, 1967.

[35] An Investigation of Permeability, Porosity, and Residual Water Saturation Relationships for Sandstone Reservoirs. Timur, A., The Log Analyst, vol. 9, No.4, July-August, 1968.

[36] Permeability-Porosity Relationships in Sedimentary Rocks. Philip H. Nelson: U.S. Geological Survey, Denver, Colorado The Log Analyst May-June, 1994.

[37] Enhanced Reservoir Description: Using Core and Log Data to Identify Hydraulic (Flow) Units and Predict Permeability in Uncored Intervals/Wells. Jude O. Amaefule and Mehmet Altunbay, Core Laboratories; Djebbar Tiab, U. of Oklahoma; David G. Kersey and Dare K. Keelan, Core Laboratories. SPE 26436 Houston October, 1993.

[38] Gas Conditioning and Processing. volume 1 & 2, by J.M. Campbell, 1981.

[39] Prediction of Minimum Gas Flow Rate Required for Liquid Removal From Gas Wells. Trans. AIME, vol 246, p. 1475, 1969.

[40] Phase Behavior Monograph. C. Whitson and M. Brule, Vol. 20, SPE 2000.

[41] Determination of the Molar mass of petroleum distillation residue using gel permeation chromatography. Paul Guieze and John M. Williams. J. Chromatography, 312, Elsevier, 1984.

[42] Reservoir Fluid Property Correlations State of the Art. W. D. McCain Jr., SPE Reservoir Engineering, May 1991.

[43] Evaluation of Empirically Derived PVT Properties for Gulf of Mexico Crude Oils. Robert P. Sutton and Farshad, SPE Reservoir Engineering, February, 1990.

[44] Volumetric and Phase Behavior of Oil Field Hydrocarbon Systems. M. Standing, SPE, 1977.

[45] A Pressure Volume Temperature Correlation For Mixtures of California Oils and Gases. Standing, M.B., Drill & Prod. Prac., API, 1947.

[46] Bubble Point Pressure Correlation. Lasater, J.A., Trans., AIME, 1958.

[47] Correlations for Fluid Physical Property Prediction. Vasquez, M.E. and Beggs, H.D., JPT, SPE, 6719, June, 1980.

[48] Generalized Pressure Volume Temperature Correlations. Glaso, Oistein, JPT, May, 1980.

[49] New correlations for formation volume factors of oil and gas mixtures. Muhammad Ali Al-Marhoun, JCPT, March, 1992.

[50] Asphaltenes and Asphalts, 1, 1994.

[51] Asphaltenes and Asphalts, 2. Edited by T.F. Yen, School of Engineering, Program of Environmental Engineering, University of Southern California, Los Angeles, CA, USA. G.V. Chilingarian, School of Engineering, University of Southern California, Los Angeles, CA, USA. Printed by Elsevier, 2000.

[52] Paraffin, Asphaltene control practices surveyed. James Herman Burlington Resources Inc. Midland, Tex. Karl Ivanhoe Chevron USA Inc. Midland, Tex. Oil & Gas Journal, July 12, 1999.

[53] Screening of Crude Oils for Asphalt Precipitation: Theory, Practice, and the Selection of Inhibitors. SPE 24987, R.B. de Boer and Klaas Leerlooyer, Shell E&P Laboratorium; M.R.P. Eigner and A.R.D. van Bergen, 1992.

[54] A practical solution to the problem of asphaltene deposits. Haskett and Tartera. JPT, April, 1965.

[55] Schlumberger Fluid Conversions in Production Log Interpretation page 35, Edition. 1974.

[56] The Properties of Gases and Liquids. Bruce E. Poling, John M. Prausnitz John O'Connell. McGraw-Hill Book Company, 2000.

[57] The Properties of Petroleum Fluids. William D. McCain, Jr. Pennwell, 2nd Edition.

[58] **SPE REPRINT SERIES N° 13 GAS TECHNOLOGY**. The reprint contains a series of selected papers published before 1977.

- The Effect of Phase Data on Liquids Recovery During Cycling of a Gas Condensate Reservoir. By Del D. Fussell and Lyman Yarborough p. 171
- Vapor-Liquid Equilibrium Ratios (K- Values) of Light Hydrocarbons at Reservoir Conditions. By Byron B. Woertz p. 178
- Compressibility Factors for Lean Natural Gas-Carbon Dioxide Mixtures at High Pressure. By Thomas S. Buxtonand John M. Campbell p. 187
- Depths to Which Frozen Gas Fields (Gas Hydrates) May Be Expected. By Donald L. Katz p. 194
- Depths to Which Frozen Gas Fields May Be Expected – Footnotes. By Donald L. Katz p. 199
- The Viscosity of Natural Gases. By Anthony L. Lee, Mario H. Gonzalez, and Bertram E. Eakin p. 201
- Calculating Viscosities of Reservoir Fluids From Their Compositions. By John Lohrenz, Bruce G. Bray, and Charles R. Clark p. 205

• The Volumetric Behavior of Natural Gases Containing Hydrogen Sulfide and Carbon Dioxide. By D.B. Robinson, C.A. Macrygeorgos, and G.W. Govier p. 211
• Predicting Phase and Thermodynamic Properties of Natural Gases With the Benedict-Webb-Rubin Equation of State. By JF Wolfe p. 218
• A New Equation of State for Z-Factor Calculations. By Kenneth R. Hall and Lyman Yarborough p. 227
• Viscosities of Binary Mixtures in the Dense Gaseous State: The Methane-Carbon Dioxide System. By Kenneth J., De Wittand George Thodos p. 236

[59] Fundamentals of Reservoir Engineering. L.P. Dake, Elsevier, 1978.

[60] How to solve equation of state for Z-factors. Lyman Yarborough and K.R. Hall SPE Reprint Series N° 13, The Oil and Gas Journal, Feb., 1974.

[61] Compressibility Factor of Sour Gases. Wichert, E., and Aziz, K., Can. J. of Chem. Eng., Vol. 49, N° 2, pp. 267-273, 1971.

[62] GPSA (Gas Processors Suppliers Association) Engineering Data Book (SI) 12th edition, 2004.

[63] Gas Well Testing Theory and Practice. Energy Resources Conservation Board Alberta Canada, 1979.

[64] An Improved Method for the Determination of the Reservoir Gas Specific Gravity for Retrogade Gases. D.K. Gold, W.D. McCain Jr. and J.W. Jennings, JPT, July, 1989.

[65] How to Estimate Equivalent Gas Volume of Stock Tank Condensate. Leshikar, A.G., World Oil, page 108, January 1961.

[66] **SPE REPRINT SERIES N° 15 PHASE BEHAVIOR 1981**. The reprint contains a series of selected papers published before 1981.

TABLE OF CONTENTS

Part 1 – Prediction of Phase Behavior

Convergence Pressure Methods

• Calculation of Pressure-Temperature Phase Behavior of Multicomponent Systems. By C.S. Kaliappan and Allen M. Rowe Jr., Soc. Pet. Eng. J., 243-251, Sept. 1971 p. 7
• The Critical Composition Method – A New Convergence Pressure Method. By Allen M. Rowe Jr., Soc. Pet. Eng. J., 54-60; Trans., A1ME, 240, March 1967 p. 16

Equations of State

• An Iterative Sequence for Phase Equilibria Calculations Incorporating the Redlich-Kwong Equation of State. By D.D. Fussell and J.L. Yanosik, Soc. Pet. Eng. J., 173-182, June 1978 p. 23
• A Technique for Calculating Multiphase Equilibria. By Lynne T. Fussell, Soc. Pet. Eng. J., 203-210, Aug. 1979 p. 33
• Two- and Three-Phase Equilibria Calculations for Systems Containing Water. By Ding-Yu Peng and Donald B. Robinson, Cdn. J. Chem. Eng., 54, No. 6, 595-599, Dec. 1976 p. 41
• A New Two-Constant Equation of State. By Ding- Yu Peng and Donald B. Robinson, I.&E.C. Fundamentals, 15, No.1, 59-64, 1976 p. 46
• On the Thermodynamics of Solutions. V – An Equation of State. Fugacities of Gaseous Solutions. By Otto Redlich and J.N.S. Kwong, Chem. Reviews, 44, 233-244, 1949 p. 52
• Equilibrium Constants From a Modified Redlich-Kwong Equation of State. By Giorgio Soave, Chem. Eng. Sci., 27, No. 6, 1197-1203, 1972 p. 64
• A New Approach for Determining Equation-of-State Parameters Using Phase Equilibria Data. By K.E. Starling, Soc. Pet. Eng. J., 363-371; Trans., A1ME, 237, Dec. 1966 p. 71

C7 + Split

• Reservoir Depletion Calculations for Gas Condensates Using Extended Analysesin the Peng-Robinson Equation of State by Abbas Firoozabadi, Yusuf Hekim, and Donald L. Katz, Cdn. J. Chem. Eng., 56, 610-615, Oct. 1978 p. 80
• A Modified Soave Equation of State for Phase Equilibrium Calculations. 1. Hydrocarbon Systems. By Michael S. Graboski and Thomas W. Daubert, I.&E.C. Process Des. Dev., 17, No. 4, 443-448, 1978 p. 86

[67] Vaporisation Equilibrium Constants in a Crude Oil-Natural Gas System. Katz, D.L. and Hachmuth, K.H., Ind. Eng. Chem, 1937.

[68] Equilibrium Constants for a Gas-Condensate System. Hoffman, A.E., Crump, J.S., and Hocott, C.R., Trans., AIME, 1953.

[69] A set of Equations for Computing Equilibrium Ratios of a Crude Oil/Natural Gas System at Pressures Below 1000 psia. J.P.T., Sept 1979.

[70] Thermodynamics: Applications in Chemical Engineering and the Petroleum Industry. Jean Vidal, Editions Technip, 2003.

[71] A Consistent Correction for Redlich-Kwong-Soave Volumes. Peneloux, A., E. Rauzy., and R. Freze, Fluid Phase Eq. 8, 7-27, 1982.

[72] Properties of Gases and Liquids. Reid, R.C. Prausnitz, J.M., and Sherwood, T.K., 3rd Ed., McGraw-Hill, 1987.

[73] Generalized liquid volume shifts for the Peng-Robinson equation of state for C_1 to C_8 hydrocarbons. B. Hoyos, Escuela de Procesos y Energía. Universidad Nacional de Colombia, A. A. 1027. Medellín, Colombia, 2004.

[74] A Method for Predicting Depletion Performance of a Reservoir Producing Volatile Crude Oil. R.H. Jacoby, V.J. Berry. Presented at the fall meeting Los Angeles, October, 1956. SPE Reprint Series N° 3 Oil and Gas Property Evaluation and Reserve Estimates.

[75] A New Depletion Performance Correlation for Gas-Condensate Reservoir Fluids. B.A. Eaton, R.H. Jacoby, SPE 1152, June, 1965.

[76] Log Interpretation Charts Schlumberger, 1972.

[77] Pressure, Volume, Temperature and Solubility Relations for Natural Gas-Water Mixtures. Dodson, C.R., and M.B. Standing, Drilling, and Production Practices, API, 1944.

[78] Effects of gas Composition and Geothermal Properties on the Thickness and Depth of Natural Gas Hydrate Zones. Holder, G.D, Malone, R.D., and Laswsa, W.F., JPT, September, 1987.

[79] Applied Petroleum Reservoir Engineering. Craft and Hawkins Prentice-Hall, 1959 and 1991.

[80] Petroleum Production Handbook. T.C. Frick, Volume 2 Reservoir Engineering, SPE, 1962.

[81] Modern Reservoir Engineering A Simulation Approach. Henry B. Crichlow, Prentice-Hall, 1977.

[82] Pressure Buildup and Flow Test in Wells. C.S. Matthews, D.G. Russel, SPE monograph, 1967.

[83] The Flow of Real Gases Through Porous Media. J.P.T. Al-Hussainy, R., Ramey, H.J., Jr. and Crawford, P.B., May: 624-636, Trans, AIME, 1966.

[84] Eléments de mécanique des fluides dans les milieux poreux. A. Houpeurt, Technip, 1975.

[85] The Application of The Laplace Transformation to Flow Problems in Reservoirs. A.F. Van Everdingen, Shell Oil Co., Houston, and W. Hurst, Petroleum Consultant, Houston. Petroleum Transactions, AIME December, 1949.

[86] SPE 6893. Interpretation of Well-Block Pressures in Numerical Reservoir Simulation. By Donald W, Peaceman, Exxon Production Research, Co. 1978.

[87] SPE 10528. Interpretation of Well-Block Pressures in Numerical Reservoir Simulation With Nonsquare Grid Blocks and Anisotropic Permeabilities. By Donald W. Peaceman, Exxon Production Research Co. Sixth SPE Symposium on Reservoir Simulation, February, 1982.

[88] Physical Principles of Oil Production. Morris Muskat, McGraw-Hill, 1949. Reprint: International Human Resources Development Corporation, 1981.

[89] Applications of Unsteady State Gas Flow Calculations. Janicek, J., and D.L. Katz, preprint, University of Michigan Publishing Services, Ann Arbor, 1955.

[90] Notes on Relative Permeability Relationships. Standing, M.B., Proc., U. of Trondheim, Norway, 1975.

[91] The Interrelation Between Gas and Oil Relative Permeabilities. Corey, A.T., Producer's Monthly, January, 1954.

[92] Reservoir Simulation with history-dependent Saturation Functions. Killough, J.E., Trans. AIME 261, pages 37-48, February 1976.

[93] Simulation of Relative Permeability Hysteresis to the Non-Wetting Phase SPE 10157. Carlson, F.M., San Antonio, 1981.

[94] Relative Permeability Hysteresis: Laboratory Measurements and Conceptual Model. Braun, E.M. and Holland, R.F., SPERE, August 1995.

[95] Steady Flow of Gas-Oil-Water Mixtures through Unconsolidated Sands. Leverett, M.C., and W.B., Lewis, Trans, AIME, 1941.

[96] Three Phase Relative Permeability. A.T. Corey, C.H. Rathjens, J.H. Henderson, and R.M.J. Wyllie, Trans. AIME, 1956.

[97] Calculation of Imbibition Relative Permeability for Two and Three Phase Flow from Rock Properties. Land, C.E., S.P.E.J., page 149-156, June, 1968.

[98] Probability Model for Estimating Three-phase Relative Permeability. H.L. Stone, JPT, 1970.

[99] Estimation of three-phase relative permeability and residual oil data. H.L. Stone, J. Can. Pet. Tech. 12, 53, 1973.

[100] Petroleum Reservoir Simulation. Khalid Aziz and Settari. Applied Science Publishers Ltd, 1979.

[101] Comparison of the three-phase oil relative permeability models. M. Delshad and G.A. Pope, J. Transport Porous Media 4, 59, 1989.

[102] The Behavior of Naturally Fractured Reservoirs. Warren, J., and Root, P., paper SPE 426 presented at the Fall Meeting of the Society of Petroleum Engineers, Los Angeles, California, 21 March, 1962.

[103] Imbibition Oil Recovery from Fractured, Water-Drive Reservoir. Mattax, C. and Kyte, J., paper SPE 187 presented at the 36th Annual Fall Meeting, Dallas, Texas, 25 April, 1961.

[104] Experimental Study of Cocurrent and Countercurrent Flows in Natural Porous Media. Bourbiaux, B. and Kalaydjian, F., paper SPE 18283 presented at the SPE Annual Technical Conference and Exhibition, Houston, 2-5 October 1988.

[105] Evaluation of Matrix-Fracture Transfer Functions for Countercurrent Capillary Imbibition. T. Babadagli, C.U. Hatiboglu, and T. Hamida, U. of Alberta. SPE Asia Pacific Oil and Gas Conference and Exhibition, 5-7 April, Jakarta, Society of Petroleum Engineers, Indonesia 2005.

[106] Measurement of Relative Permeabilities by the Welge Method (Investigation). Revue de l'Institut Français du Pétrole (1973) 28, N° 5.

[107] Mbal user guide.

[108] Eclipse Technical Description.

[109] VIP-Executive Technical Reference.

[110] Corner Point Geometry in Reservoir Simulation by D.K. Ponting; Proceedings of the Joint IMA/SPE European Conference on Mathematics of Oil Recovery, Cambridge, July 1989.

[111] A Method for Calculating Multi-Dimensional Immiscible Displacement. Jim Douglas, D.W. Peaceman, H.H. Rachford SPE 2021, 1968. SPE REPRINT SERIES N° 11 Numerical Simulation SPE, 1973.

[112] An Efficient Fully Implicit Simulator. By Ian M. Cheshire, John R. Appleyard, and Derek Banks, Atomic Research Establishment; Robert J. Crozier, British National Oil Corp.; Jonathan

A. Holmes, Atomic Energy Authority. Paper EUR 179 at European Offshore Conference & Exhibition, London, October, 1980.

[113] Special Techniques for Fully Implicit Simulators. Appleyard, J.R., Cheshire, I.M. and Pollard, R.K., Proc. European Symposium on Enhanced Oil Recovery, Bournemouth, England, 1981.

[114] Reservoir Simulation Using an Adaptive Implicit Method. Thomas, G.W. and D.H. Thurnau, paper SPE 10120 presented at the 56th Annual Fall Technical Conference, San Antonio, 1981.

[115] The Mathematical Basis of The Adaptive Implicit Method by G.W. Thomas and D.H. Thurnau, Scientific Software Corp. SPE 10495 Sixth SPE Symposium on Reservoir Simulation, New Orleans, 1982.

[116] An Adaptive Implicit Switching Criteria Based on Numerical Stability Analysis. By L.S-K Fung, D.A.C. Collins, and L. Nghiem, Computer Modeling Group. SPE 16003 9th SPE Symposium on Reservoir Simulation, San Antonio, 1987.

[117] IMPES Stability: The Stable Step by K.H Coats; Coats Engineering, Inc.SPE 69225 SPE Symposium on Reservoir Simulation, Houston, 2001.

[118] High-Order Implicit Flux Limiting Schemes for Black Oil Simulation; Rubin, B. and Blunt, M.J. SPE 21222 11th SPE Symposium on Reservoir Simulation, Anahein, 1991.

[119] Direct Methods in Reservoir Simulation. H.S. Price, and K.H. Coats, 3rd SPE Symposium on numerical simulation, Houston, January, 1973. SPE Reprint Series N° 11 Numerical Simulation, 1973. SPEJ, June, 1974.

[120] Nested Factorization by J.R. Appleyard and I.M. Cheshire, Exploration Consultants Ltd. SPE 12264 7th SPE Symposium on Reservoir Simulation, San Francisco, Nov., 1983.

[121] Orthomin, an iterative Method for Solving Sparse Banded Sets of Simultaneous Linear Equations. Vinsome, P.K.W., SPE 5729 4th SPE Symposium, Los Angeles, 1979.

[122] Comparison of Nested Factorization, Constrained Pressure Residual, and Incomplete Factorization Preconditionings. By A. Behie, Computer Modelling Group. SPE 13531, 8th SPE Symposium on Reservoir Simulation, Dallas, February, 1985.

[123] Constrained Residual Acceleration of Conjugate Residual Methods by J.R. Wallis, R.P. Kendall, and T.E. Little, J.S. Nolen & Assocs. Inc. SPE 13536 8th SPE Symposium on Reservoir Simulation, Dallas, Feb., 1985.

[124] GMRES; A Generalized Minimal Residual Algorithm for Solving Non-Symmetric Linear Systems. By Saad, Y. and Schultz, M., SIAM J. Sci. Stat. Comput. 7 (3): 856-869, July 1986.

[125] Incomplete Gaussian Elimination as a Preconditioning for Generalized Conjugate Gradient Acceleration by J.R. Wallis, Scientific Software-Intercomp. SPE 12265 7th SPE Symposium on Reservoir Simulation, San Francisco, Nov., 1983.

[126] Matrix Iterative Analysis. Varga, R.S., Englewood Cliffs, N.J., Prentice-Hall, 1962.

[127] The Use of Flexible Gridding for Improved Reservoir Modeling. Quandalle, P., and Besset, P., paper SPE 12239 presented at the 7th SPE Symposium on Reservoir Simulation, San Francisco, November 1983.

[128] Reduction of Grid Effects due to Local Sub-Gridding in simulations Using a Composite Grid. Quandalle, P., and Besset, P., paper SPE 13527 presented at the SPE 1985 Reservoir Simulation Symposium, Dallas, February 1985.

[129] Efficient Iterative Linear Solution of Locally Refined Grids using Algebraic Multilevel Approximate Factorizations. Wallis, J.R. and Nolen, J.S., SPE 25239, presented at the 12th SPE Symposium on Reservoir Simulation, New Orleans, February 1993.

[130] A General-Purpose Parallel Reservoir Simulator. Killough, John E., Forster, John A., Nolen, James S., Wallis, John R., and Xiao, Jason, presented at the 5th European Conference on the Mathematics of Oil Recovery, Leoben, Austria, Sept, 1996.

[131] Quiet Revolution Information Technology and the Reshaping of the Oil and Gas Business. Cambridge Energy Research Associates, 1996.

Author index

Subject index

Pierre Donnez

ESSENTIALS OF RESERVOIR ENGINEERING

The book covers the basic techniques of reservoir engineering necessary for a professional to master. The approach consists of starting from the fundamental physical laws down to the practical applications in reservoir engineering. Emphasis is placed on assumptions and limits attached to each concept and the link between theory and field applications.

A lot of effort has been developed to clarify the issue of the unit systems. The theory in this book is developed with a homogenous unit system with useful formulas expressed in practical units. We get:

- Rock properties described to satisfy the reservoir engineer requirements and help geologists in electrical log interpretation.
- Fluid behavior properties explained through a complete PVT report for oil and gas.
- Laboratory techniques described to help the engineer to communicate with the laboratory staff.

Material balance is discussed extensively for oil and gas reservoirs. Attention is given to the importance of the aquifer match before starting a reservoir simulation. Associated gas reservoir development issues are presented.

The last chapter is devoted to reservoir simulation. The theory focuses on the modern tools used in the industry. Calculation techniques are explained to help the user to master the algorithms and optimize the management of the reservoir study. Numerous references are provided to guide the students for further reading.

The book content will help students in their first approach to reservoir engineering and professionals to familiarize themselves with modern techniques.

Pierre Donnez *holds a Master's degree in aeronautics. He spent 12 years working for Schlumberger Wireline Services and 22 years for Total in the reservoir engineering department. Currently he is teaching at the IFP School, Rueil-Malmaison.*

ISBN 978-2-7108-0892-3

www.editionstechnip.com

design K